Universidad Zaragoza
1542

Trabajo Fin de Grado

CAPACITY EVALUATION OF LINE-OF-SIGHT MULTI-ANTENNA COMMUNICATIONS

EVALUACION DE CAPACIDAD SOBRE ENLACES DE VISION DIRECTA EN COMUNICACIONES CON MULTIPLES ANTENAS

Autor

Eduardo Almazán Galisteo

Director

Emil Björnson

Ponente

Pedro Luis Carro Ceballos

Escuela de Ingeniería y Arquitectura

Septiembre 2016

TRABAJOS DE FIN DE GRADO / FIN DE MÁSTER

Escuela de Ingeniería y Arquitectura Universidad Zaragoza

DECLARACIÓN DE AUTORÍA Y ORIGINALIDAD

(Este documento debe acompañar al Trabajo Fin de Grado (TFG)/Trabajo Fin de Máster (TFM) cuando sea depositado para su evaluación).

D./Dª. Eduardo Almazán Galisteo,

con nº de DNI 76923871A en aplicación de lo dispuesto en el art. 14 (Derechos de autor) del Acuerdo de 11 de septiembre de 2014, del Consejo de Gobierno, por el que se aprueba el Reglamento de los TFG y TFM de la Universidad de Zaragoza,

Declaro que el presente Trabajo de Fin de (Grado/Máster) Grado, (Título del Trabajo) CAPACITY EVALUATION OF LINE-OF-SIGHT MULTI-ANTENNA COMMUNICATIONS,

es de mi autoría y es original, no habiéndose utilizado fuente sin ser citada debidamente.

Zaragoza, 29 de Agosto de 2016

Fdo: EAG

A mis padres y mi hermana

Agradecimientos

Me gustaría agradecer el apoyo de mi director de proyecto Emil Björnson y mi ponente Pedro Luis Carro, sin sus consejos y ayuda no habría sido posible este Trabajo Fin de Grado.

Agradecer también a la Universidad de Zaragoza en la que he pasado esta etapa de mi vida que en parte finaliza con este proyecto y a la Universidad de Linköping, en la que ha transcurrido mi último año, y me ha dado la oportunidad de vivir nuevas experiencias.

A mi familia, por su apoyo y comprensión durante todos estos años en los que hemos compartido tanto buenos como malos momentos.

Por último, agradecer a mis compañeros de grado con los que he disfrutado estos últimos cuatro años, a mis amigos del instituto con los que he compartido tantas experiencias, a todas aquellas personas que conocí en Linköping durante este último año y a mis amigos de la playa, los cuales han estado apoyándome durante la redacción de este trabajo.

A todas las personas que han hecho esto posible, gracias.

Eduardo Almazán Galisteo
18 de Septiembre de 2016

CAPACITY EVALUATION OF LINE-OF-SIGHT MULTI-ANTENNA COMMUNICATIONS

EVALUACION DE CAPACIDAD SOBRE ENLACES DE VISIÓN DIRECTA EN COMUNICACIONES CON MÚLTIPLES ANTENAS

RESUMEN

CAPÍTULO 1

Introducción

En esta sección se explicaran los objetivos que se han llevado a cabo en este trabajo Fin de Grado, además de un pequeño resumen del trabajo realizado y de la metodología utilizada.

1.1 Objetivo y alcance

Los sistemas de comunicación inalámbrica han estado presentes en nuestras vidas desde hace tiempo. Hoy en día estamos acostumbrados a que estos sistemas nos ayuden tanto en el ámbito personal como el empresarial, convirtiéndose en algo fundamental para nuestras vidas. Considerando el desarrollo de las tecnologías actuales y de los sistemas, es posible plantear mejoras y desarrollar nuevas tecnologías en este ámbito que abran el abanico de posibilidades de las comunicaciones inalámbricas. En este proyecto se ha realizado un estudio sobre el grado de importancia de la posición de las antenas en un enlace de múltiple entrada y múltiple salida con línea de visión directa, estudiando para ello sus modelos teóricos y posteriormente evaluándolos en distintas simulaciones que han sido desarrolladas a partir de los datos recopilados. A partir de los datos conseguidos se analizará la posibilidad de aplicar técnicas como el multiplexado espacial para la mejora del enlace.

El proyecto comienza con la idea de recopilar información y realizar un estudio de los diferentes modelos teóricos que serán aplicados a la práctica posteriormente, generalizándolos para así ser posible el análisis de cualquier composición de antenas posible. Para ello se realizaran modelos de simulación con ayuda del software de cálculo matemático MATLAB. Finalmente se realizará un análisis de los resultados obtenidos y serán comparados para así obtener nuestras conclusiones finales. Debido a la enorme cantidad de simulaciones posibles que se pueden realizar al ser posible variar cualquier parámetro del sistema, el trabajo se limitará a aquellas que aporten datos más relevantes para las conclusiones.

1.2 Concepto del TFG

Los modelos usados para las simulaciones se han desarrollados usando la capacidad multiplexada de canales MIMO [**1**][**9**] deterministas usando las matrices de canal H, que representan el modelo matemático y las características de un canal de comunicaciones y que varían según las propiedades de este, el número de antenas en recepción y transmisión y la localización de estas. Mirando la capacidad y la matriz que representa al canal, es posible indicar si el canal es capaz de soportar multiplexado espacial y el nivel aplicable de este. Para ello se utilizará la descomposición en valores singulares, que permite conocer la capacidad resultante de los canales simulados.

Esta matriz depende del modelado físico del canal que estemos utilizando, en el proyecto podemos diferenciar cinco tipos diferentes de canales.

- **Entrada simple salida múltiple (SIMO)**: Sistemas con una sola antena en transmisión y múltiples antenas en recepción.

- **Entrada multiple salida simple (MISO):** Sistemas con múltiples antenas en transmisión y una sola antena en recepción.

- **Entrada múltiple salida múltiple (MIMO):** Sistemas con múltiples antenas tanto en transmisión como en recepción. Este modelo mezclan los modelos SIMO y MISO en uno más general.

- **Antenas de transmisión geográficamente separadas (GSTA):** Sistemas con antenas separadas a gran distancia en transmisión. En este tipo de sistemas se encontraran presentes dos antenas diferentes en transmisión las cuales se separarán una distancia comparable a la distancia del enlace. En recepción se utilizara un sistema de antenas múltiples como el del modelo SIMO.

- **Antenas de recepción geográficamente separadas (GSRA):** Sistemas con antenas separadas a gran distancia en recepción. En este tipo de sistemas se encontraran presentes dos antenas diferentes en recepción que se separarán una distancia comparable a la distancia del enlace. En transmisión se utilizara un sistema de antenas múltiples como el del modelo MISO.

Finalmente, con todos los algoritmos implementados se simularán los cinco modelos con diferentes conjuntos de parámetros que permitirán comprobar las ventajas y desventajas de estos y obtener conclusiones.

1.3 Metodologia

Las herramientas utilizadas para el desarrollo de este proyecto incluyen el software cálculo numérico MATLAB [**4**] y los modelos teóricos utilizados, implementados desde una colección de diferentes artículos y libros.

MATLAB es un programa de computación con su propio lenguaje de programación que permite cálculos matriciales, gráficos e implementación de algoritmos, además de ser compatible con otros lenguajes de programación. Es un programa muy utilizado en el ámbito de las telecomunicaciones por lo que no fue necesario tiempo extra para familiarizarse con el entorno de trabajo debido al uso previo y conocimiento de este.

Con todas estas herramientas, se pueden ver diferentes pasos en la progresión del proyecto y como estos han sido ejecutados y solucionados.

1. Recolección de toda la información disponible, artículos y familiarización con la idea principal del Proyecto y los conceptos que van a ser implementados en el futuro.

2. Estudio de los principales conceptos de los sistemas MIMO, de los fundamentos teóricos y de cómo implementar estos modelos y crear los algoritmos para una simulación.

3. Implementacion de los algoritmos de los cinco modelos iniciales que son vistos en toda la información disponible.

4. Mejora de los modelos iniciales para permitir cualquier conjunto de antenas posible tanto en recepción como en transmisión. Tras esto se comprobará la funcionalidad de los modelos.

5. Ajuste, corrección y mejora de los modelos ya generados para depurar los algoritmos y conseguir simulaciones lo más reales posibles.

6. Interpretación de los resultados obtenidos y evaluación de estos. Análisis de las causas y consecuencias de estos resultados.

7. Escritura de la memoria. Esta fase y la anterior son realizadas conjuntamente debido a la necesidad de escribir los resultados obtenidos y las conclusiones de estos.

1.4 Cronograma

En el siguiente cronograma se encuentra resumida una aproximación del número de horas dedicadas a cada apartado del trabajo.

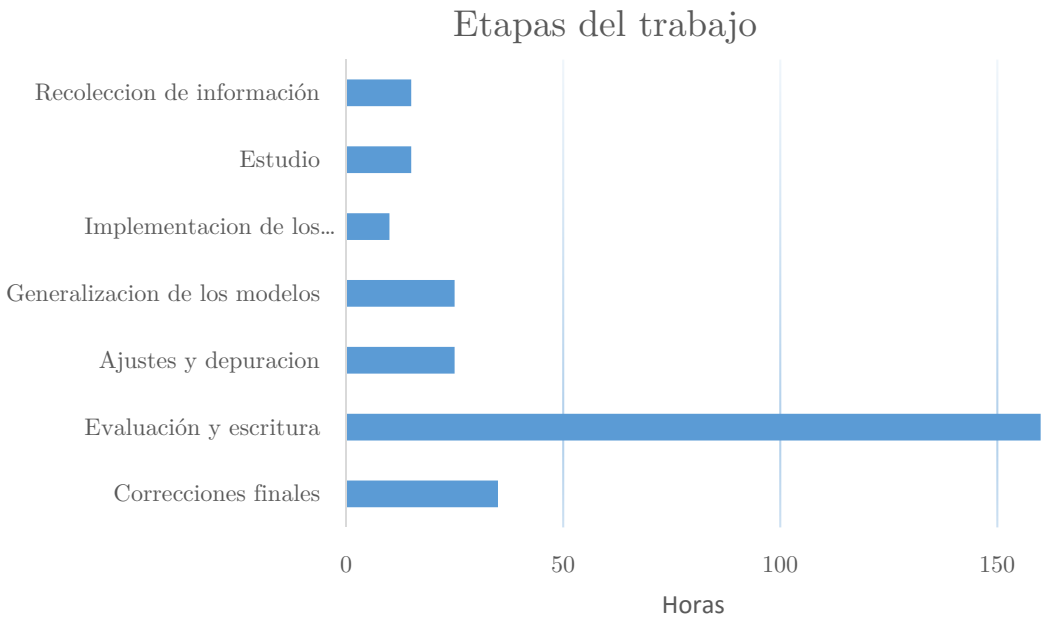

Figura 1.1: Cronograma de trabajo

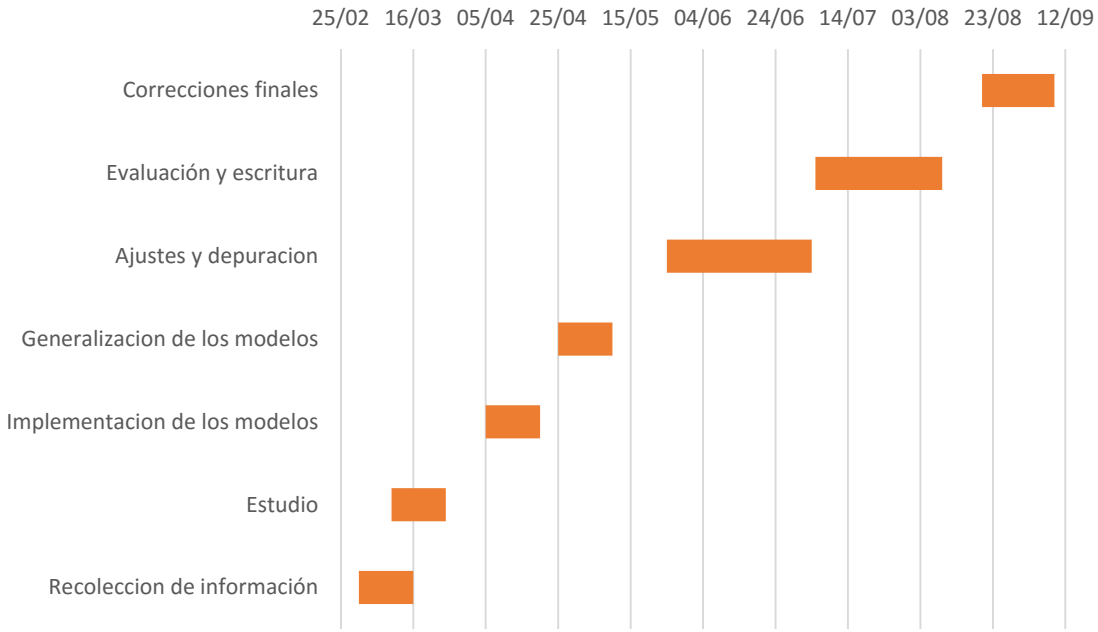

Figura 1.2: Diagrama de Gantt

CAPÍTULO 2

Aspectos teóricos

En esta capitulo se realizará un estudio sobre los modelos teóricos utilizados en las simulaciones y como se ha obtenido la capacidad de estos.

2.1 Capacidad

Un canal invariante en el tiempo puede ser descrito con una ecuación que relaciona la señal transmitida con la matriz que describe el comportamiento del canal, tal que:

$$\boldsymbol{y = Hx + w} \tag{2.1}$$

donde **y** representa la señal recibida como un vector de dimensión $\boldsymbol{n_r \times 1}$, **x** representa la señal transmitida con un vector de dimensión $\boldsymbol{n_t \times 1}$, **H** representa el canal junto con su comportamiento y características mediante una matriz de dimensiones $\boldsymbol{n_r \times n_t}$ y **w** representa una distribución gaussiana que modela el ruido blanco que entra a la transmisión y es añadido al resultado de la multiplicación entre la señal transmitida la matriz de canal, es representado por un vector $\boldsymbol{n_r \times 1}$.

Este es modelo general que representa todo sistema de telecomunicaciones desde el punto de vista lineal y usando la notación matricial puede ser particularizado para los modelos que se propondrán aquí. Este proyecto se centrará en la matriz de canal **H** y en la capacidad que se puede obtener en las transmisiones en diferentes casos particulares.

La capacidad de un canal MIMO es obtenida mediante la extensión de la ecuación de la información mutua para un canal de entrada simple salida simple, para el cual utilizaremos la capacidad de Shannon [**8**] [**15**]. La capacidad de Shannon es la mayor velocidad que el canal puede soportar decodificando la señal recibida con sin error. La capacidad (**C**) es el máximo de la información mutua respecto a la distribución $\boldsymbol{p(x)}$

$$\boldsymbol{C = \max_{p(x)} I(X;Y) = \max_{p(x)} [H(Y) - H(Y|X)]} \tag{2.2}$$

La medida de la información mutua mide la dependencia entre las dos variables y cuantifica la cantidad información obtenida. Se puede expresar esta información mutua en términos de la entropía. La definición de entropía marca que $\boldsymbol{H\ (Y/X)\ =\ H\ (w)}$, que es la entropía del ruido. Esto provoca que maximizar la información mutua equivalga a maximizar la entropía en **y**. A su vez la información mutua de **y** depende de su matriz de covarianza $\mathbf{R}_y$, por lo que el modelo MIMO de banda estrecha es dado por la siguiente formula donde $\mathbf{R}_x$ es la covarianza de la entrada.

$$\boldsymbol{R_y = E[yy^H] = HR_xH^H + I_{M_r}} \tag{2.3}$$

La información mutua puede mostrarse como,

$$\boldsymbol{I(X;Y) = B\,log_2\,det[HR_xH^H + I_{M_r}]} \tag{2.4}$$

siendo B el ancho de banda del sistema.

2.1.1 Descomposicion en valores singulares

El canal es un vector gaussiano que permite calcular la capacidad mediante la descomposición en valores singulares de la matriz de canal [**13**]. En el álgebra lineal, esta descomposición es una factorización de una matriz real o compleja y es definida como la descomposición en valores propios de una matriz positiva semidefinida a otra matriz mediante descomposición polar.

$$\boldsymbol{H\ =\ U\Sigma V^*} \tag{2.5}$$

Las matrices **U** y **V** son las matrices de rotación unitarias de la descomposición, mientras que la matriz central contiene los valores singulares de la matriz **H** en su diagonal. Esta descomposición permite entender la descomposición paralela del canal que es obtenida al definir una transformación en la entrada y salida del canal mediante un pre cifrado y un cambio de forma en recepción.

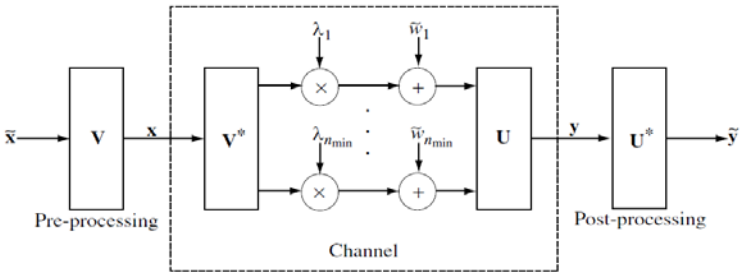

Figura 2.1: Esquema descomposición SVD [1]

Esto permite transformar el canal MIMO en un conjunto de canales SISO [**7**] paralelos con $\tilde{\boldsymbol{x}}$ como entrada y $\tilde{\boldsymbol{y}}$ como salida, tal y como se puede ver en la figura **2.1**.

$$\begin{aligned}\tilde{\boldsymbol{y}} &= \boldsymbol{U^H}(\boldsymbol{Hx}+\boldsymbol{w})\\ &= \boldsymbol{U^H}(\boldsymbol{U\Sigma Vx}+\boldsymbol{w})\\ &= \boldsymbol{U^H}\left(\boldsymbol{U\Sigma VV^H}\tilde{\boldsymbol{x}}+\boldsymbol{w}\right)\\ &= \boldsymbol{U^H U\Sigma VV^H}\tilde{\boldsymbol{x}}+\boldsymbol{U^H w}\\ &= \Sigma\tilde{\boldsymbol{x}}+\tilde{\boldsymbol{w}}\end{aligned} \qquad \textbf{(2.6)}$$

2.1.2 Distribucion de potencia

En la expresión para calcular la capacidad del canal, se puede observar que en vez de la potencia es utilizado el algoritmo de distribución de potencia para distribuir la potencia transmitida por cada canal [**5**] [**6**]. Este algoritmo se emplea para estrategias de ecualización en canales de comunicación. El algoritmo usa el concepto de la ley de Pascal, cada canal utiliza cierta cantidad de la potencia que depende de la **SNR** disponible, para alcanzar individualmente la potencia necesaria, compensando la diferencia entre canales.

$$\boldsymbol{P_i^*} = \left(\boldsymbol{\mu} - \frac{\boldsymbol{N_0}}{\boldsymbol{\lambda_i^2}}\right)^+ \qquad \textbf{(2.7)}$$

Cada $\boldsymbol{\lambda_i}$ representa un canal propio. La existencia de más de uno de estos canales hace posible el multiplexado espacial de diferentes tramas en sistemas MIMO. Este sistema permite adaptarnos a las características del sistema y de la señal de entrada, localizando iguales cantidades de potencia para altos valores de SNR o solo en el modo principal para bajos valores de SNR, como se muestra en la figura **2.2.**

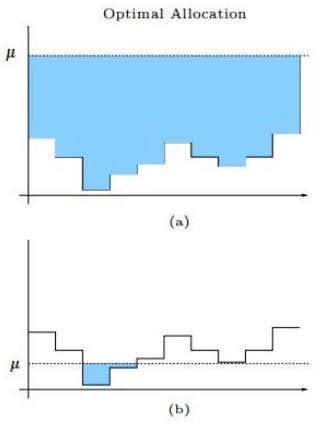

Figure 2.2: Distribución de potencia [3]

Maximizando la información mutua sobre las matrices de covarianza a la entrada satisfaciendo la restricción de potencia, la capacidad de un sistema MIMO es descrita por:

$$C = \sum_{i=1}^{n_{min}} log\left(1 + \frac{P_i^* \lambda_i^2}{N_0}\right) \frac{bits}{s} / Hz \tag{2.8}$$

Donde $P_1^*, \ldots, P_{n_{min}}^*$ son las distribuciones localizadas de potencia.

2.2 Modelado de los canales a estudiar

En este apartado de la memoria se introducen teóricamente los diferentes modelos desarrollados. En todos los casos se habla de comunicaciones con línea de visión directa, ya que en este proyecto se intenta averiguar la importancia de la colocación de las agrupaciones de antenas. Colocar efectos de reflexión, multicamino y dispersión causaría que la posición de estas antenas fuera mucho menos decisiva debido a las diferentes interferencias constructivas y destructivas que estos efectos generan.

2.3.1 SIMO

El canal SIMO con línea de visión directa posee una separación entre las antenas en recepción de $\Delta_r \lambda_c$. La dimensión total de la agrupación de antenas es mucho menor que la de la distancia total **d**. Podemos ver el esquema en la figura **2.3**.

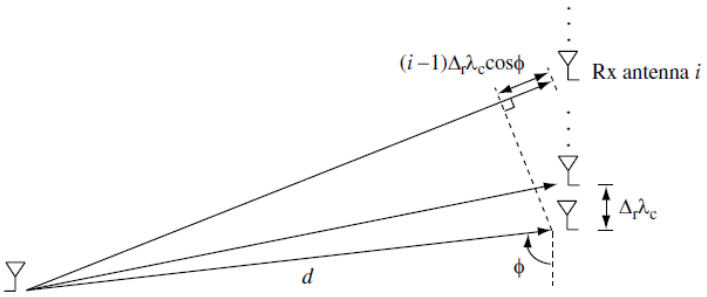

Figura 2.3 Esquema SIMO [1]

Con este esquema y la premisa de que $^{d_i}/_{c} \ll {}^{1}/_{B}$ donde B es el ancho de banda de transmisión, se puede describir la ganancia del canal como:

$$h_i = a\, exp\left(-\frac{j2\pi d_i}{\lambda_c}\right) \tag{2.9}$$

El vector de ganancia del canal se denomina firma espacial inducida en el conjunto de antenas receptoras. Calculando las distancias relativas a cada componente de una distribución lineal simple, se obtiene la matriz de canal final definida junto a la firma espacial unitaria del coseno director $\left(e_r(\Omega)\right)$ como:

$$h = a\, exp\left(-\frac{j2\pi d}{\lambda_c}\right)\sqrt{n_r}\, e_r(\Omega) = a\, exp\left(-\frac{j2\pi d}{\lambda_c}\right)\begin{bmatrix} 1 \\ \dots \\ exp(-j2\pi(n_r-1)\Delta_r\Omega) \end{bmatrix} \tag{2.10}$$

2.3.2 MISO

El canal MISO es reciproco y equivalente al canal SIMO, presentando las mismas propiedades y características que el canal anterior, cambiando los parámetros de recepción por los de transmisión. La firma espacial del canal MISO es exactamente la misma que la descrita por el canal anterior. El modelo queda descrito en la figura **2.4**.

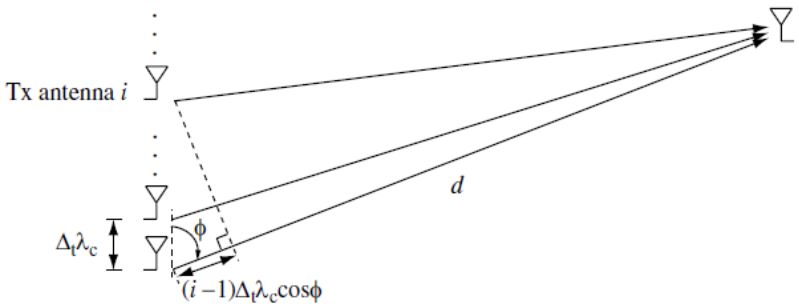

Figura 2.4: Esquema MISO [1]

Usando las mismas distancias relativas, se puede definir la matriz de canal final definida junto a la firma espacial unitaria del coseno director $\left(\boldsymbol{e_t(\Omega)}\right)$ como:

$$\boldsymbol{h = a\, exp\left(-\frac{j2\pi d}{\lambda_c}\right)\sqrt{n_t}\, e_t(\Omega) = a\, exp\left(-\frac{j2\pi d}{\lambda_c}\right)\begin{bmatrix} 1 \\ \dots \\ exp(-j2\pi(n_t-1)\Delta_t\Omega) \end{bmatrix}} \quad \textbf{(2.11)}$$

En una transmisión óptima los desfases entre los componentes se equilibran y añaden constructivamente. La capacidad final obtenida es la misma que la del canal SIMO, dependiendo únicamente del número de antenas en transmisión. El canal SIMO y el canal MISO proveen de ganancia en potencia, pero no ganancia por grados de libertad.

2.3.3 MIMO

Ahora al considerar el canal MIMO con línea de visión directa, el más general de todos los estudiados en este proyecto, se puede modificar la ecuación de la firma espacial de un canal SIMO y generalizarla para un mayor número de antenas en transmisión. El resultado obtenido es:

$$\boldsymbol{h_{ij} = a\, exp\left(-\frac{j2\pi d_{ij}}{\lambda_c}\right)} \quad \textbf{(2.12)}$$

Los parámetros de la formula son los mismos de los canales anteriores, y continuamos asumiendo la misma atenuación para todos los enlaces. La distancia entre cada una de las antenas será el mayor factor para describir el cambio de fase entre los diferentes elementos de los conjuntos. Combinando ambas firmas espaciales unitarias de los anteriores modelos, es posible describir la matriz de canal del modelo MIMO:

$$\boldsymbol{H = a\, exp\left(-\frac{j2\pi d}{\lambda_c}\right)\sqrt{n_t n_r}\, e_r(\Omega_r) e_t(\Omega_t)^*} \quad \textbf{(2.13)}$$

Al igual que los anteriores modelos, el canal MIMO provee de ganancia en potencia pero no en grados de libertad, por lo que solo es proyectado en un único canal. La capacidad final es la misma que en los casos anteriores, pero en este caso depende tanto del número de antenas en transmisión y recepción.

2.3.4 GSTA

En todos los modelos vistos obteníamos ganancia en potencia pero no en grados de libertad. Ahora, al colocar dos antenas separadas entre ellas con una distancia comparable a la distancia del enlace se puede obtener una separabilidad en función de los ángulos que permitirá obtener más de un canal propio de la matriz de canal. Esta matriz será una composición de dos enlaces SIMO. Se puede ver el esquema en la figura **2.5**.

$$\boldsymbol{h_k = a_k\, exp\left(-\frac{j2\pi d_{1k}}{\lambda_c}\right)\sqrt{n_r}\, e_r(\Omega_{rk})} \qquad \textbf{(2.14)}$$

Al poseer dos valores singulares diferentes y distintos de cero, permite dos grados de libertad. Para que estos dos grados existan, y las dos columnas sean independientes en la matriz de canal, ambos cosenos directores deben ser diferentes, y al estar contenido su valor en [-1,1] y no poder diferir en más que 2, debe que cumplirse que el espaciado entre antenas debe ser menor que $\Delta_r \leq 1/2$.

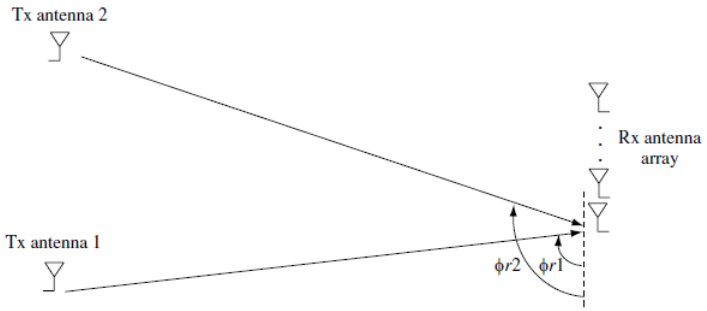

Figura 2.5: Esquema GSTA [1]

La separación angular describe el nivel de condicionamiento de los grados de libertad de la matriz y la posibilidad de utilizarlos efectivamente. Esto está determinado por cómo se encuentran las firmas espaciales alineadas. Utilizando,

$$\boldsymbol{\cos\theta \coloneqq e_r(\Omega_{r1})^* e_r(\Omega_{r2})} \qquad \textbf{(2.15)}$$

se puuede definir el número de condición que describe como de bien condicionada es la matriz. Si el valor de este número es cercano a uno, no es posible usar ambos canales.

$$\frac{\lambda_1}{\lambda_2} = \sqrt{\frac{1 + |cos\,\theta|}{1 - |cos\,\theta|}} \tag{2.16}$$

2.3.5 GSRA

Finalmente, si en vez de basar el modelo anterior en enlaces de tipo SIMO con múltiples antenas en recepción, se usa un sistema MISO transmisión múltiple y recepción única, obteniendo un sistema paralelo al anterior con las mismas propiedades. El esquema está descrito en la figura **2.6**.

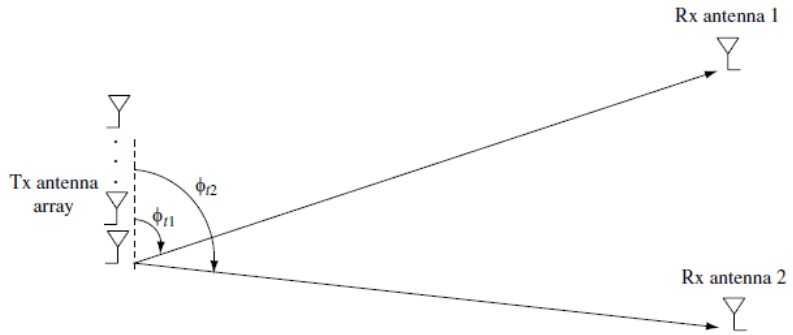

Figura 2.6: Esquema GSRA [1]

Paralelamente, la matriz de canal estará compuesta por dos matrices modeladas mediante enlaces MISO usando la ecuación:

$$h_i = a_i\, exp\left(-\frac{j2\pi d_{i1}}{\lambda_c}\right)\sqrt{n_t}\, e_t(\Omega_{it}) \tag{2.17}$$

Este modelo comparte junto a GSTA ambos grados de libertad junto a la ganancia en potencia, estos grados podrán ser efectivos siempre y cuando cumplan las condiciones pertinentes para ser utilizables en el enlace de comunicaciones.

2.3.6 Generalizacion de los modelos

Los modelos teóricos previamente presentados están diseñados para conjuntos de antenas simples equidistantes. Por tanto se generalizaran estos modelos para así poder aplicar cualquier conjunto de antenas tanto en recepción como en transmisión.

Es posible observar que en todos los modelos la matriz se compone de la ganancia base de canal en la dirección principal y por la firma espacial unitaria. Esta última describe las diferencias de distancias entre los elementos del conjunto.

Los modelos generales son capaces de calcular todas las distancias relativas entre componentes y generar una matriz que contenga estas distancias relativas. La matriz es

procesada por el algoritmo añadiendo las atenuaciones y las frecuencias de portadora, obteniendo así la matriz de canal final. Este desarrollo se basa en la ecuación **(2.9)**, usando directamente la distancia relativa entre las antenas en vez de utilizar series y formulas generalizadas como los modelos simplificados.

CAPÍTULO 3

Modelos y simulaciones

Este capítulo contiene una descripción sobre los modelos usados en las simulaciones, así como una breve descripción de éstos junto con los resultados obtenidos mediante las simulaciones.

3.1 Algoritmos y modelos

Los modelos teóricos previamente explicados y generalizados han sido implementados mediante algoritmos en MATLAB para que sea posible probarlos matemáticamente. Los algoritmos usan dos sistemas de coordenadas cartesianas independientes para describir tanto la posición de las antenas en transmisión como en recepción. Ambos sistemas son combinados en uno utilizando como origen el sistema de coordenadas de transmisión y la separación general **d** entre antenas.

Con esta información ya procesada, es sencillo obtener todas las distancias relativas entre ambos conjuntos de antenas y con ellas calcular las firmas espaciales y los distintos desfases. El algoritmo también contiene una corrección angular para rotar los conjuntos si fuera necesario en cualquier número de grados.

El algoritmo acepta como entrada todos los posibles parámetros en la simulación del modelo. Para los cálculos se utilizará una frecuencia de portadora que pertenezca al rango UHF y SHF, que son las más usadas en comunicaciones móviles con frecuencias alrededor de los GHz. También se utilizará un ancho de banda de usuario de 10 MHz.

En las siguientes secciones se presentan más detalladamente los modelos usados para los factores de atenuación del sistema, el ruido y las potencias transmitidas.

3.1.1 Atenuación

Como modelo de atenuación se ha elegido un modelo de micro celdas con línea de visión directa basado en el COST 231 Walfish – Ikegami [**2**], ya que es más preciso que otros modelos. La distancia d se expresa en metros y la frecuencia f en MHz.

$$PL(dB) = -35.4 + 26log_{10}(d) + 20log_{10}(f) \quad (3.1)$$

Este modelo permite estimaciones desde los 20 metros, en vez de 1 km como en el modelo Okomura – Hata.

3.1.2 SNR y modelo de ruido

Para que las simulaciones sean realistas, se elegirán valores para la potencia de transmisión prácticos. Se usaran valores de 10, 20, 30 y 40 dBm que representan un rango de potencias comprendido entre 10 mW y los 10 W, potencias que pueden ser encontradas en sistemas como GSM, UMTS o 3G [**10**].

También se necesitará un modelo de ruido para calcular la capacidad. Para ello se utilizará un valor de -174 dBm/Hz [**11**] que representa el ruido blanco térmico para un ancho de banda de 1Hz a temperatura ambiente. Este valor será multiplicado por el ancho de banda de 10 MHz de la señal, obteniendo una potencia de ruido de -104 dBm para las simulaciones.

3.2 Configuraciones de Antenas bajo Test

En esta sección se describen los diferentes modelos de distribución de las antenas que se han utilizado en los conjuntos de transmisión y recepción. Estos diferentes conjuntos han sido diseñados para intentar comprobar las diferencias existentes en la capacidad resultante. Los algoritmos crean la distribución de antenas que es usada como entrada, aproximando la separación entre elementos a la mitad de la longitud de onda de la frecuencia portadora, que estará en torno al valor de decenas de centímetros.

3.2.1 Agrupación lineal

La distribución linear es exactamente la misma utilizada en los modelos simplificados. Usando el número de antenas N y la separación entre elementos S se pueden localizar los elementos mediante un bucle, obteniendo resultados prácticamente idénticos en las antenas generadas mediante este modelo y los modelos simplificados (**Figura 3.1**).

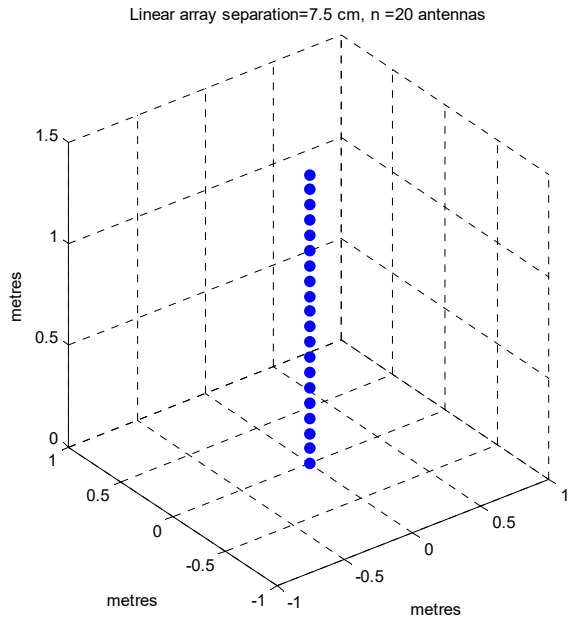

Figura 3.1: Agrupación lineal

3.2.2 Agrupación Circular

El algoritmo genera un conjunto que contiene N antenas separadas por una distancia aproximada de S en una distribución circular. Para ello obtiene la longitud de la circunferencia mediante los parámetros de entrada, calculando así el radio necesario. Finalmente tan solo hace falta colocar las antenas de una en una incrementando el ángulo progresivamente hasta alcanzar la circunferencia completa (**Figura 3.2**).

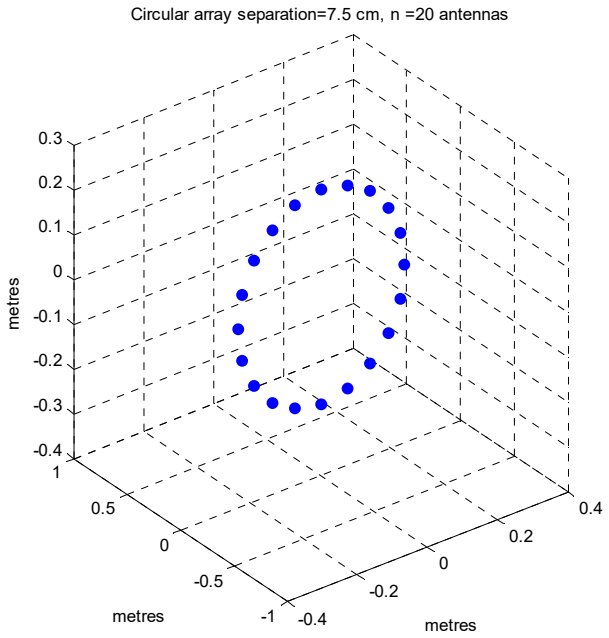

Figura 3.2: Agrupación circular

3.2.3 Agrupación cuadrangular

Genera una distribución con forma de cuadrado, obteniendo la longitud de este mediante la multiplicación de los parámetros de entrada y con ello la longitud de los lados. Las antenas serán colocadas progresivamente utilizando la separación necesaria, y comprobando donde se encuentran los ángulos del cuadrado para no romper la formación (**Figura 3.3**).

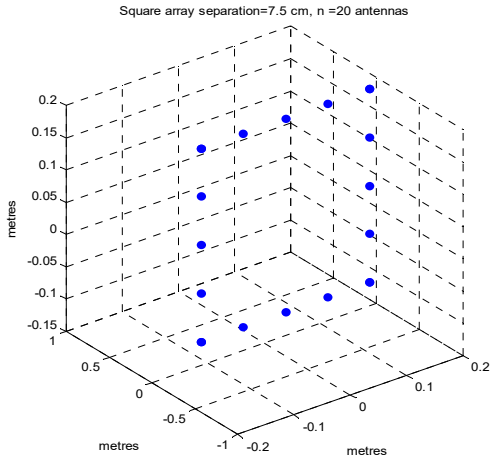

Figura 3.3: Agrupación cuadrangular

3.2.4 Agrupación cuadrangular concéntrica

Crea una distribución compuesta por cuadrados concéntricos que contienen una antena en cada una de sus esquinas. El cuadrado inicial tendrá sus elementos separados por la distancia introducida, aumentando esta progresivamente en el resto de cuadrados de la distribución (**Figura 3.4**).

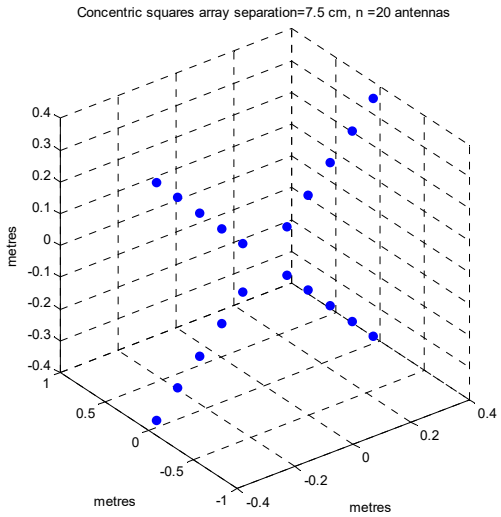

Figure 3.4: Agrupación cuadrangular concéntrica

3.2.5 Agrupación Cúbica

Por ultimo de generará una antena tridimensional cúbica compuesta por 27 antenas en vez de los anteriores ejemplos bidimensionales para observar las diferencias entre estos. Cada uno de los lados estará compuesto por 9 antenas, junto con una central que coincidirá con el origen de coordenadas (**Figura 3.5**).

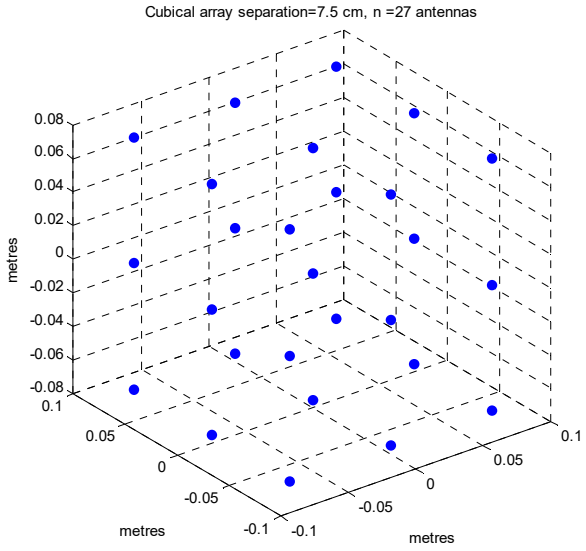

Figura 3.5: Agrupación cúbica

3.3 Simulaciones

A continuación se encuentran las gráficas y resultados obtenidos mediante los modelos programados anteriormente. En el siguiente capítulo se analizaran los resultados de las simulaciones bajo las condiciones que se han explicado.

3.3.1 Sistema SIMO

Los algoritmos son simulados para obtener la capacidad final del sistema SIMO simulado mediante los modelos generales, alternando las distribuciones de antenas en recepción y usando diferentes conjuntos de parámetros. Las gráficas y resultados obtenidos se encuentran en el segundo capítulo del Anexo A. En las figuras **3.6** y **3.7** se encuentran una de las simulaciones del sistema SIMO como ejemplo orientativo de las cifras obtenidas.

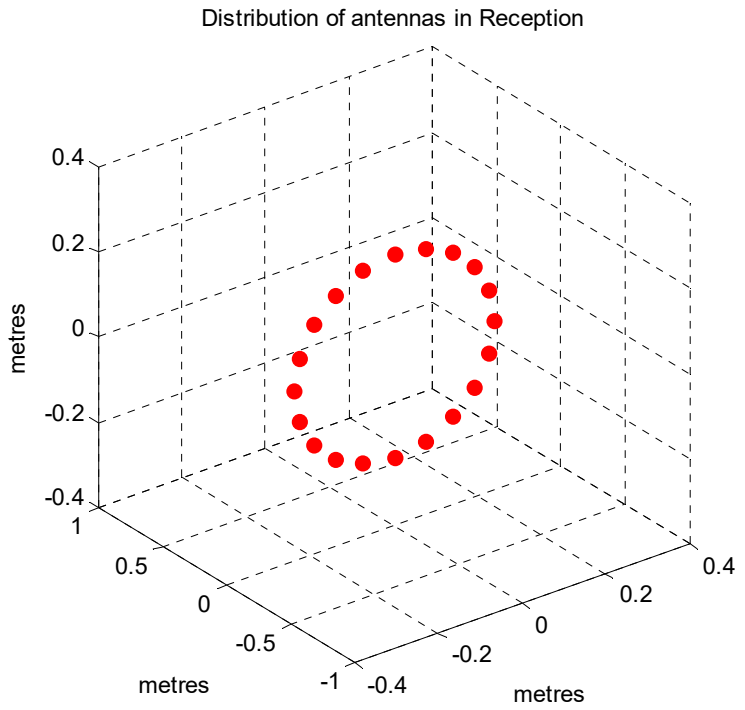

Figura 3.6: Agrupación circular SIMO en recepción N_r =20

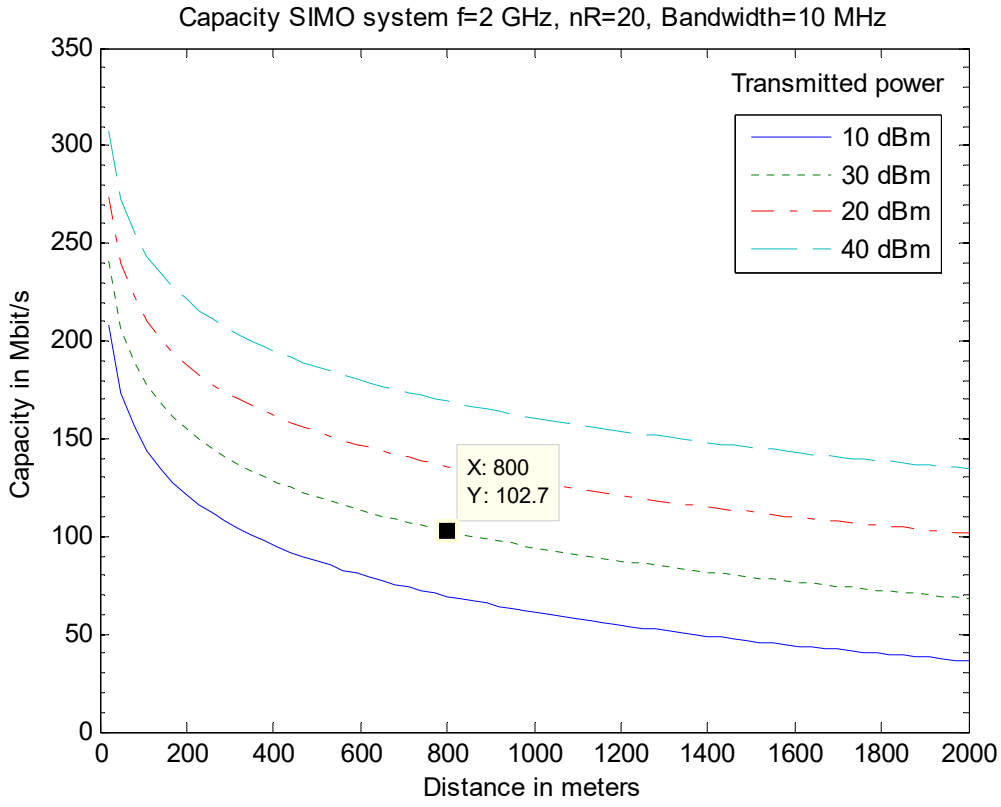

Figura 3.7: Capacidad agrupación circular SIMO N_r=20

3.3.2 Sistema MISO

Los algoritmos son simulados para obtener la capacidad final del sistema MISO simulado mediante los modelos generales, alternando las distribuciones de antenas en transmisión y usando diferentes conjuntos de parámetros. Las gráficas y resultados obtenidos se encuentran en el segundo capítulo del Anexo A.

3.3.3 Sistema MIMO

Los algoritmos son simulados para obtener la capacidad final del sistema MIMO simulado mediante los modelos generales, alternando las distribuciones de antenas tanto en recepción como en transmisión y usando diferentes conjuntos de parámetros. Las gráficas y resultados obtenidos se encuentran en el segundo capítulo del Anexo A. En las figuras **3.8** y **3.9** se encuentran una de las simulaciones del sistema MIMO como ejemplo orientativo de las cifras obtenidas.

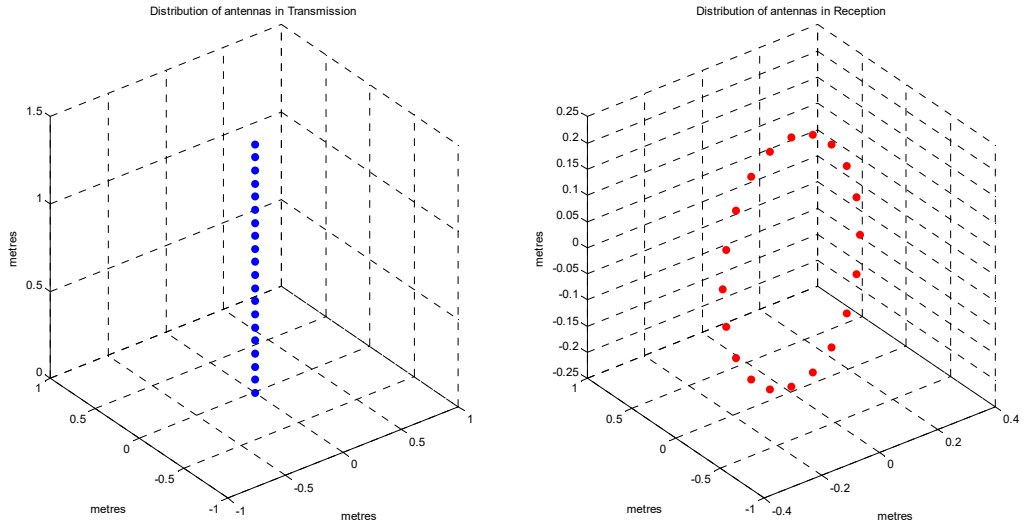

Figura 3.8: Agrupación lineal en transmision N_t=20 y agrupación circular en recepción N_r =20 en sistema MIMO

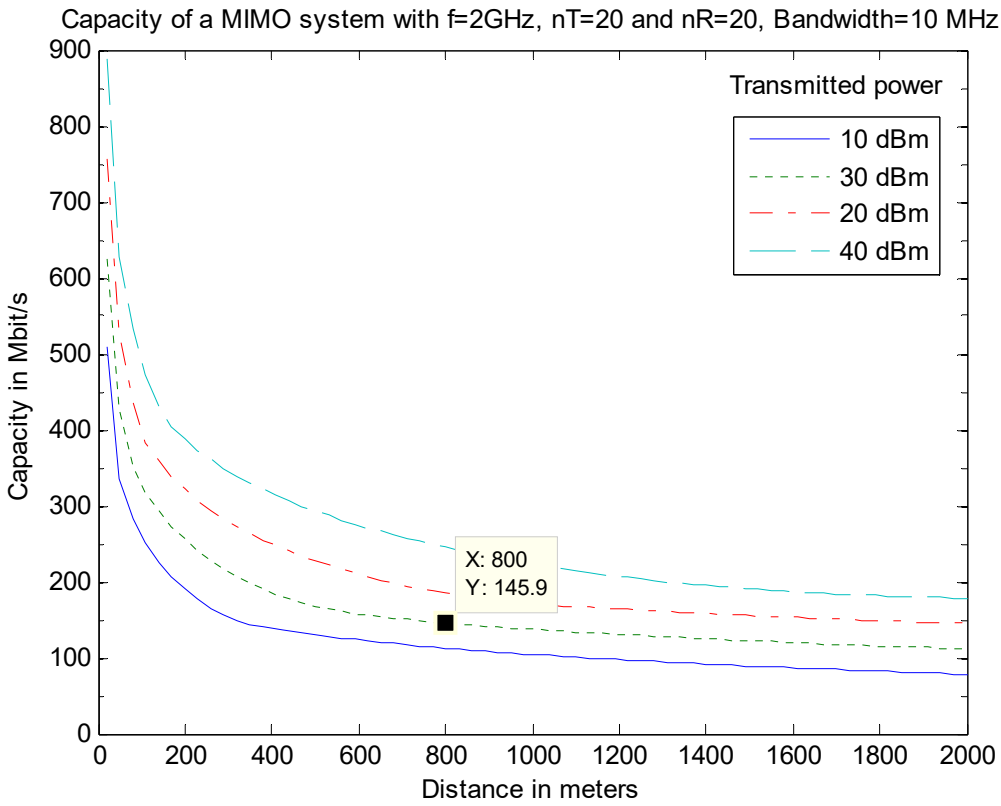

Figura 3.9: Capacidad agrupación lineal N_t=20 y agrupación circular N_r=20 en sistema MIMO

3.3.4 Sistema GSTA

Los algoritmos son simulados para obtener la capacidad final del sistema GSTA simulado mediante los modelos generales, alternando las distribuciones de antenas en recepción y usando diferentes conjuntos de parámetros. Las gráficas y resultados obtenidos se encuentran en el segundo capítulo del Anexo A. En las figuras **3.10** y **3.11** se encuentran una de las simulaciones del sistema GSTA como ejemplo orientativo de las cifras obtenidas.

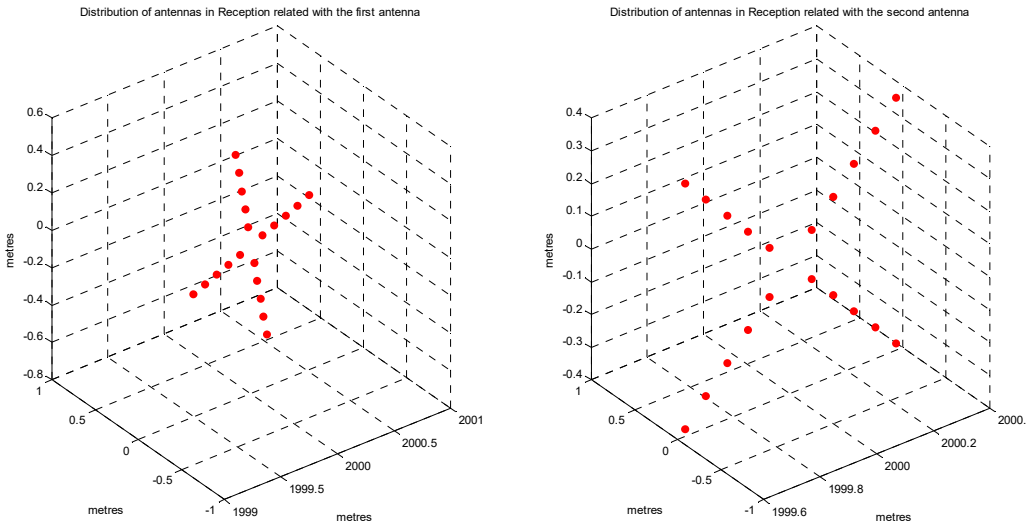

Figura 3.10: Agrupación concéntrica cuadrangular GSTA en recepción $N_r = 20$ $\emptyset_1 = \frac{\pi}{3}$ $\emptyset_2 = 0$

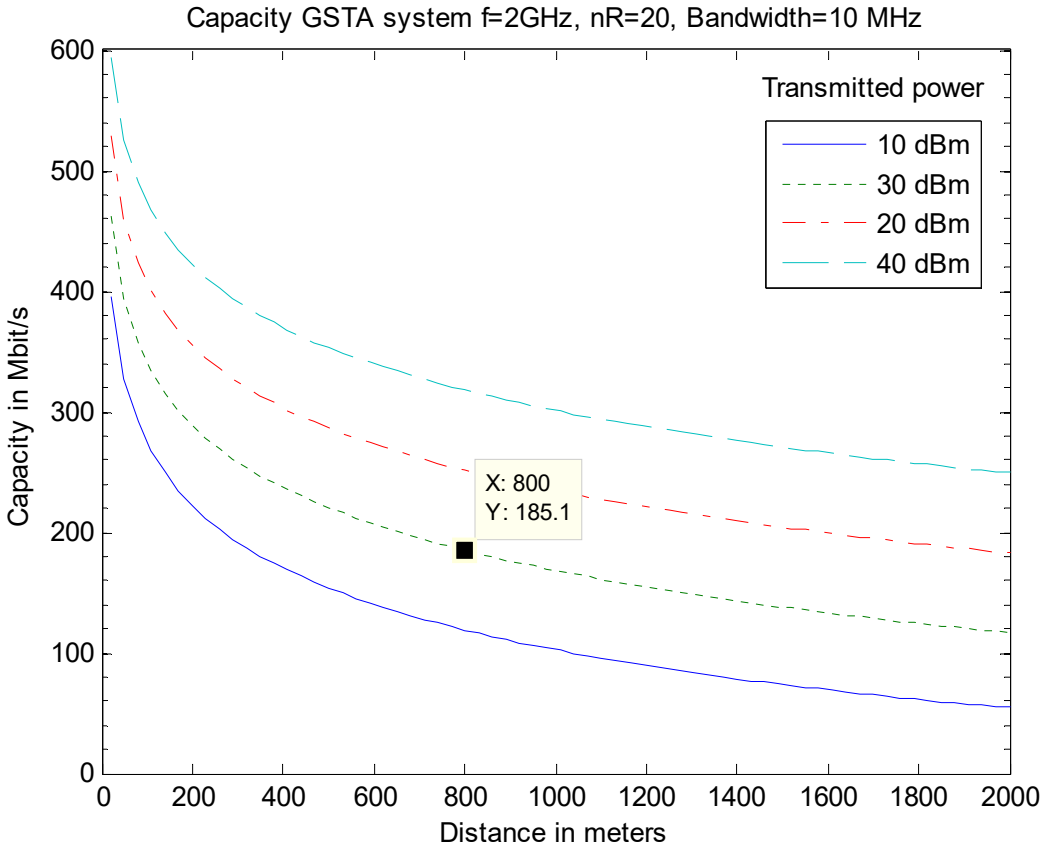

Figura 3.11: Capacidad agrupación concéntrica cuadrangular GSTA $N_r = 20$ $\emptyset_1 = \frac{\pi}{3}$ $\emptyset_2 = 0$

3.3.5 Sistema GSRA

Los algoritmos son simulados para obtener la capacidad final del sistema GSRA simulado mediante los modelos generales, alternando las distribuciones de antenas en transmisión y usando diferentes conjuntos de parámetros. Las gráficas y resultados obtenidos se encuentran en el segundo capítulo del Anexo A.

CAPÍTULO 4

Resultados

Este capítulo contiene una descripción de los resultados finales obtenidos en cada uno de los modelos implementados y simulados anteriormente. Todos los resultados presentados han sido medidos a una distancia de 800 metros.

4.1 SIMO

Podemos observar en las gráficas la variación de la capacidad aumenta proporcionalmente dependiendo del número de antenas en recepción, obteniendo 102.7 Mbit/s con 20 antenas y 107 Mbit/s con 27 antenas. Comparando los resultados de las diferentes antenas se obtienen resultados muy parecidos, debido a la pequeña distancia utilizada en la separación de las antenas y al hecho que el sistema SIMO no posee ganancia en grados de libertad.

La variación en la posición de las antenas modifica la matriz de canal como se puede observar en las tablas contenidas en el anexo incluido al final del documento. Sin embargo el valor singular obtenido de estas gráficas es prácticamente el mismo, variando únicamente con la variación del número de antenas y no con la posición de estas, generando capacidades casi idénticas. La ausencia de ganancia en grados de libertad debido a la obtención de un único valor singular de la matriz de canal, hace imposible el uso del multiplexado espacial en este tipo de sistemas.

4.2 MISO

El modelo MISO es reciproco al anterior, obteniendo resultados casi idénticos, variando únicamente la configuración en recepción por la de transmisión. Al igual que en el modelo anterior, se obtienen 102.7 Mbit/s con 20 antenas y 107 Mbit/s con 27 antenas, variándose este valor únicamente con el número de antenas. Esto es debido a las mismas razones que han sido explicadas en el modelo SIMO.

La ausencia de ganancia en grados de libertad debido a la obtención de un único valor singular de la matriz de canal, hace imposible el uso del multiplexado espacial en este tipo de sistemas.

4.3 MIMO

Los sistemas MIMO combinan ambos modelos en uno más general. Los valores obtenidos mediante las simulaciones se encuentran alrededor de los 145 Mbit/s con 20 antenas en ambos sentidos, 150 Mbit/s con 20 antenas en transmisión y 27 en recepción y 155 Mbit/s con 27 antenas en ambos sentidos. La variación en la capacidad de los diferentes sistemas es muy baja en comparación a la capacidad media obtenida, destacando únicamente en ciertos casos como en el uso de conjuntos lineales que reportan una capacidad de 174.9 Mbit/s con 27 antenas.

Para la realización de estas simulaciones se ha considerado el paralelismo que existe entre antenas, variando los modelos únicamente en uno de los puntos para poder ahorrar en el número de simulaciones. Al igual que SIMO y MISO, tan solo es posible obtener un valor singular de la matriz de canal, siendo así imposible el uso del multiplexado espacial en estos sistemas. Si se aumenta progresivamente la distancia entre las antenas de la agrupación, se ganaría separabilidad espacial, siendo posible así la obtención de más de un valor singular en la matriz de canal y por tanto ganancia en cuanto a los grados de libertad.

4.4 GSTA

El modelo GSTA considera dos antenas separadas geográficamente por una distancia comparable a la distancia de enlace, haciendo uso de esta forma de dos enlaces SIMO. Para simplificar las simulaciones y los cálculos, se utilizará en ambos enlaces la misma distancia. Este modelo sí que es afectado por la ganancia en grados de libertad, siendo posible la obtención de dos valores singular diferentes que hacen posible el uso del multiplexado espacial para la mejora del enlace. Para ello el receptor tendrá que ser capaz de separar y resolver ambas señales por separado, lo que dependerá del ángulo utilizado.

Usando como ángulos de transmisión $\emptyset_1 = \frac{\pi}{3}$ $\emptyset_2 = 0$, se obtienen capacidades de 185.4 Mbit/s con 20 antenas 194 Mbit/s con 27 antenas, ambas capacidades alcanzadas con el uso de conjuntos lineales, obteniendo capacidades ligeramente más bajas con el resto de distribuciones pero también muy similares. También se han obtenido 117 Mbit/s con 27 antenas utilizando el mismo ángulo en varios enlaces, siendo así imposible separar ambas señales y anulando así el posible uso del multiplexado espacial y la ganancia adicional en grados de libertad.

4.5 GSRA

Finalmente el sistema GSRA reporta resultados muy similares al anterior debido a que este está compuesto por dos enlaces MISO en vez de SIMO y comparte un gran número de características con este. Como en el modelo previo, se mantendrá la misma distancia para ambos enlaces durante las simulaciones de este modelo.

Utilizando como ángulos de transmisión $\boldsymbol{\emptyset_1 = \pi\ \emptyset_2 = -\frac{\pi}{12}}$, se han obtenido unos resultados de 198.7 Mbit/s con 20 antenas y 213.7 Mbits/s con 27 antenas, usando para ambos conjuntos lineales. Si en vez de estos conjuntos se usa una configuración con forma circular o cuadrangular, la capacidad obtenida se ve reducida hasta 190 Mbit/s y 150 Mbit/s con una agrupación. Este se debe a que estos dos últimos modelos son mucho más sensibles al posicionamiento de las antenas y los ángulos con estas que los anteriores, debido al efecto que esto produce en la diferencia entre los dos valores singulares obtenidos de la matriz de canal y su repercusión directa en la capacidad resultante.

Variando los ángulos para comprobar esta sensibilidad, obtenemos 212.5 Mbit/s con ángulos de $\boldsymbol{\emptyset_1 = \pi\ \emptyset_2 = -\frac{\pi}{5}}$ con 27 antenas y 200.2 Mbit/s con 20 antenas. Con estos resultados se observa como el modelo es afectado de la misma manera que GSTA y como la obtención de varios valores singulares permite obtener un mejor comportamiento del modelo en función del valor y a diferencia entre estos, así como posibilitando el uso del multiplexado espacial en estos sistemas.

CAPÍTULO 5

Conclusiones finales y lineas futuras

Este capítulo final contiene las conclusiones que han sido recopiladas mediante este trabajo fin de grado y de las posibles líneas de futuro y desarrollos que podrían tomar como punto de partida este trabajo fin de grado.

5.1 Conclusiones

El estudio de los diferentes medios de transmisión y sus variaciones en las comunicaciones inalámbricas pueden ayudarnos en el presente y futuro para mejorar los sistemas de comunicaciones.

Por estas razones, en los capítulos anteriores se ha desarrollado como estudiar e implementar diferentes modelos de transmisión y los efectos que tienen en la capacidad resultante los diferentes parámetros presentes en la comunicación.

En la siguiente tabla se encuentran resumidas los resultados obtenidos en los distintos modelos y las mejores capacidades alcanzadas junto con su configuración principal.

Capacidades alcanzadas en los modelos

Model	$\mathbf{N_T}$	$\mathbf{N_R}$	**Antena en transmisión**	**Antena en recepción**	**Capacidad**	**Multiplexado espacial**
SIMO	1	20	-	Todas	102.7 Mbit/s	No
SIMO	1	27	-	Todas	107 Mbit/s	No
MISO	20	27	Todas	-	102.7 Mbit/s	No
MISO	20	27	Todas	-	107 Mbit/s	No
MIMO	20	20	Lineal	Lineal	148.5 Mbit/s	No
MIMO	20	27	Circular	Cúbica	150.2 Mbit/s	No

MIMO	27	27	Lineal	Lineal	174.9 Mbit/s	No
GSTA	2	20	-	Lineal	185.4 Mbit/s	Si
GSTA	2	27	-	Lineal	194 Mbit/s	Si
GSRA	20	2	Lineal	-	198.7 Mbit/s	Si
GSRA	27	2	Lineal	-	213.7 Mbit/s	Si

Tabla 5.1 Resultados finales

Con estos resultados se puede concluir que en situaciones normales los mejores resultados se obtienen mediante el uso de conjuntos lineales, aunque la diferencia en ganancia con el resto de conjuntos es bastante baja. También se ha visto la importancia de la ganancia de grados de libertad presente en los modelos GSTA y GSRA en comparación con los demás, permitiendo el uso del multiplexado espacial en los enlaces y haciendo cobrar una mayor importancia a la localización de las antenas en comparación con el resto de los modelos.

Finalmente se puede concluir que estos resultados pueden aprovecharse en un futuro y ayudar en próximos sistemas, considerando este proyecto como un éxito y considerando la posibilidad de aplicar estos modelos y técnicas en un futuro para alcanzar mejoras en las prestaciones de los sistemas de comunicación inalámbrica.

5.2 Lineas futuras

Observando los resultados obtenidos y la metodología empleada, se puede continuar con el este proyecto tomando en cuenta los resultados obtenidos y creando nuevas líneas de trabajo.

En primer lugar, podríamos investigar como pasar de los modelos MIMO a GSTA/GSRA aumentando la separación entre antenas y analizando las dimensiones para obtener un mayor número de grados de libertad tanto en transmisor como en receptor.

Se puede continuar con la implementación de diferentes antenas y con el número de simulaciones realizadas para obtener modelos y resultados mucho más precisos, en vez de considerar tan solo los casos principales como ocurre en este proyecto debido a la gran cantidad de diferentes simulaciones que se puede realizar.

También sería posible aumentar la dificultad de los modelos añadiendo efectos de reflexión, multicamino y dispersión a los modelos para así poder determinar su repercusión. Esto añadiría en ciertos casos un mayor número de grados de libertad a los enlaces, siendo así posible el uso del multiplexado espacial y obteniendo así aumentos en las capacidades resultantes.

Finalmente se podría reajustar los modelos de ruido y atenuación para aumentar la precisión de las simulaciones para entornos más particulares, además de añadir otros efectos al enlace como el desvanecimiento.

CAPACITY EVALUATION OF LINE-OF-SIGHT MULTI-ANTENNA COMMUNICATIONS

AUTHOR

EDUARDO ALMAZAN GALISTEO

DIRECTOR

EMIL BJÖRNSON

Index

List of Abbreviations

SIMO	*Single Input Multiple Output*
MISO	*Multiple Input Single Output*
MIMO	*Multiple Input Multiple Output*
GSTA	*Geographically Separated Transmission Antennas*
GRSA	*Geographically Separated Reception Antennas*
SISO	*Single Input Single Output*
SVD	*Singular Value Decomposition*
SNR	*Signal to Noise Ratio*
UHF	*Ultra-High Frequency*
SHF	*Super High Frequency*
GSM	*Global System mobile communications*
UMTS	*Universal mobile telecommunications system*
3G	*Third Generation*
LOS	*Line of sight*
NLOS	*None line of sight*
COST	*European Cooperation in Science and Technology*
BS	*Base Station*

CHAPTER 1

Introduction

In this first chapter we offer a general scope of the developed project, introducing the main concepts of the project and the objectives. We will explain about the different methods that have been used and the theoretical aspects that fundament it.

1.1 Scope

Wireless communications systems have been present since a long time ago. We can find this systems in a huge quantity of places that are around us, including the ones that are intended for the users (in systems such as WiFi and cellular communications) and the different enterprises, and have become something fundamental in our lives. The improvements in security and capacity in this systems can help us to have better experiences either for users or enterprises. We can achieve this developing of the new technologies with new types of modulations, software and hardware architectures. We have made a study of the degree of importance of the position of the antennas in the line-of-sight MIMO communications at transmission and reception at different types of theoretical models, and then evaluate the benefits and difference in our simulations.

This project starts with theoretical models of our antenna systems that we can found at different situations, varying the number of antennas, the position and the distance between them, and with that models we will generalize them for the use of any position for our array of antennas, and then we will developed the MATLAB models that will allow us to do simulations and compare the different behavior of the systems. Due to the huge amount of possible simulations, we will take just a few of them to get the results that can provide us more information about the developed models and see the more easily the differences between the models, using different patterns for the positions of the antennas in the modeled simulations

1.2 Overview

The models used for the simulations have been developed according to the multiplexing capability of deterministic MIMO channels, using the generated deterministic matrix H. H represents the mathematical model of the channel, and depends of the properties of this, the number of antennas in transmission and reception and the position of these ones. Looking at the capacity of the channel, , that describes the maximum amount of information that the channel can transport in a reliable way measure in bits/s, we can know how much spatial multiplexing can the channel support, and for that we will use the singular value decomposition, that allow us to compute the capacity of each simulated channel.

This channel matrix depends on the physical modelling of the channel, in which we can differentiate five different models:

- **Single Input Multiple Output (SIMO)**: Systems with a single antenna in transmission and multiple number of antennas in reception.

- **Multiple Input Single Output (MISO):** Systems with multiple antennas in transmission and just one antenna in reception.

- **Multiple Input Multiple Output (MIMO):** Systems with multiple antennas in transmission and reception, this model will mix both previous models into a one more general.

- **Geographically Separated Transmission Antennas (GSTA):** Systems with geographically separated transmit antennas. In this type of systems we will consider two different antennas in transmission separated by a very big distance, and a system of multiple antennas in reception like the ones that have been used in the SIMO model.

- **Geographically Separated Reception antennas (GSRA):** Systems with geographically separated antennas at reception. In this type of systems we will consider two different antennas in reception separated by a very big distance, and a system of multiple antennas in transmission like the ones that have been used in the MISO model.

Finally, with all the channel models implemented, we will simulate the five different scenarios with different sets of parameters (frequency, number of antennas, shape, separation…) that will allow us to check the advantages and disadvantages of our physical models and draw conclusions on how the antenna deployment affects the capacity.

1.3 Methods

The tools used for the development of this project includes the numerical computing program MATLAB, and the theoretical models that have been studied and implemented from a collection of different articles and books.

MATLAB is a multi-paradigm numerical computing program with his own programming language that allows matrix calculations, plotting of functions and data, implementation of algorithms and interfacing with programs written in other languages like C, C++ or Java. MATLAB is a well-known program in the field of Telecommunications and Systems, so the use of it was an advantage, because it wasn´t necessary time learn how to use it.

With all these resources, we can see different steps in the progression of the project and how these steps has been executed and solved:

1. Collect all the available information and articles about MIMO channels and modelling and familiarity with the main idea of the project and the concepts that are going to be implemented in the future.

2. Study the main concepts of the MIMO systems, the theoretical fundaments, and think about to implement these models and create the algorithms for simulations of the channel capacity.

3. Implement the algorithms of the five initial theoretical.

4. Improve the basics models with any position of the antennas in reception and transmission and check the functionality of this models.

5. Adjust and correct some aspects of the capacity computation to improve them and obtained more accurate simulations.

6. Interpretation of the obtained results of the simulations and evaluation of them. Analysis of the causes and consequences of the results.

7. Writing of the project report. This phase and the previous one are made at the same time due to the necessity to write the obtained results and the conclusions of them.

1.4 Organization of the project report

In addition of this chapter that summarised the whole project, this report contain four more chapters.

- **Chapter 2 – Theoretical Aspects:** An overview of the theoretical tools, models and fundaments that have been use to implement the final models of the simulation.

- **Chapter 3 – Simulations:** Explanation of how the code has been implement, how the different antenna distributions that have been chosen works, how the five models have been implemented, and the final set of simulations results.

- **Chapter 4 – Discussion of the results:** In this chapter we will analyse the simulations and comment on obtained results and the explanation to them.

- **Chapter 5 – Conclusions and future lines:** Finally, we will extract the conclusion of the work and describes briefly the possible future lines of work that can continue this project.

CHAPTER 2

Theoretical Aspects

2.1 Introduction

This chapter describes the theoretical concepts and defines the capacity of MIMO channels that this project evaluates. In the next paragraphs we will use for describe the models the number of antennas in transmission $\mathbf{n_t}$, and the number of antennas in reception $\mathbf{n_r}$.

2.2 Capacity via SVD

A time invariant channel can be describe with an equation that related the transmitted signals with the matrix that describes the behaviour of a narrowband channel, and can be represented as a sum and multiplication of matrix and vectors

$$\boldsymbol{y = Hx + w} \tag{2.1}$$

Where:

- **y:** represents the received signal as a vector with a dimension of $\boldsymbol{n_r \times 1}$. Each component of the vector represents the receive signal at one of the $\boldsymbol{n_r}$ antennas at the receiver.

- **x:** represents the transmitted signal that enters in the system, with a vector of dimension $\boldsymbol{n_t \times 1}$. Each component of the vector represents the signal that is transmitted from one of the $\boldsymbol{n_t}$ antennas of the transmitter.

- **H:** represents the channel and it behaviour and characteristics. This matrix is deterministic and is assumed to be constant at all times and known to both, the transmitter and the receiver. The dimension of the channel matrix is $\boldsymbol{n_r \times n_t}$, and each component of the matrix $\boldsymbol{h_{ij}}$ corresponds with the particular channel between the transmission antenna j and the reception antenna $\boldsymbol{i}$. In the next pages we will see how to obtain the capacity of the channel using this matrix

with the help of the single value decomposition (SVD) and the capacity theorem of Shannon.

- **w:** is a random variable with Gaussian distribution that models the noise that is added in the hardware of the receiver. This distribution has zero mean and a variance that depends of the noise power of the channel. This amount of noise will depend also of different factors such as the bandwidth that our communications systems use. The dimension of this vector is $n_r \times 1$.

This is the general model that is presented in some communication system, and using the matrix notation we will particularized it to our MIMO models. In this project we will concentrate on the matrix channel H and the capacity that we can obtain with different channel models.

The capacity of a MIMO channel is obtained from the channel matrix using the extension of the mutual information formula for a SISO (Single input single output) channel, for that we will use the Shannon capacity. The capacity is the highest data rate (bit/symbol) that the communication channel supports, in the sense that the the signal can be decoded without error if the number symbols is infinitely long. (One can also measure capacity in bit/s, then the capacity is achieved if the transmission is done for infinitely long time).

The capacity is the maximum of the mutual information, with respect to the input distribution $p(x)$

$$C = \max_{p(x)} I(X;Y) = \max_{p(x)} [H(Y) - H(Y|X)]. \quad (2.2)$$

The mutual information measures the dependence between two variables, and quantifies the amount of information obtained about one random variable, through the observing the other random variable. We can express this mutual information in terms of the entropy, where:

- $H(Y)$: is the marginal entropy

- $H(Y|X)$: is the conditional entropy that quantifies the amount of uncertainty of the random variable Y given that the value of the known random value X.

The definition of entropy yields that $H(Y|X) = H(w)$ for the model described in equation **(2.1)**, the entropy of the noise. Since this noise has fixed entropy independent of the channel input, so maximizing the mutual information is equivalent to maximizing the entropy in y.

The mutual information of y depends on its covariance matrix, which for the narrowband MIMO model is given by the next formula, where $\mathbf{R}_x$ is the covariance of the MIMO channel input

$$R_y = E[yy^H] = HR_xH^H + I_{M_r}. \quad (2.3)$$

The mutual information can be show to be

$$I(X;Y) = B\,log_2\,det[HR_xH^H + I_{M_r}]. \quad (2.4)$$

2.2.1 SVD Decomposition

The channel is a vector Gaussian channel, and that allow us to compute the capacity using a Singular Value Decomposition (SVD), decomposing the vector channel into a set of parallel, independent scalar Gaussian sub-channels. In linear algebra, the SVD is a factorization of a real or complex matrix, and it's define as the Eigen decomposition of a positive semidefinite normal matrix. Formally, the singular value decomposition of an $m \times n$ real or complex matrix H is a factorization of the form

$$H = U\Sigma V^* . \quad (2.5)$$

Where:

- **U:** is an $m \times m$ real or complex matrix. The columns of U are called the left-singular vectors of H, which are a set of orthogonal eigenvectors of HH^*. U is an unitary matrix (a unitary matrix satisfies $U^*U = I$).

- **Σ:** is an $m \times n$ rectangular diagonal matrix with non-negative real numbers on the diagonal. The diagonal elements $\lambda_1 \geq \lambda_2 \geq \ldots \geq \lambda_{n_{min}}$ of the matrix are the ordered singular values of the matrix H, where $n_{min} := min(n_t,n_r)$. This singular values are the square roots of the non-zero eigenvalues of both H^*H and HH^*.

- **V:** is an $n \times n$ real or complex matrix. . The columns of V are called the right-singular vectors of H, which are the set of orthogonal eigenvectors of H^*H. V is a unitary matrix. In the formula we use the conjugate transpose of **V**, **V***.

  Using the multiplication between matrixes we can obtain

$$HH^* = U\Sigma\,\Sigma^t U^* \quad (2.6)$$

This square singular values that we obtained are the eigenvalues of the matrix $\boldsymbol{HH^*}$ and also of the matrix $\boldsymbol{H^*H}$. The SVD decomposition allow us to understand the parallel decomposition of the channel that is obtained by defining a transformation on the channel input x and output y through transmit precoding and receiver shaping.

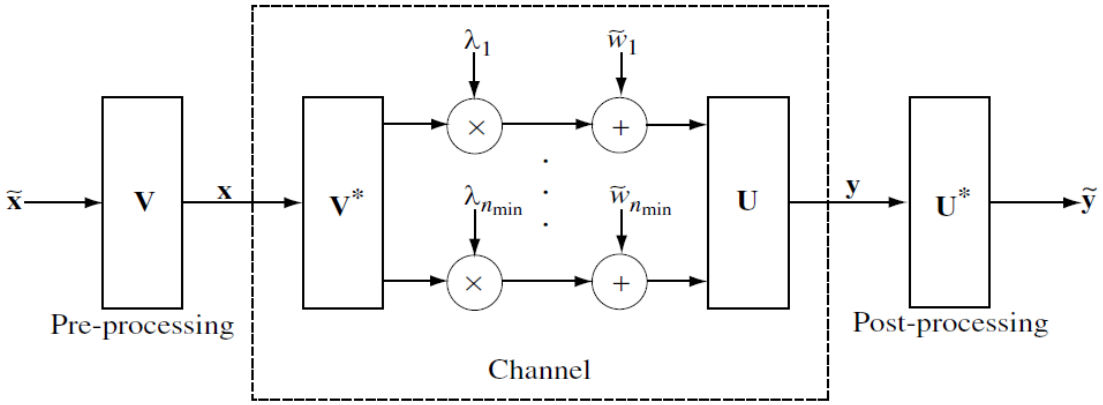

Figure 2.1: SVD decomposition schematic [1]

The transmit precoding and receiver shaping transform the MIMO channel into a parallel SISO channels with input $\tilde{\boldsymbol{x}}$ and output $\tilde{\boldsymbol{y}}$, as we can see in the **Figure 2.1** since from the SVD we have

$$\begin{aligned}\tilde{\boldsymbol{y}} &= \boldsymbol{U^H}(\boldsymbol{Hx}+\boldsymbol{w}) \\ &= \boldsymbol{U^H}(\boldsymbol{U\Sigma Vx}+\boldsymbol{w}) \\ &= \boldsymbol{U^H}\left(\boldsymbol{U\Sigma VV^H}\tilde{\boldsymbol{x}}+\boldsymbol{w}\right) \\ &= \boldsymbol{U^H U\Sigma VV^H}\tilde{\boldsymbol{x}}+\boldsymbol{U^H w} \\ &= \Sigma\tilde{\boldsymbol{x}}+\tilde{\boldsymbol{w}}\end{aligned} \qquad \textbf{(2.7)}$$

Where $\tilde{\boldsymbol{w}}$ has the same distribution as $\boldsymbol{w}$, obtaining with that the representation as a parallel Gaussian channel. The SVD decomposition can be interpreted as a two coordinate transformation, in which we can say that the input is expressed with a new system of coordinates whose base is defined in the columns of the **V** matrix, and the output is expressed with another system of coordinates whose base is defined in the columns of the **U** matrix. With this simplification of the relation between the input and the output, we can see that the equation **(2.10)** is a representation of the original channel **(2.1)** with the input and output represented with a new coordinates systems.

2.2.2 Waterfilling power allocation

In our capacity formula we can notice that we use the water filling algorithm to calculate the power that each channel has. The water filling algorithm is use for equalization strategies in communications channels. The algorithm uses the concepts of the Pascal´s law. Each channel is amplify to the required power level compensating for the channel inequalities.

$$P_i^* = \left(\mu - \frac{N_0}{\lambda_i^2}\right)^+ \tag{2.8}$$

With μ chosen to satisfy the total power constrain $\sum_i P_i^* = P$. Each λ_i corresponds to an eigen mode of the channel. Each non-zero eigen channel can support a data stream, which makes it possible the spatial multiplexing of multiple streams in MIMO systems. The water filling power allocations allow us to adapt the systems to the characteristics of the channel and the SNR (Signal to Noise Ratio), that compares the level of a desired signal to the level of background noise, of the input signal. In the **Figure 2.2** are represented these different cases.

- **High values of SNR:** the algorithm allocate equal amounts of power to each non-zero Eigen channel and the policy is asymptotically optimal.

- **Low values of SNR:** the optimal policy of the algorithm is to allocate all the power only to the strongest Eigen mode.

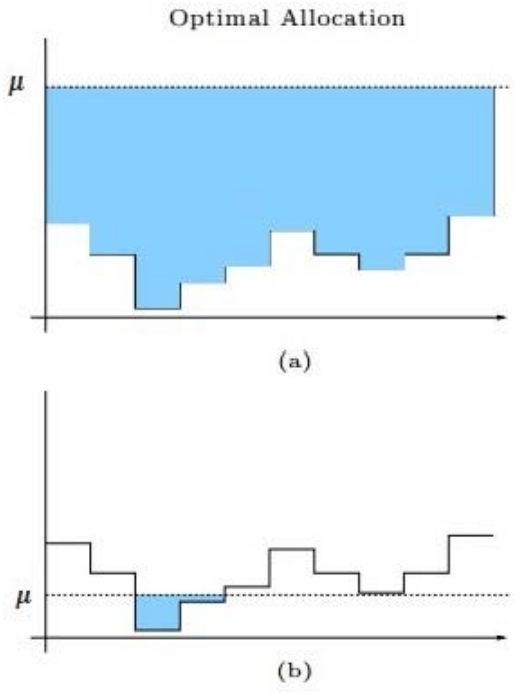

Figure 2.2: Waterfill power allocation [3]

If instead of looking into the SNR we analyse the eigenvalues of the matrix $\boldsymbol{H}$, we can see that the number of non-zero $\boldsymbol{\lambda_i}$ values correspond with the number of spatial degrees of freedom per second per hertz, that represents the dimension of the transmitted signal modified by the MIMO channel. This values will bring a better behaviour of the channel the less spread their values are. This is defined as the condition number, the matrix is said to be well-conditioned if the condition number is close to one, facilitating communications in the high SNR regime

$$\boldsymbol{condition\ number} = \frac{\boldsymbol{\max_i \lambda_i}}{\boldsymbol{\min_i \lambda_i}} \tag{2.9}$$

The MIMO capacity is achieved by maximizing the mutual information over all input covariance matrixes $\boldsymbol{R_x}$ satisfying the power constraint. Substituting the matrix SVD of H into C and using properties of unitary matrices we get the MIMO capacity and the water filling power allocation that are explained in the next sections, we can summarized the capacity of the channel as

$$\boldsymbol{C} = \sum_{i=1}^{n_{min}} \boldsymbol{B\ log}\left(\mathbf{1} + \frac{P_i^* \lambda_i^2}{N_0}\right)\frac{bits}{s}. \tag{2.10}$$

Where $\boldsymbol{P_1^*, \dots, P_{n_{min}}^*}$ are the water filling power allocations.

2.3 Physical modelling of MIMO Channels

In this part of the report we will define the theoretical explanation of the five different models that have been developed and simulated. In all the cases we are talking about line-of-sight communications without obstacles, due to in this project we are trying to evaluate the importance of the position of the antennas at MIMO systems and the effects that it has on the capacity of the channel. If we add to the systems different effects as multipath, the position of the antennas in transmission and reception is less important due to the different constructive and destructive interferences that this effect creates.

In the next sections the models will be just arrays that have all the antennas located in a line with equidistant separations to simplify the theoretical calculations. At the end of the section it's explained how to generalize this models to a more general model that admits all type of positions in transmission and reception.

2.3.1 SIMO

The SIMO channel has line-of-sight vision between the transmission antenna and the receiver array of antennas. As we have explain, there is only free space without factors that can create a multipath effect. The antenna separation in the reception is $\boldsymbol{\Delta_r \lambda_c}$, where $\boldsymbol{\lambda_c}$ is the carrier wavelength and $\boldsymbol{\Delta_r}$ is the normalized receive antenna separation, normalized to the unit of the carrier wavelength. The total dimension of the array is much smaller than the total distance $\boldsymbol{d}$ between the transmission and the reception antennas. In the **Figure 2.3** there is represented the model.

The general equation of the channel for the ith element of the receive array antenna can be describe with the basic continuous time impulse response.

$$\boldsymbol{h_i(\tau) = a\delta\left(\tau - {}^{d_i}/_{c}\right), \quad i = 1, \dots, n_r} \tag{2.11}$$

Where:

- $\boldsymbol{\delta}$**:** represents the Dirac delta function that models the impulse response.
- $\boldsymbol{d_i}$**:** the distance between the transmit antenna and the ith receive antenna.
- $\boldsymbol{c}$**:** the speed of light
- $\boldsymbol{a}$**:** attenuation of the channel, we assume the same attenuation for each antenna pairs.

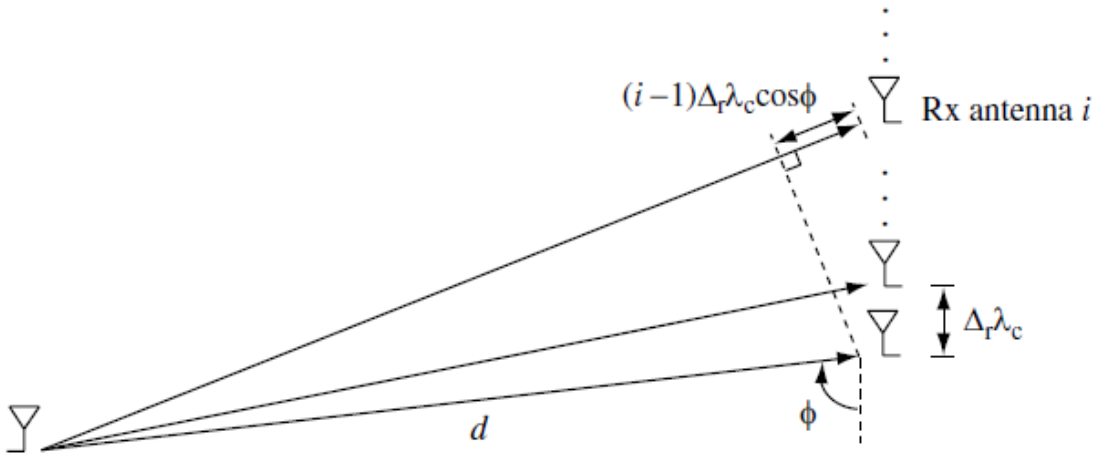

Figure 2.3 SIMO Model [1]

With this parameters and with the assumption of ${}^{d_i}/_{c} \ll {}^{1}/_{B}$ where $\boldsymbol{B}$ is the transmission bandwidth, we describe the gain of the channel as

$$h_i = a\,exp\left(-\frac{j2\pi d_i}{\lambda_c}\right) \tag{2.12}$$

Where h_i represents each of the components of the channel matrix that defines the model.

The SIMO channel can be written with the equation **(2.1)**. The vector of the channel gains is called the spatial signature induced on the receive antenna array by the transmit signal. In the basic model that use a linear equidistant array of antennas, we can calculate the relative distance of each component of the array to the initial one. This distance will be the cause of the phase difference in the reception antennas. If we describe the angle of incidence as the directional cosine: $\Omega := cos\,\phi$, the relative distance of each antenna is describe by

$$d_i = d + (i-1)\,\Delta_r \lambda_c \Omega \tag{2.13}$$

Finally, we define the unit spatial signature in the directional cosine $(e_r(\Omega))$, obtaining the final capacity matrix of the channel:

$$h = a\,exp\left(-\frac{j2\pi d}{\lambda_c}\right)\sqrt{n_r}\,e_r(\Omega) = a\,exp\left(-\frac{j2\pi d}{\lambda_c}\right)\begin{bmatrix} 1 \\ \vdots \\ exp(-j2\pi(n_r-1)\Delta_r\Omega) \end{bmatrix} \tag{2.14}$$

The optimal receiver projects the noisy into the signal direction, adjusting the delays of the antennas and combining it constructively, this result capacity can be expressed as

$$C = log_2\left(1+\frac{Pa^2 n_r}{N_0}\right)\frac{bits}{s}/Hz \tag{2.15}$$

The SIMO channel provides power gain due to the contribution that multiple antennas give to the beamforming, but no degree-freedom gain because the antennas are to close between them to be resolve by the transmitter. We will study this capacity in the simulations of the developed theoretical models.

2.3.2 MISO

The MISO channel is reciprocal to the SIMO channel. It uses a single antenna in reception and an array of multiple antennas in transmission. The antenna separation in the transmission is $\Delta_t \lambda_c$, where Δ_t is the normalized receive antenna separation,

normalized to the unit of the carrier wavelength. The MISO channel can be written with the equation **(2.1)**. The spatial signature of the channel is the same that in the SIMO channel, described in the equation **(2.14)**. The **Figure 2.4** resumes the model.

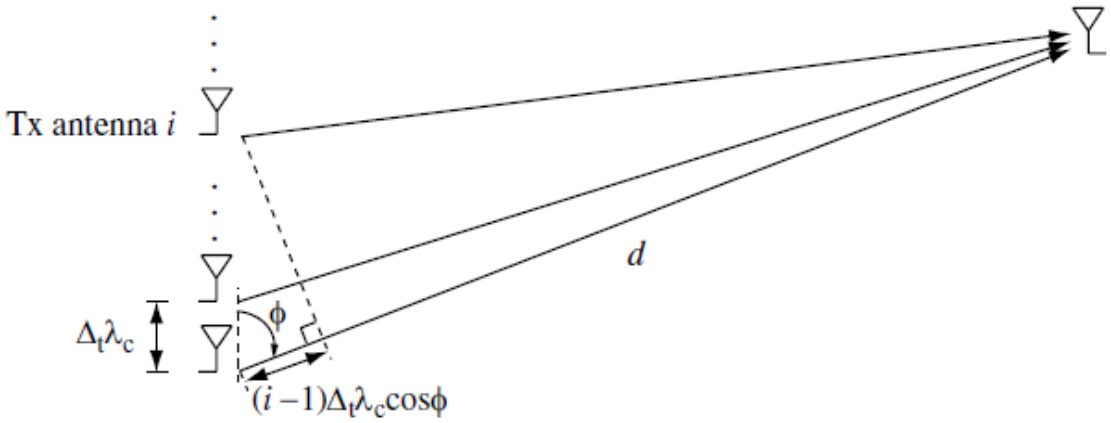

Figure 2.4: MISO Model [1]

The relative distance of each antenna uses the same equation **(2.15)** of the SIMO model. If we define the unit spatial signature in the directional cosine $(\boldsymbol{e_t(\Omega)})$, we obtain the final capacity matrix of the channel:

$$\boldsymbol{h = a\, exp\left(-\frac{j2\pi d}{\lambda_c}\right)\sqrt{n_t}\, e_t(\Omega) = a\, exp\left(-\frac{j2\pi d}{\lambda_c}\right)\begin{bmatrix} 1 \\ \vdots \\ exp(-j2\pi(n_t-1)\Delta_t\Omega) \end{bmatrix}} \qquad \textbf{(2.16)}$$

In an optimal transmission, the phase of the signal from each transmit antenna is adjusted and added constructively. The final capacity is the same that the equation of SIMO channel, but in this case it depends of the number of transmission antennas.

$$\boldsymbol{C = log_2\left(1+\frac{Pa^2 n_t}{N_0}\right)\frac{bits}{s}/Hz} \qquad \textbf{(2.17)}$$

The SIMO channel provides power gain, but no degree-freedom gain. We will study this capacity in the simulations of the developed theoretical models.

2.3.3 MIMO

Now we will consider a MIMO channel with direct line-of-sight paths between the transmission and the receiver antennas. Suppose the normalized antenna separation $\boldsymbol{\Delta_t}$ in transmission and the normalized antenna separation in reception $\boldsymbol{\Delta_r}$, we can modify the equation of the spatial signature of SIMO channel and generalize it for

multiple antennas in transmission. The result equation of the MIMO spatial signature is

$$\boldsymbol{h_{ij} = a\, exp\left(-\frac{j2\pi d_{ij}}{\lambda_c}\right)} \tag{2.18}$$

The parameters of the formula are the same as in the cases of SIMO and MISO, we continue assuming the same attenuation for all the links. $\boldsymbol{d_{ij}}$ is the distance of the transmission antenna $\boldsymbol{i}$ and the reception antenna $\boldsymbol{j}$. This distance will be the main factor for describe the change in the phase between the different elements of the arrays. We can describe this distance in terms of the parameters of the system:

$$\boldsymbol{d_{ij} = d + (i-1)\Delta_r \lambda_c \Omega_r - (k-1)\,\Delta_t \lambda_c \Omega_t} \tag{2.19}$$

Where $\boldsymbol{d}$ is the main distance between the initial components of both arrays and $\boldsymbol{\Omega_r}$, $\boldsymbol{\Omega_t}$ are the directional cosines in reception and transmission respectively. If we expand the expression **(2.20)** we obtain:

$$\boldsymbol{h_{ij} = a\, exp\left(-\frac{j2\pi d}{\lambda_c}\right) exp(j2\pi(k-1)\,\Delta_t \Omega_t)\, exp(-j2\pi(i-1)\Delta_r \Omega_r)} \tag{2.20}$$

Using the description of the unit spatial signature of SIMO and MISO channels, and the matrix properties, we can observe that the expression of the MIMO channel is a combination of the expression of SIMO and MISO, and transform the expression **(2.22)** in a combined one using the expressions of **(2.18)** and (**2.16**), obtaining:

$$\boldsymbol{H = a\, exp\left(-\frac{j2\pi d}{\lambda_c}\right)\sqrt{n_t n_r}\, e_r(\Omega_r) e_t(\Omega_t)^*} \tag{2.21}$$

The final capacity is the same that the equations of SIMO and MISO channel, but in this case it depends of the number of antennas in transmission and reception, due to the singular value of the matrix varies with them:

$$\boldsymbol{C = log\left(1 + \frac{Pa^2 n_t n_r}{N_0}\right)\frac{bits}{s}/Hz} \tag{2.22}$$

The MIMO channel provides power gain but no degree-of-freedom as the SIMO and MISO channels. Although there are multiple transmit and multiple receive antennas, the transmitted signals are all projected onto a single-dimensional space (the

only non-zero eigenmode) and thus only one spatial degree of freedom is available. The number of available spatial degrees of freedom does not increase even though there are multiple transmit and multiple receive antennas. that's the reason why only one degree of freedom is available.

2.3.4 GSTA

In previous models we have seen that they provide us power gain to our transmission but no a degree-freedom-gain. Now we will use two antennas for transmission and we will place it with a separation of the order of the distance between the transmission and the reception antennas, as we can see in the **Figure 2.5**.

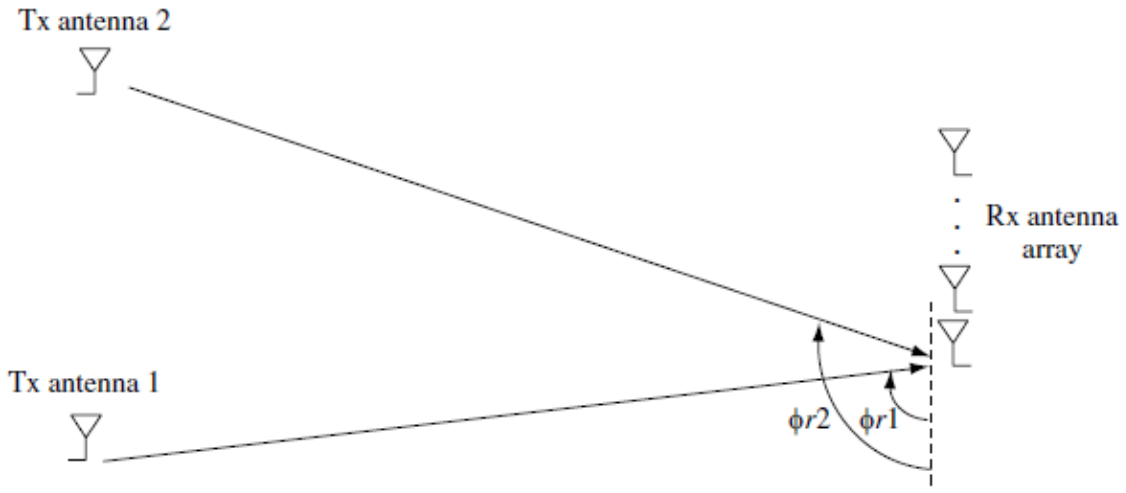

Figure 2.5: GSTA Model [1]

The channel matrix will be a composition of two SIMO modelled matrices, using the equation:

$$\boldsymbol{h_k = a_k\, exp\left(-\frac{j2\pi d_{1k}}{\lambda_c}\right)\sqrt{n_r}\, e_r(\Omega_{rk})\ ,\quad k = 1,2} \tag{2.23}$$

Due to the paths used on the transmission are too different because of the separation between the transmission antennas, the attenuations used are different. The final channel matrix will have the form

$$\boldsymbol{H = [h_1, h_2]} \tag{2.24}$$

This channel matrix have two non-zero singular values, and allows two degrees of freedom and the power gain. Now the signal can be receive in two different directions, allowing to the receive array to resolve this direction. To make this possible, and have two independent columns in the channel matrix that allows both degrees of freedom, both directional cosines lie in [−1,1] and cannot differ by more than 2 and both must be different, reducing to the simpler condition when the antenna spacing must be less than ½, $\Delta_r \leq 1/2$.

The angular separation describes how well-conditioned are the two degrees of freedom of the matrix and the possibility for use both of them effectively. This is determined by how aligned are both spatial signatures, the less aligned the better conditioning. This angle between both spatial signatures depends only of this difference:

$$\cos\boldsymbol{\theta} = \boldsymbol{f_r}(\boldsymbol{\Omega_r}) \coloneqq \boldsymbol{e_r}(\boldsymbol{\Omega_{r1}})^{*}\boldsymbol{e_r}(\boldsymbol{\Omega_{r2}}) \tag{2.25}$$

Computing the previous result, we can obtain the expression of the angle in terms of the angular separation, the normalized length of the antenna array ($\boldsymbol{L_r} := \boldsymbol{n_r}\Delta_r$) and the number of antennas.

$$|\boldsymbol{cos\,\theta}| = \left|\frac{\boldsymbol{sin}(\boldsymbol{\pi L_r \Omega_r})}{\boldsymbol{sin}(\boldsymbol{\pi L_r \Omega_r}/\boldsymbol{n_{r)}})}\right| \tag{2.26}$$

With this parameters we can define the condition number that describes if the channel matrix is ill-conditioned and only is possible to use one of the channels and when is well-conditioned and is possible the use of both levels of freedom. If this value is near to one the matrix is ill-conditioned, and is well-conditioned otherwise.

$$\frac{\boldsymbol{\lambda_1}}{\boldsymbol{\lambda_2}} = \sqrt{\frac{\boldsymbol{1} + |\boldsymbol{cos\,\theta}|}{\boldsymbol{1} - |\boldsymbol{cos\,\theta}|}} \tag{2.27}$$

The resolvability of the signals also depends of the bandwidth $\boldsymbol{B}$ and the length of the array $\boldsymbol{L_r}$. The parameter $\boldsymbol{1/B}$ measures the resolvability of signals in the time domain: multipath arriving at time separation much less of $\boldsymbol{1/B}$ cannot be resolved by the receiver. The parameter $\boldsymbol{1/L_r}$ measures the resolvability of signals in the angular domain. Signals that arrive within an angle difference much less than $\boldsymbol{1/L_r}$ cannot be resolved by the receiver.

2.3.5 GSRA

The GSTA model uses two separated antennas in transmission to achieve two degrees of freedom. Using the same concept, we can model the reception antennas in the same way, separating them a distance of the order of the distance between the transmitter and the receiver. The **Figure 2.6** describes the model.

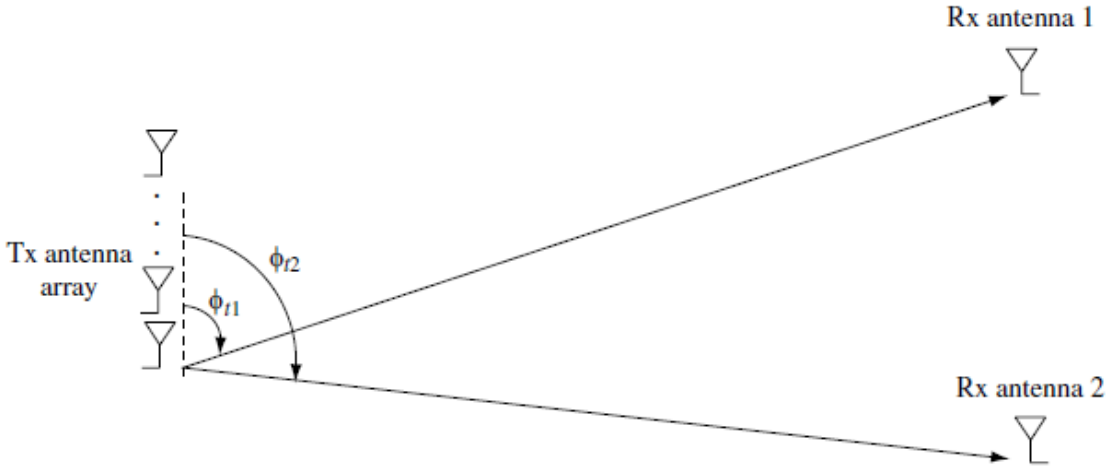

Figure 2.6: GSRA Model [1]

The channel matrix will be a composition of two MISO modelled matrixes, using the equation:

$$\boldsymbol{h_i = a_i\, exp\left(-\frac{j2\pi d_{i1}}{\lambda_c}\right)\sqrt{n_t}\, e_t(\Omega_{it})} \qquad \textbf{(2.28)}$$

Due to the paths used on the transmission are different because of the separation between the transmission antennas, the attenuations used are different. The final channel matrix will have the same form of the equation **(2.24)**. This model share with the GSRA model the two degrees of freedom due to the channel matrix have two independent columns that allows both degrees of freedom. Now the signal can be receive in two different directions, allowing to the receive array to resolve this direction. To make this possible, and have two independent columns in the channel matrix that allows both degrees of freedom, both directional cosines lie in $[-1,1]$ and cannot differ by more than 2 and both must be different, reducing to the simpler condition when the antenna spacing must be less than ½, $\Delta_r \leq 1/2$.

2.3.6 Generalization of the models

The previous theoretical models and equations are designed for simple linear arrays with the antennas placed equidistant. With this models we generalize them to be able to use them with any distribution and localization of the antennas.

In all the models we can observe that in the equations **(2.14)**, **(2.16)**, **(2.21)**, **(2.23)** and **(2.28)** the matrix channel is composed by the channel gain $\left(\boldsymbol{exp}\left(-\frac{\boldsymbol{j2\pi d}}{\boldsymbol{\lambda_c}}\right)\right)$ in the principal direction $\boldsymbol{d}$ and the unit spatial signature in the directional cosine. The unit spatial signature in the directional cosine describe the difference on the phase between the antennas in the array.

The basic formulas allows us to describe iteratively all the phase difference thanks to the regularity of the array. The general models are able to calculate all the relative distance between de antennas of the arrays in transmission and reception, and generate a matrix with all the relative distances. This matrix is processed by the algorithm adding the attenuation and the carrier frequency, obtaining the channel matrix. This development is based in the equation **(2.12)**, using directly the relative distance between each antenna instead of generalize the formulas like in the previous models.

CHAPTER 3

Models and Simulations

3.1 Introduction

In this section we will talk about the simulations and the algorithms that have been developed using the theoretical models. We will analyse the functioning of the algorithms implemented and present the simulation results that will be analysed in the next chapter.

3.2 Algorithms

The generalized theoretical models have been implement in MATLAB applying the needed modifications to be able to work with any distribution of the antennas. One of the purposes of this project is analyse if it exists any difference between the colocation of the antennas in the transmission and reception arrays and the direct consequences in the total capacity of the systems.

The algorithms use two independent systems of Cartesian coordinates to describe the exactly position of the antennas in transmission and reception, and another one that contains both arrays of antennas. The algorithm use the origin of the coordinate system that is used to describe the antennas in transmission as the origin of the whole system of the common system of coordinates. It uses the general distance $\boldsymbol{d}$, that describes the separation between the antennas that are in the same point as the origin of both system of coordinates, to recalculate the position of the reception antennas to the origin of the transmission coordinate system, obtaining as result of it the position of all the antennas in the general system of coordinates.

With that processed information it is easy to obtain all the relative distances between the transmission and reception antennas and calculate the changes in the phase. The algorithm also includes an angular correction that allows to turn the antennas in transmission and reception a certain amount of degrees, using the rotation matrix:

$$\boldsymbol{R(\theta)} = \begin{bmatrix} \boldsymbol{\cos\theta} & \boldsymbol{-\sin\theta} & \boldsymbol{0} \\ \boldsymbol{\sin\theta} & \boldsymbol{\cos\theta} & \boldsymbol{0} \\ \boldsymbol{0} & \boldsymbol{0} & \boldsymbol{1} \end{bmatrix} \quad \textbf{(3.1)}$$

The algorithm allows as input all the parameters that are needed for the model, being possible to adjust the simulation to our needs. In our simulations we will use a carrier frequency that belongs to the UHF (ultra-high frequency, 300 MHz – 3 GHz) and SHF (super high frequency, 3 GHz – 30 GHz) bands, that are the more uses to mobile communications nowadays using frequency around the GHz (Gigahertz). We also can adjust the used bandwidth in the communications, and we will place it in a value of 10 MHz, as a normal value that we can find in normal communications.

In the next sections is more detailed the models used for the attenuation factor of the channel and the model used for the noise and the transmitted powers.

3.2.1 SNR and Noise

To have realistic simulations, we must choose values for the transmission power that can be achievable in the real life systems. For that reason, the simulations will use as transmission powers the values of 10, 20, 30 and 40 dBm, that represent a range of values between 10 mW to 10 W of power, that can be found in systems like GSM (Global System mobile communications), UMTS (Universal mobile telecommunications system) or 3G (third generation) mobile communications

We also need a noise model to calculate the final capacity and complete the simulations. For that we will use the value of -174 dBm/Hz that represents the thermal noise power for a bandwidth of 1 Hz at room temperature (23ºC approx.). This value will be multiplied to our bandwidth of 10 MHz, obtaining a value for the noise of -104 dBm of noise power ($4*10^{-14}$ Watts approx.).

3.2.2 Attenuation

To fulfil our simulation models, we must enter a model for the attenuation channel to complete the channel matrix. A lot of different models exists, but we will use microcell LOS (line of sight) pathloss is based on the COST 231 Walfish - Ikegami street canyon model with the same parameters as in the NLOS (non-line of sight) case. The distance $\boldsymbol{d}$ is at least 20m, with $\boldsymbol{d}$ measure in metres and $\boldsymbol{f}$ measure in MHz.

$$\boldsymbol{PL(dB) = -35.4 + 26log_{10}(d) + 20log_{10}(f)} \quad \textbf{(3.2)}$$

This model is used for urban microcells, with a distance of less than 1km distance BS (Base station) to BS, and depends also of the carrier frequency, adapting itself different situations. This models is the one that is the more accurate for nowadays general models. Also, the Walfish – Ikegami model is more accurate and complex than other models. This model allows estimations of 20 metres.

3.3 Implemented antennas

This section describes different models of distribution of the antennas in the transmission and reception arrays. Five different algorithms have been implemented to create different arrays to test the simulations and try to discover if it exists any difference in the capacity of the channel if the position of this antennas changes.

The algorithms that creates the distribution of the antennas use as input the number of antennas that will compose the array and the approx. separation between the elements. The separation will depends of the wavelength of the carrier frequency, using a separation of ***wavelength/2***. As the value of the carrier frequency used is around the GHz, the separation between antennas will have a value of tens of centimetres.

3.3.1 Array

The linear array distribution is exactly the same that is use in the simplified version of the models, but with this algorithm we can use it too with the general models. Using the number of antennas $\boldsymbol{N}$ (if the array is placed in transmission $\boldsymbol{N = n_t}$, if its placed in reception $\boldsymbol{N = n_r}$) and the separation between elements $\boldsymbol{S}$ it's possible to locate the elements in the right coordinates with just the use of a loop.

The results obtained in the simple models and the general models (**Figure 3.1**) using this linear array with the same parameters are practically identical, with a little margin of error.

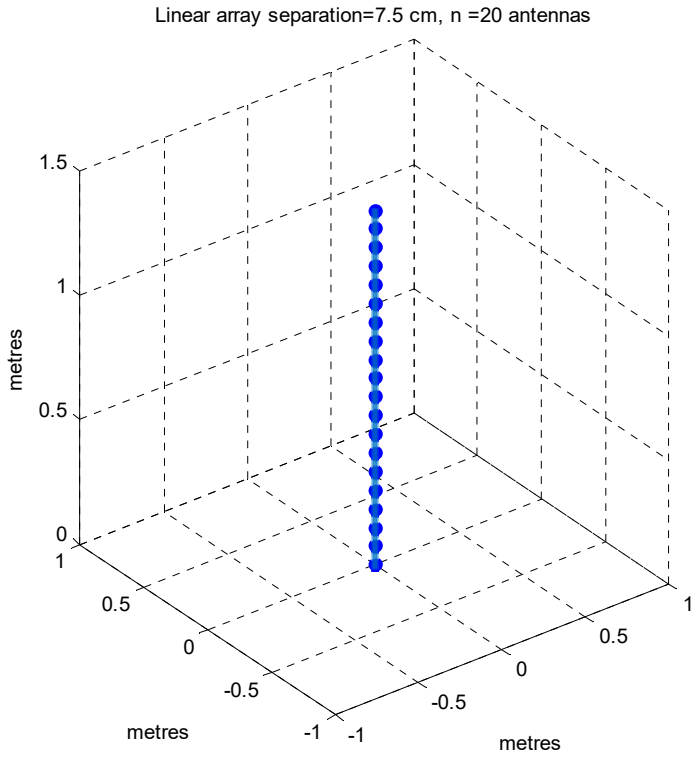

Figure 3.1: Linear array

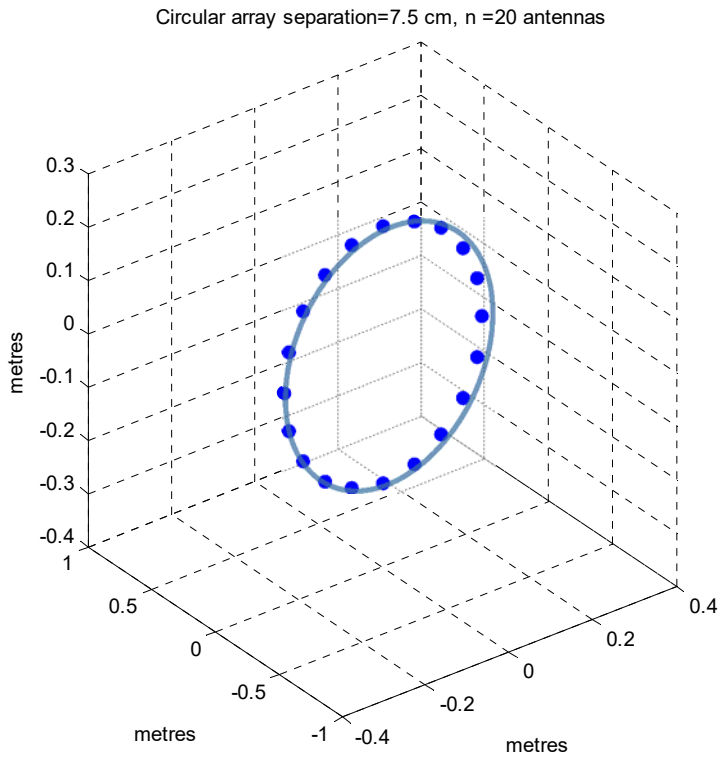

Figure 3.2: Circular array

3.3.2 Circle

The algorithm creates an array that contains ***N*** antennas separated by a distance of ***S***. To locate the elements, the algorithm multiplies the number of antennas and the separation to calculate the longitude of the circumference. With this value, we can calculate the radius of the circumference, and with the number of antennas we can calculate the angle separation between antennas.

With this two values it is easy to locate all the elements one by one increment the angle until we reach the whole circumference (**Figure 3.2**).

3.3.3 Square

The square algorithm creates an array that contains ***N*** antennas separated by a distance of ***S***. To locate the elements, the algorithm multiplies the number of antennas and the separation to calculate the longitude of the square, the same method that is used in the circumference array. With the longitude, we can calculate the measure of the sides of the square and the position of the four edges.

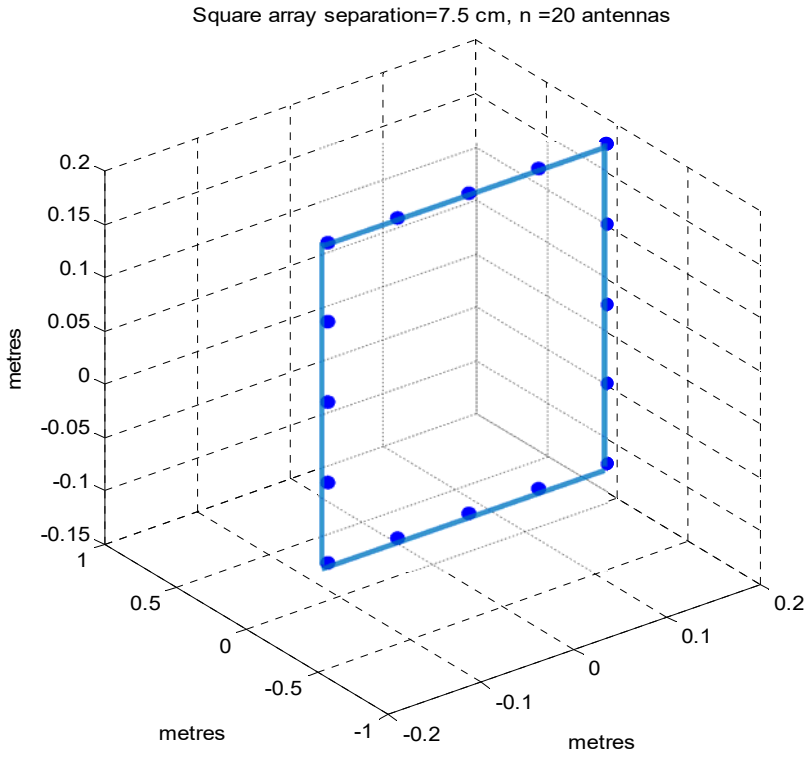

Figure 3.3: Square array

To locate the antennas, the algorithm starts in one of the edges and moves in one of the four directions (depends of the initial edge, but the movement is clockwise), and locate a new antenna. Before placing the antenna, it is checked if the total longitude of the antennas located in the side is bigger than the side of the square. If it´s bigger, the algorithm changes the direction and places the antenna in the next side (**Figure 3.3**).

3.3.4 Concentric Squares

We will locate the antennas creating an array composed by concentrically squares. The method to create it is the same that in the square case, but the first four antennas will be placed directly in the edges of the square, and the rest of them will form squares with the same centre as the original one, but increasing the value of the side of the original side by the same factor as the number of the square. If the number of antennas is not dividable by four, the last concentric square will be incomplete (**Figure 3.4**).

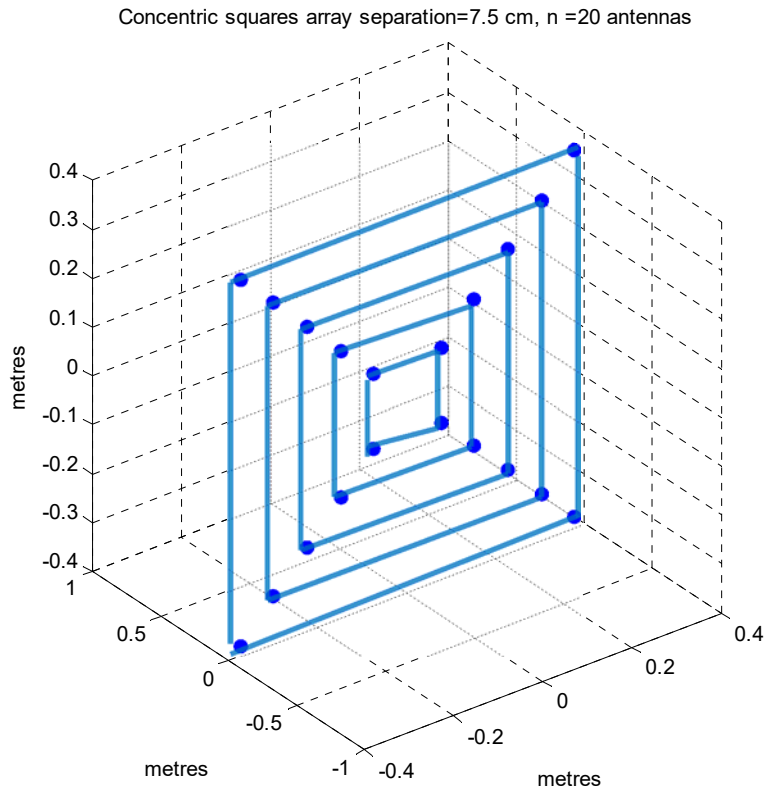

Figure 3.4: Concentric squares array

3.3.5 Cubical antenna

Finally, we will try with a three dimensional antenna instead of the antennas that have been implanted previously. For that purpose, we will use a cube that is implemented by twenty seven antennas, nine in each side and a central one, that we will locate in the centre of our coordinates system. To create the cube we will locate the twenty seven antennas with loop and then move the resultant cube to locate the centre of the cube in the origin of the coordinates system (**Figure 3.5**).

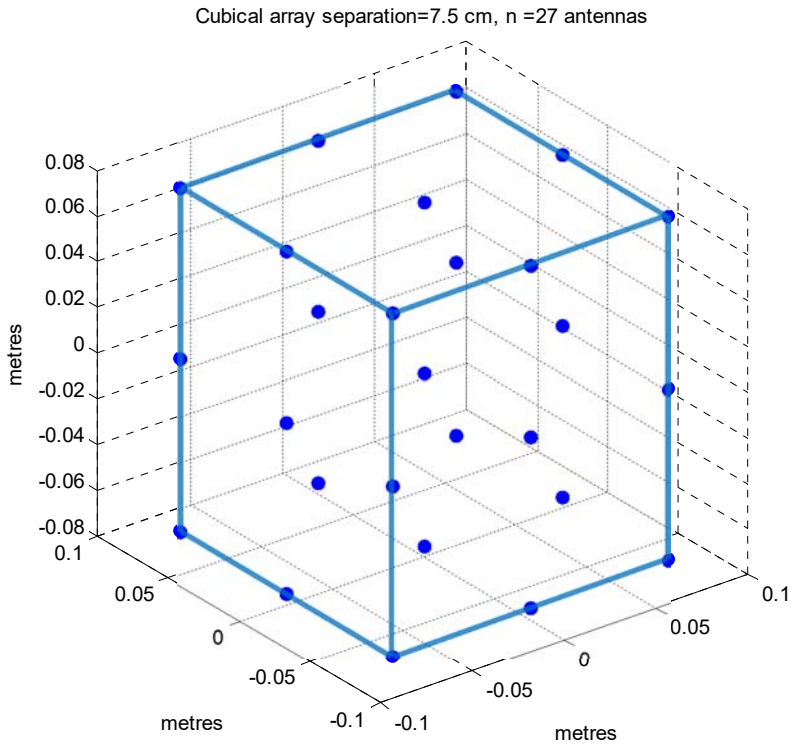

Figure 3.5: Cubical array

3.4 Simulations

This section contains the main simulations results that have been obtained with the implemented models variating the types of the distribution of the antennas to check the resulting capacities.

3.4.1 SIMO

The algorithms are simulated to obtain the final capacity of the systems with the SIMO general models, alternating the distribution of the antennas in reception and using as parameters the next values:

- ***Carrier frequency (f_c):*** 2 GHz
- ***Number of antennas in reception (n_r):*** 20 antennas or 27 antennas
- ***Bandwidth (B):*** 10 MHz
- ***Separation between reception antennas ($\Delta_r \lambda_c$):*** 7.5 cm (λ/2)
- ***Angle of incidence (∅): $\pi/2$***
- ***Transmitted power (P):*** 10, 20, 30 and 40 dBm
- ***Noise power (N_0):*** -104 dBm (-174 dBm/Hz)

In the next graphs **(Figure 3.6 to Figure 3.15)** are described the spatial distribution that have been used for the antennas and the resulting capacities. In the capacity graphs it has been selected one point at 800 metres to have a more detailed information about the exact capacity of the system to see easily the differences.

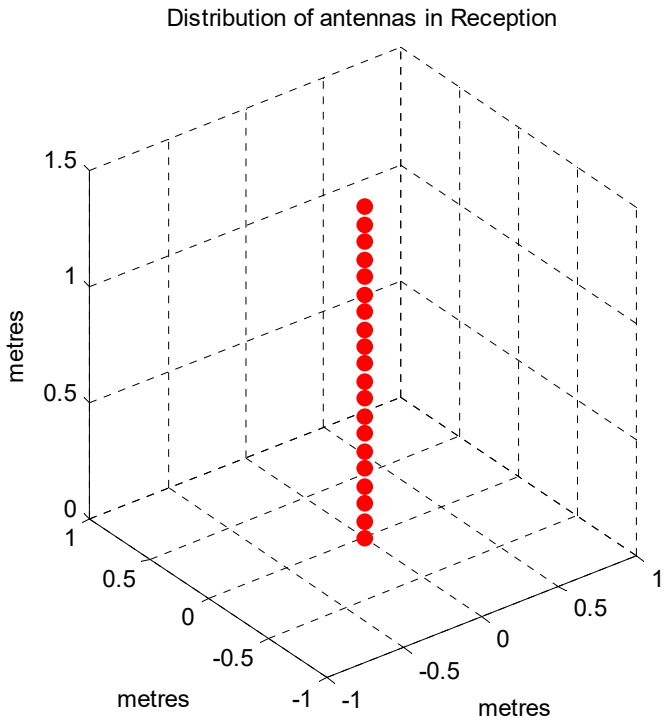

Figure 3.6: SIMO Linear array at reception N_r=20

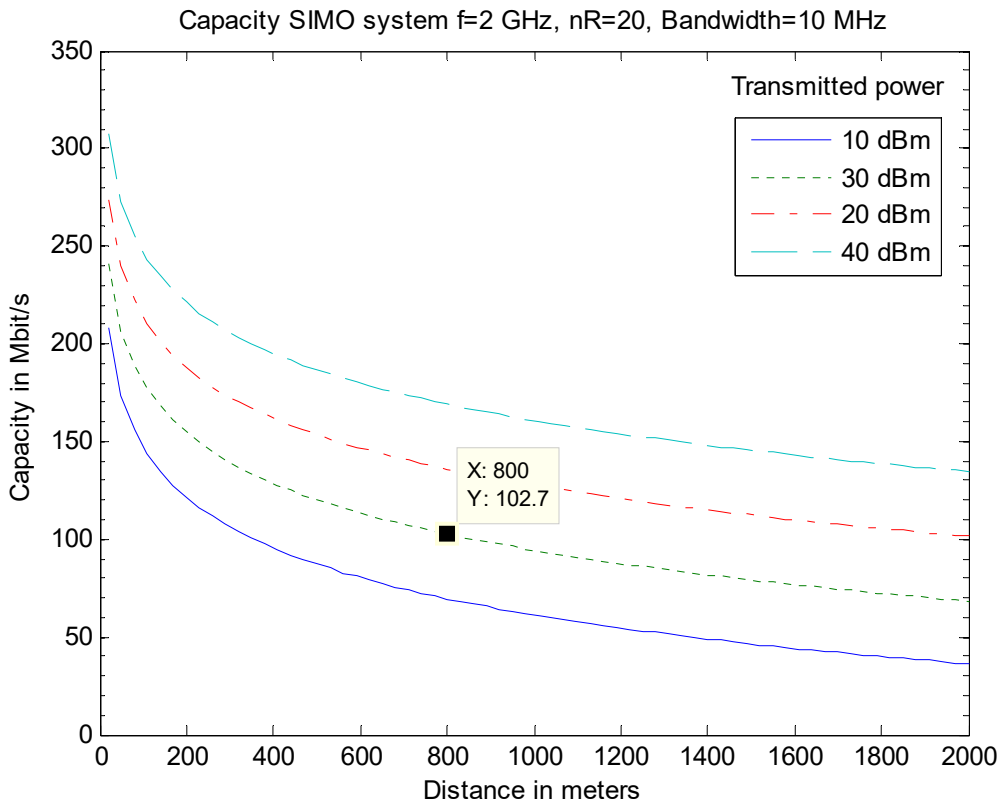

Figure 3.7: Capacity of SIMO Linear array N_r=20

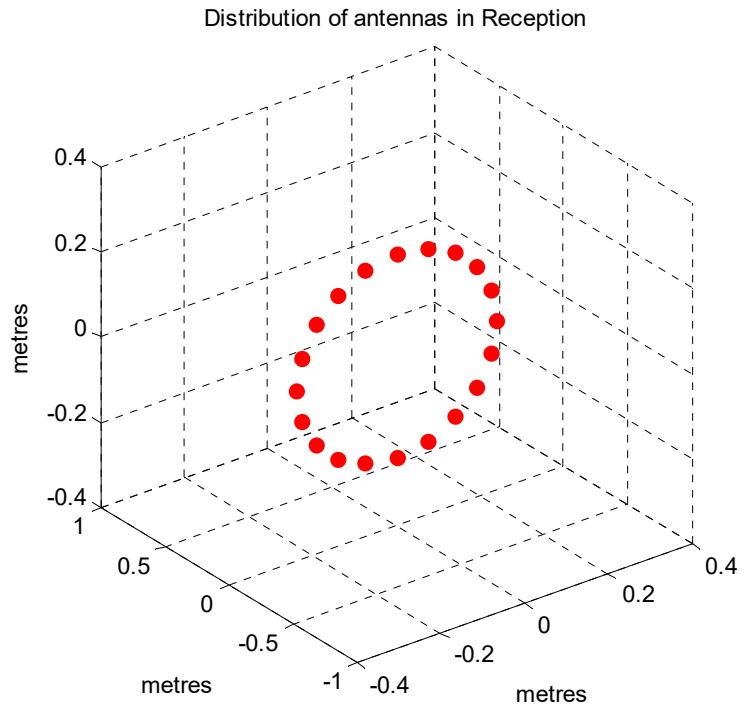

Figure 3.8: SIMO Circular array at reception N_r=20

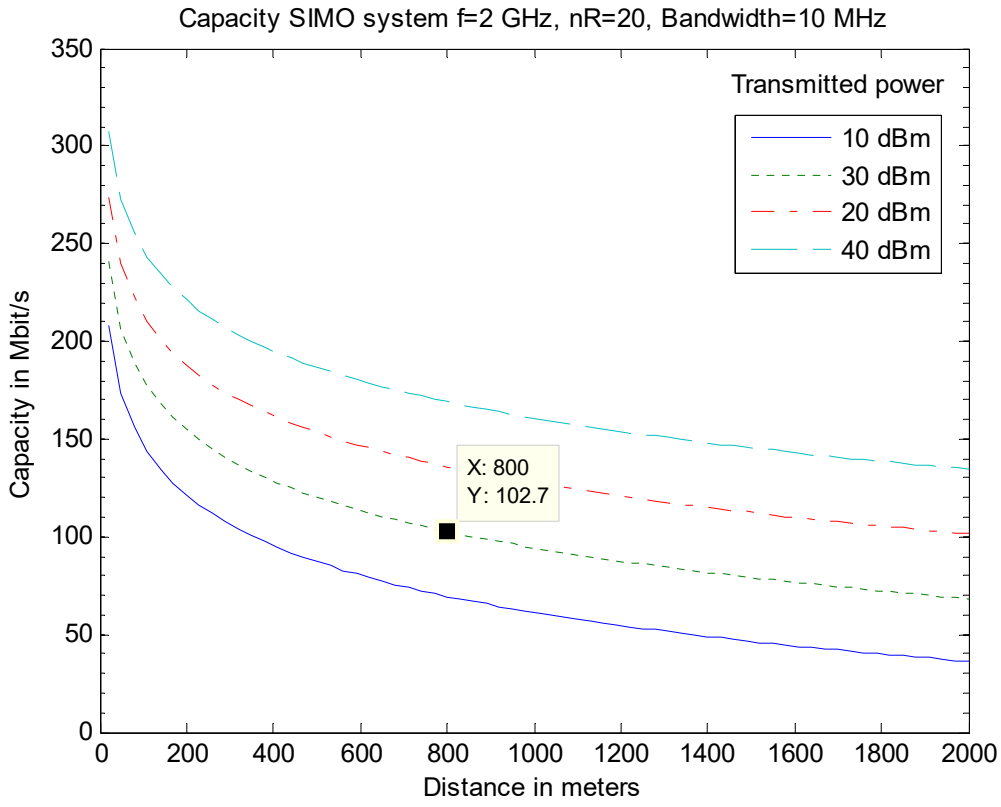

Figure 3.9: Capacity of SIMO Circular array N_r=20

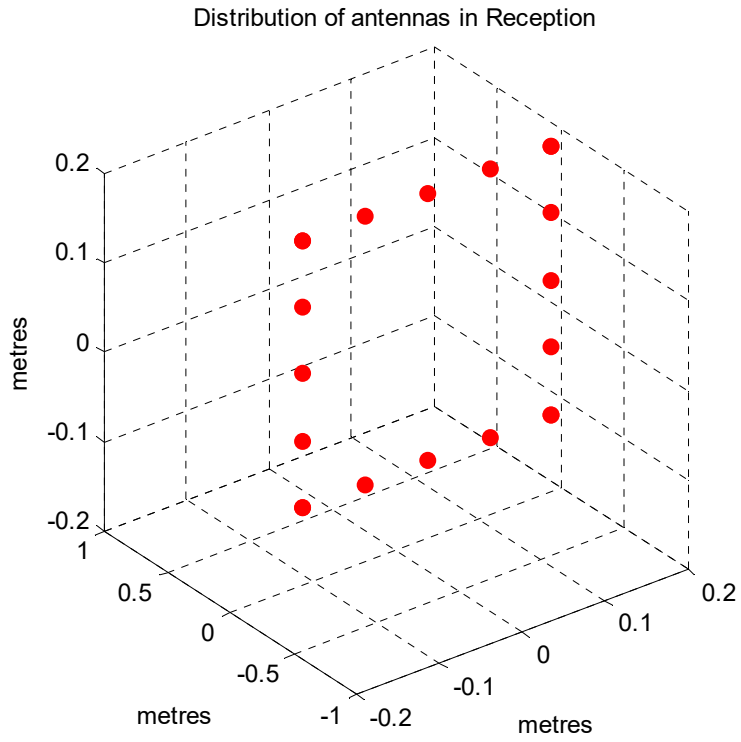

Figure 3.10: SIMO Square array at reception N_r=20

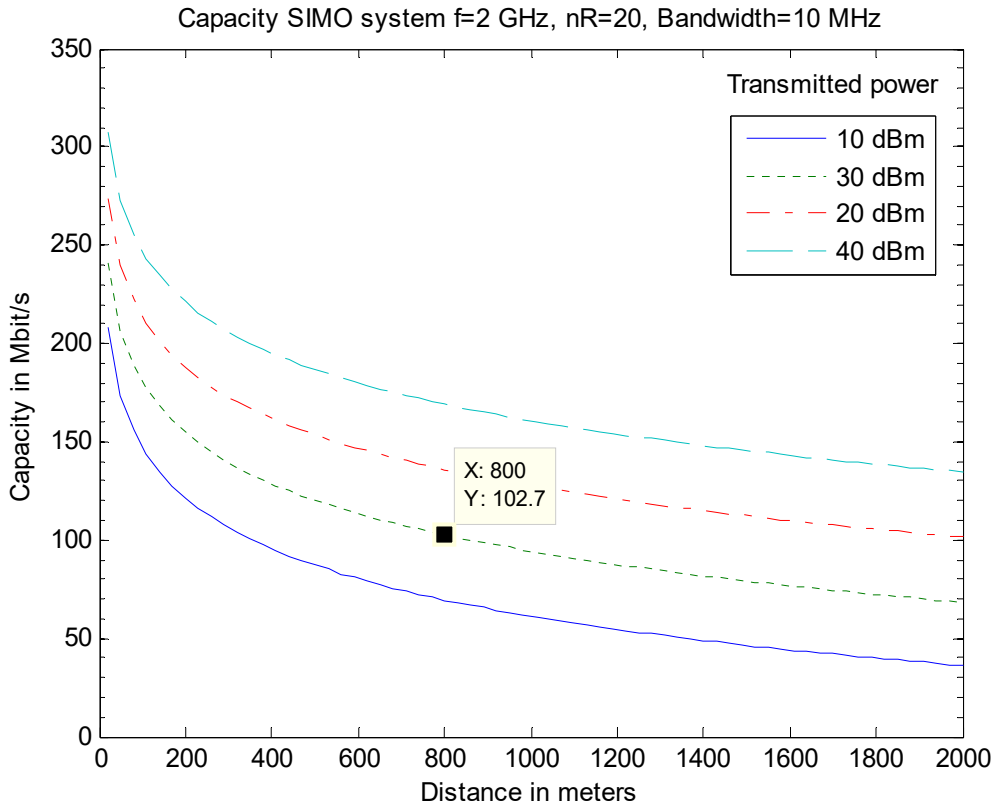

Figure 3.11: Capacity of SIMO square array N_r=20

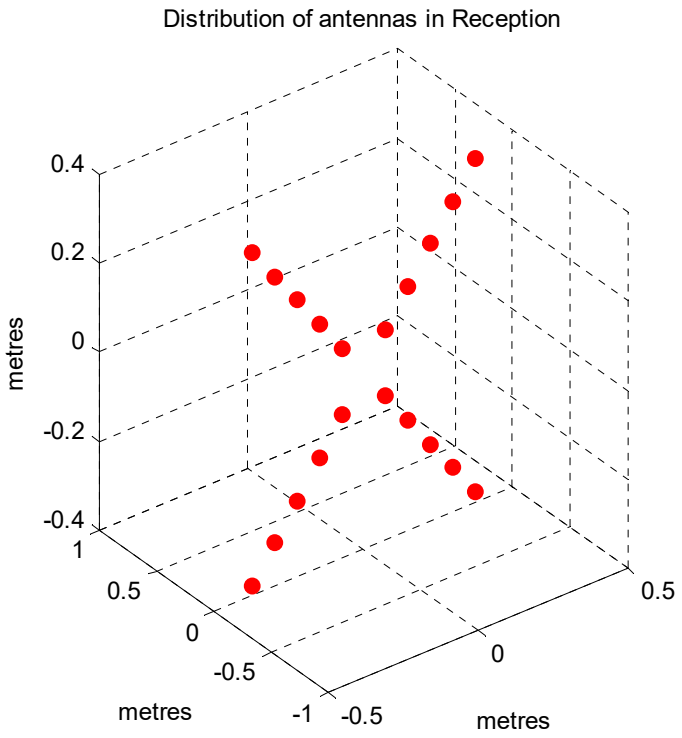

Figure 3.12: SIMO C. Squares array at reception N_r=20

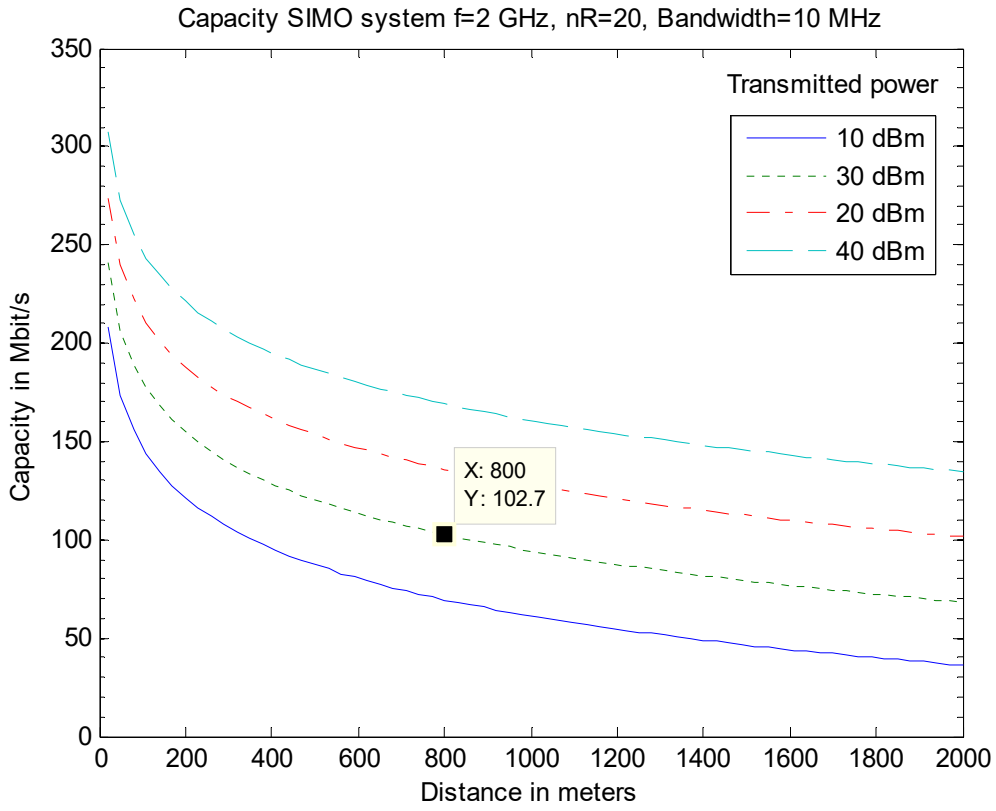

Figure 3.13: Capacity of SIMO C. Squares array N_r=20

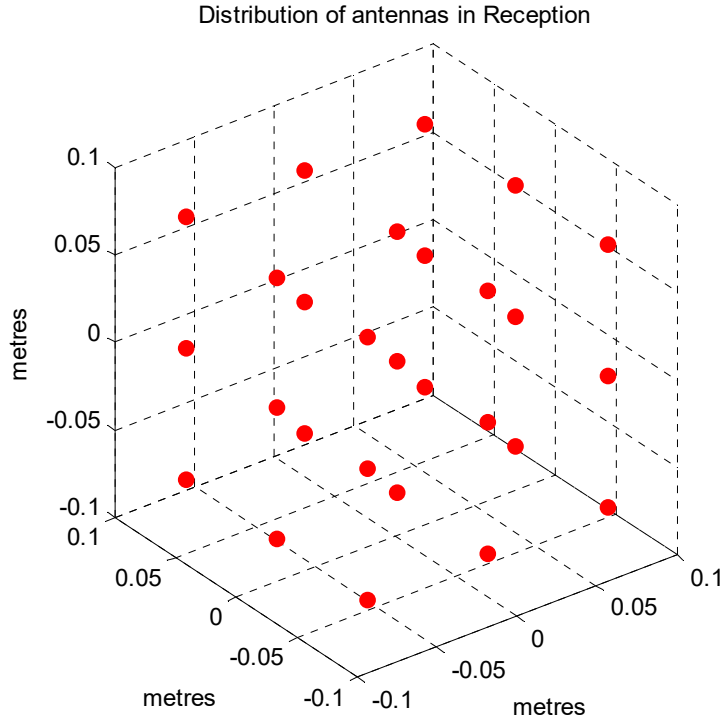

Figure 3.14: SIMO Cubical array at reception N_r=27

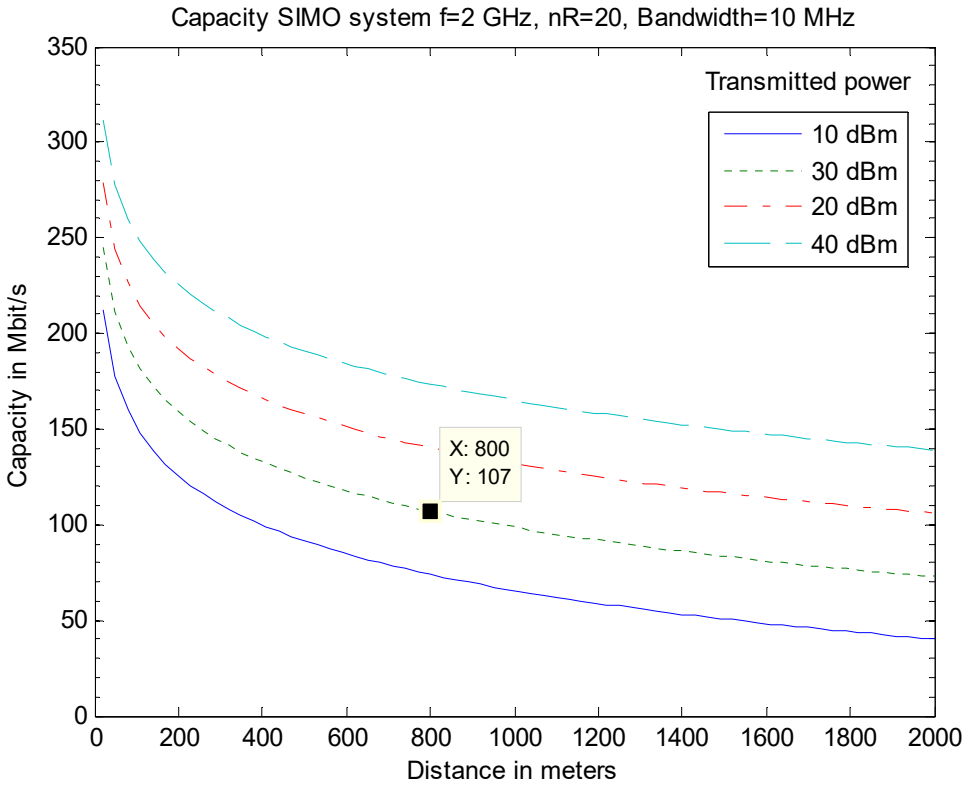

Figure 3.15: Capacity of SIMO Cubical array N_r=27

3.4.2 MISO

The algorithms are simulated to obtain the capacity of the systems with the MISO general models, alternating the distribution of the antennas in reception and using as parameters the next values:

- ***Carrier frequency (f_c):*** 2 GHz
- ***Number of antennas in transmisson (n_t):*** 20 antennas or 27 antennas
- ***Bandwidth (B):*** 10 MHz
- ***Separation between transmission antennas ($\Delta_t \lambda_c$):*** 7.5 cm (λ/2)
- ***Angle of incidence (∅): $\pi/2$***
- ***Transmitted power (P):*** 10, 20, 30 and 40 dBm
- ***Noise power (N_0):*** -104 dBm (-174 dBm/Hz)

In the next graphs **(Figure 3.16 to Figure 3.25)** are described the spatial distribution that have been used for the antennas and the resulting capacities. In the capacity graphs it has been selected one point at 800 metres to have a more detailed information about the exact capacity of the system to see easily the differences.

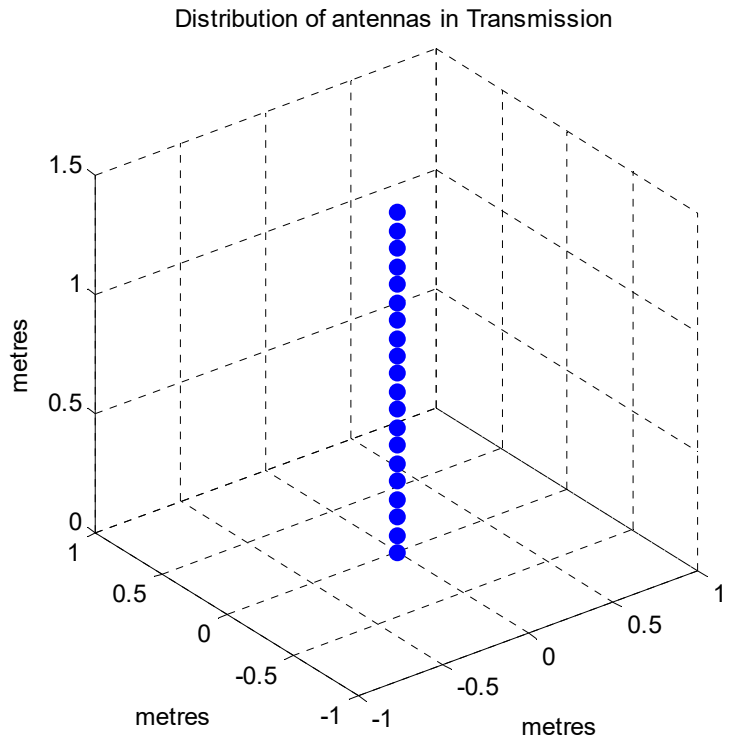

Figure 3.16: MISO Linear array at transmission N_t=20

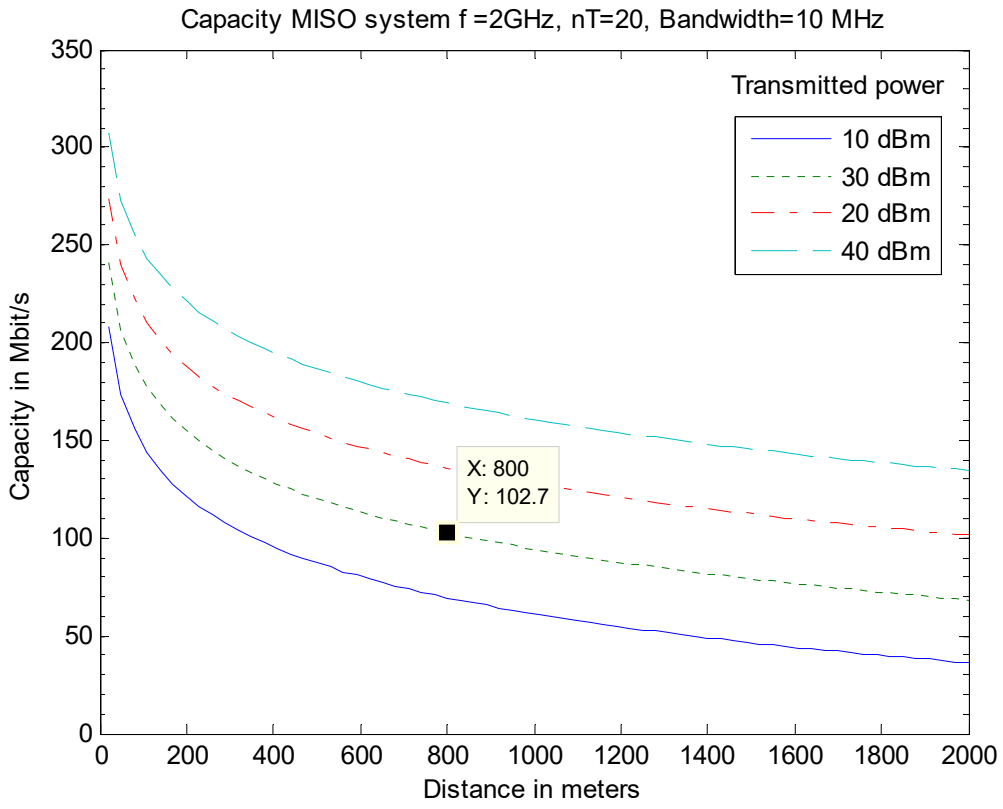

Figure 3.17: Capacity of MISO Linear array N_t=20

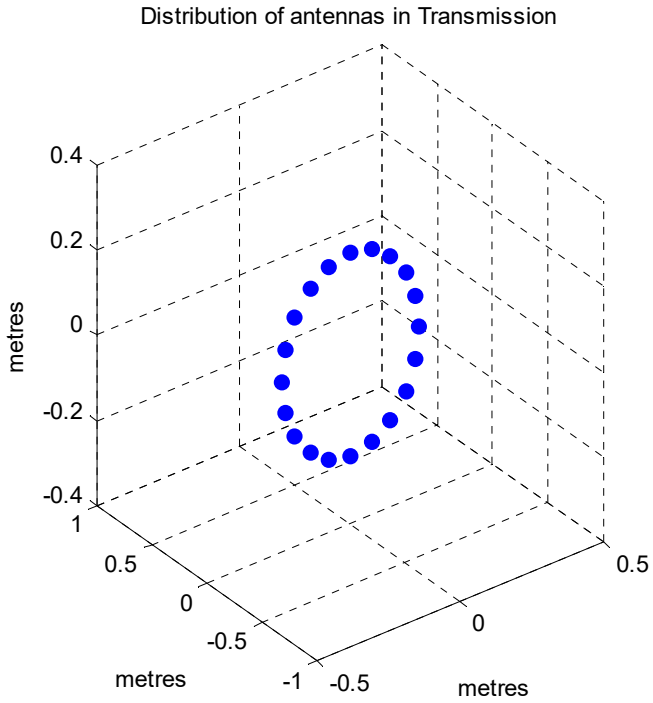

Figure 3.18: MISO Circular array at transmission N_t=20

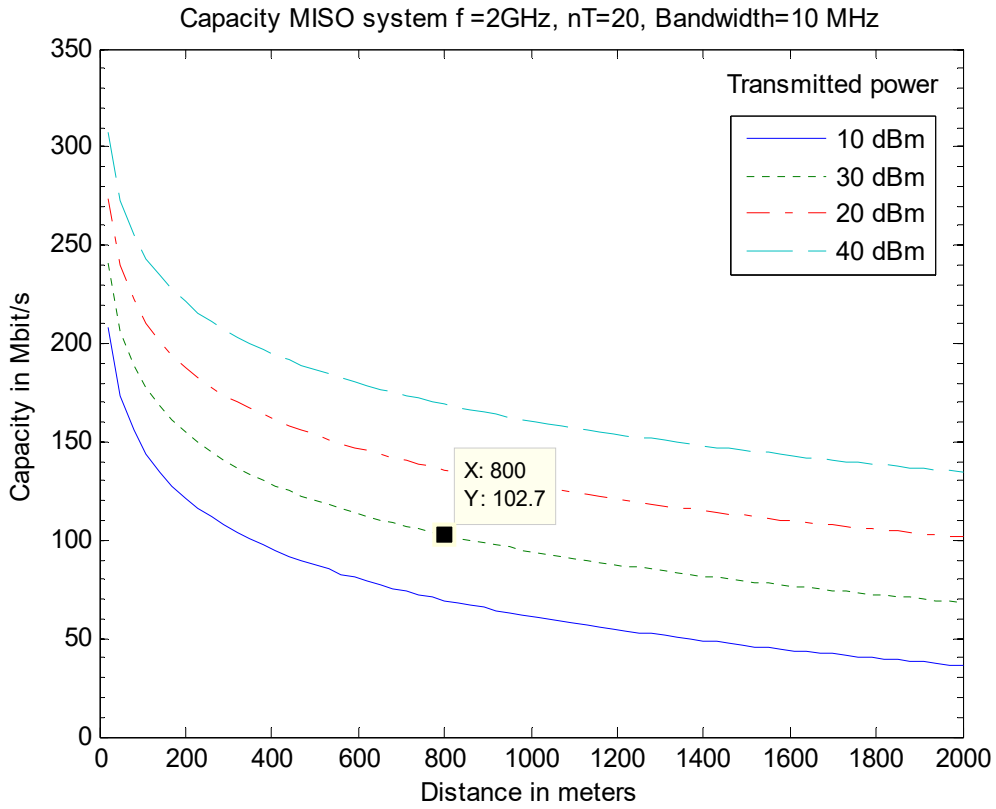

Figure 3.19: Capacity of MISO Circular array N_t=20

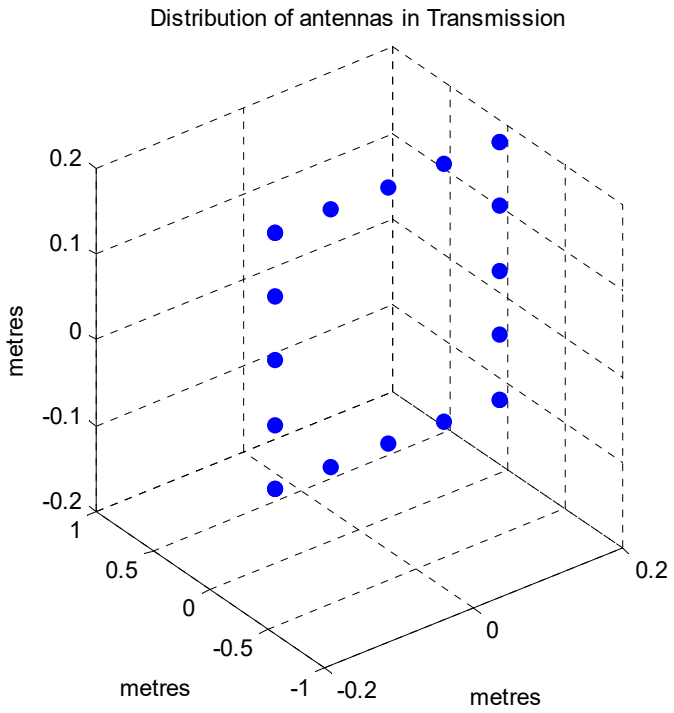

Figure 3.20: MISO Square array at transmission N_t=20

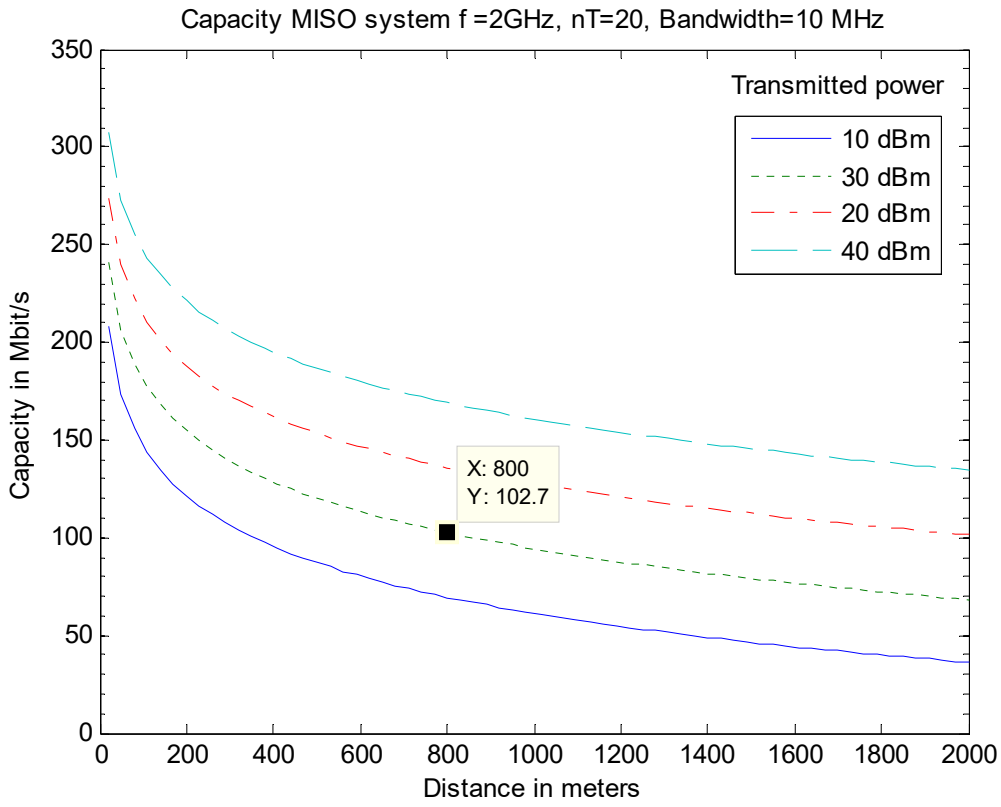

Figure 3.21: Capacity of MISO Squares array N_t=20

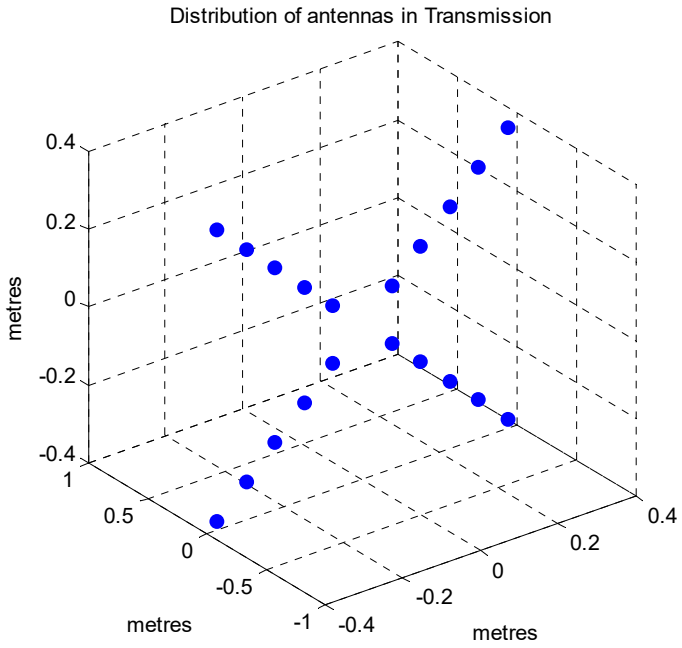

Figure 3.22: MISO C. Squares array at transmission N_t=20

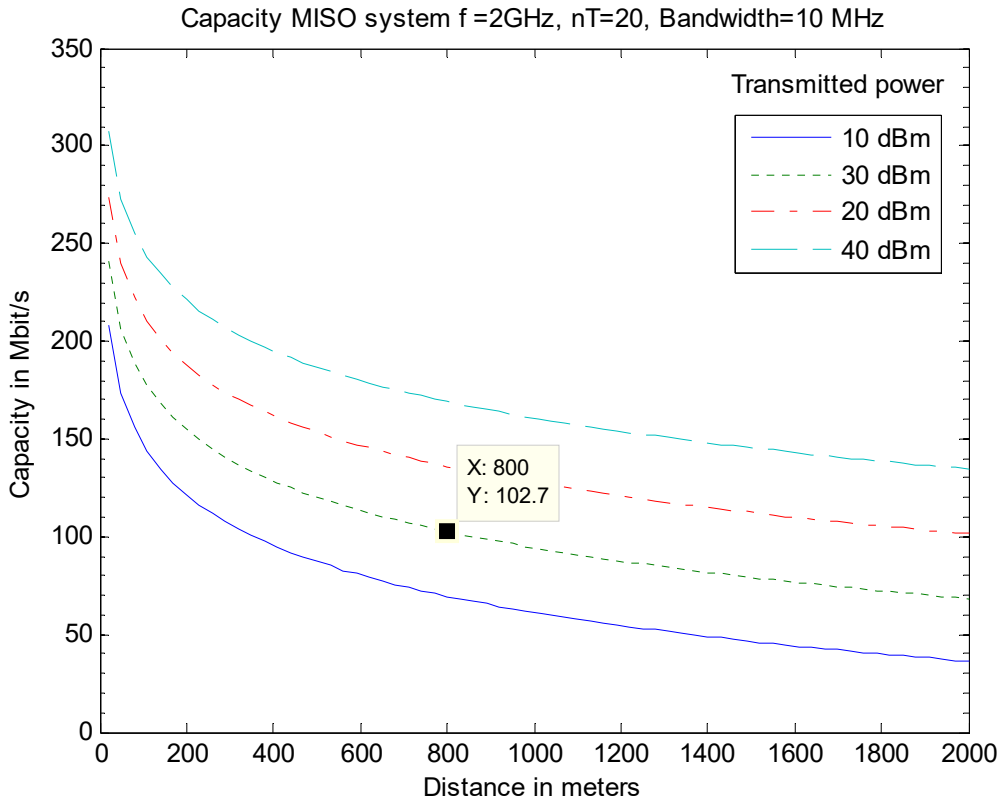

Figure 3.23: Capacity of MISO C. Squares array N_t=20

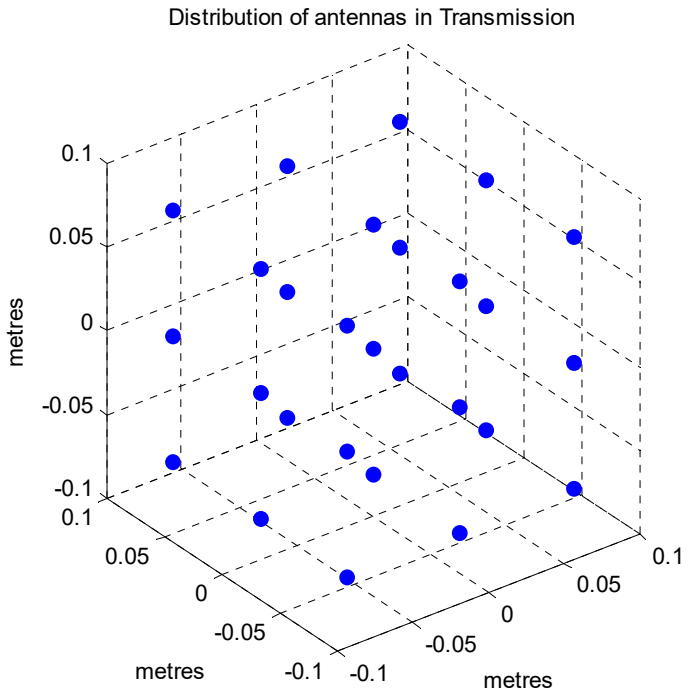

Figure 3.24: MISO Cubical array at transmission N_t=27

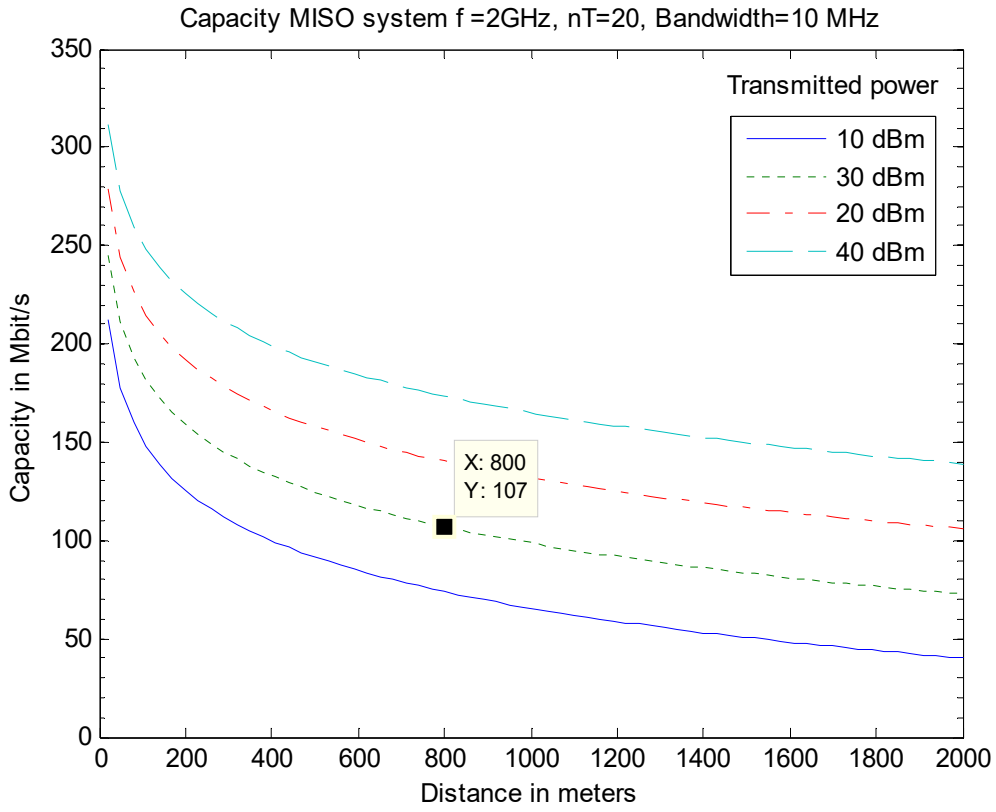

Figure 3.25: Capacity of MISO Cubical array N_t=27

3.4.3 MIMO

The algorithms are simulated to obtain the capacity of the systems with the MIMO general models, alternating the distribution of the antennas in reception and using as parameters the next values:

- ***Carrier frequency (f_c):*** 2 GHz
- ***Number of antennas in reception (n_r):*** 20 antennas or 27 antennas
- ***Number of antennas in transmission (n_t):*** 20 antennas or 27 antennas
- ***Bandwidth (B):*** 10 MHz
- ***Separation between reception antennas ($\Delta_r \lambda_c$):*** 7.5 cm (λ/2)
- ***Separation between transmission antennas ($\Delta_t \lambda_c$):*** 7.5 cm (λ/2)
- ***Angle of incidence (∅): $\pi/2$***
- ***Transmitted power (P):*** 10, 20, 30 and 40 dBm
- ***Noise power (N_0):*** -104 dBm (-174 dBm/Hz)

In the next graphs **(Figure 3.26 to Figure 3.39)** are described the spatial distribution that have been used for the antennas and the resulting capacities. In the capacity graphs it has been selected one point at 800 metres to have a more detailed information about the exact capacity of the system to see easily the differences.

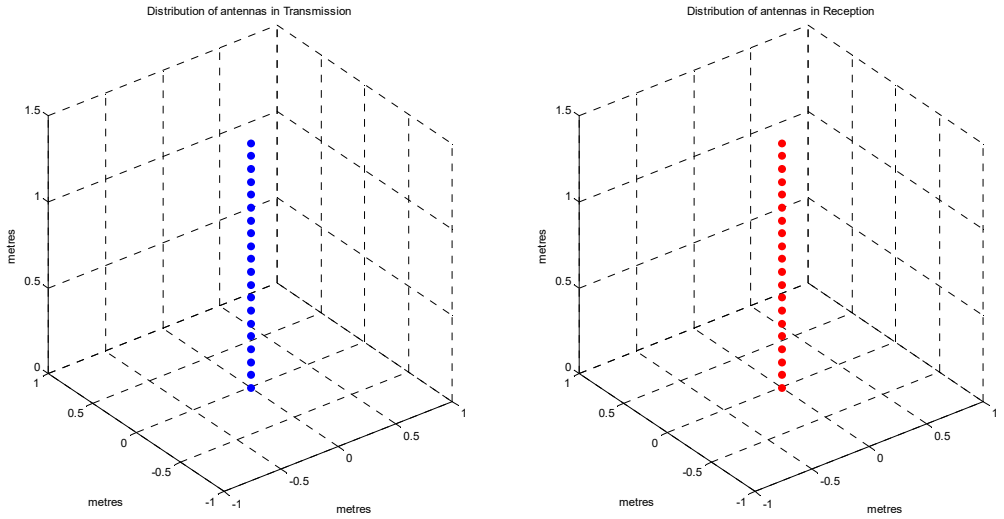

Figure 3.26: MIMO Linear array at transmission N_t=20 and Linear array at reception N_r =20

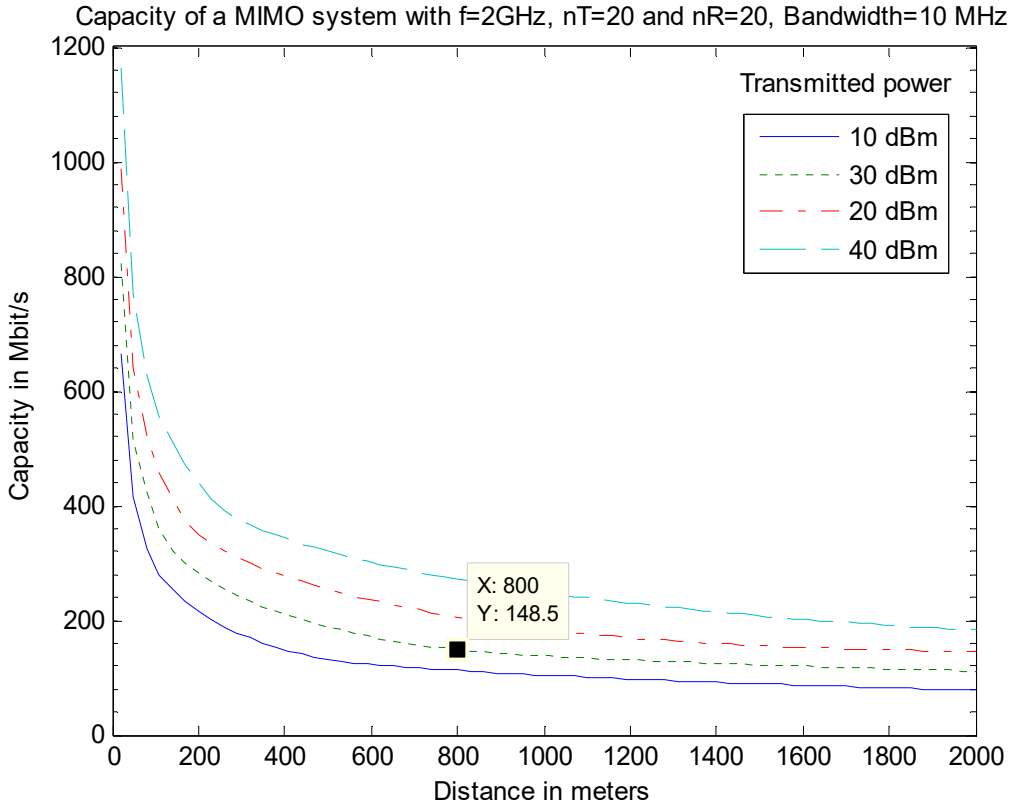

Figure 3.27: Capacity of MIMO Linear array N_t=20 and Linear array N_r=20

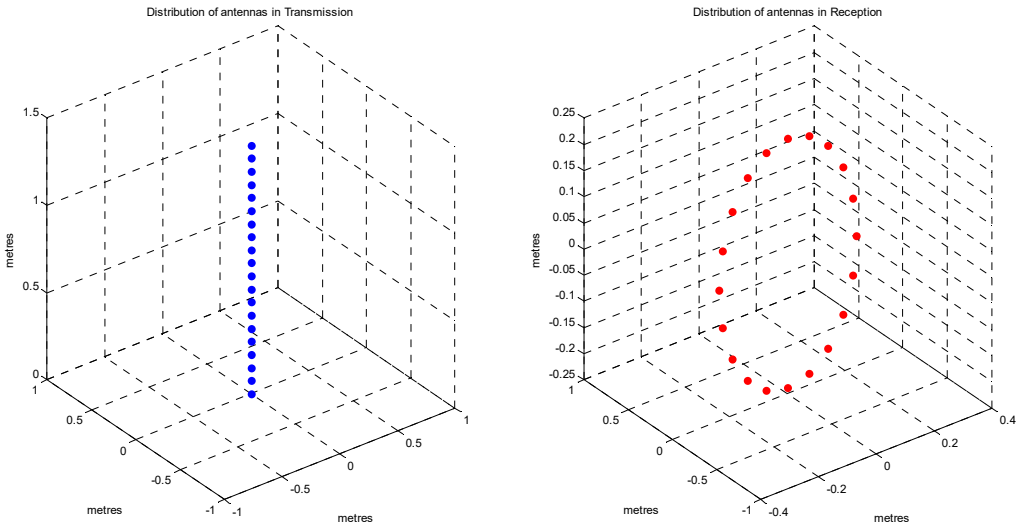

Figure 3.28: MIMO Linear array at transmission N_t=20 and Circular array at reception N_r =20

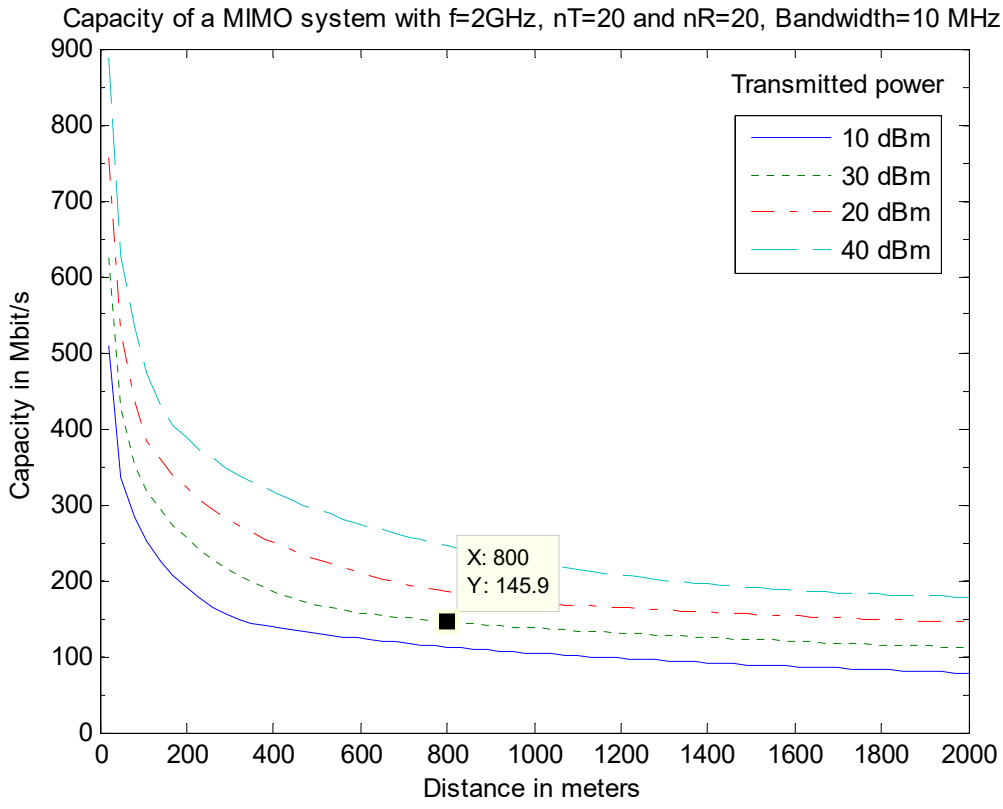

Figure 3.29: Capacity of MIMO Linear array N_t=20 and Circular array N_r=20

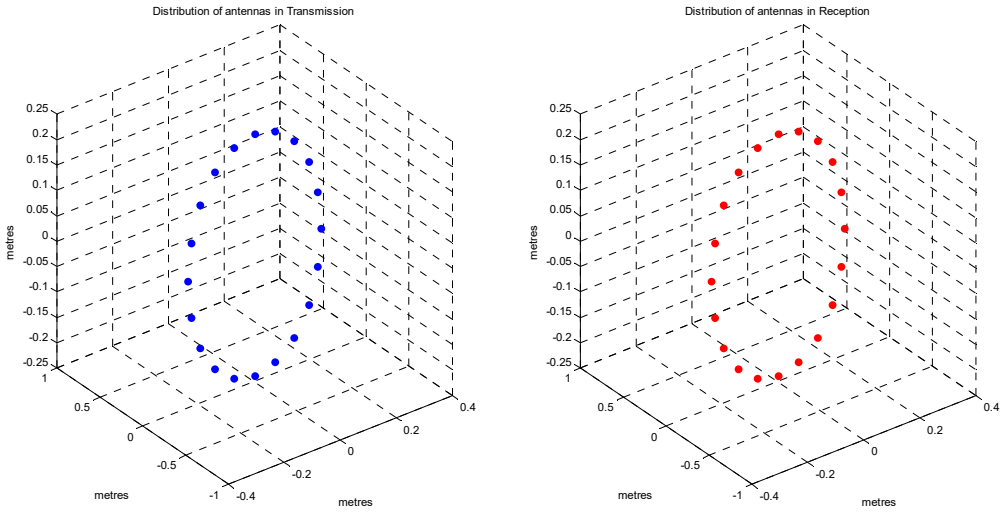

Figure 3.30: MIMO Circular array at transmission N_t=27 and Circular array at reception N_r =27

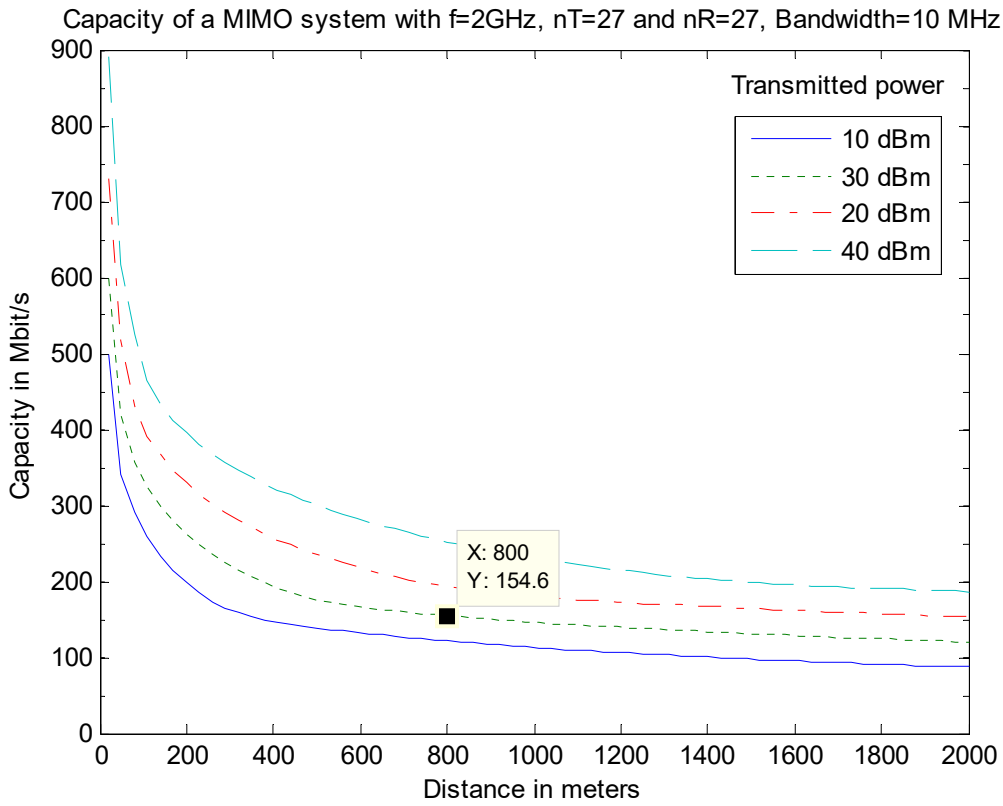

Figure 3.31 Capacity of MIMO Circular array N_t=27 and Circular array N_r=27

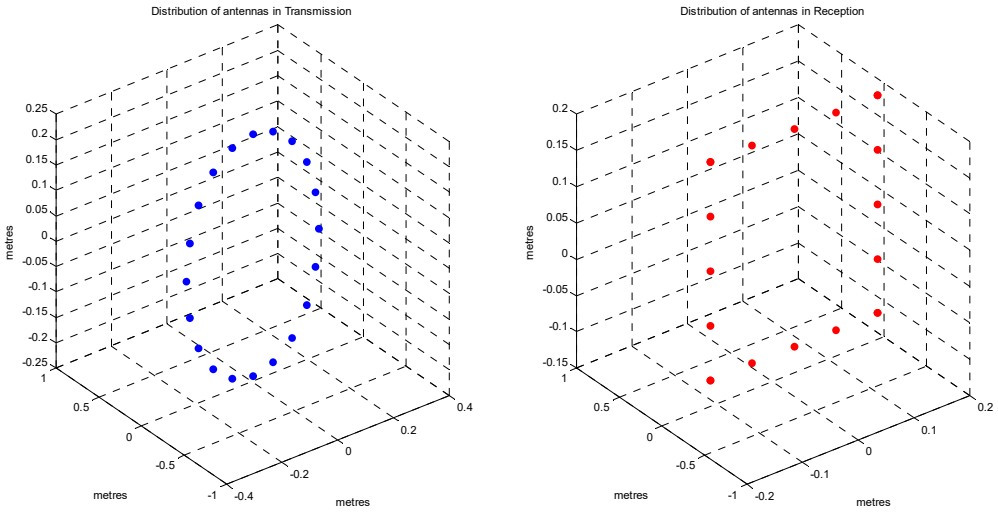

Figure 3.32: MIMO Circular array at transmission N_t=27 and Square array at reception N_r =27

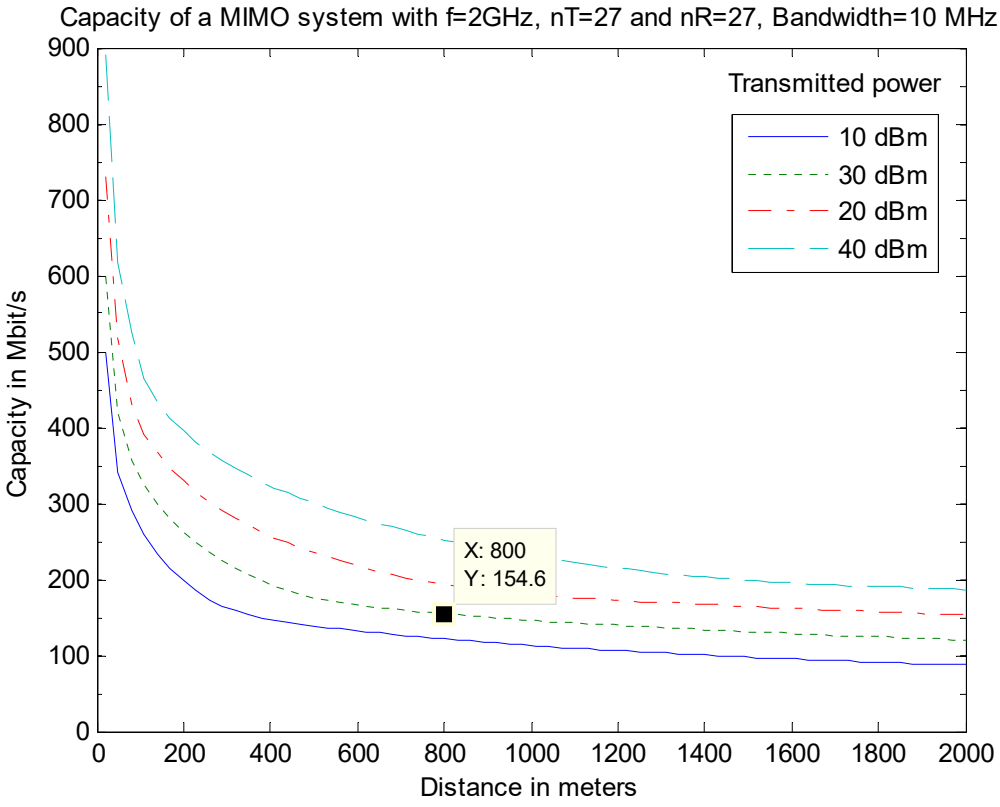

Figure 3.33: Capacity of MIMO Circular array N_t=27 and Square array N_r=27

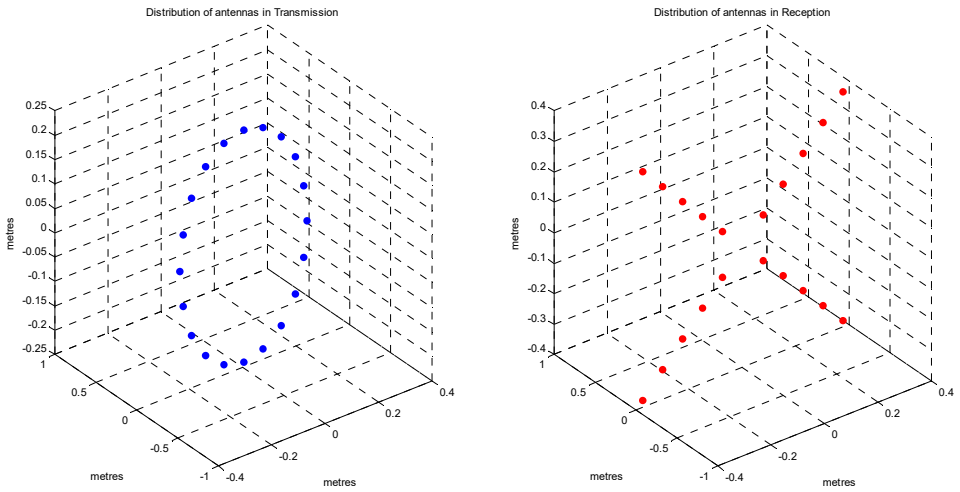

Figure 3.34: MIMO Circular array at transmission N_t=27 and C. Squares array at reception N_r =27

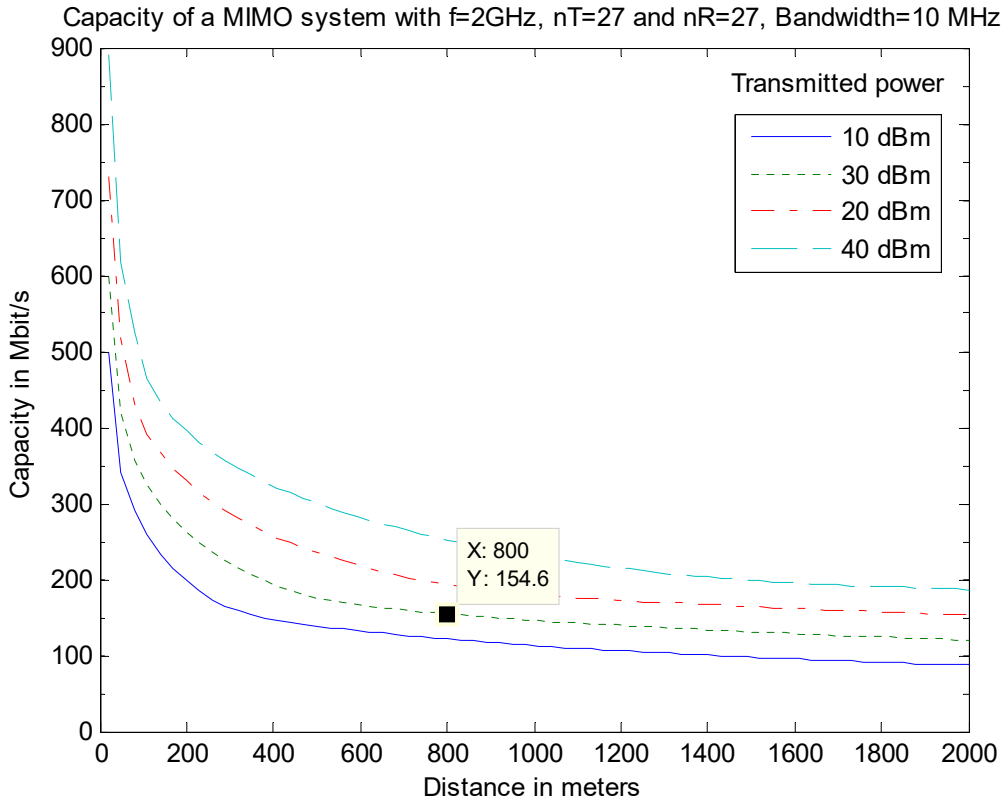

Figure 3.35: Capacity of MIMO Circular array N_t=27 and C. Squares array N_r=27

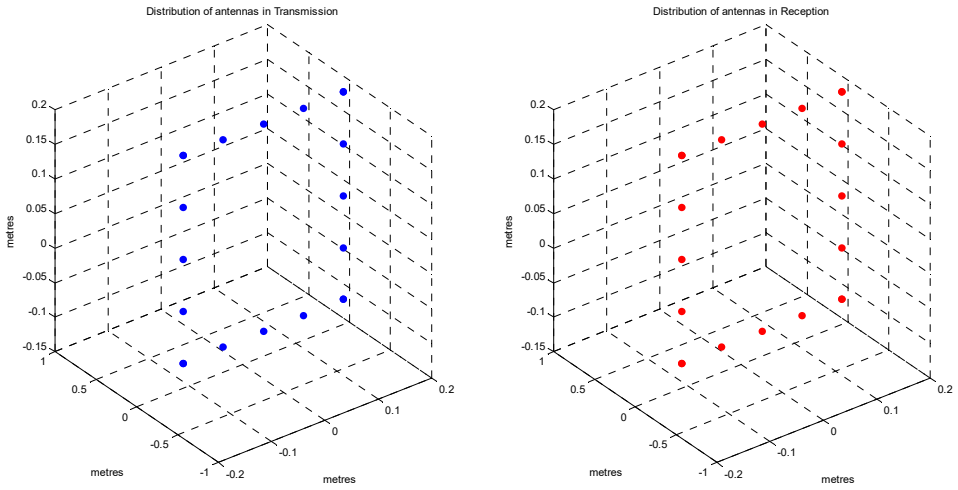

Figure 3.36: MIMO Square array at transmission N_t=27 and Square array at reception N_r =27

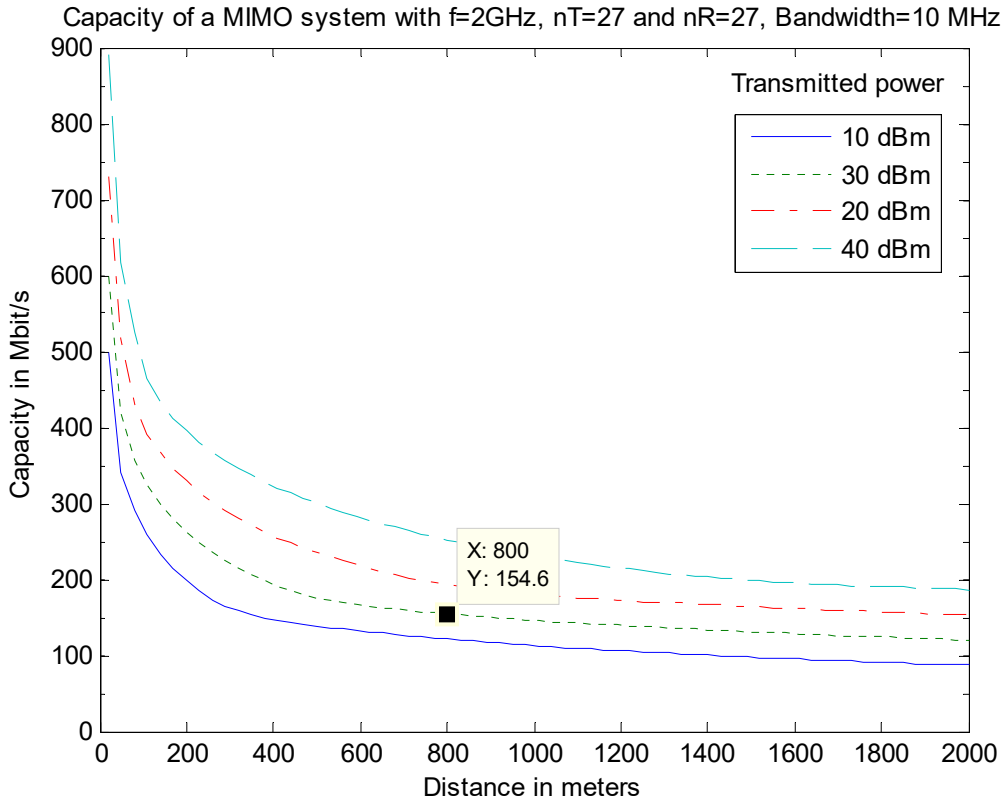

Figure 3.37: Capacity of MIMO Square array N_t=27 and Square array N_r=27

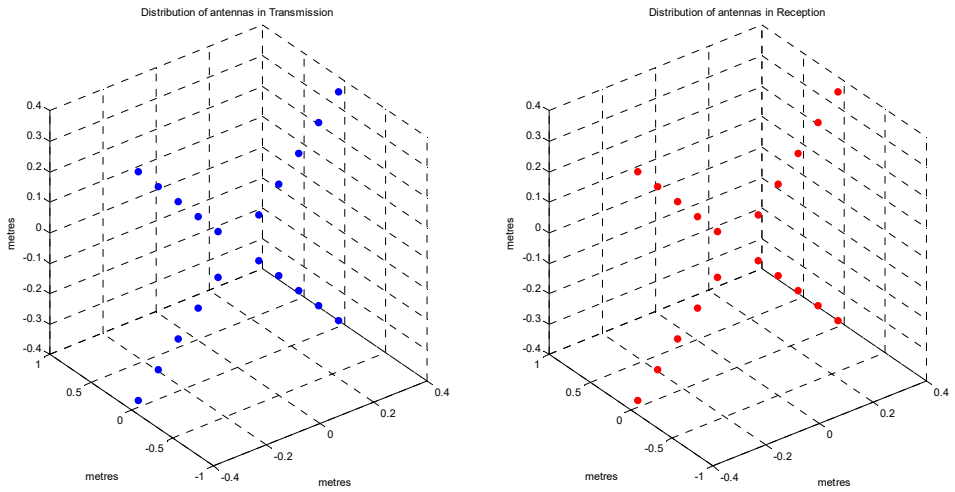

Figure 3.38: MIMO C. Squares array at transmission N_t=27 and C. Squares array at reception N_r =27

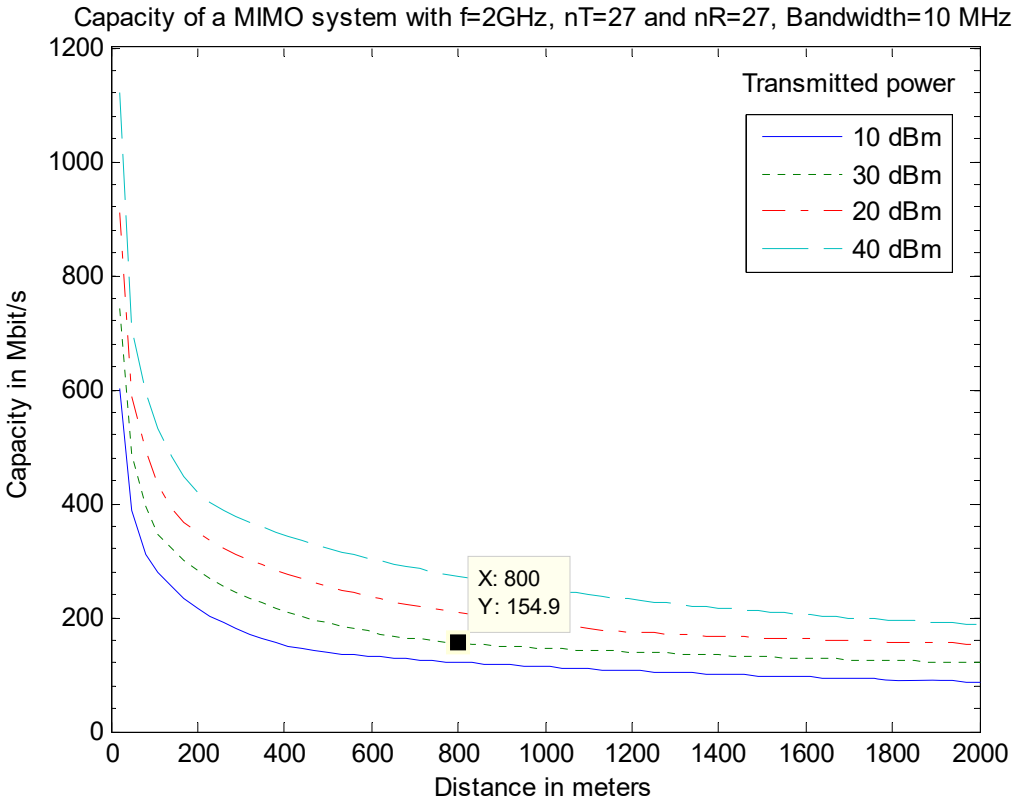

Figure 3.39: Capacity of MIMO C. Squares array N_t=27 and C. Squares array N_r=27

3.4.4 GSTA

The algorithms are simulated to obtain the capacity of the systems with the GSTA general models, alternating the distribution of the antennas in reception and using as parameters the next values:

- ***Carrier frequency (f_c):*** 2 GHz
- ***Number of antennas in reception (n_r):*** 20 antennas or 27 antennas
- ***Bandwidth (B):*** 10 MHz
- ***Separation between reception antennas ($\Delta_r \lambda_c$):*** 7.5 cm (λ/2)
- ***Angle of incidence1 ($\emptyset 1$): $\pi/3$***
- ***Angle of incidence2 ($\emptyset 2$): 0***
- ***Transmitted power (P):*** 10, 20, 30 and 40 dBm
- ***Noise power (N_0):*** -104 dBm (-174 dBm/Hz)

In the next graphs **(Figure 3.40 to Figure 3.49)** are described the spatial distribution that have been used for the antennas and the resulting capacities. In the capacity graphs it has been selected one point at 800 metres to have a more detailed information about the exact capacity of the system to see easily the differences.

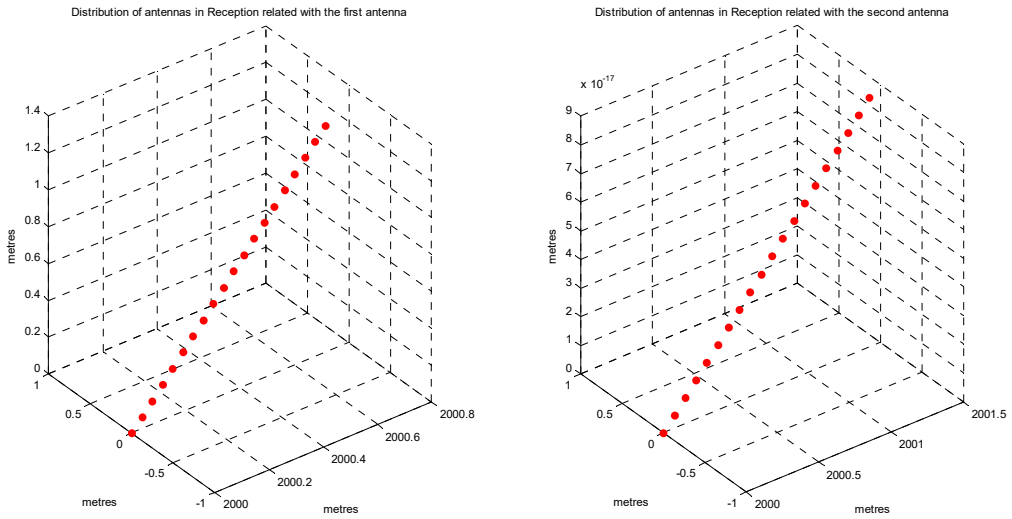

Figure 3.40: GSTA Linear array at reception N_r =20 $\emptyset_1 = \frac{\pi}{3}$ $\emptyset_2 = 0$

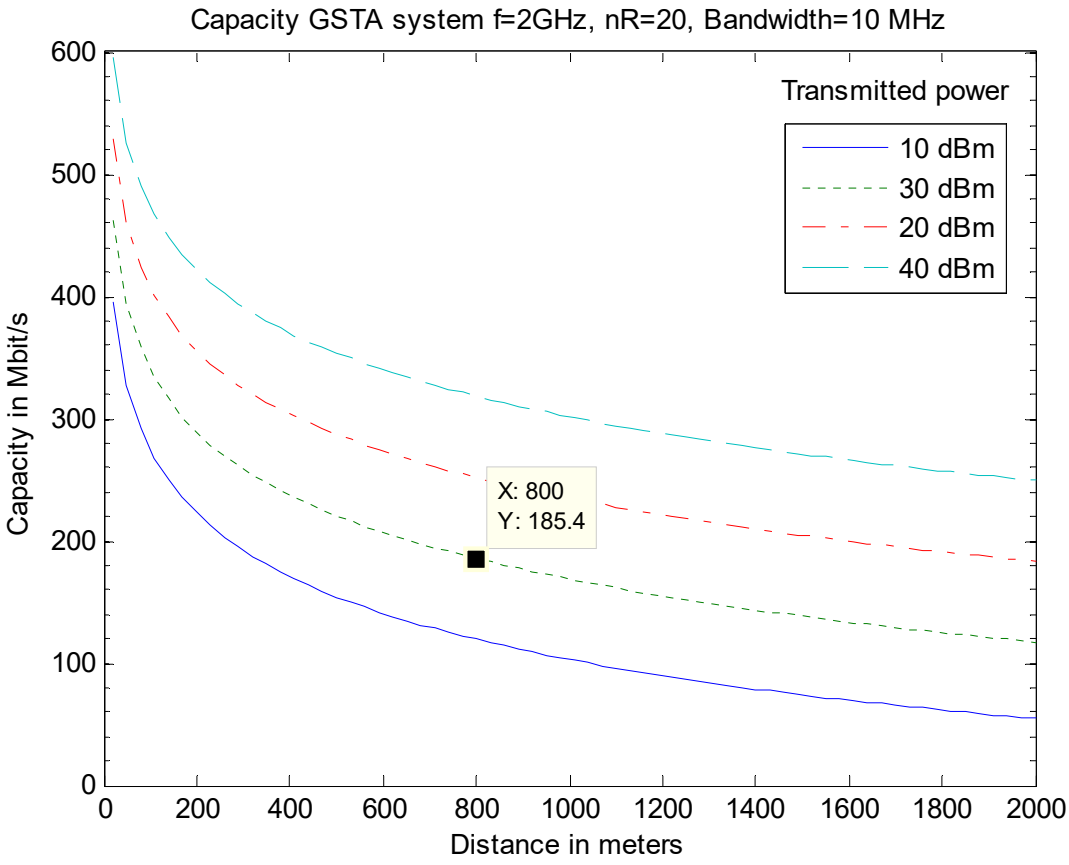

Figure 3.41: Capacity of GSTA Linear array N_r=20 $\emptyset_1 = \frac{\pi}{3}$ $\emptyset_2 = 0$

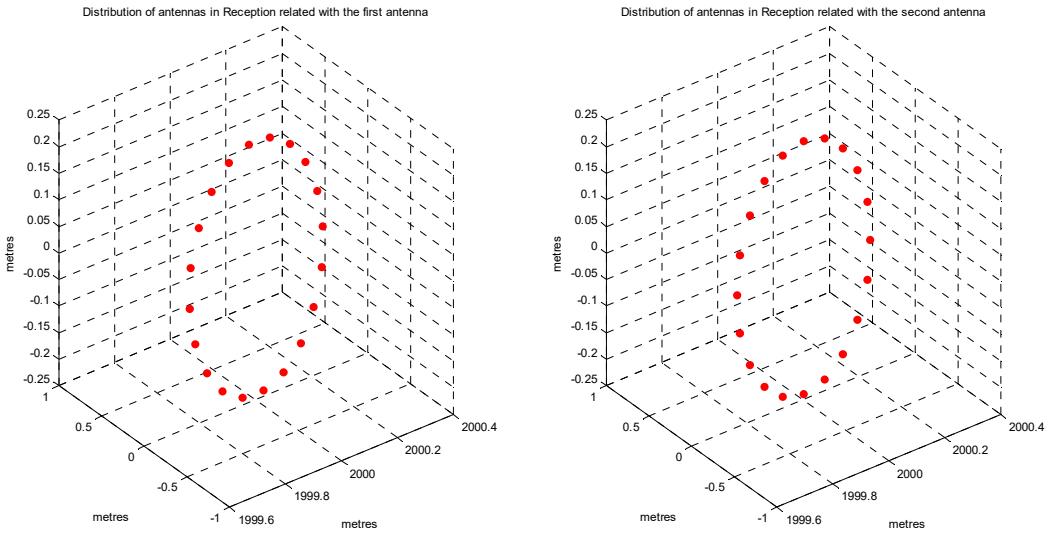

Figure 3.42: GSTA Circular array at reception N_r=20 $\emptyset_1 = \frac{\pi}{3}$ $\emptyset_2 = 0$

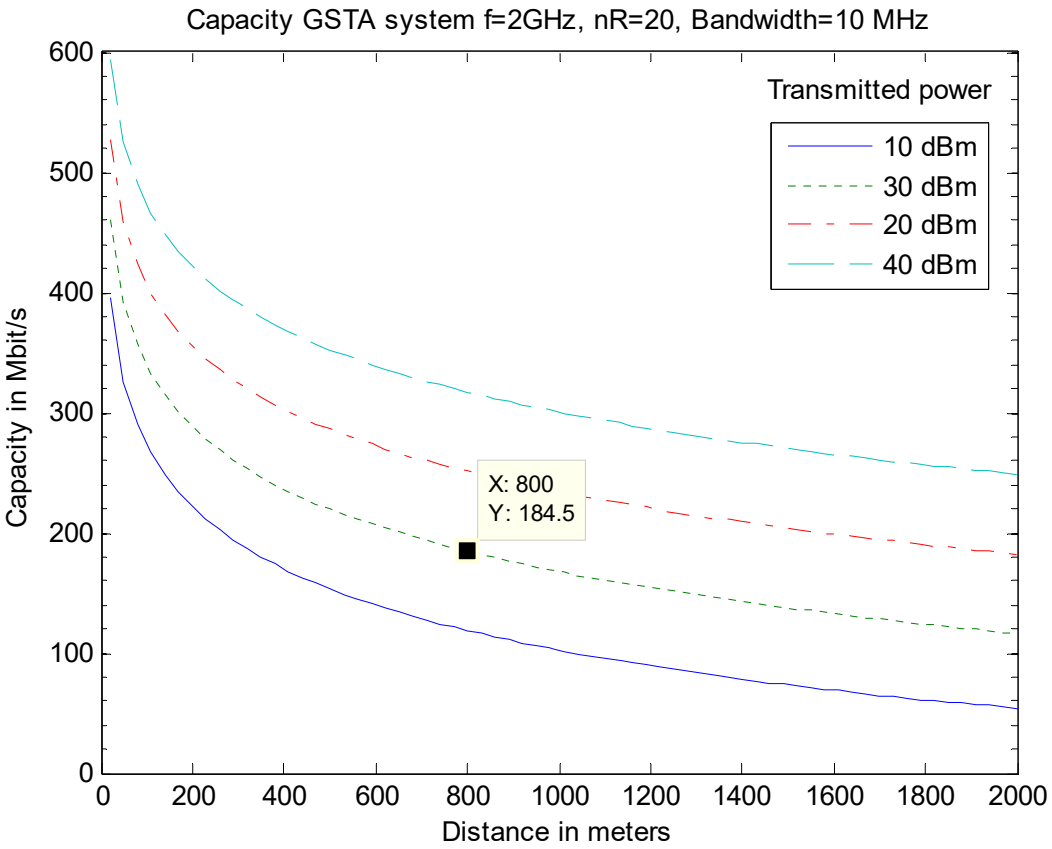

Figure 3.43: Capacity of GSTA Circular array N_r=20 $\emptyset_1 = \frac{\pi}{3}$ $\emptyset_2 = 0$

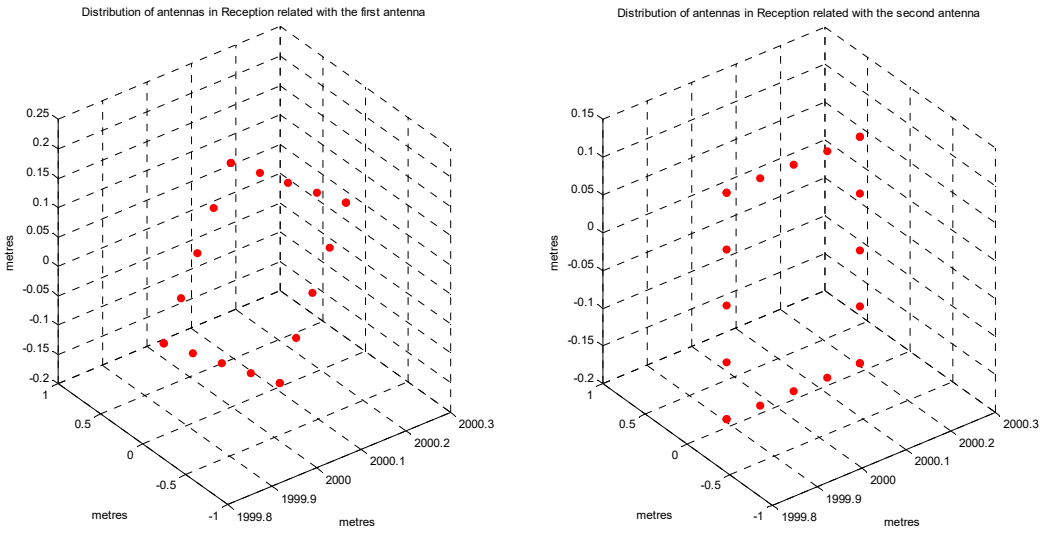

Figure 3.44: GSTA Square array at reception N_r =20 $\emptyset_1 = \frac{\pi}{3}$ $\emptyset_2 = 0$

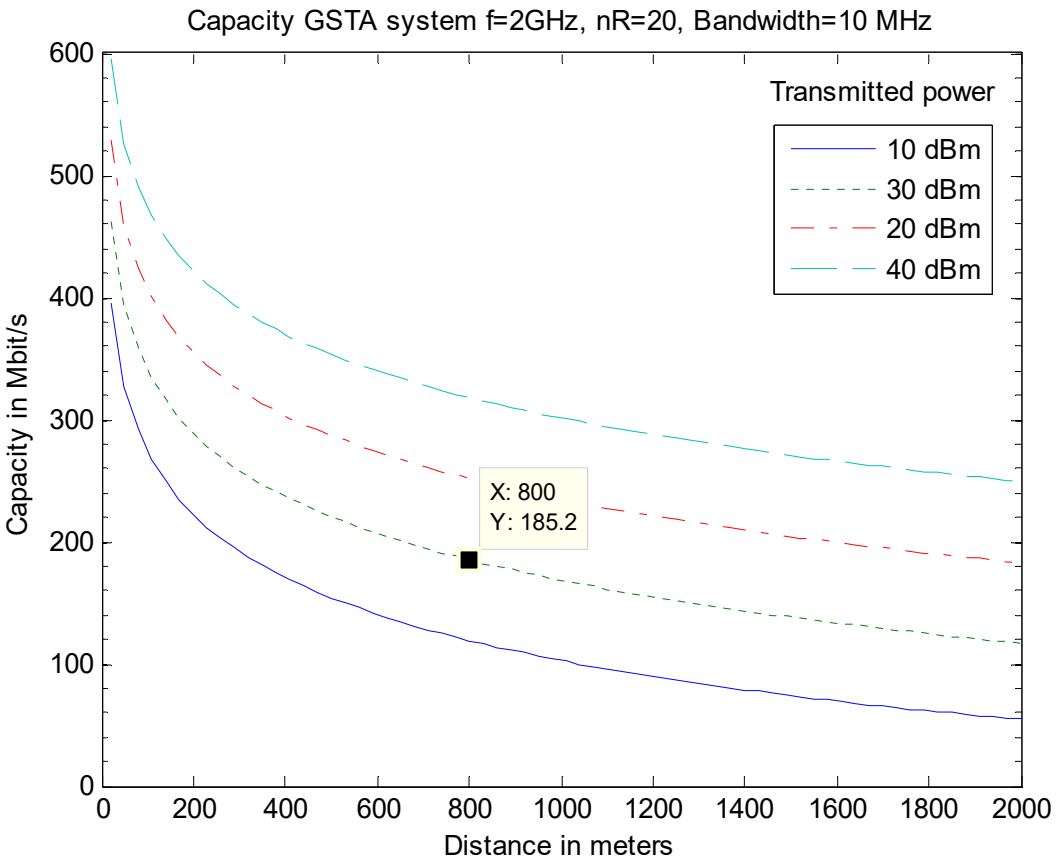

Figure 3.45: Capacity of GSTA Square array N_r=20 $\emptyset_1 = \frac{\pi}{3}$ $\emptyset_2 = 0$

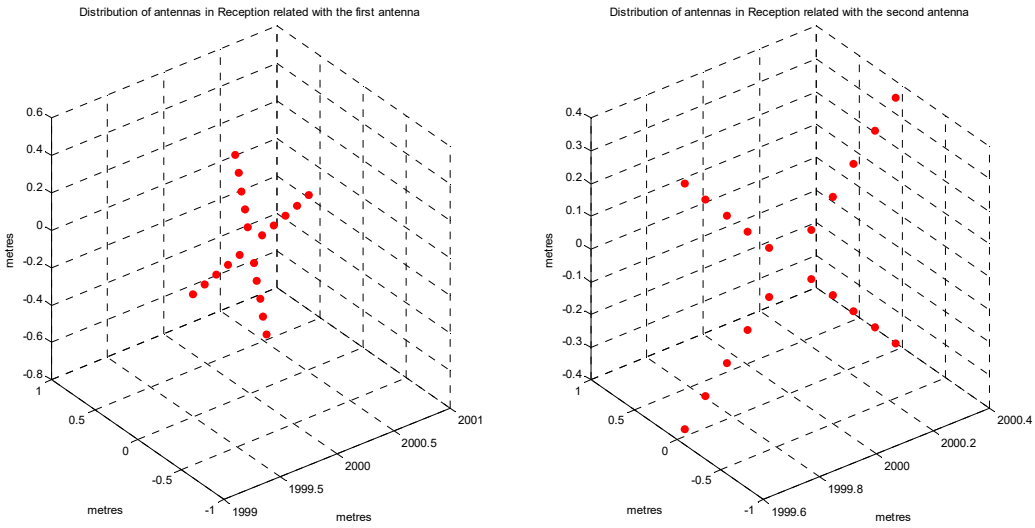

Figure 3.46: GSTA C. Squares array at reception N_r =20 $\emptyset_1 = \frac{\pi}{3}$ $\emptyset_2 = 0$

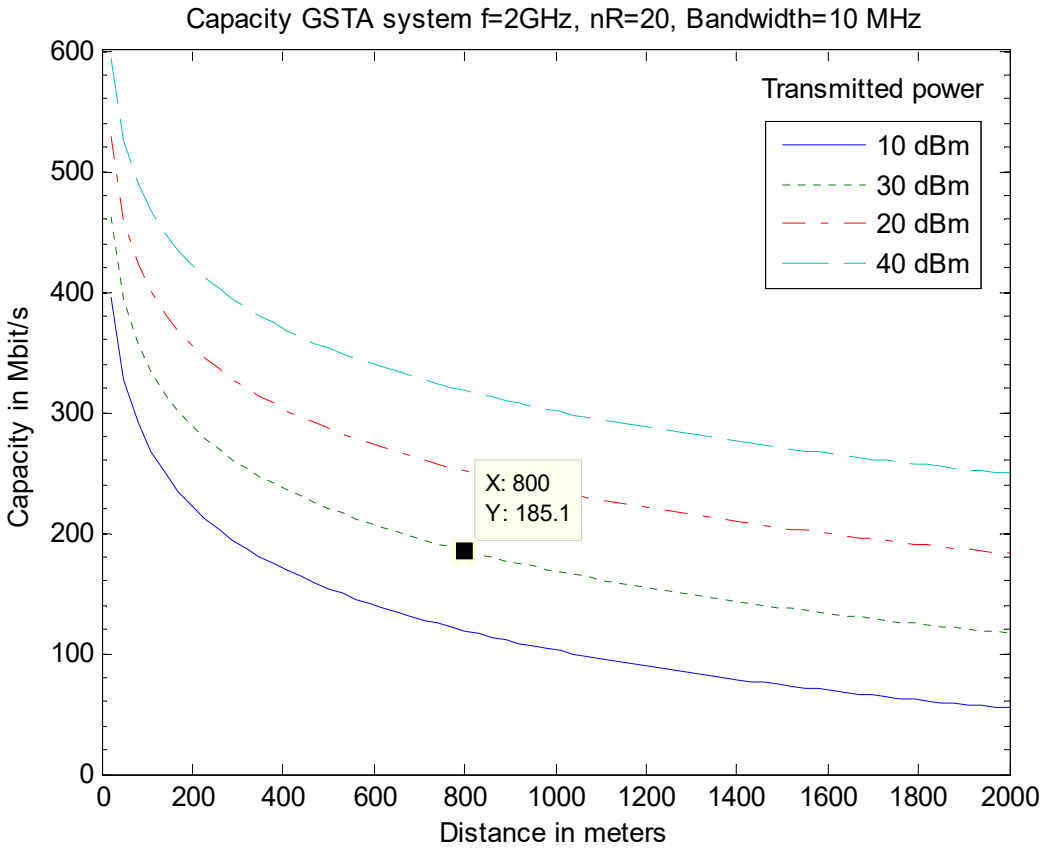

Figure 3.47: Capacity of GSTA C. Squares array N_r=20 $\emptyset_1 = \frac{\pi}{3}$ $\emptyset_2 = 0$

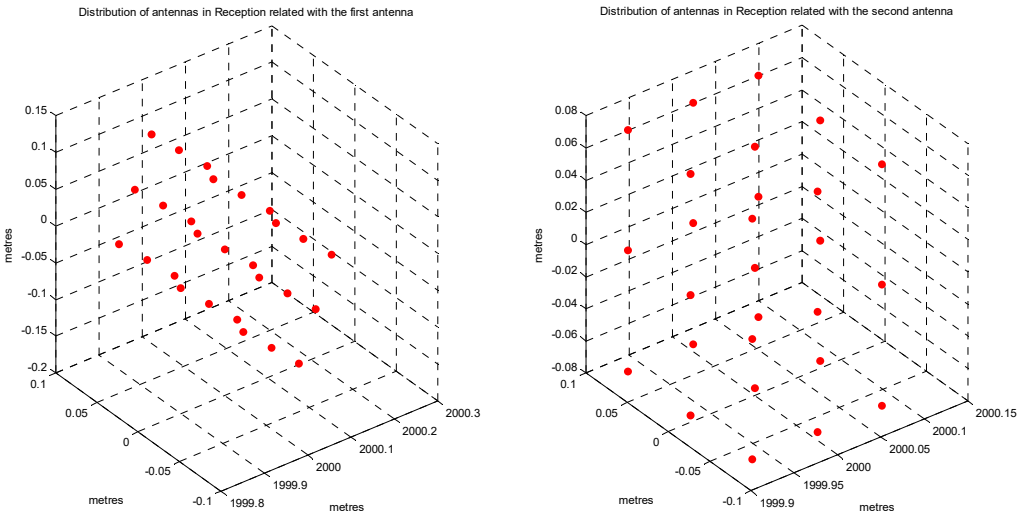

Figure 3.48: GSTA Cube array at reception N_r =27 $\emptyset_1 = \frac{\pi}{3}$ $\emptyset_2 = 0$

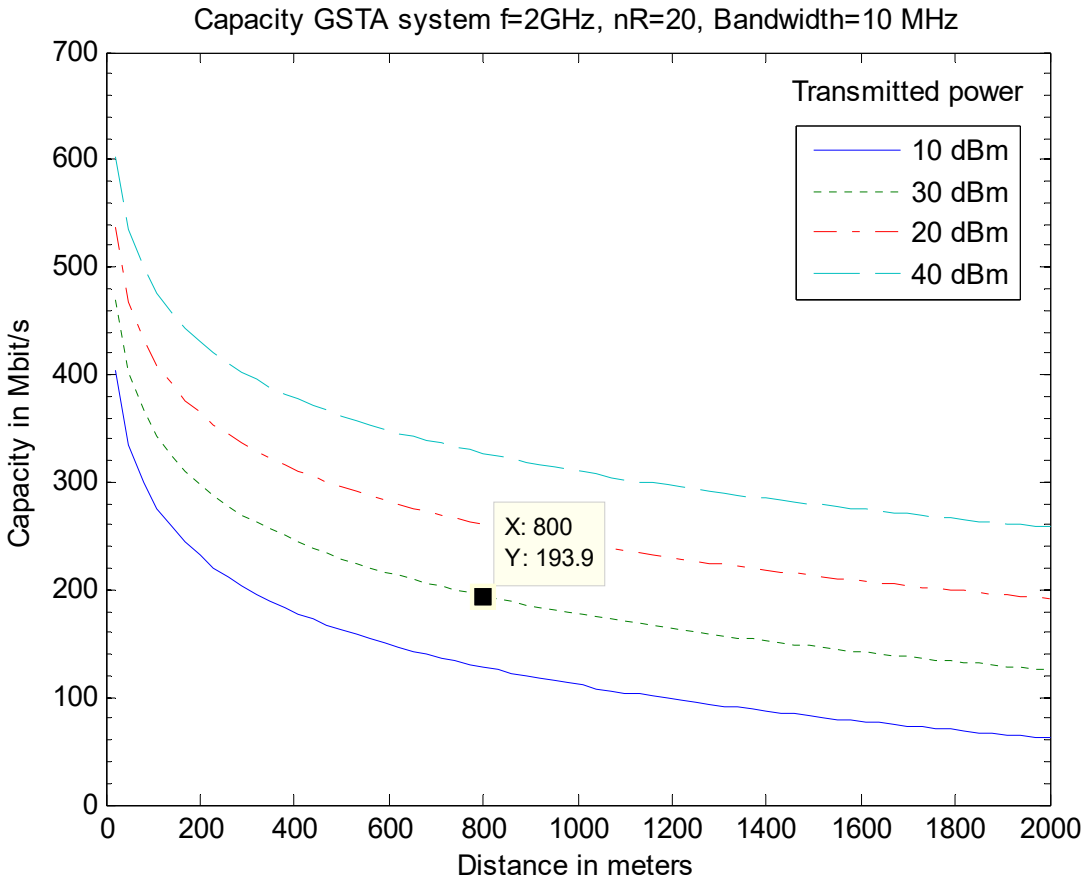

Figure 3.49: GSTA Cube array at reception N_r =27 $\emptyset_1 = \frac{\pi}{3}$ $\emptyset_2 = 0$

3.4.5 GSRA

The algorithms are simulated to obtain the capacity of the systems with the GSRA general models, alternating the distribution of the antennas in reception and using as parameters the next values:

- ***Carrier frequency (f_c):*** 2 GHz
- ***Number of antennas in transmission (n_t):*** 20 antennas or 27 antennas
- ***Bandwidth (B):*** 10 MHz
- ***Separation between transmission antennas ($\Delta_t \lambda_c$):*** 7.5 cm (λ/2)
- ***Angle of incidence1 ($\emptyset 1$): π***
- ***Angle of incidence2 ($\emptyset 2$): $-\pi/12$***
- ***Transmitted power (P):*** 10, 20, 30 and 40 dBm
- ***Noise power (N_0):*** -104 dBm (-174 dBm/Hz)

In the next graphs **(Figure 3.50 to Figure 3.59)** are described the spatial distribution that have been used for the antennas and the resulting capacities. In the capacity graphs it has been selected one point at 800 metres to have a more detailed information about the exact capacity of the system to see easily the differences.

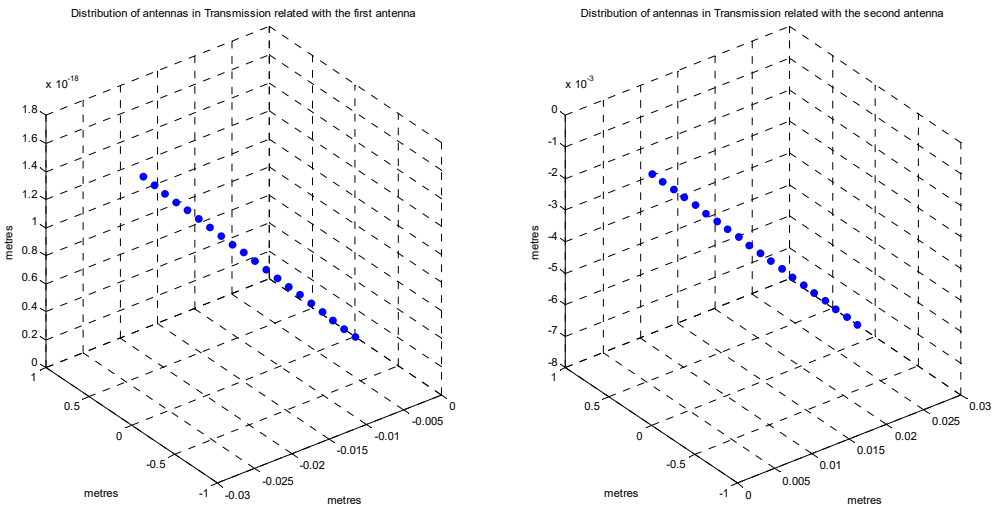

Figure 3.50: GSRA Linear array at transmission N_t =20 $\emptyset_1 = \pi$ $\emptyset_2 = -\frac{\pi}{12}$

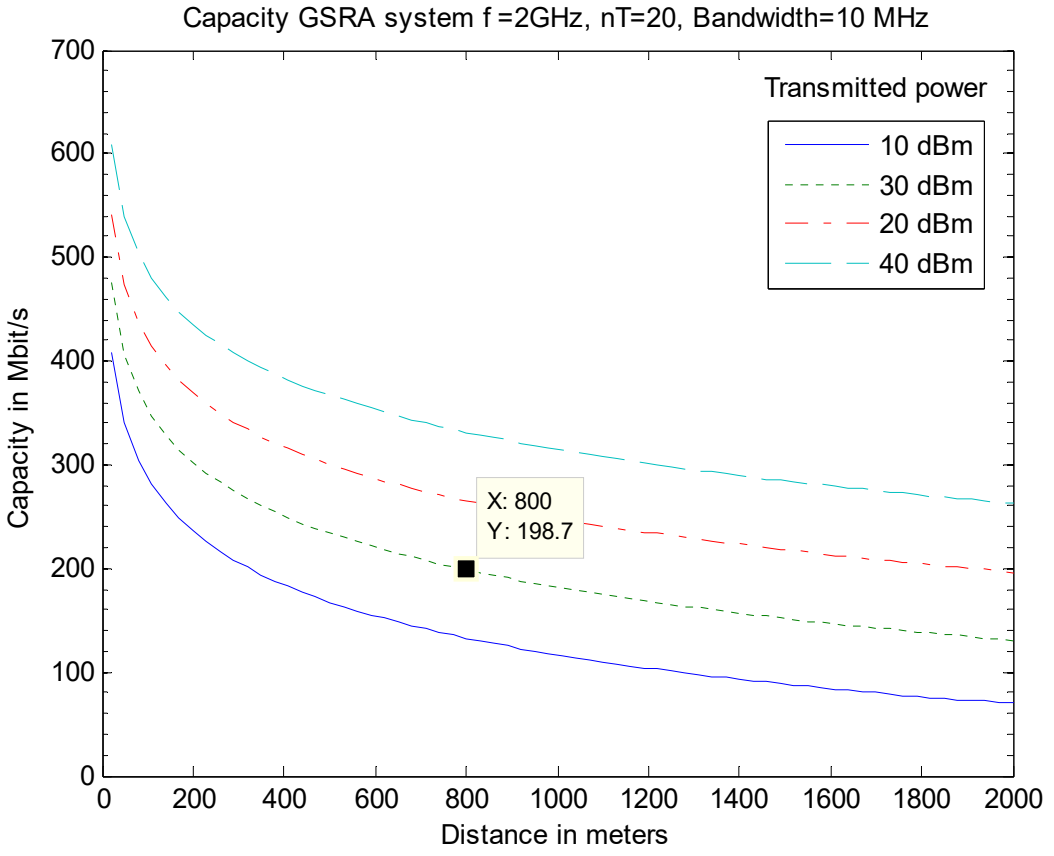

Figure 3.51: GSRA Linear array at transmission N_t =20 $\emptyset_1 = \pi$ $\emptyset_2 = -\frac{\pi}{12}$

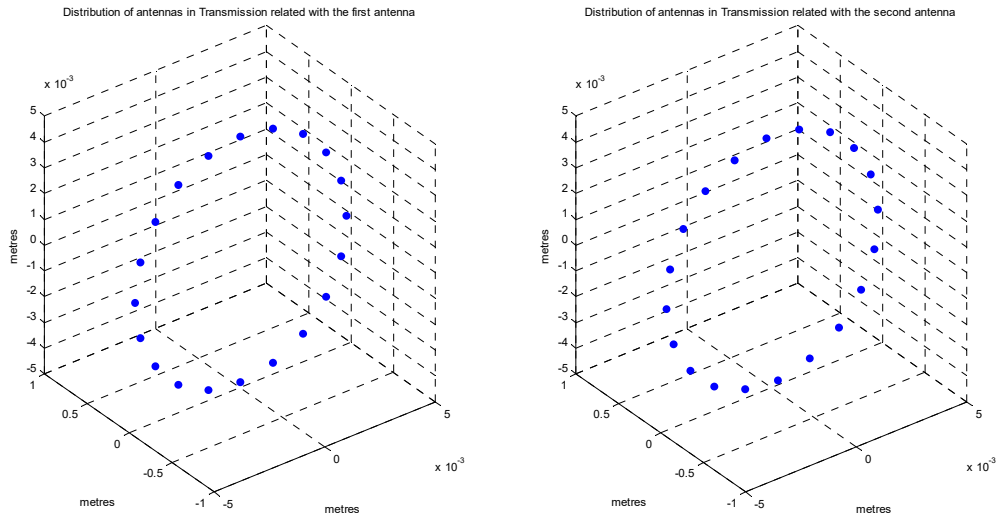

Figure 3.52: GSRA Circular array at transmission N_t =20 $\emptyset_1 = \pi$ $\emptyset_2 = -\frac{\pi}{12}$

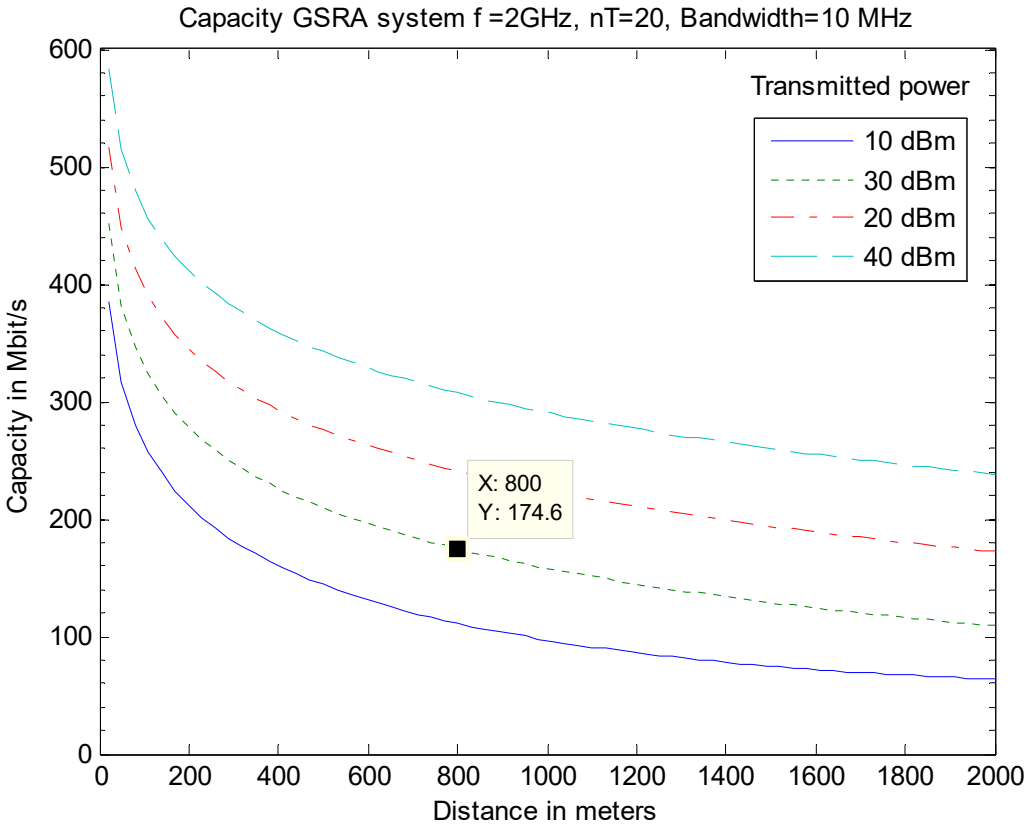

Figure 3.53: GSRA Circular array at transmission N_t =20 $\emptyset_1 = \pi$ $\emptyset_2 = -\frac{\pi}{12}$

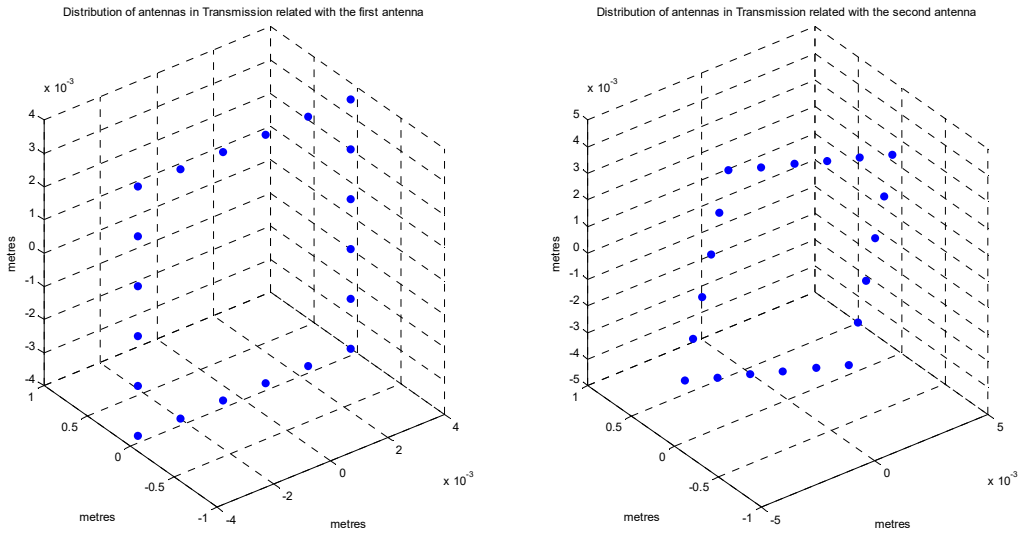

Figure 3.54: GSRA Square array at transmission N_t =20 $\emptyset_1 = \pi$ $\emptyset_2 = -\frac{\pi}{12}$

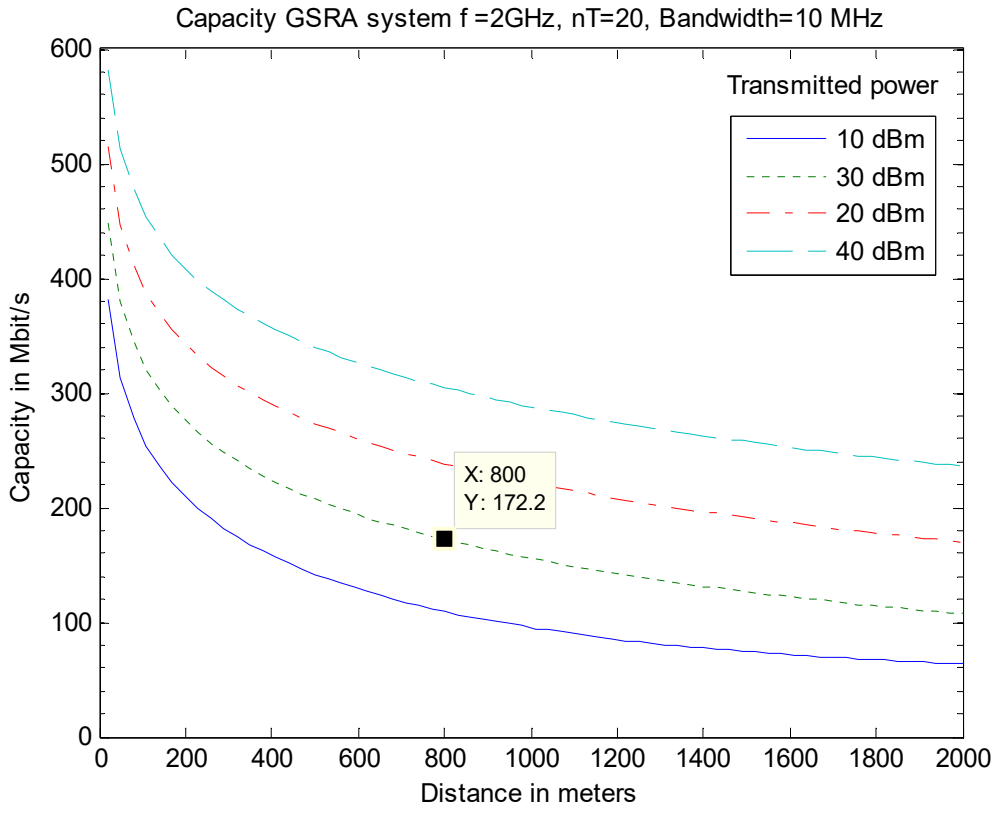

Figure 3.55: GSRA Square array at transmission N_t =20 $\emptyset_1 = \pi$ $\emptyset_2 = -\frac{\pi}{12}$

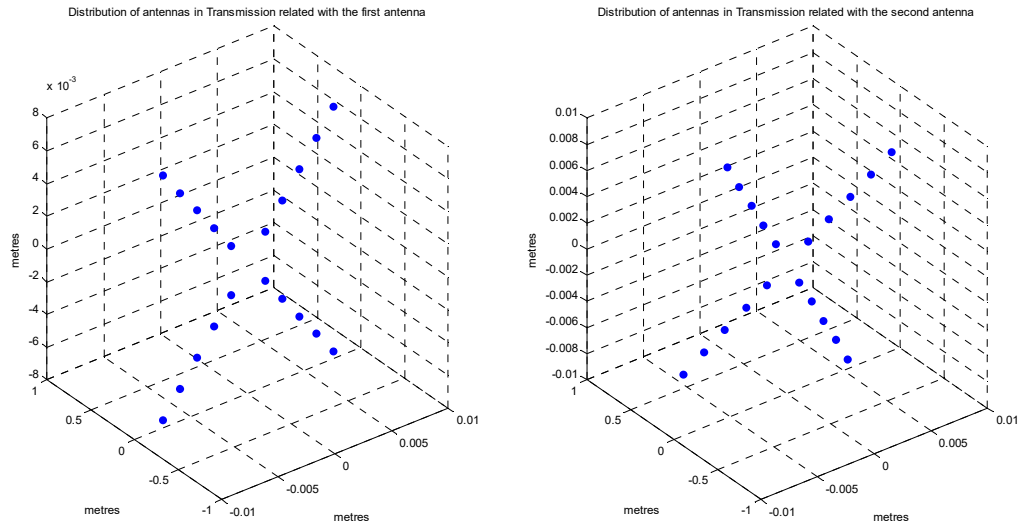

Figure 3.56: GSRA C. Squares array at transmission N_t =20 $\emptyset_1 = \pi$ $\emptyset_2 = -\frac{\pi}{12}$

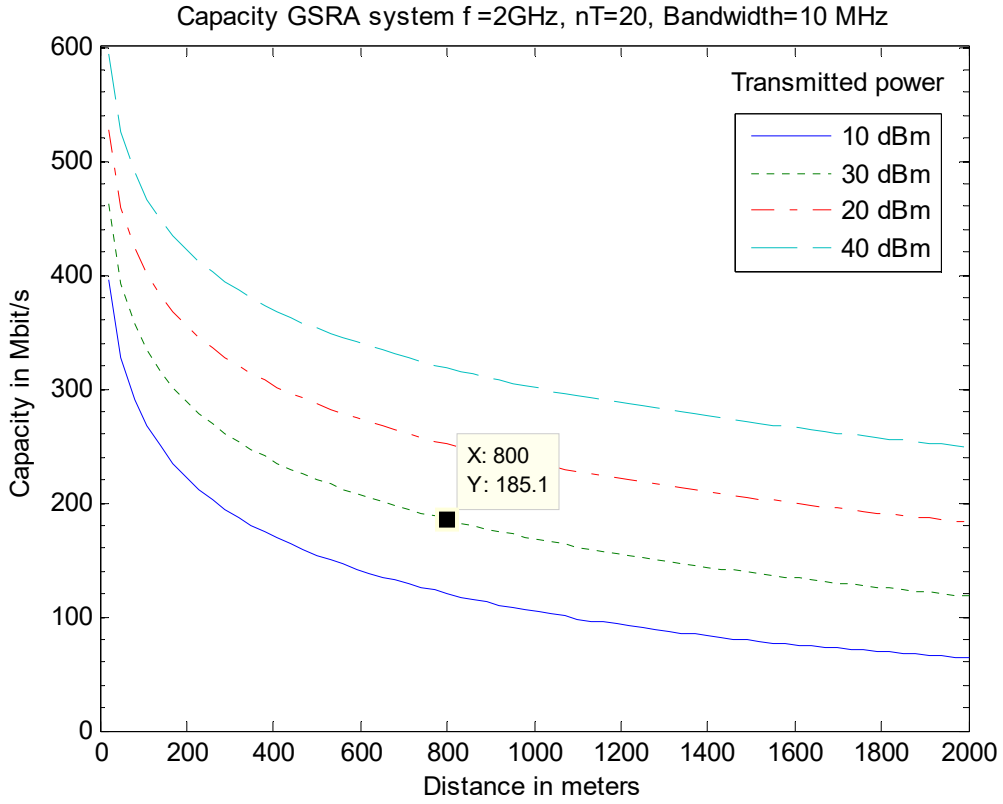

Figure 3.57: GSRA C. Squares array at transmission N_t =20 $\emptyset_1 = \pi$ $\emptyset_2 = -\frac{\pi}{12}$

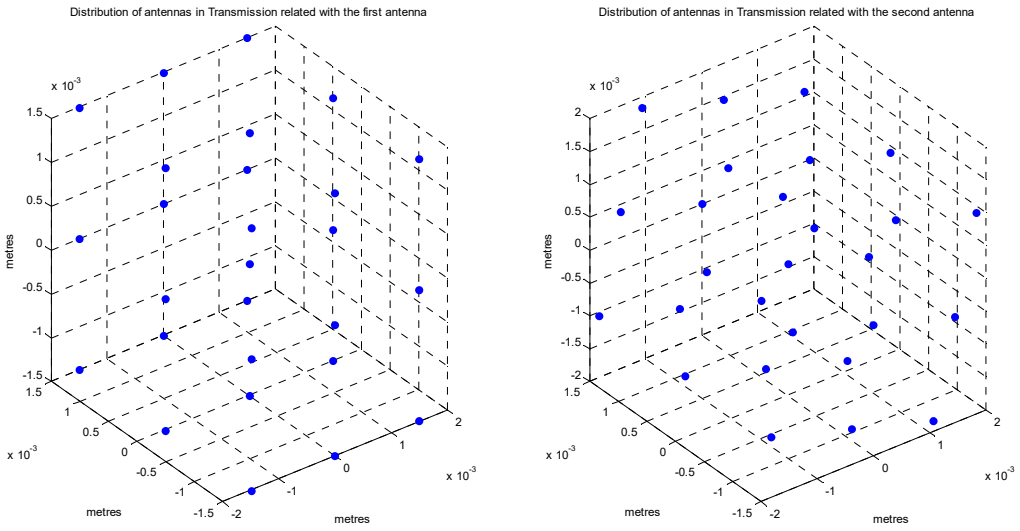

Figure 3.58: GSRA Cube array at transmission N_t =27 $\emptyset_1 = \pi$ $\emptyset_2 = -\frac{\pi}{12}$

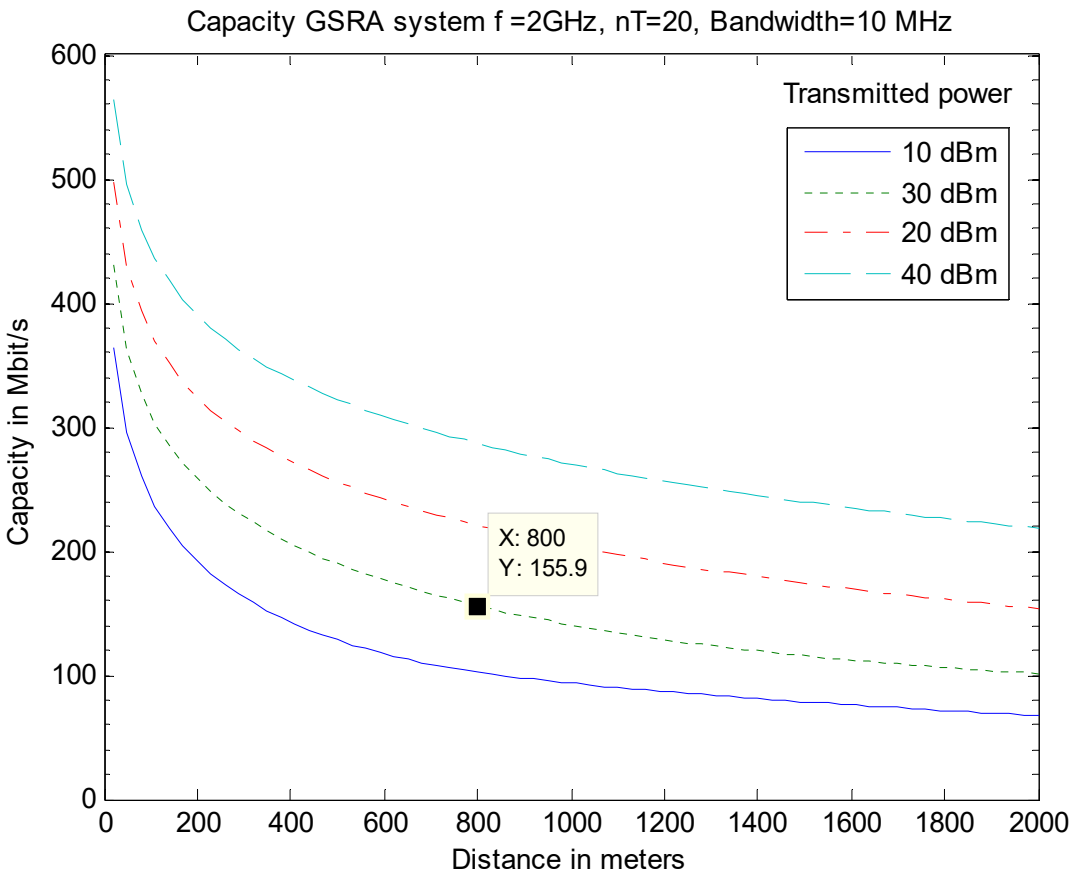

Figure 3.59: GSRA Cube array at transmission N_t =27 $\emptyset_1 = \pi$ $\emptyset_2 = -\frac{\pi}{12}$

CHAPTER 4

Results and discussion

4.1 Introduction

In this section discusses the results that have been obtained from the simulations and theoretical models that have been implemented. Due to the huge amount of parameters that are involved in the models of the simulation, it is impossible to vary all the parameters to cover all the different possibilities. For that reason, we have varied the main values that can involve significant changes in the models and give results for our project.

4.2 SIMO

The SIMO model has been simulated variating the number of antennas and comparing the resulting capacities at 800 metres. Since all the graphs are to similar and hard to compare them just by looking at them.

We can observe in all the graphs that the capacity varies with number of antennas as is describe in (**2.17**). Obtaining as result a capacity of 102.7 Mbit/s at 800 metres with 20 antennas in reception and 107 Mbit/s at 800 metres with 27 antennas. Moreover, the five different antenna configurations have been used to compare the difference in the resultant capacities, but due to the small wavelength and the fact that the SIMO channel only provides power gain and not degree freedom gain, the differences between them are very small. The change of phase in the reception antennas is compensate creating a constructive effect in the receive waves that compensate the phase change.

The optimal receiver projects the noise into the signal direction, adjusting the delays of the antennas and combining them constructively. The variation of the type of antenna and the position of them changes the channel matrix as is shown in the tables that are included in the third paragraph of the Annex A that is included at the end of the document. In spite of the change in the matrices, the singular value that is obtained of them is practically the same, and only change with the variation of the number of antennas, the SNR relation and the attenuation of the channel, that varies

with the distance as is explained in the **Chapter 3.2.2.** As only one singular value can be obtained, it is impossible to use the spatial multiplexing in this systems.

4.3 MISO

The MISO model is reciprocal to the SIMO model, obtaining identical results. The method use is the same that have been used in the simulations of the MISO model, varying the principal parameters of the simulation and observing the changes in the graphs at a fix distance.

The resulting capacities obtained are identical at SIMO model, with 102.7 Mbit/s at 800 metres with 20 antennas and 107 Mbit/s at 800 metres with 27 antennas. We can observe in the tables of the Annex A that the channel matrices are very similar to the channel matrices of the SIMO model, due to both models are reciprocals between them. The reasons are the same that the SIMO model, due to the singular value obtained from the channel matrix, is the same and is independent of the location of the antennas, and only depends of the number of antennas in transmission, as is described in (**2.19)** the SNR relation and the attenuation of the models that have been use, the same parameters as the SIMO model.

The MISO model only has power gain, and don't obtain gain from the degree of freedom, because only it is possible to obtained one singular value from the channel matrix, and is impossible to use the spatial multiplexing in this systems, as the same occurs in the MISO system.

4.4 MIMO

The MIMO model combines both previous models into a unique one in which is it possible to vary the number and location of the antennas in transmission and reception.

The main values considered in this simulation are the number of antennas and the form of the arrays in transmission and reception, proving with different combinations between them. The results achieved are around 145 Mbit/s at 800 metres with 20 antennas in reception and transmission, around 150 Mbit/s at 800 metres with 20 antennas in transmission and 27 antennas in reception, and 155 Mbit/s at 800 metres with 27 antennas in transmission and 27 antennas in reception. The variations achieved with the different locations of antennas are very low compared with the mean capacity between the all simulations. The more significant gain is achieve using a linear array in transmission and reception, obtaining 174.9 Mbit/s with 27 antennas in both transmission and reception, 150.2 Mbit/s with 20 antennas in transmission and 27 in reception using the circle, square or concentrically squares as transmission antennas and the cubical antennas as reception antennas, and 148.5 Mbit/s with 20 antennas in

both reception and transmission, using again two linear arrays. All these measures have been made at 800 metres.

As it happens in the previous models, the singular values obtained from the channel matrices are very similar, and that is the reason why the variation between the resultant capacities is lower. The unique singular value obtained due to the non degree of freedom of the channel makes impossible to use the spatial multiplexing in this models. The resultant capacities also vary with the number of antennas in reception and transmission as the principal change, as is describe in (**2.24)**.

When doing the simulations, we have only consider the variation of the antennas location in one of the side, because it has been prove using the simulations that the final results are the same if we change the form of the transmission and the reception antennas, that fact makes easier for us doing the simulations, due to the number of them decrease.

4.5 GSTA

The GTSA model combines two antennas geographically separated in transmission with an array in reception. To analyse the changes, we will vary the number of antennas in reception to see the variation in the capacity, the degrees of the angles that the transmission antennas form with the reception arrays and the form of the arrays, as we have done in the previous models.

We consider the same distance between the transmission antennas and the reception arrays, but if it was necessary this distance could be change. The main component of the simulation that is affected by the distance is the total attenuation of the models, that's why varying the distance in one of the antennas will increase or decrease the capacity.

This models is affected by the degree of freedom, because it is possible to obtain two different singular values from the channel matrix and separate the transmission power and the data that is send in the channel in both channels of transmission. The relation between this singular values depends of the position of the antennas in the reception array and the angles of incidence that describes the separation between the transmission antennas. That makes that the difference between different locations affect more to the resultant capacity that in the other models, obtaining in some cases higher capacities.

Using as angles of transmission $\emptyset_1 = \frac{\pi}{3}\ \emptyset_2 = 0$ to try to achieve two singular values the more equal possible and the lowest possible value in the multiplication between the spatial signatures of both links. The capacities obtained are 185.4 Mbits/s with 20 antennas in the reception arrays at 800 metres and 194 Mbits/s with 27 antennas in reception at 800 metres, both capacities have been achieve using linear arrays at reception, obtaining similar results with the rest of the arrays with a bit lower capacities, around 5% lower. Also we have achieved capacities of 117 Mbits/s with 27

antennas using the same angle in both links, to compare the difference of having just one singular values for sending date instead of both of them.

4.6 GSRA

The GSRA model is reciprocal to the GSTA model as SIMO is to MISO, due to GSRA is made using the same concepts of the MISO models. Instead of placing the geographically separated antennas in transmission and the array in reception, we will invert the system, using the same methods for the simulation, variating the angles of reception of the separated antennas and the number and form of the antennas in the transmission array.

As we have made in the previous model, we will maintain in all the simulations the same distance between the both links to simplify the calculations. Using as reception angles $\emptyset_1 = \pi\, \emptyset_2 = -\frac{\pi}{12}$, we obtain as result capacities 198.7 Mbits/s with 20 antennas in transmission at 800 metres, and 213.7 Mbits/s with 27 antennas in transmission at 800 metres, using in both systems the linear arrays to obtain the best results. If we use instead of the linear array a circle antenna or a square antenna, the capacity with 27 antennas decrease around 190 Mbits/s, and around 150 Mbits/s with the cubical antenna due to the decrease of the relation between both singular values. If we variate the angles to variate the multiplication between the unit spatial signatures of both links, we obtain as maximum capacity 212.5 Mbits/s at 800 metres with the angles $\emptyset_1 = \pi\, \emptyset_2 = -\frac{\pi}{5}$ and 200.2 Mbits/s with 27 antennas using the concentric squares to locate the antennas in transmission.

With these results we can see that the models affect in the same way as GSTA because of the degree of freedom model that the two singular values gives to the system, allowing us to use this model with the spatial multiplexing to send the data and take advantage of the properties of the system. It is shown too that the position of the antennas is not the most important aspect of the simulation, giving similar results in the simulations of the models with the different antennas.

CHAPTER 5

Conclusions and future lines

5.1 Introduction

In this chapter will summarise all the project that has been made, the conclusions that have been obtained from the simulations, graphs and tables and a critical evaluation of the whole work. Also is described the possible future lines that can be achieve in the future, taking advantage of the results of this project.

5.2 Conclusions

The study of the different methods of transmission and variations in the wireless communications can help us in the present and in the future to improve our systems and obtains better properties and quality, increasing the capacity, reliability and security of them. The use of arrays of different forms and size in different models of communications can offer to us an advantage in our communications and in the capacity of our systems due to the power gain due to the beamforming and the degrees of freedom of some models.

For this reasons, the previous chapters have described how we have studied and implemented five different theoretical models to do an analysis of the variations that we obtain in the capacity with the variation of the parameters of the system (frequency, spacing, number of antennas, bandwidth…). We also have proved the difference between different models of antennas that we have implemented, and the relation between them and the final results. The next table summarises the results obtained and the best performance achieved in our models.

Capacities achieve in all the models

Model	$\mathbf{N_T}$	$\mathbf{N_R}$	**Transmission antenna**	**Reception antenna**	**Capacity**	**Spatial Multiplexing**
SIMO	1	20	-	All	102.7 Mbit/s	No

SIMO	1	27	-	All	107 Mbit/s	No
MISO	20	27	All	-	102.7 Mbit/s	No
MISO	20	27	All	-	107 Mbit/s	No
MIMO	20	20	Array	Array	148.5 Mbit/s	No
MIMO	20	27	Circle	Cube	150.2 Mbit/s	No
MIMO	27	27	Array	Array	174.9 Mbit/s	No
GSTA	2	20	-	Array	185.4 Mbit/s	Yes
GSTA	2	27	-	Array	194 Mbit/s	Yes
GSRA	20	2	Array	-	198.7 Mbit/s	Yes
GSRA	27	2	Array	-	213.7 Mbit/s	Yes

Table 5.1 Final results

With these results we can conclude that in line-of-sight situations the best performance is achieve using equidistant linear arrays, although the difference in the capacity with the rest of the antennas is very low. We can also describe the importance of the degree of freedom gain that the GSTA and GSRA models obtain in comparison to the rest of the models. That makes more important the location of the antennas in this models due to the singular values obtained from the model that describes the capacity are dependant of the angles of transmission between both links and the value of the multiplication between both unit spatial signatures.

5.3 Future lines

Looking to the results that have been obtained, it is possible to continue with the project taking advantage of the results obtained, and creating new lines of work.

In the first place, we can investigate the from the MIMO models to the GSTA/GSRA models increasing the separations between the antennas and analyse how large should the antenna distances be at the transmitter and the receiver in order to obtain more degrees of freedom.

Secondly, we can continue implementing the number of antennas, the location of them and variate the parameters of the system to obtain a more accurate model and description of the model. This has not been done because as has been described previously, the number of possible simulations and changes is too much to be measure in this project entirely, so we have only consider the main cases and the parameters that can give us the best performances and change in the capacity.

Also we can include multipath effects and scattering to our systems, changing our models to a complex one that can simulate this effects. Adding these properties can add more degree of freedom to our models, making possible the use of the spatial multiplexing for our models, and obtaining an increase in the capacity of the systems.

Finally we can adjust the attenuation models to a more accurate model that can allow us make precisely simulations in particular environments and adding other important facts to our models as narrowband fading.

ANNEX A

A.1 Introduction

In this annex are detailed all the results that have been obtained and are not in the main project report.

A.2 Graphs

This section contains all the simulations of the models that have been use to achieve the final results and the conclusions. Some of this graphs are presented in the main sections, but have been included here too to have an order in all the data.

A.2.1 SIMO

- ***Carrier frequency (f_c):*** 2 GHz
- ***Number of antennas in reception (n_r):*** 20 antennas
- ***Bandwidth (B):*** 10 MHz
- ***Separation between reception antennas ($\Delta_r \lambda_c$):*** 7.5 cm (λ/2)
- ***Angle of incidence (∅): $\pi/2$***
- ***Transmitted power (P):*** 10, 20, 30 and 40 dBm
- ***Noise power (N_0):*** -104 dBm (-174 dBm/Hz)

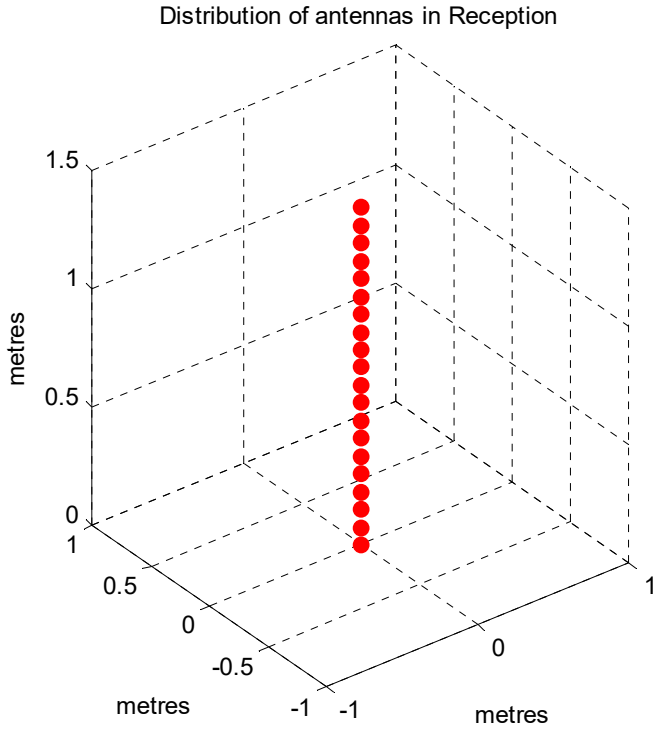

Figure A.1: SIMO Linear array at reception N_r=20

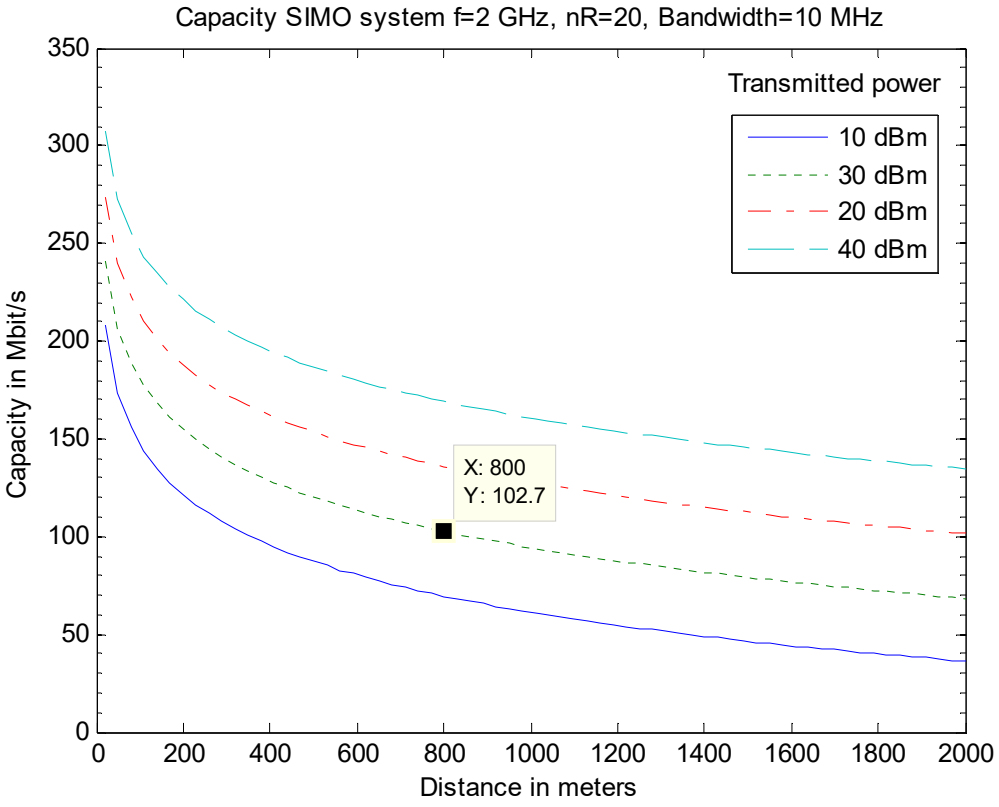

Figure A.2: Capacity of SIMO Linear array N_r=20

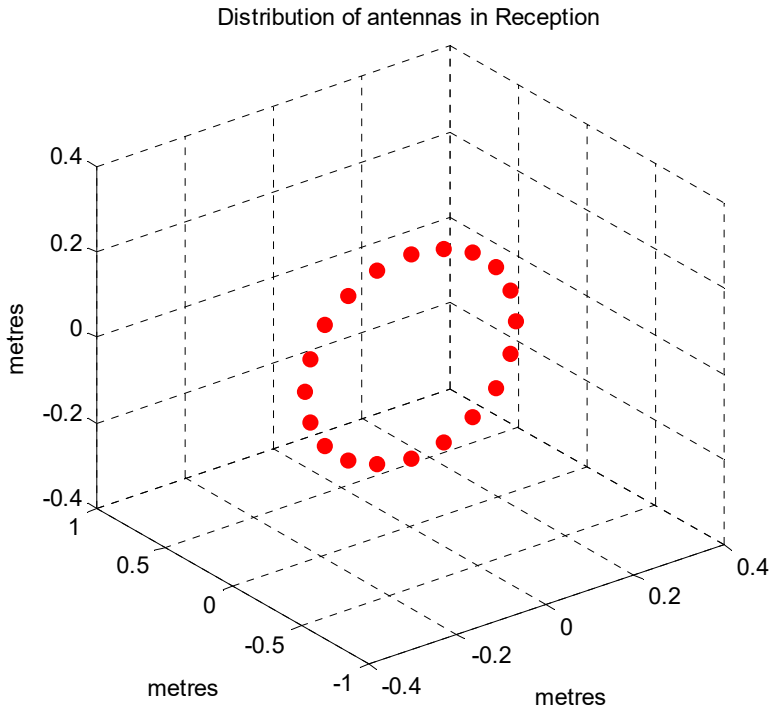

Figure A.3: SIMO Circular array at reception N_r=20

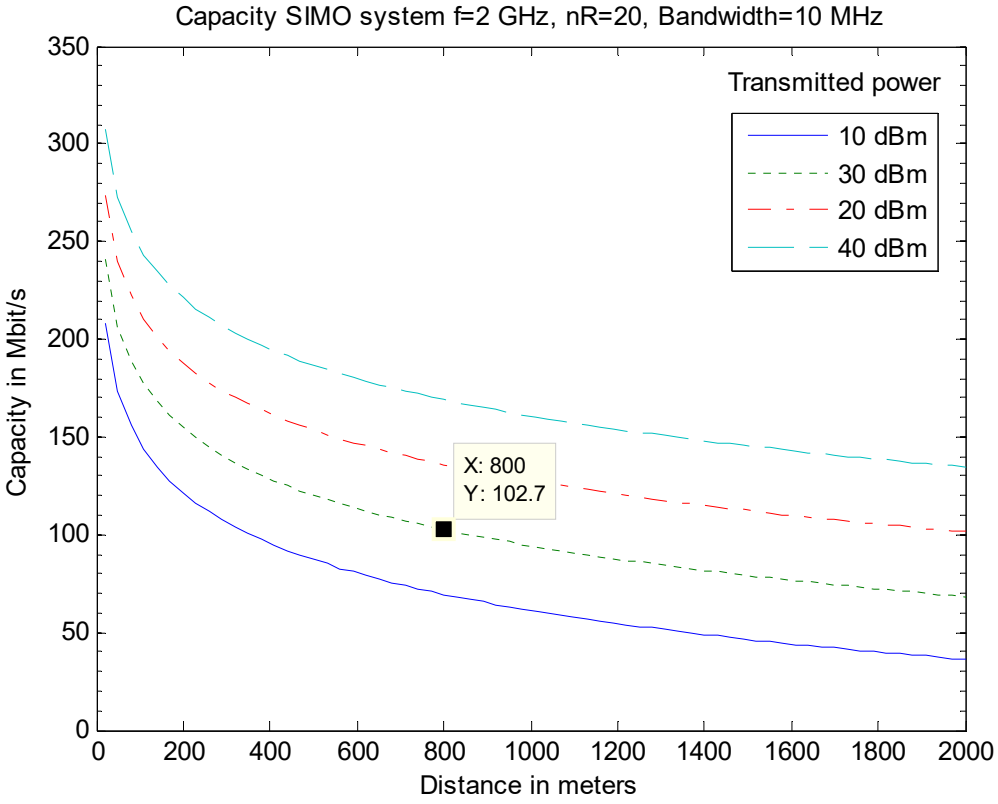

Figure A.4: Capacity of SIMO Circular array N_r=20

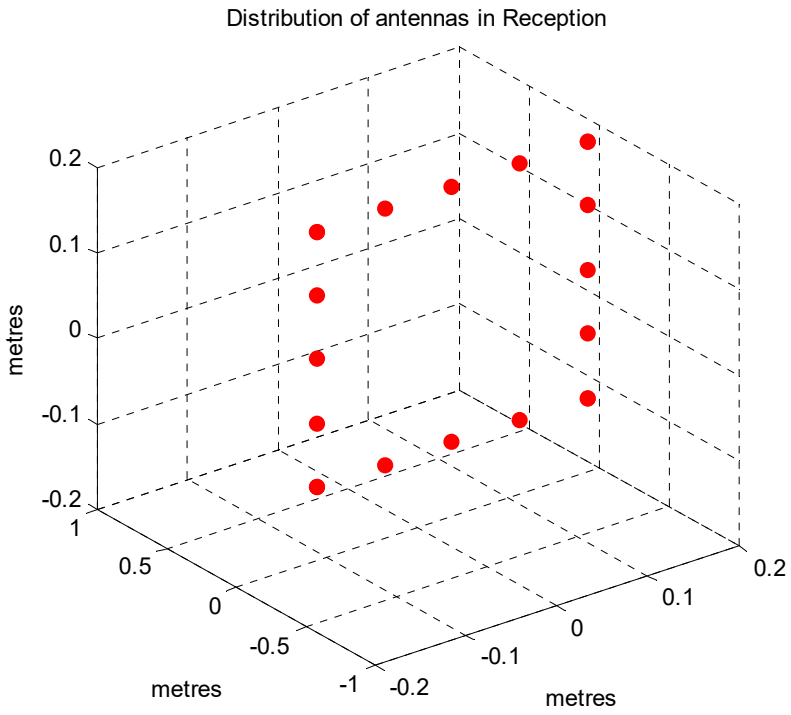

Figure A.5: SIMO Square array at reception N_r=20

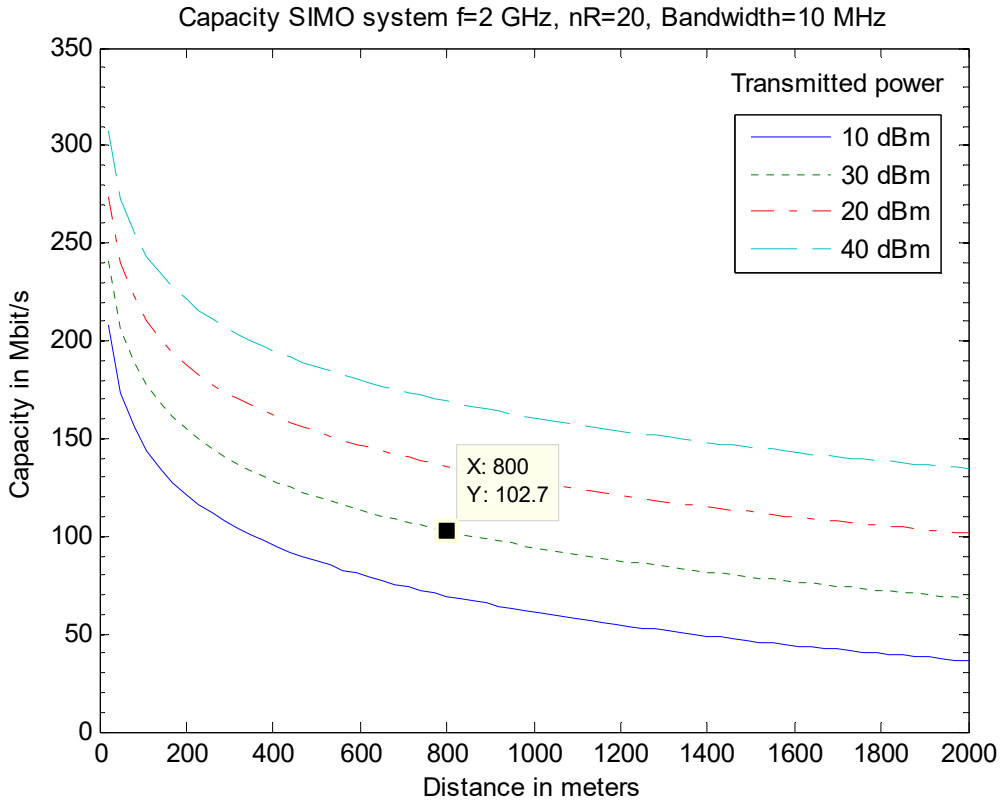

Figure A.6: Capacity of SIMO square array N_r=20

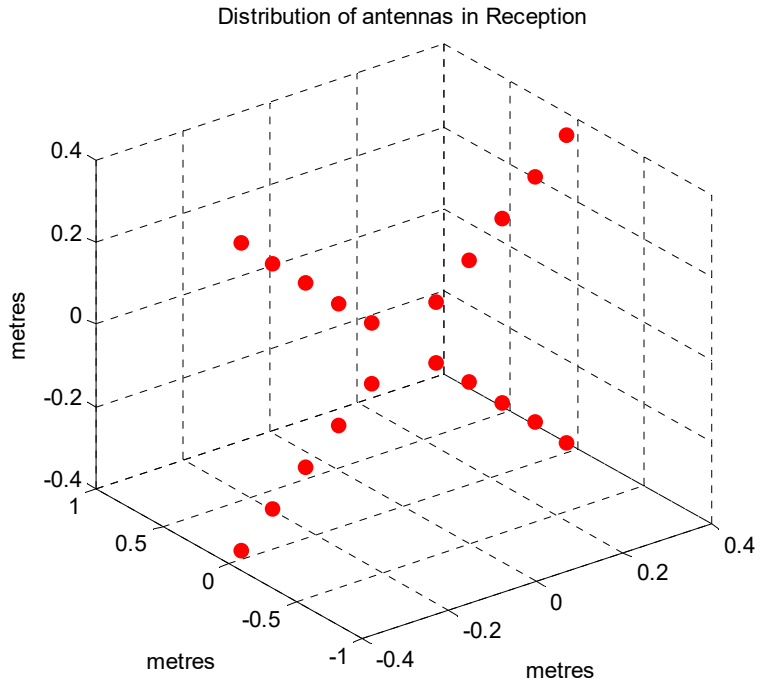

Figure A.7: SIMO C. Squares array at reception N_r=20

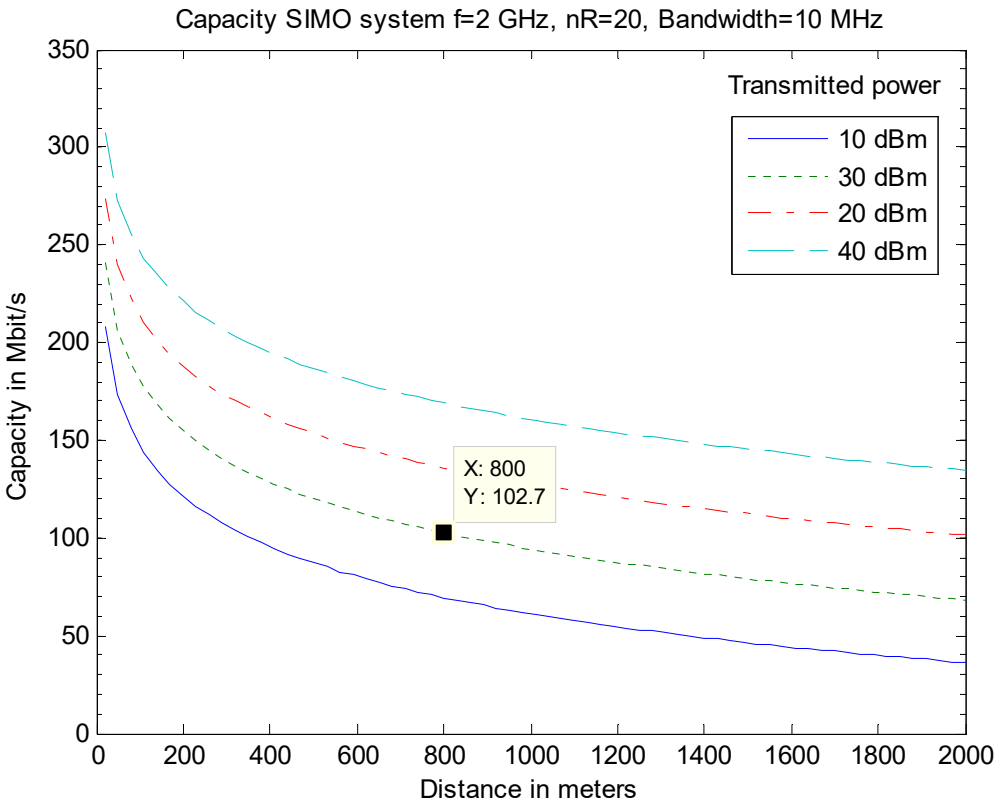

Figure A.8: Capacity of SIMO C. Squares array N_r=20

- ***Carrier frequency (f_c):*** 2 GHz
- ***Number of antennas in reception (n_r):*** 27 antennas
- ***Bandwidth (B):*** 10 MHz
- ***Separation between reception antennas ($\Delta_r \lambda_c$):*** 7.5 cm (λ/2)
- ***Angle of incidence (∅): $\pi/2$***
- ***Transmitted power (P):*** 10, 20, 30 and 40 dBm
- ***Noise power (N_0):*** -104 dBm (-174 dBm/Hz)

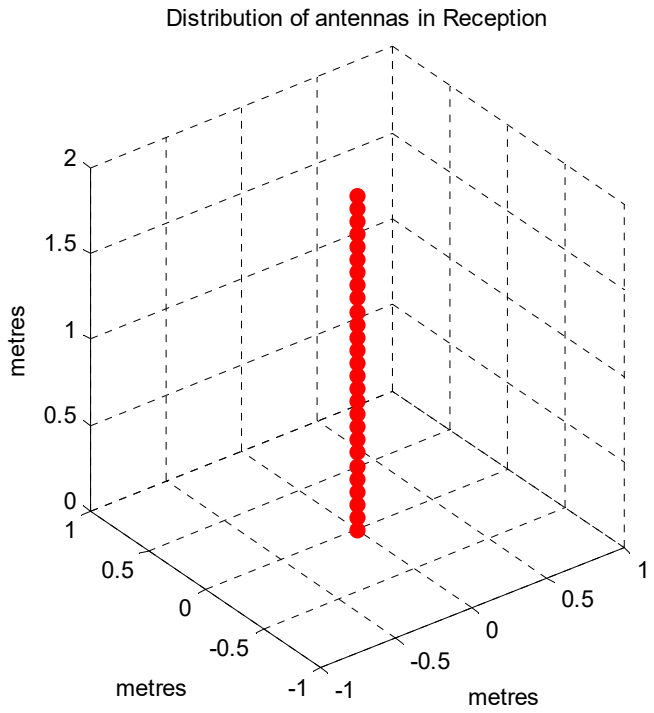

Figure A.9: SIMO Linear array at reception N_r=27

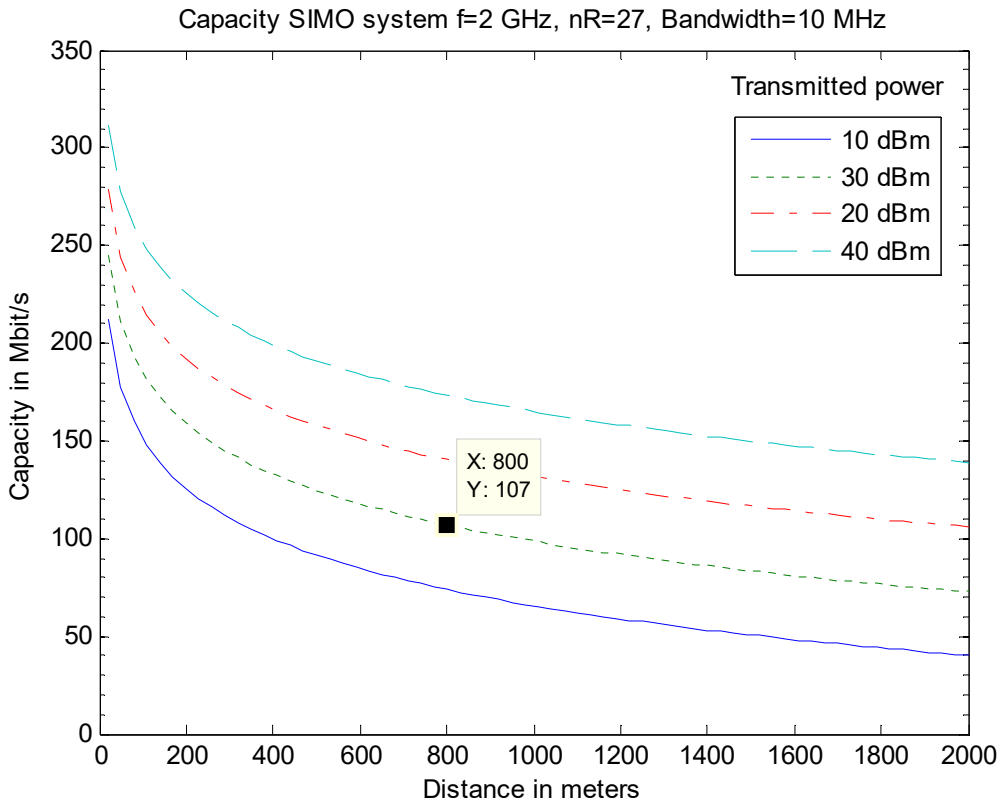

Figure A.10: Capacity of SIMO Linear array N_r=27

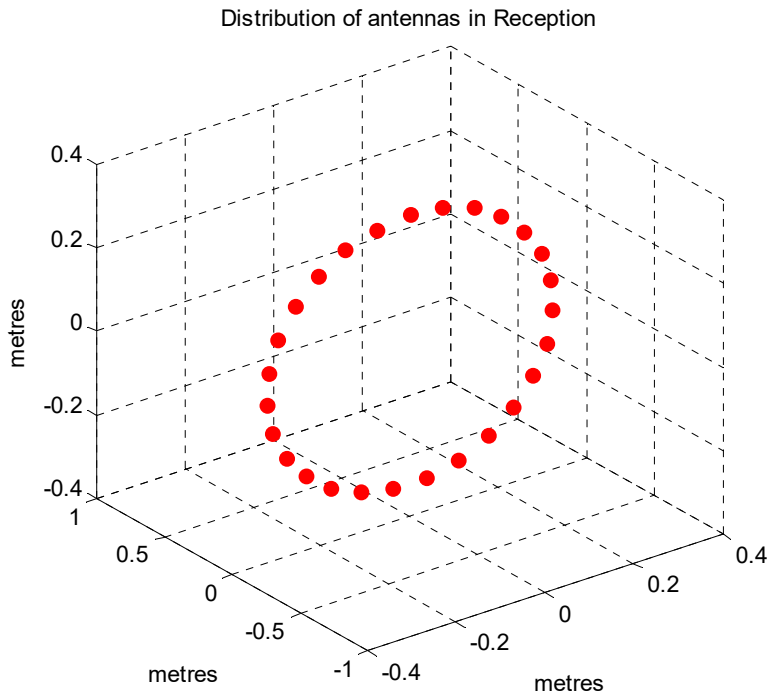

Figure A.11: SIMO Circular array at reception N_r=27

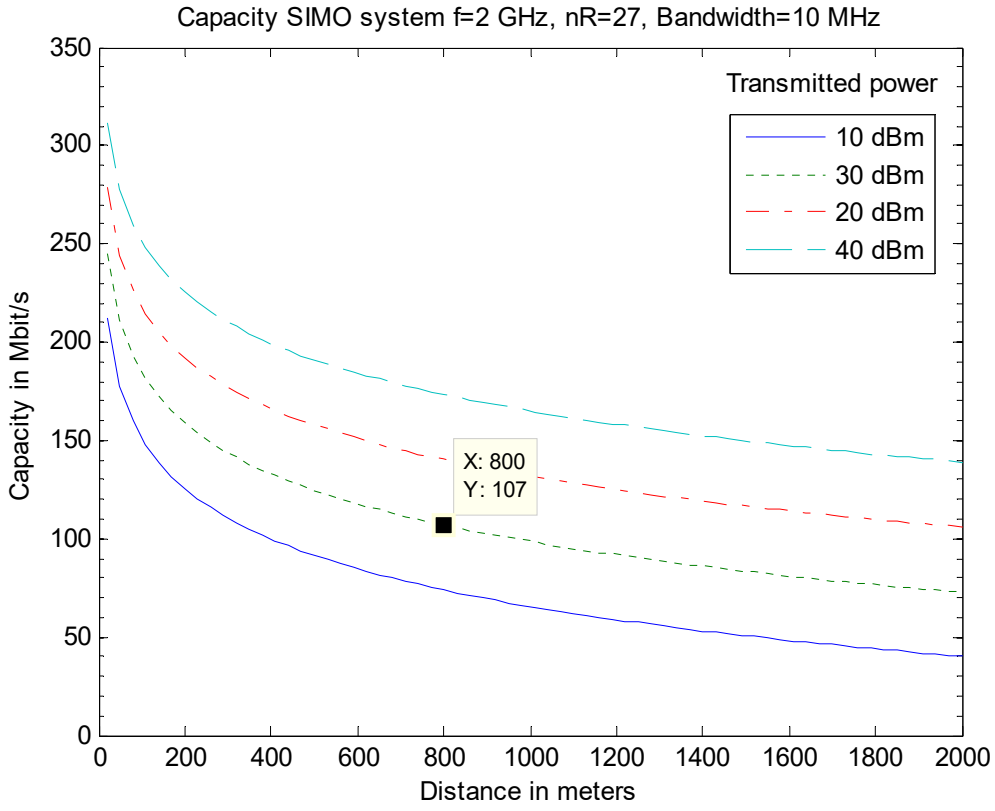

Figure A.12: Capacity of SIMO Circular array N_r=27

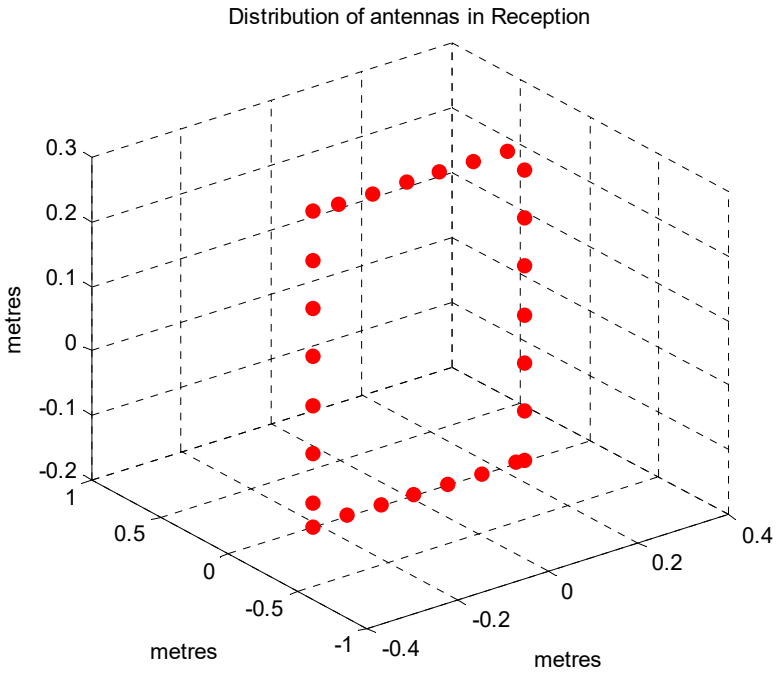

Figure A.13: SIMO Square array at reception N_r=27

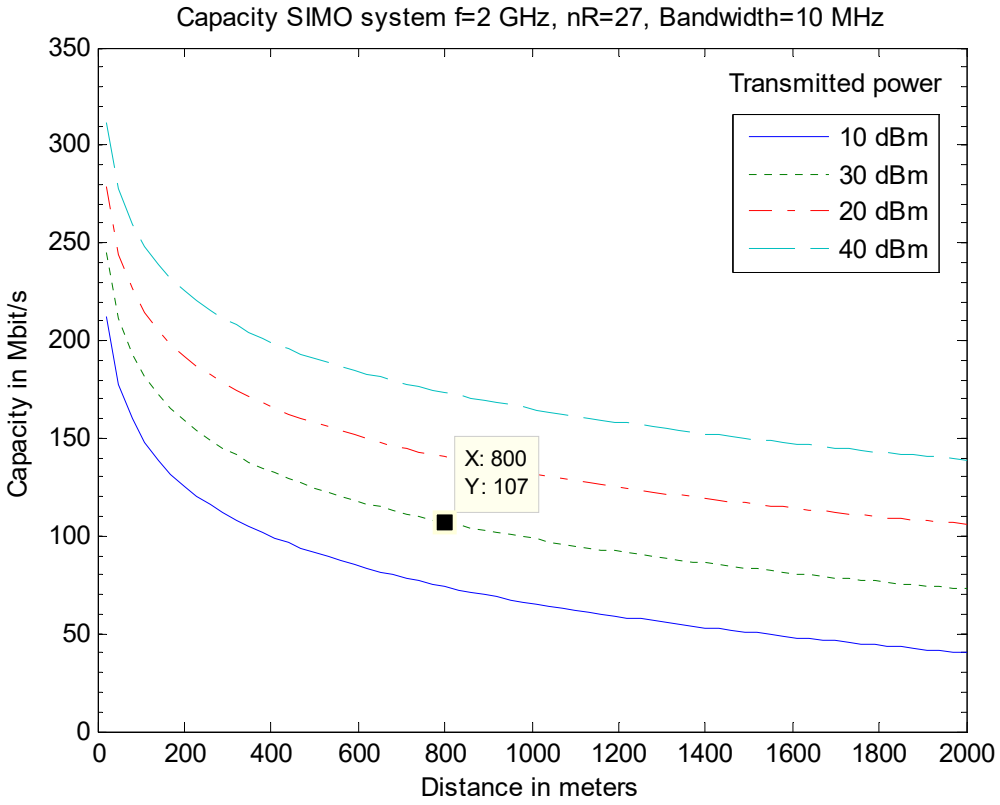

Figure A.14: Capacity of SIMO Square array N_r=27

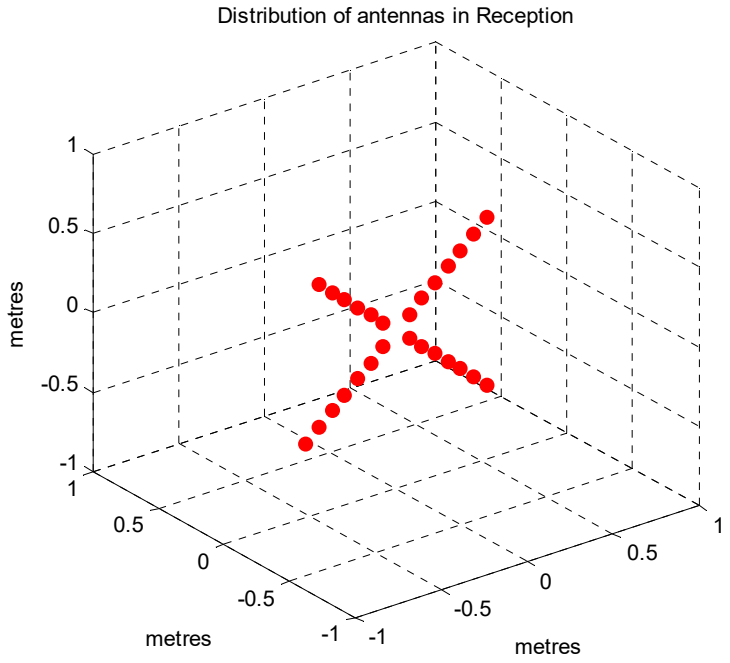

Figure A.15: SIMO C. Squares array at reception N_r=27

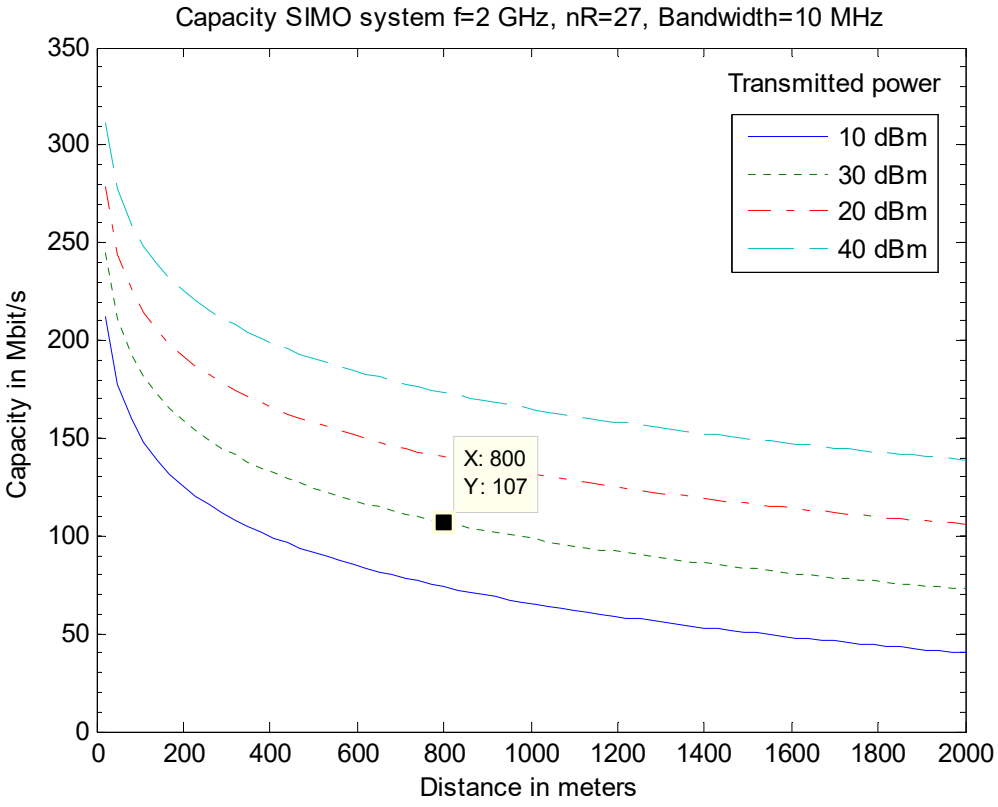

Figure A.16: Capacity of SIMO C. Squares array N_r=27

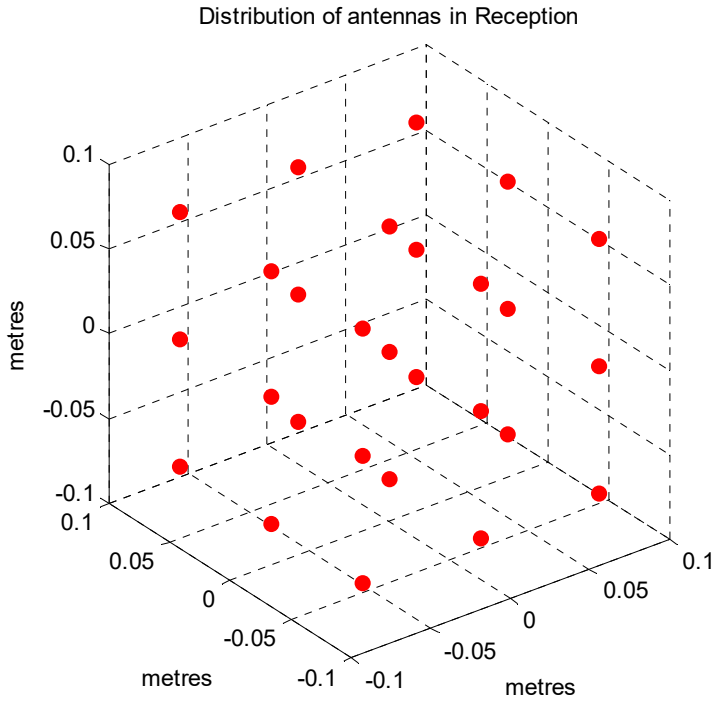

Figure A.17: SIMO Cubical array at reception N_r=27

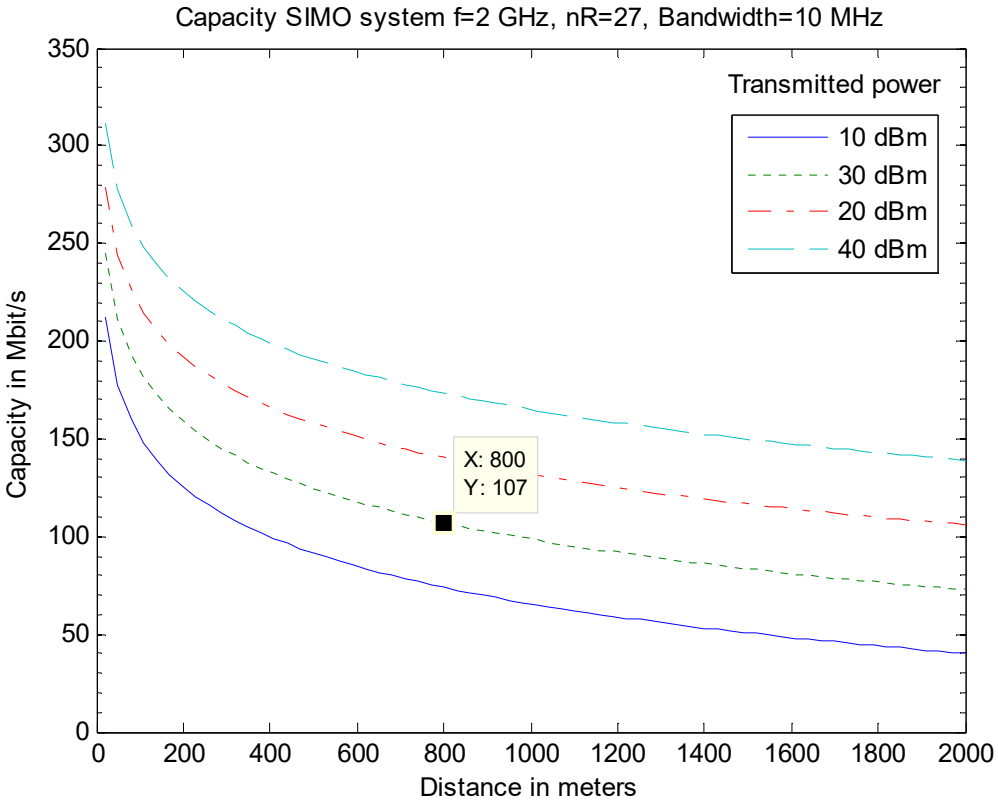

Figure A.18: Capacity of SIMO Cubical array N_r=27

A.2.2 MISO

- ***Carrier frequency (f_c):*** 2 GHz
- ***Number of antennas in transmission (n_t):*** 20 antennas
- ***Bandwidth (B):*** 10 MHz
- ***Separation between transmission antennas ($\Delta_t \lambda_c$):*** 7.5 cm (λ/2)
- ***Angle of incidence (∅): $\pi/2$***
- ***Transmitted power (P):*** 10, 20, 30 and 40 dBm
- ***Noise power (N_0):*** -104 dBm (-174 dBm/Hz)

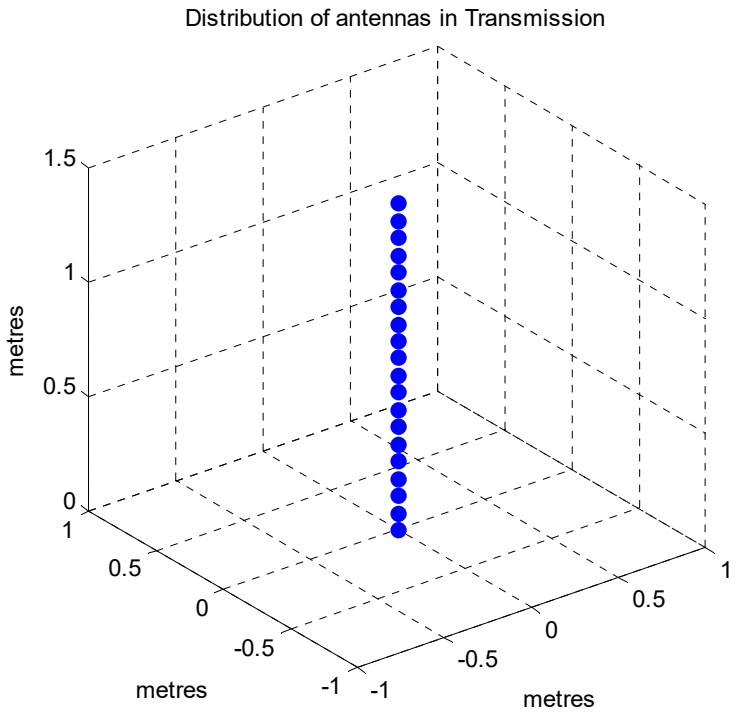

Figure A.19: MISO Linear array at transmission N_t=20

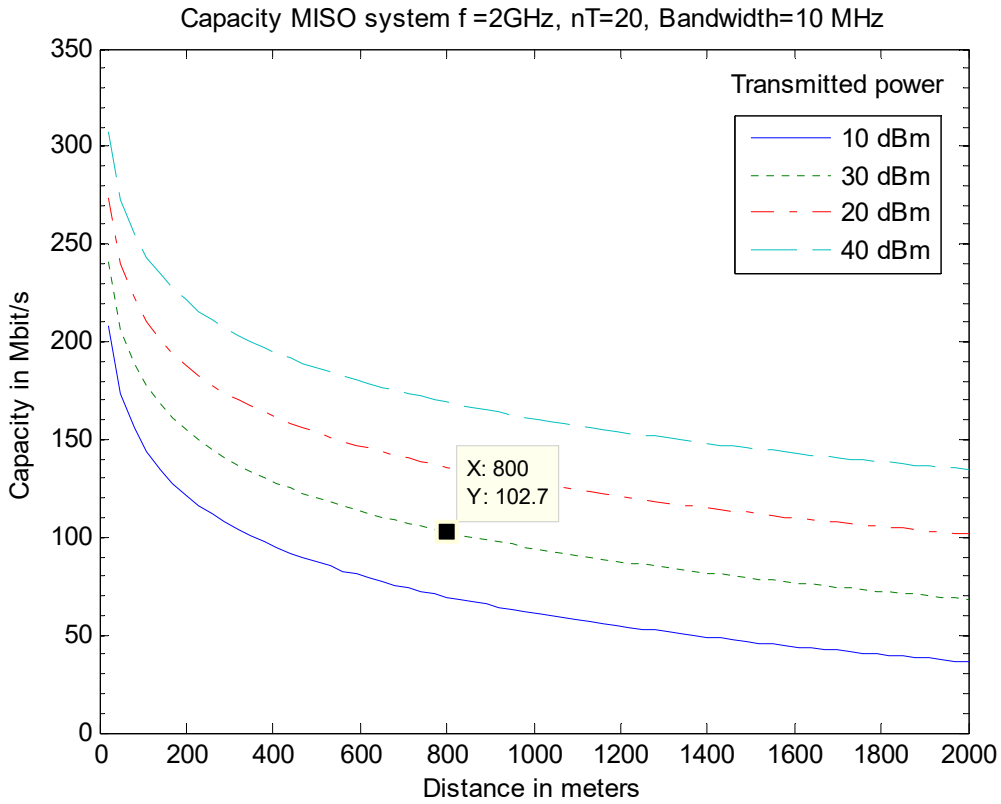

Figure A.20: Capacity of MISO Linear array N_t=20

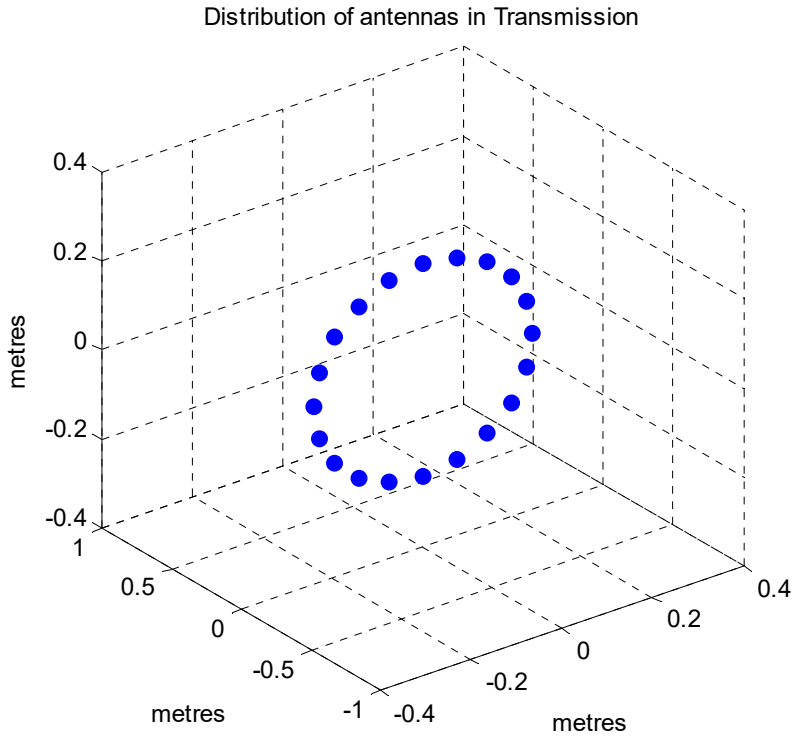

Figure A.21: MISO Circular array at transmission N_t=20

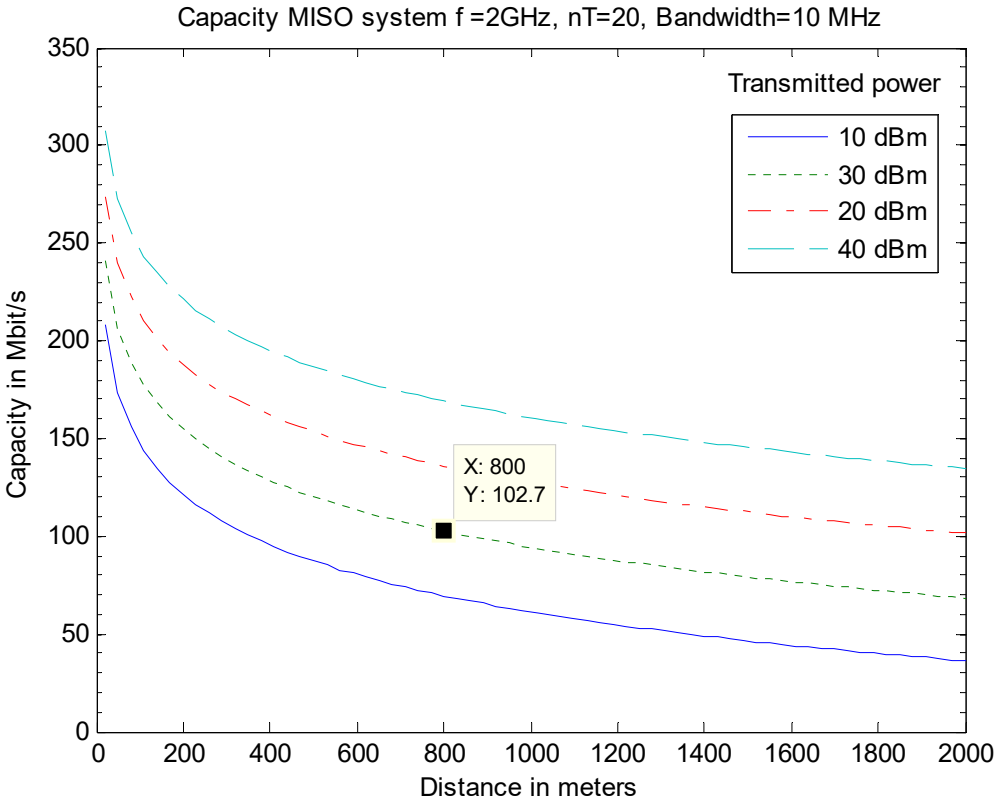

Figure A.22: Capacity of MISO Circular array N_t=20

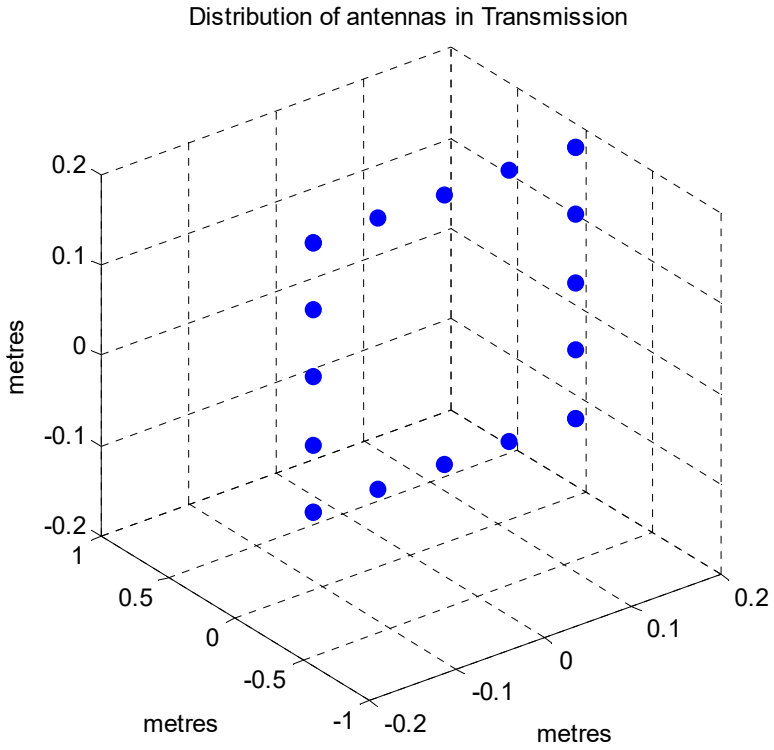

Figure A.23: MISO Square array at transmission N_t=20

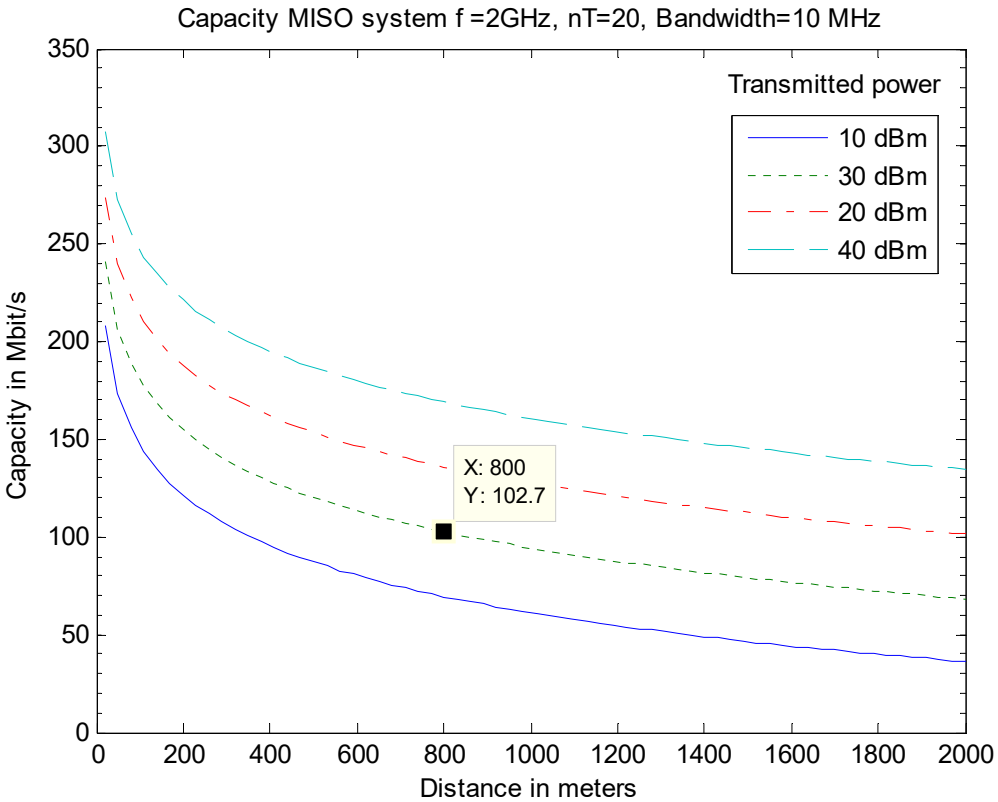

Figure A.24: Capacity of MISO Squares array N_t=20

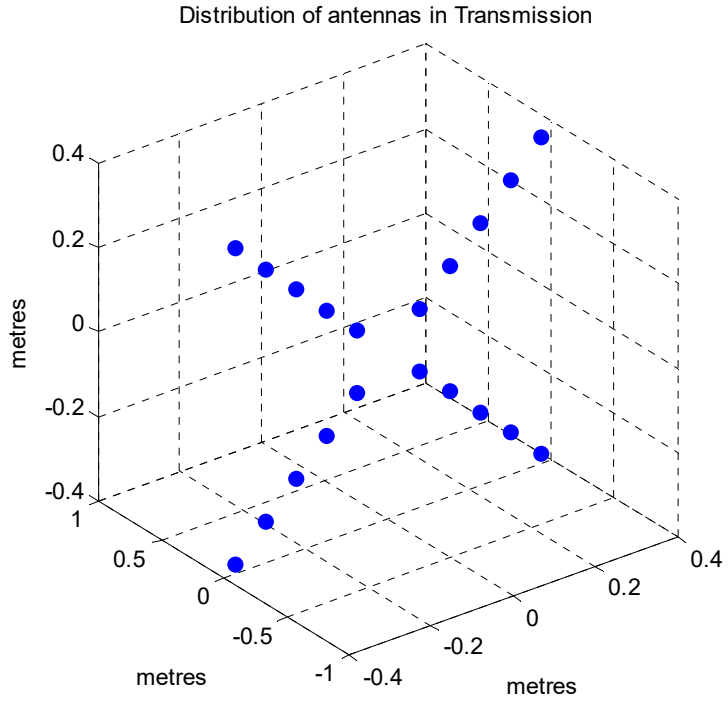

Figure A.25: MISO C. Squares array at transmission N_t=20

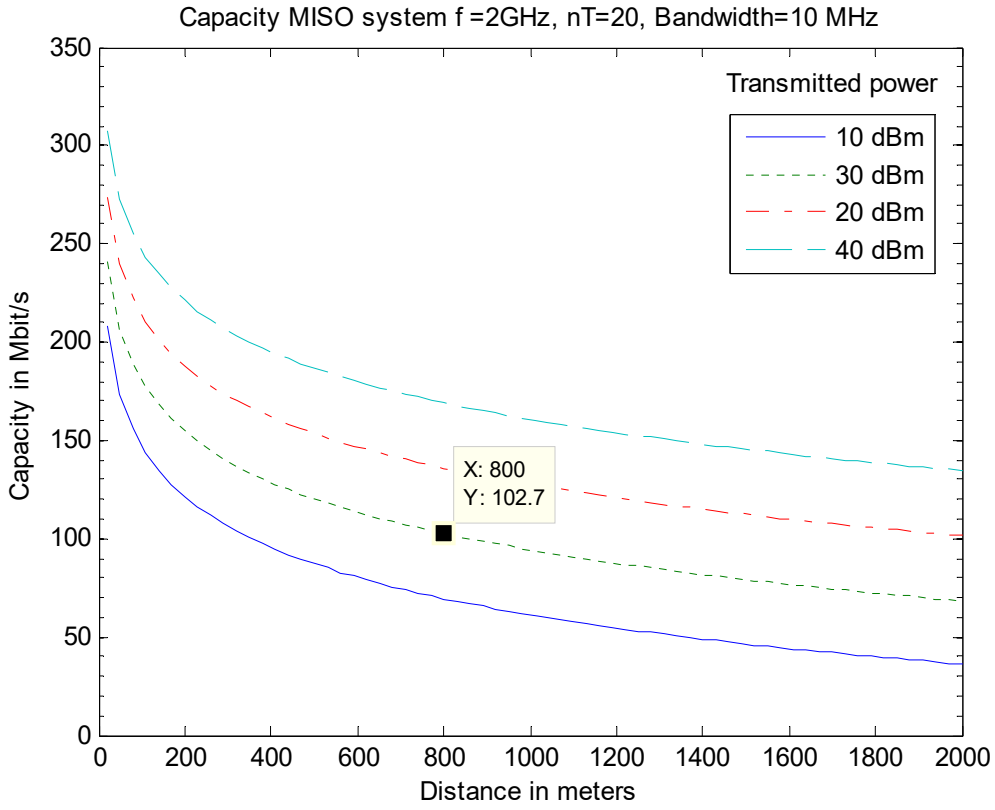

Figure A.26: Capacity of MISO C. Squares array N_t=20

- ***Carrier frequency (f_c):*** 2 GHz
- ***Number of antennas in transmission (n_t):*** 27 antennas
- ***Bandwidth (B):*** 10 MHz
- ***Separation between transmission antennas ($\Delta_t \lambda_c$):*** 7.5 cm (λ/2)
- ***Angle of incidence ($\emptyset$): $\pi/2$***
- ***Transmitted power (P):*** 10, 20, 30 and 40 dBm
- ***Noise power (N_0):*** -104 dBm (-174 dBm/Hz)

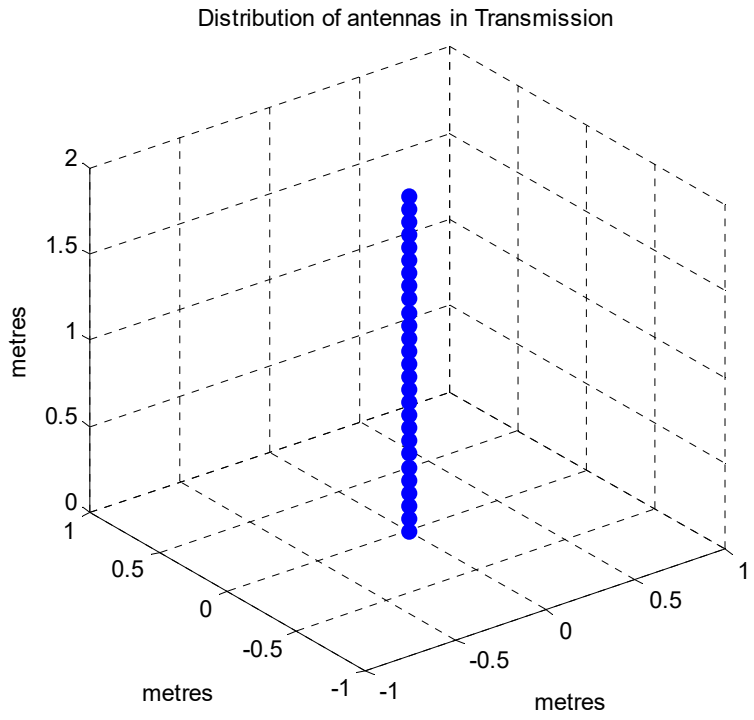

Figure A.27: MISO Linear array at transmission N_t=27

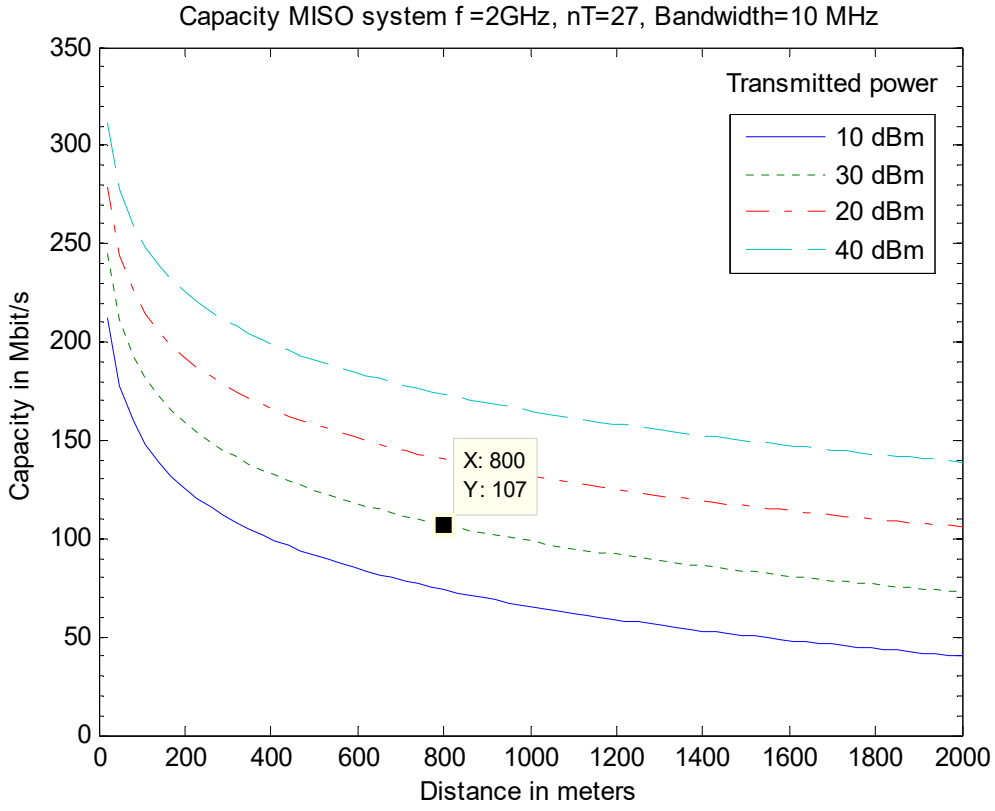

Figure A.28: Capacity of MISO Linear array N_t=27

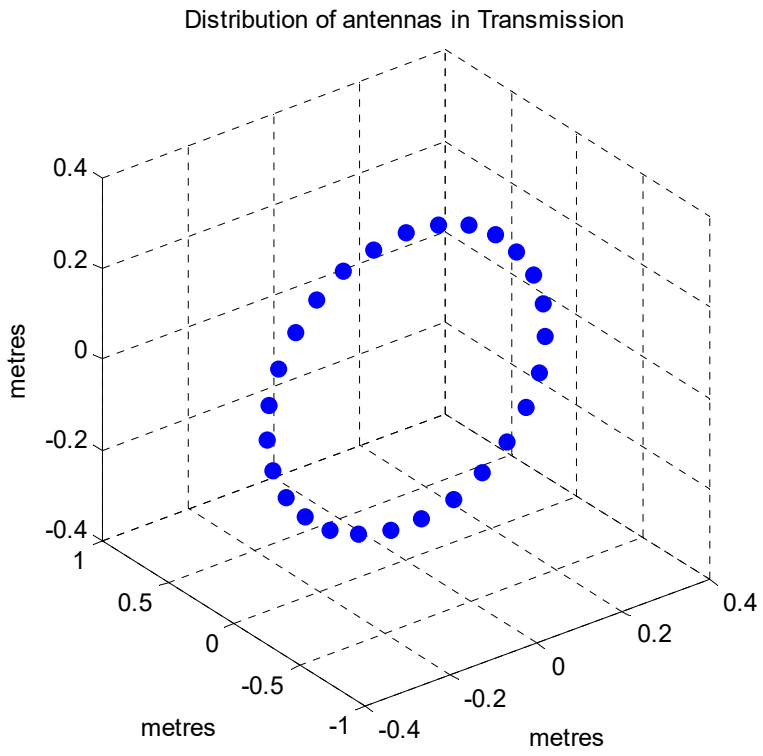

Figure A.29: MISO Circular array at transmission N_t=27

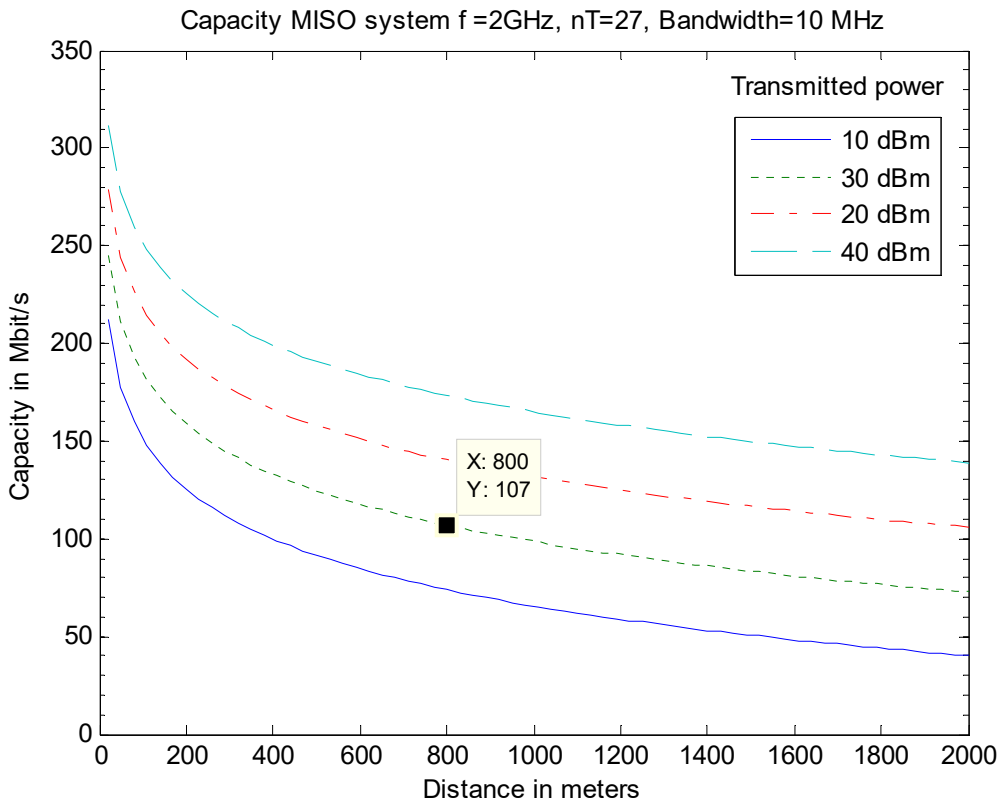

Figure A.30: Capacity of MISO Circular array N_t=27

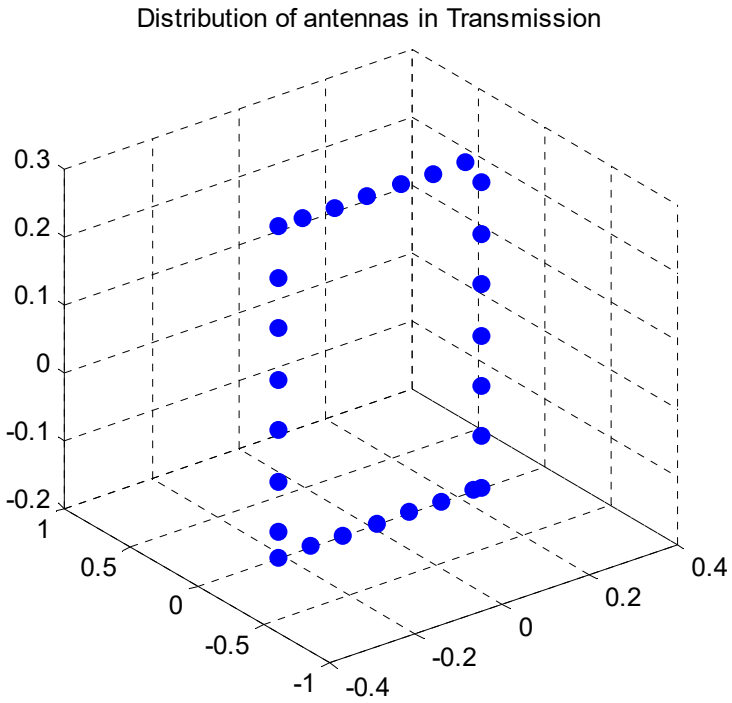

Figure A.31: MISO Square array at transmission N_t=27

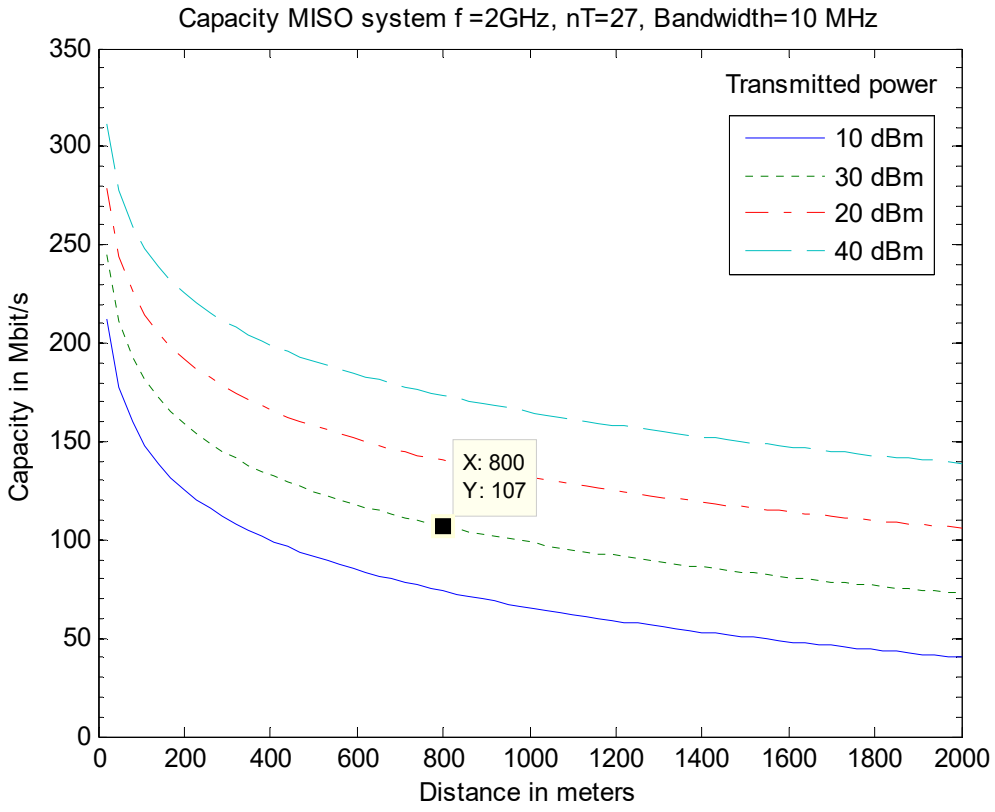

Figure A.32: Capacity of MISO Square array N_t=27

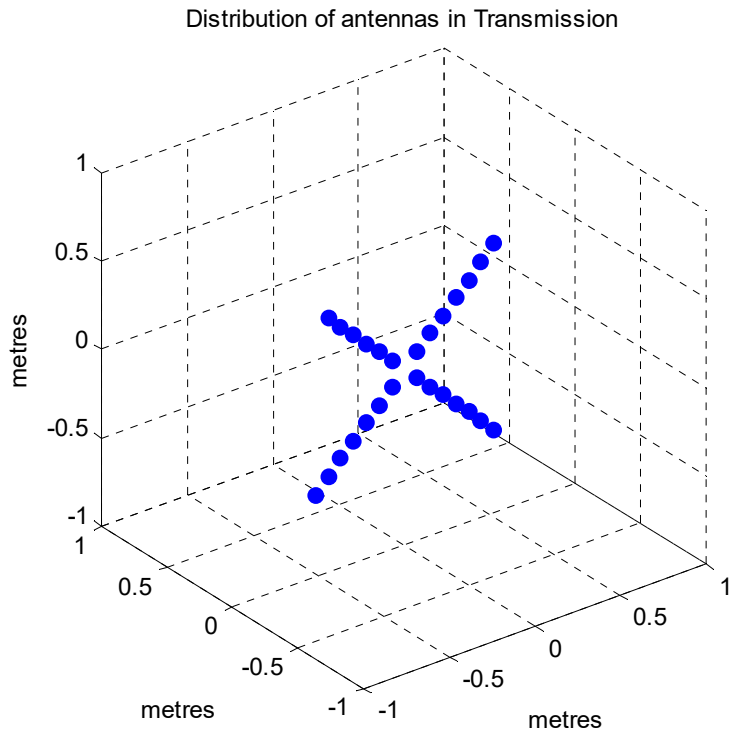

Figure A.33: MISO C. Squares array at transmission N_t=27

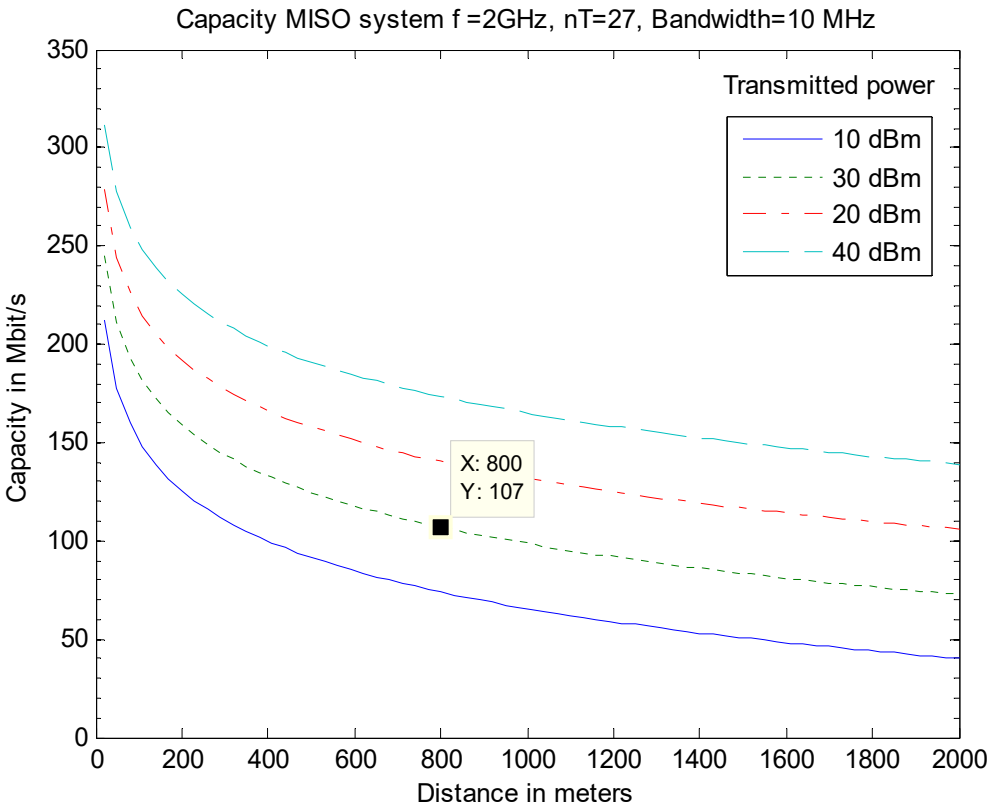

Figure A.34: Capacity of MISO C. Squares array N_t=27

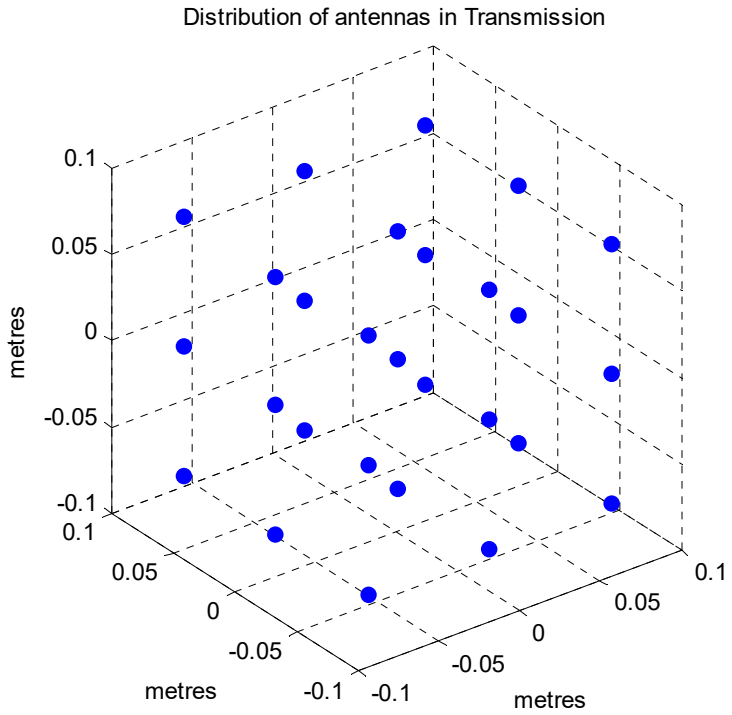

Figure A.35: MISO Cubical array at transmission N_t=27

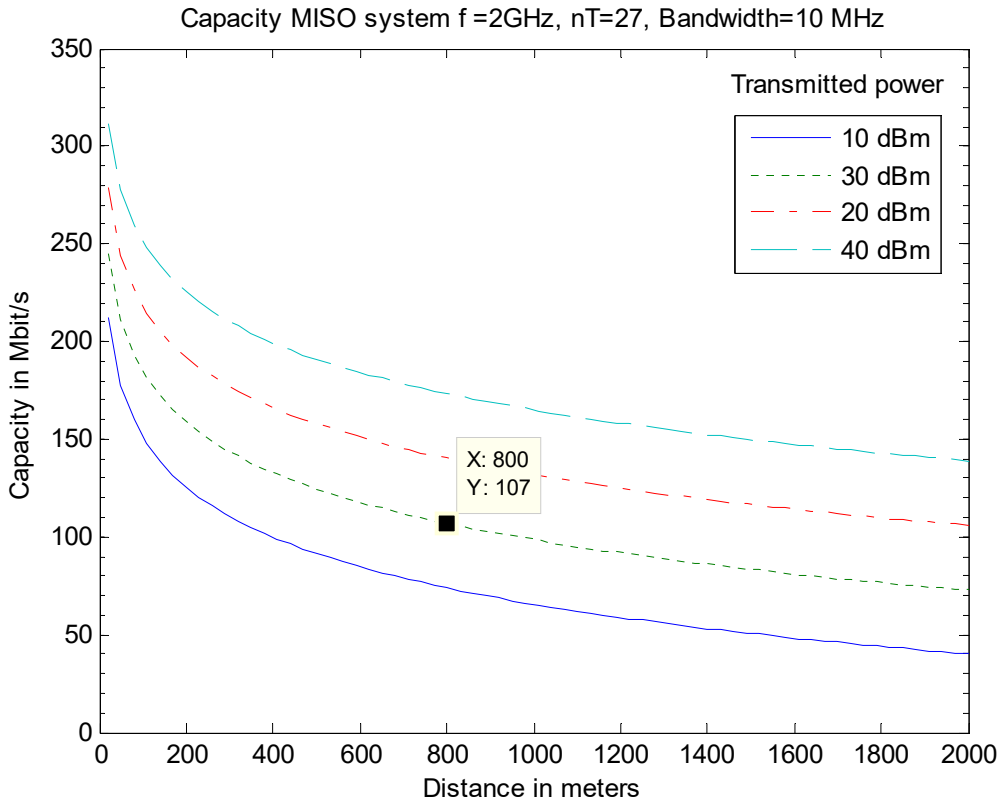

Figure A.36: Capacity of MISO Cubical array N_t=27

A.2.3 MIMO

- ***Carrier frequency (f_c):*** 2 GHz
- ***Number of antennas in reception (n_r):*** 20 antennas
- ***Number of antennas in transmission (n_t):*** 20 antennas
- ***Bandwidth (B):*** 10 MHz
- ***Separation between reception antennas ($\Delta_r \lambda_c$):*** 7.5 cm (λ/2)
- ***Separation between transmission antennas ($\Delta_t \lambda_c$):*** 7.5 cm (λ/2)
- ***Angle of incidence (∅): $\pi/2$***
- ***Transmitted power (P):*** 10, 20, 30 and 40 dBm
- ***Noise power (N_0):*** -104 dBm (-174 dBm/Hz)

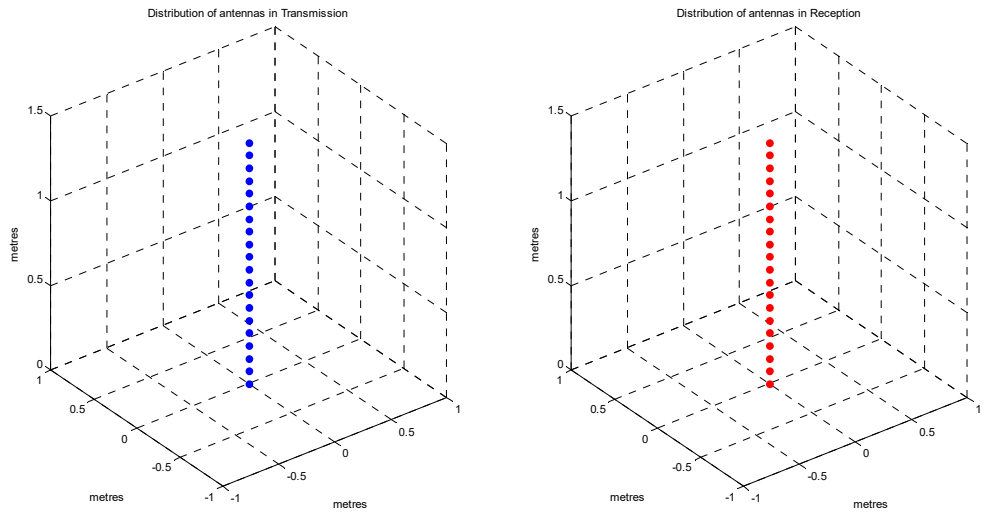

Figure A.37: MIMO Linear array at transmission N_t=20 and Linear array at reception N_r =20

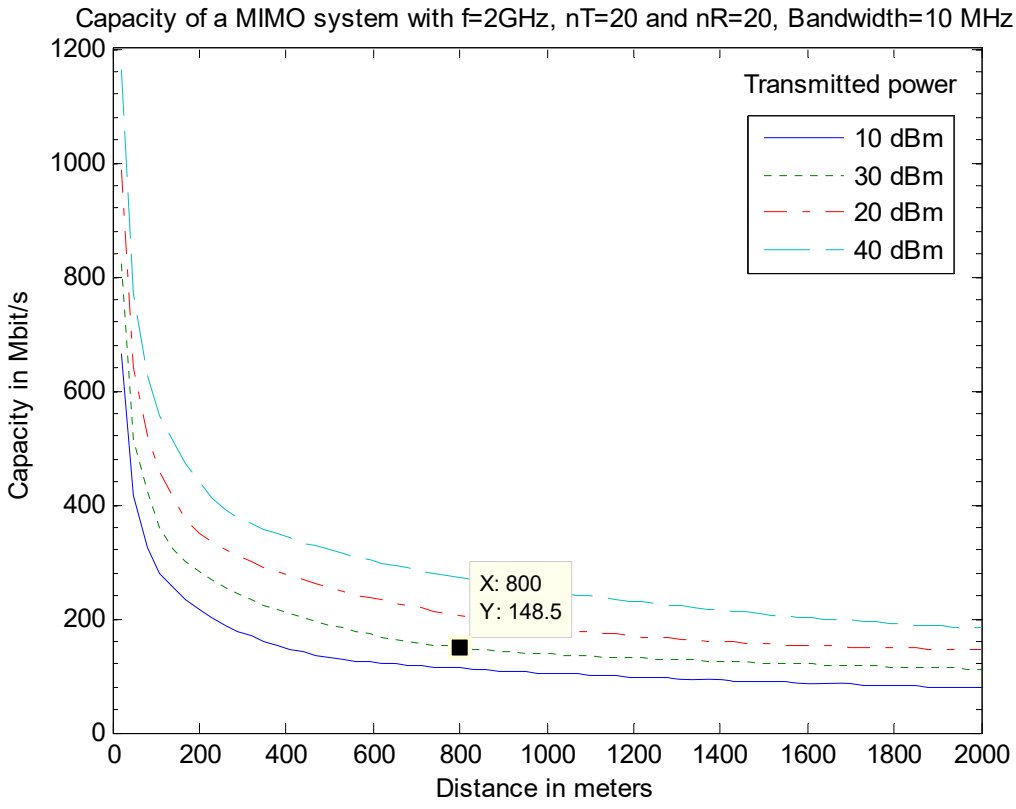

Figure A.38: Capacity of MIMO Linear array N_t=20 and Linear array N_r=20

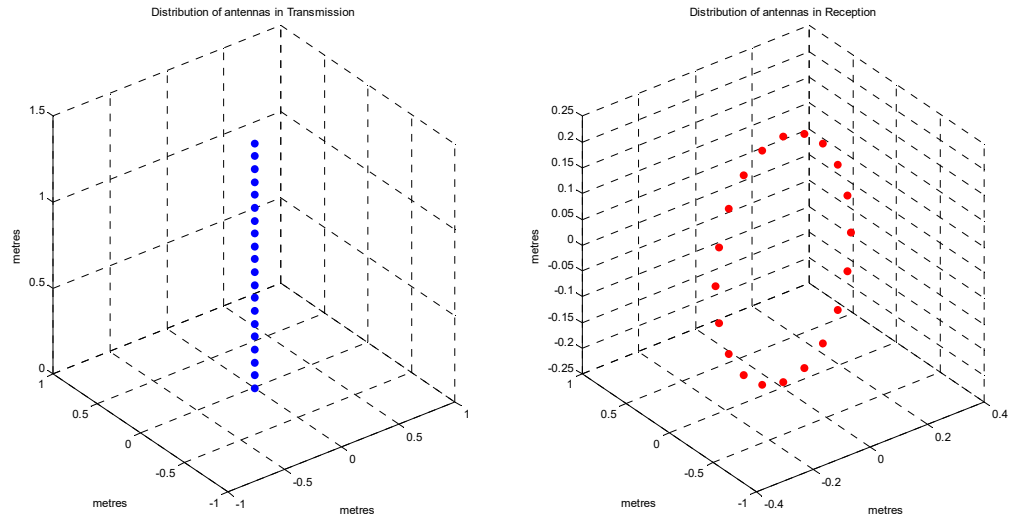

Figure A.39: MIMO Linear array at transmission N_t=20 and Circular array at reception N_r =20

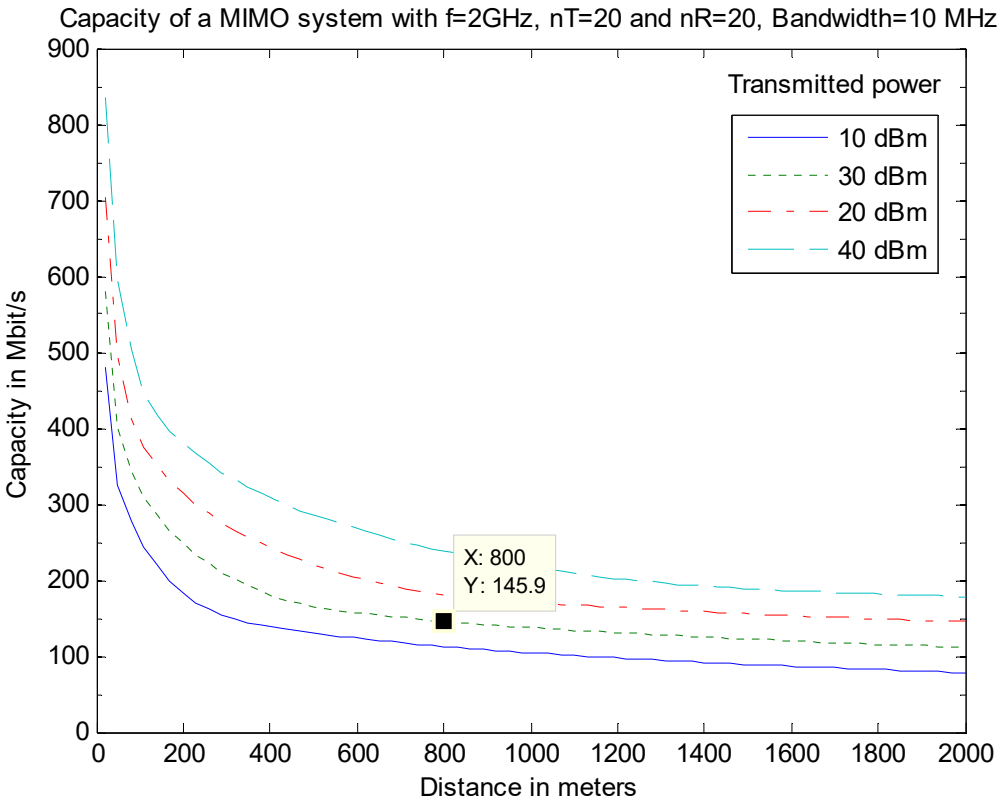

Figure A.40: Capacity of MIMO Linear array N_t=20 and Circular array N_r=20

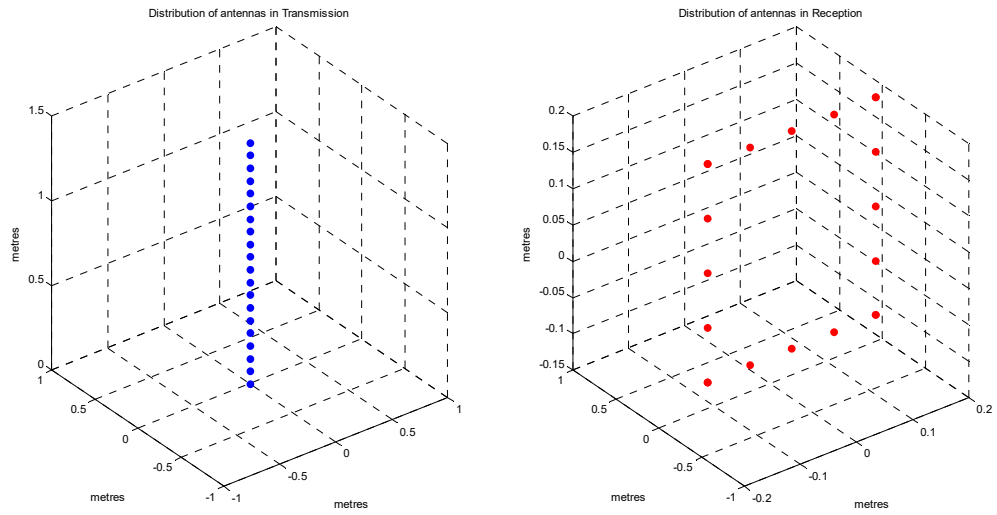

Figure A.41: MIMO Linear array at transmission N_t=20 and Square array at reception N_r =20

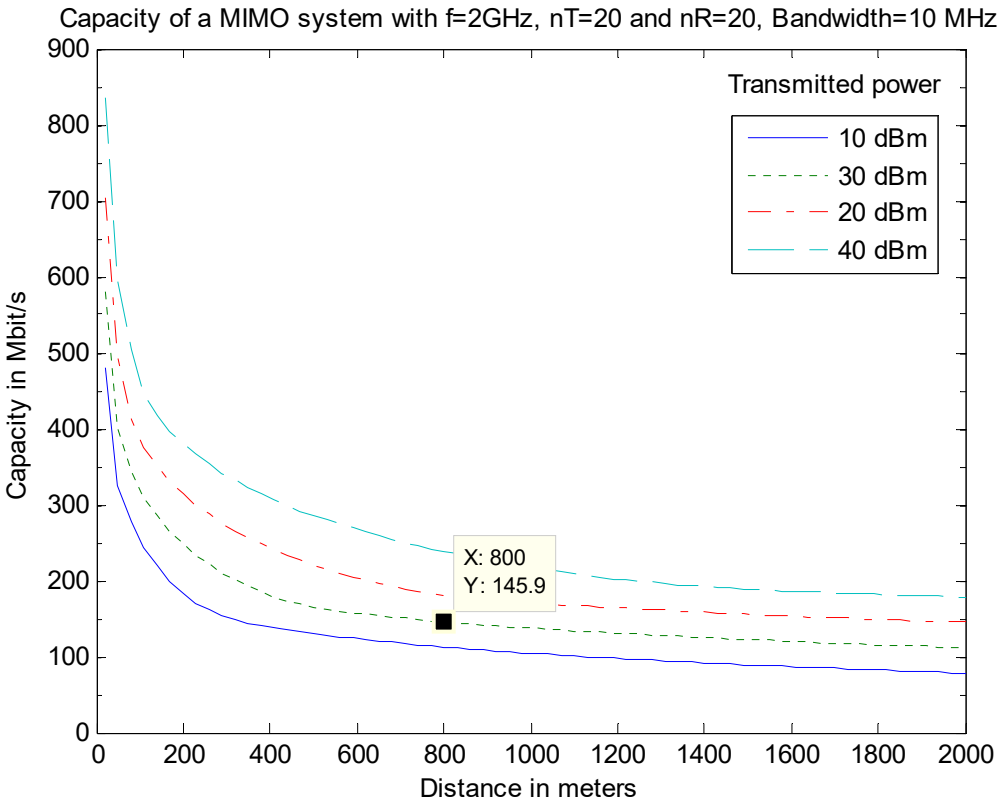

Figure A.42: Capacity of MIMO Linear array N_t=20 and Square array N_r=20

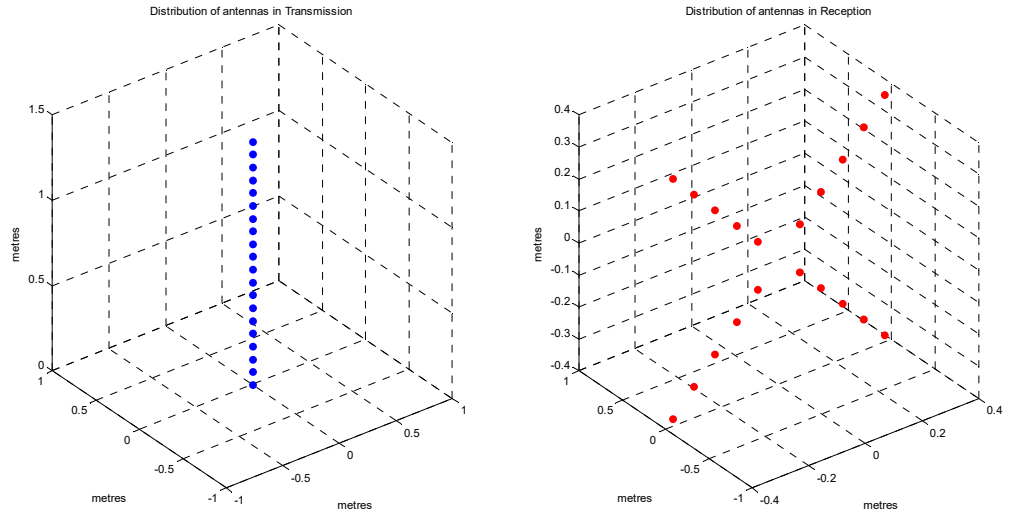

Figure A.43: MIMO Linear array at transmission N_t=20 and C. Squares array at reception N_r =20

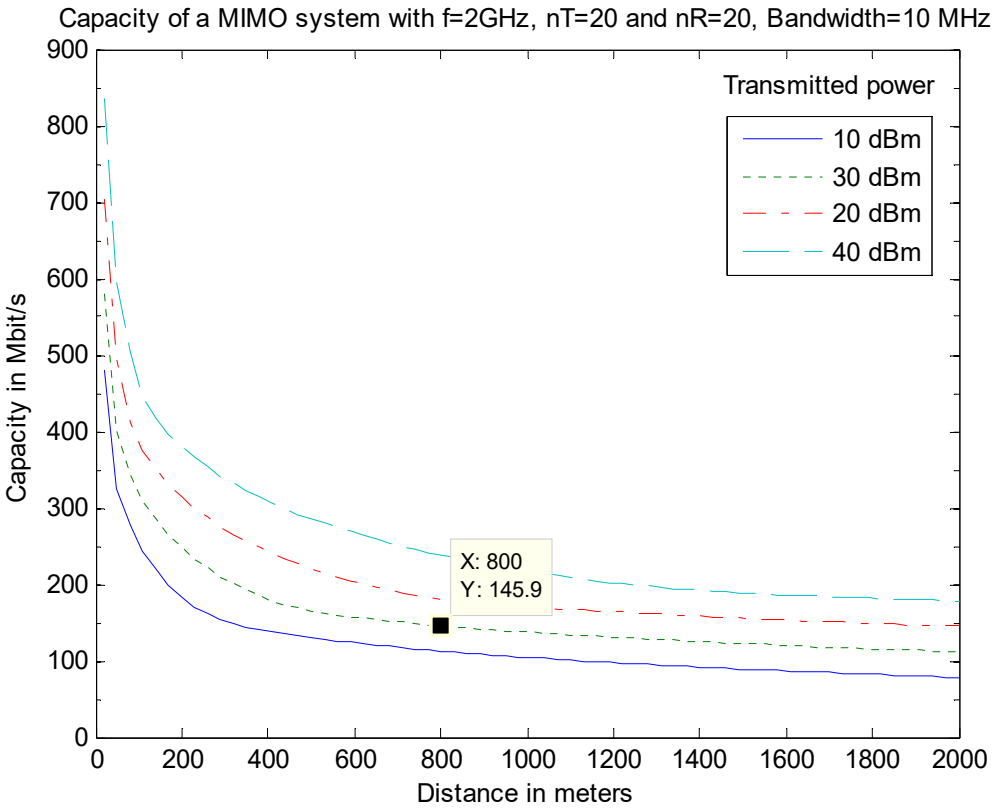

Figure A.44: Capacity of MIMO Linear array N_t=20 and C. Squares array N_r=20

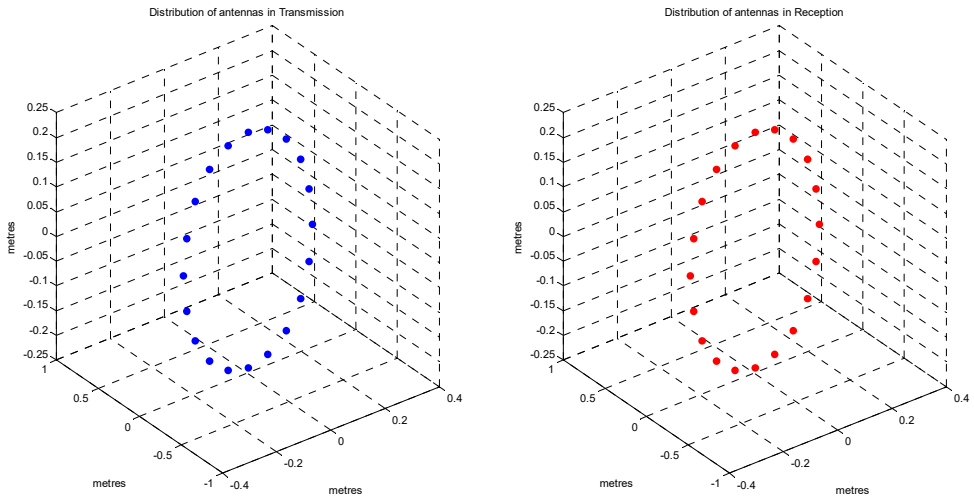

Figure A.45: MIMO Circular array at transmission N_t=20 and Circular array at reception N_r =20

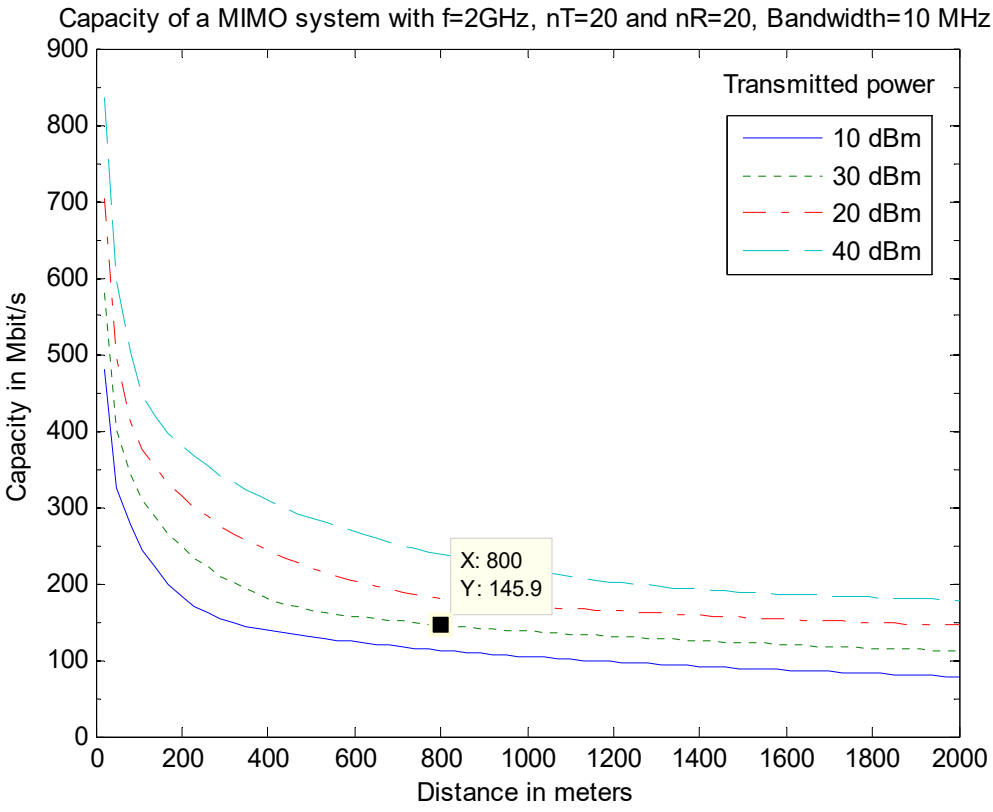

Figure A.46: Capacity of MIMO Circular array N_t=20 and Circular array N_r=20

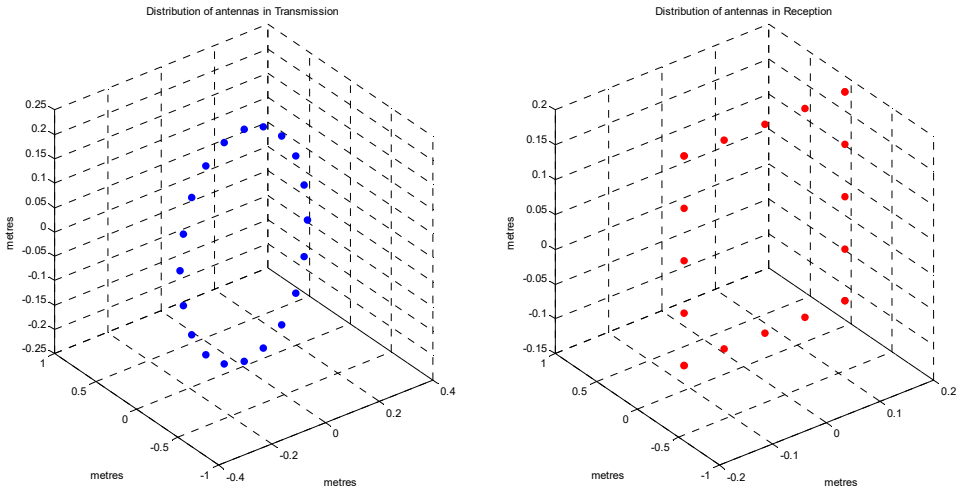

Figure A.47: MIMO Circular array at transmission N_t=20 and Square array at reception N_r =20

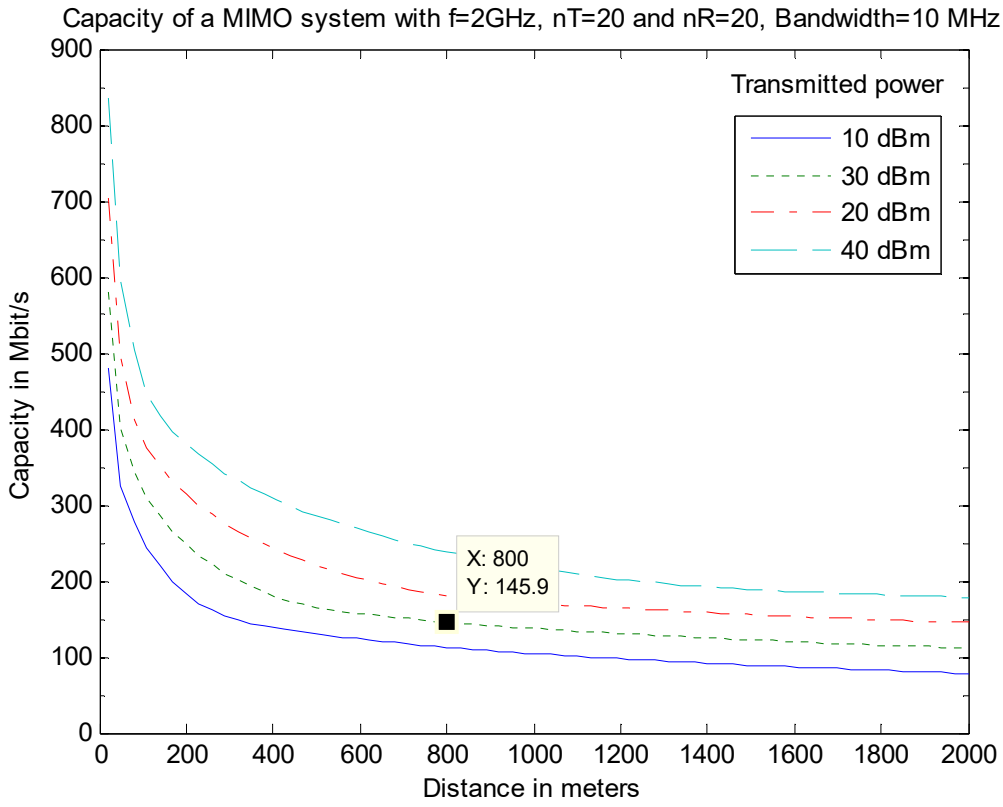

Figure A.48: Capacity of MIMO Circular array N_t=20 and Square array N_r=20

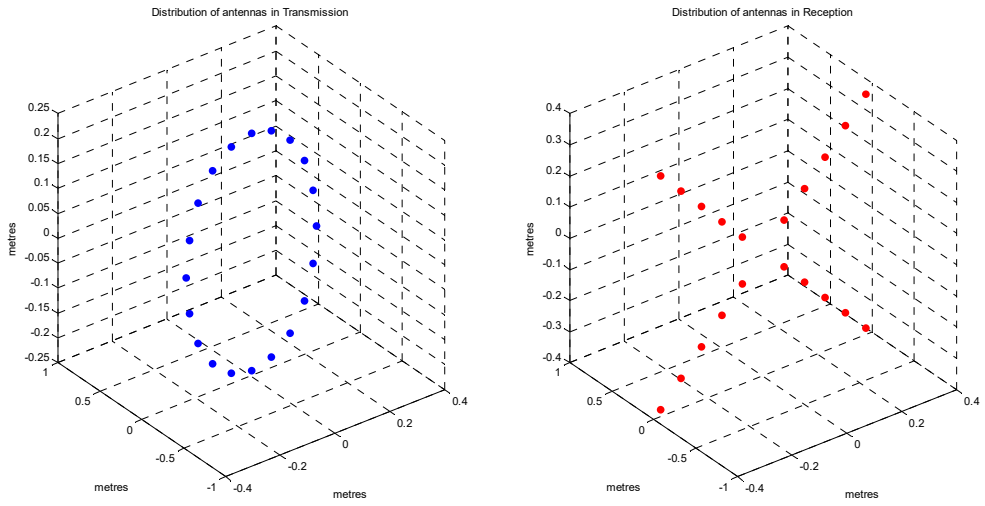

Figure A.49: MIMO Circular array at transmission N_t=20 and C. Squares array at reception N_r =20

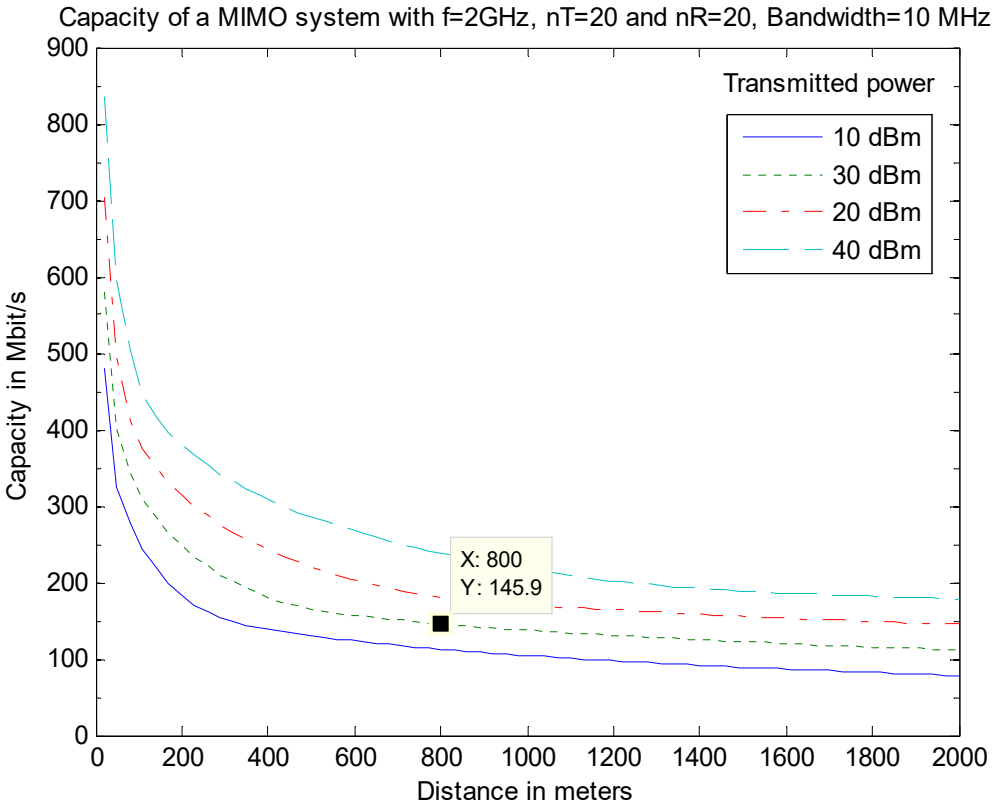

Figure A.50: Capacity of MIMO Circular array N_t=20 and C. Squares array N_r=20

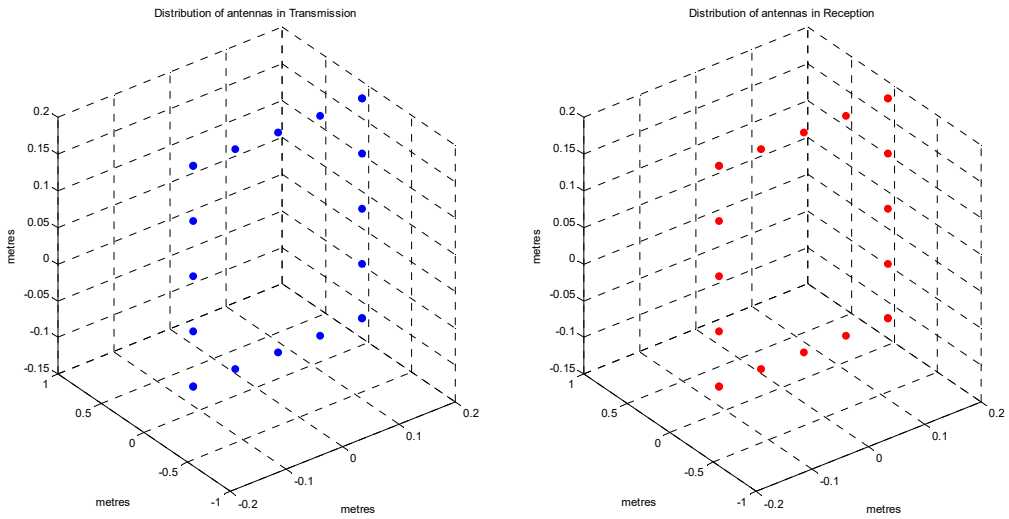

Figure A.51: MIMO Square array at transmission N_t=20 and Square array at reception N_r =20

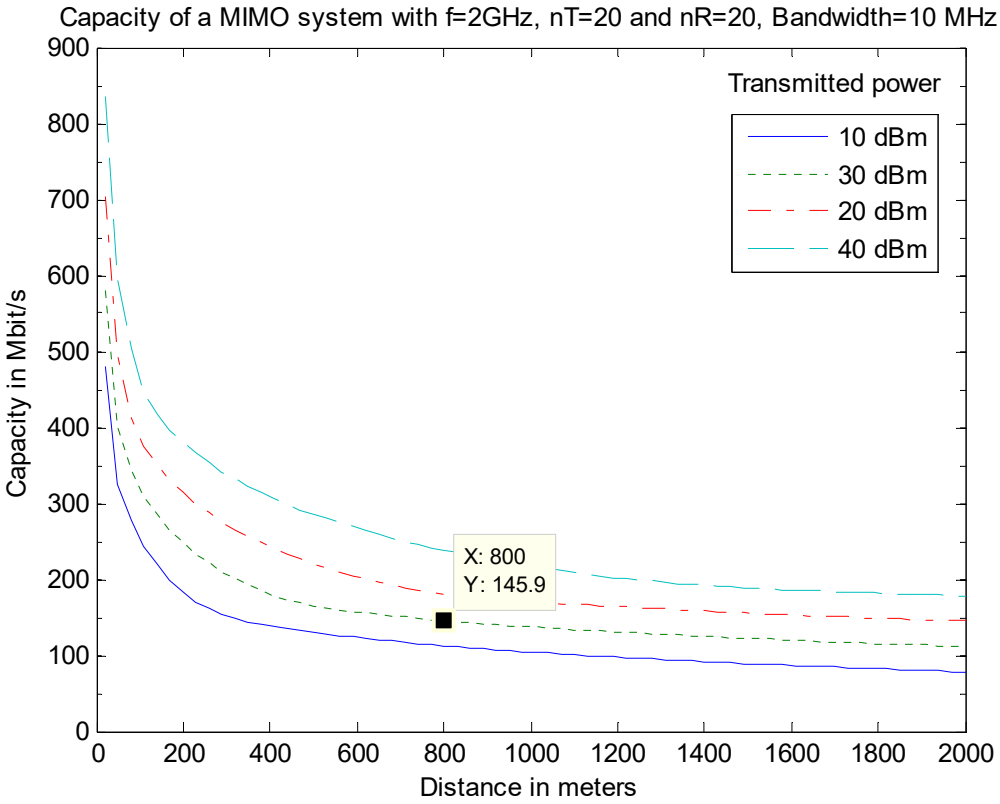

Figure A.52: Capacity of MIMO Square array N_t=20 and Square array N_r=20

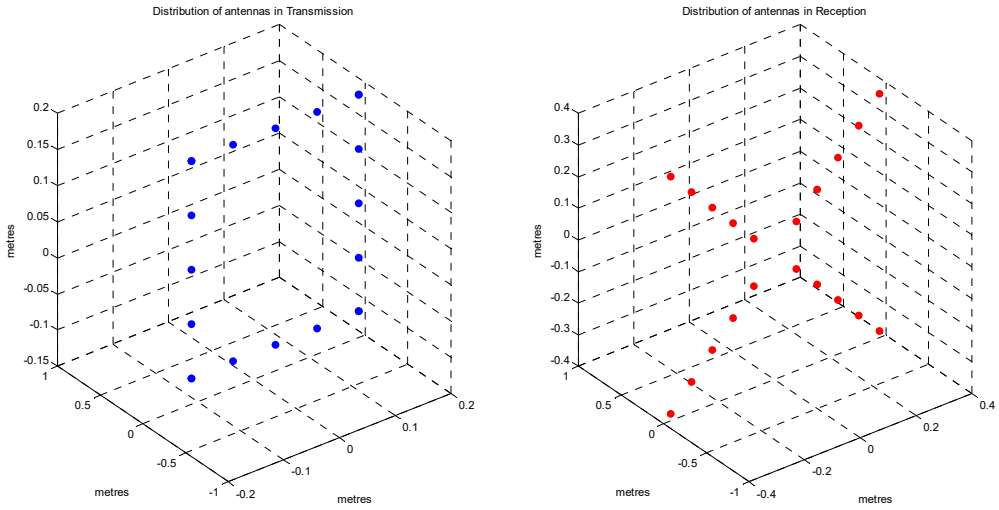

Figure A.53: MIMO C. Squares array at transmission N_t=20 and C. Squares array at reception N_r =20

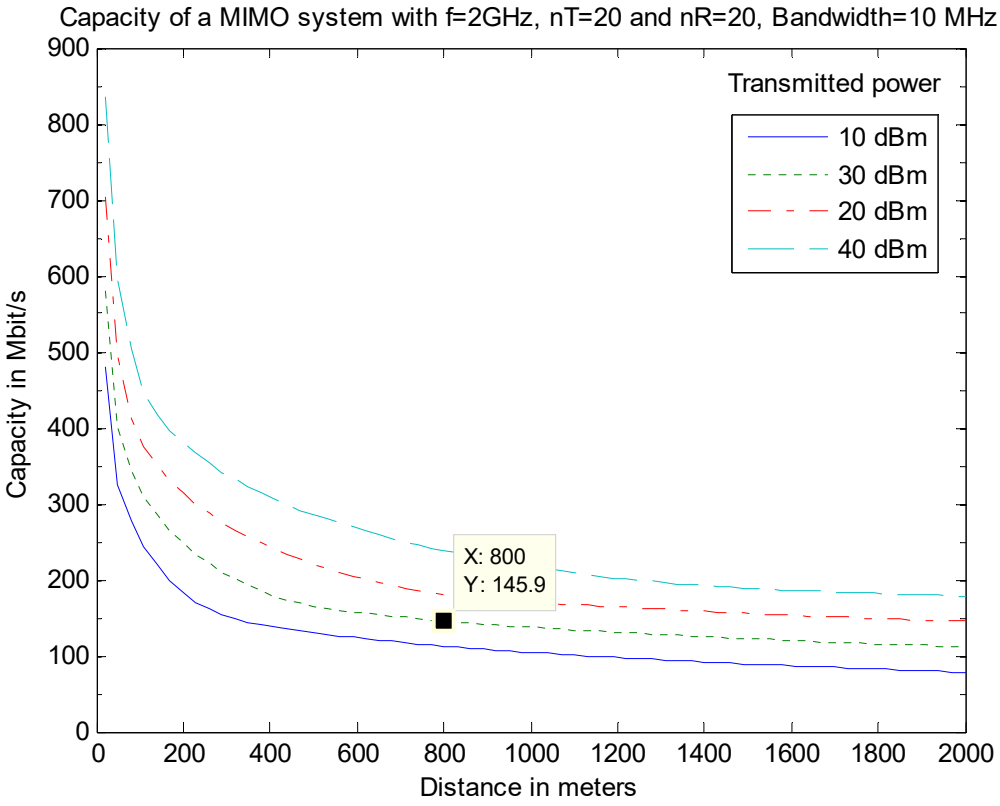

Figure A.54: Capacity of MIMO C. Squares array N_t=20 and C. Squares array N_r=20

- ***Carrier frequency (f_c):*** 2 GHz
- ***Number of antennas in reception (n_r):*** 27 antennas
- ***Number of antennas in transmission (n_t):*** 20 antennas
- ***Bandwidth (B):*** 10 MHz
- ***Separation between reception antennas ($\Delta_r \lambda_c$):*** 7.5 cm (λ/2)
- ***Separation between transmission antennas ($\Delta_t \lambda_c$):*** 7.5 cm (λ/2)
- ***Angle of incidence (∅): $\pi/2$***
- ***Transmitted power (P):*** 10, 20, 30 and 40 dBm
- ***Noise power (N_0):*** -104 dBm (-174 dBm/Hz)

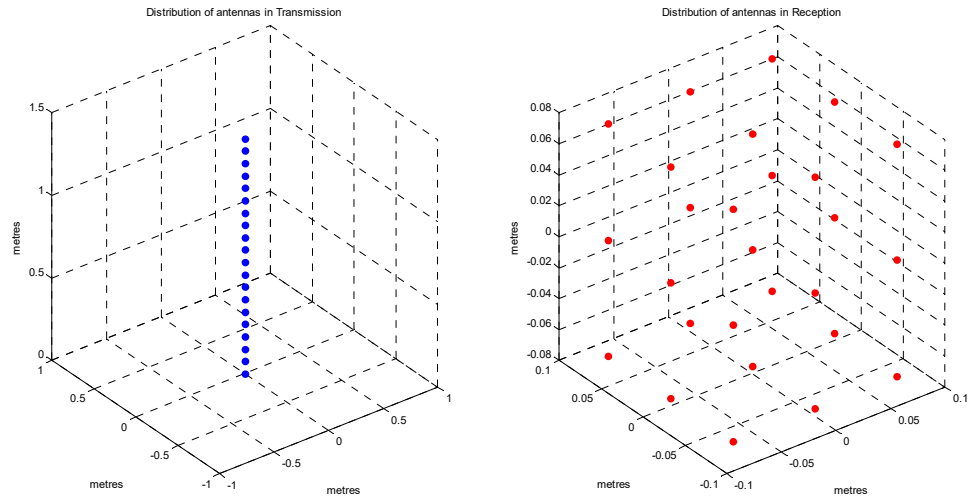

Figure A.55: MIMO Linear array at transmission N_t=20 and Cube array at reception N_r =27

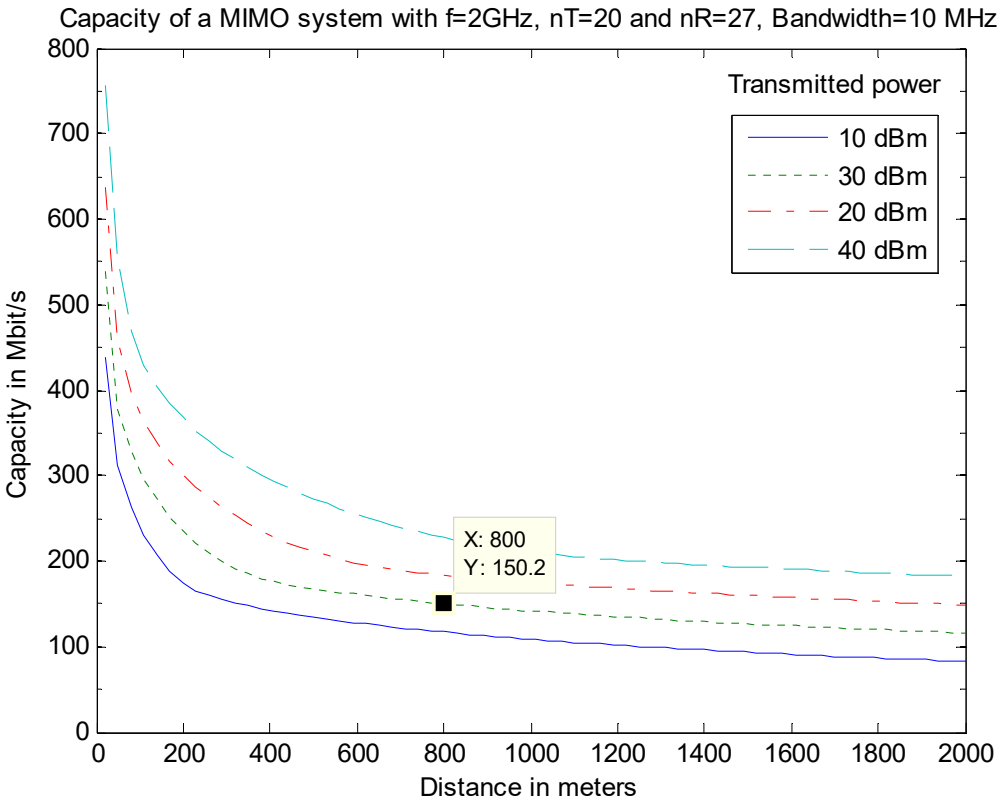

Figure A.56: Capacity of MIMO Linear array N_t=20 and Cube array N_r=27

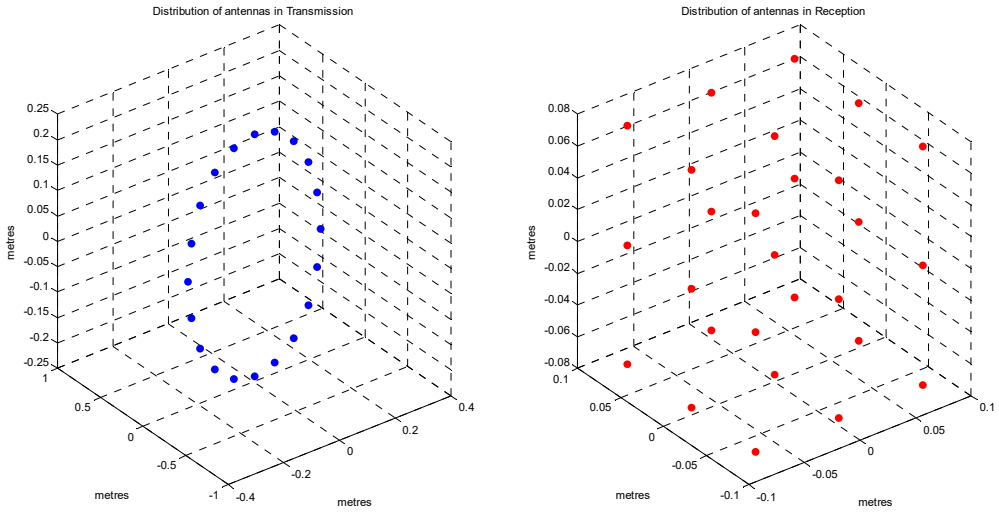

Figure A.57.: MIMO Circular array at transmission N_t=20 and Cube array at reception N_r =27

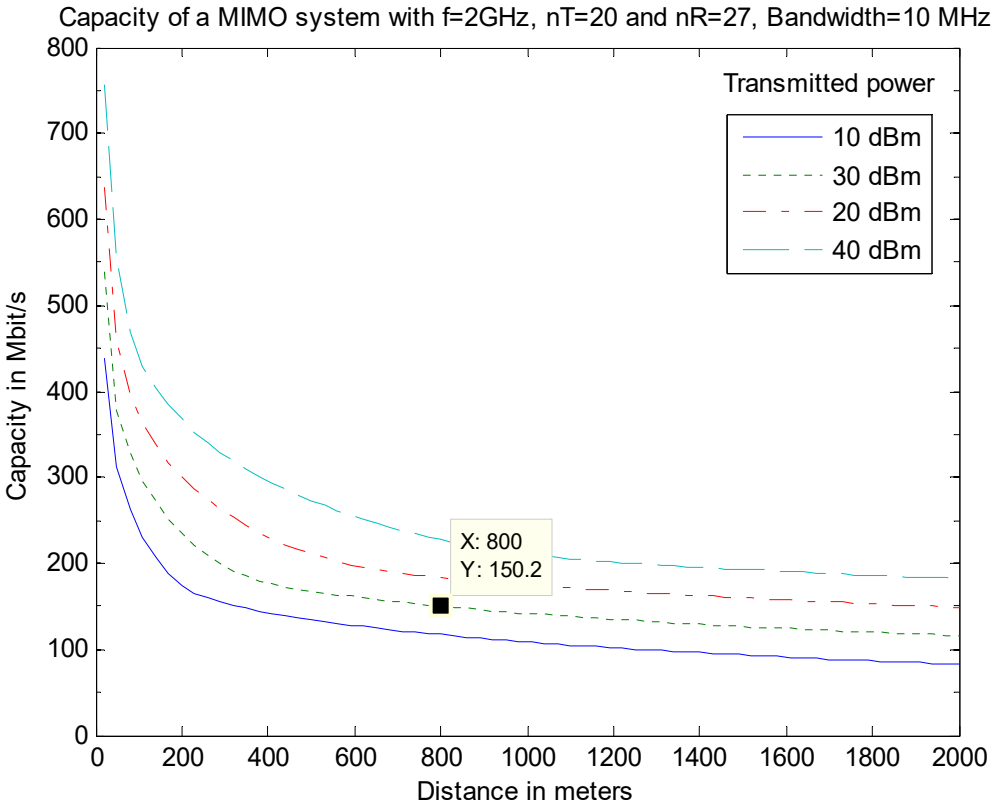

Figure A.58: Capacity of MIMO Circular array N_t=20 and Cube array N_r=27

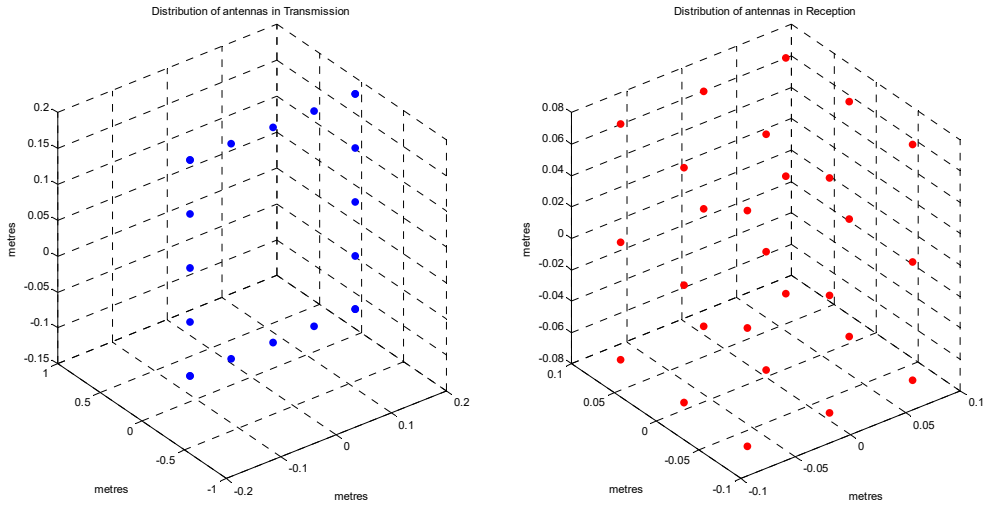

Figure A.59: MIMO Square array at transmission N_t=20 and Cube array at reception N_r =27

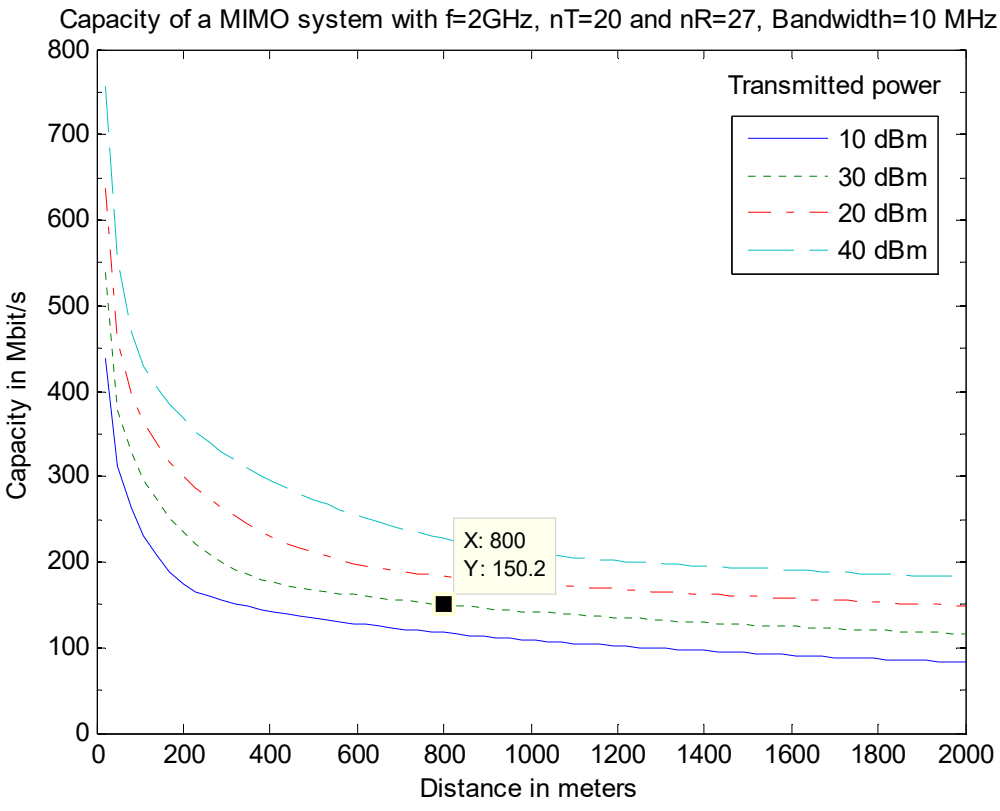

Figure A.60: Capacity of MIMO Square array N_t=20 and Cube array N_r=27

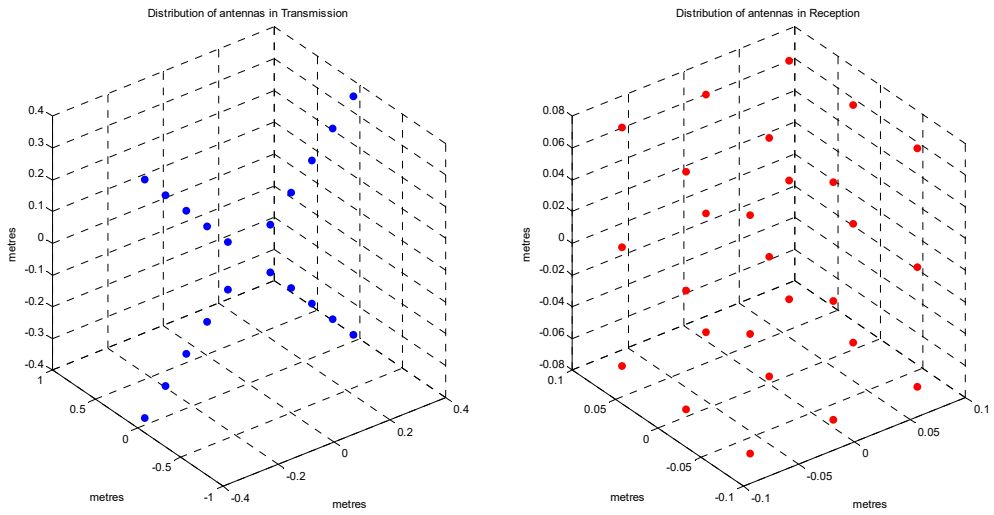

Figure A.61: MIMO C. Squares array at transmission N_t=20 and Cube array at reception N_r =27

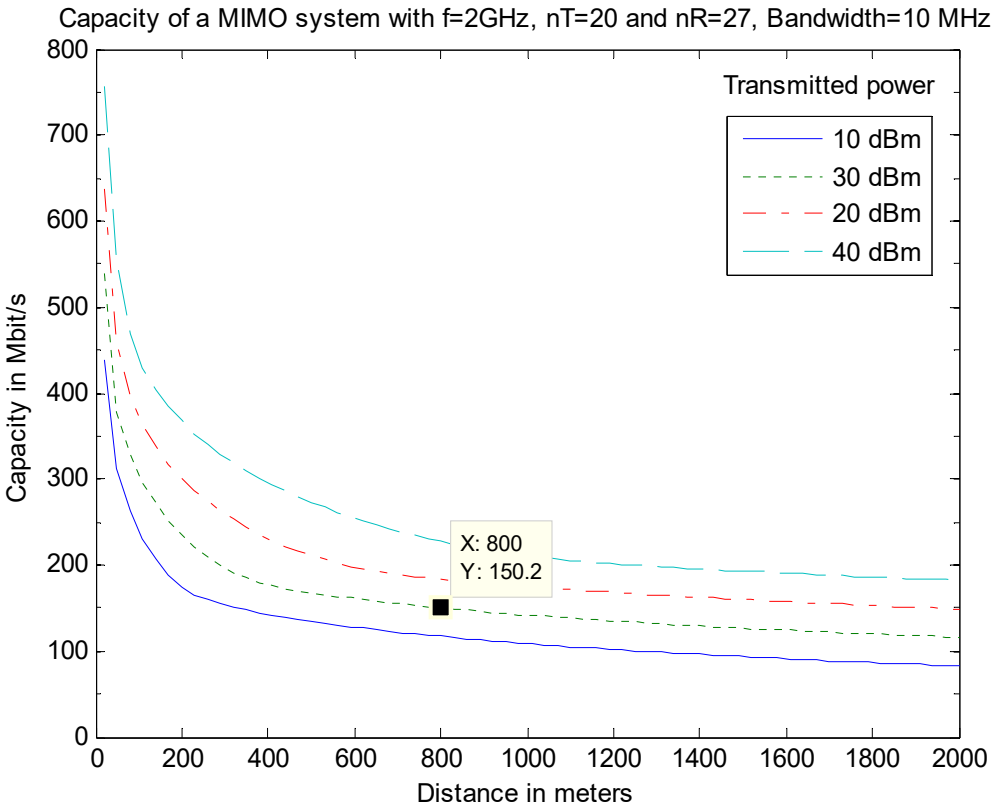

Figure A.62: Capacity of MIMO C. Squares array N_t=20 and Cube array N_r=27

- ***Carrier frequency (f_c):*** 2 GHz
- ***Number of antennas in reception (n_r):*** 27 antennas
- ***Number of antennas in transmission (n_t):*** 27 antennas
- ***Bandwidth (B):*** 10 MHz
- ***Separation between reception antennas ($\Delta_r \lambda_c$):*** 7.5 cm (λ/2)
- ***Separation between transmission antennas ($\Delta_t \lambda_c$):*** 7.5 cm (λ/2)
- ***Angle of incidence ($\emptyset$): $\pi/2$***
- ***Transmitted power (P):*** 10, 20, 30 and 40 dBm
- ***Noise power (N_0):*** -104 dBm (-174 dBm/Hz)

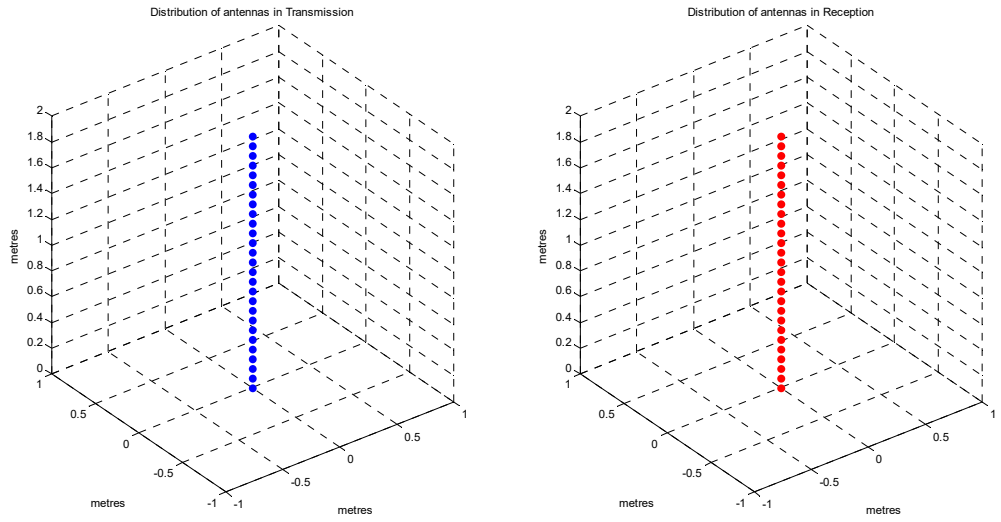

Figure A.63: MIMO Linear array at transmission N_t=27 and Linear array at reception N_r =27

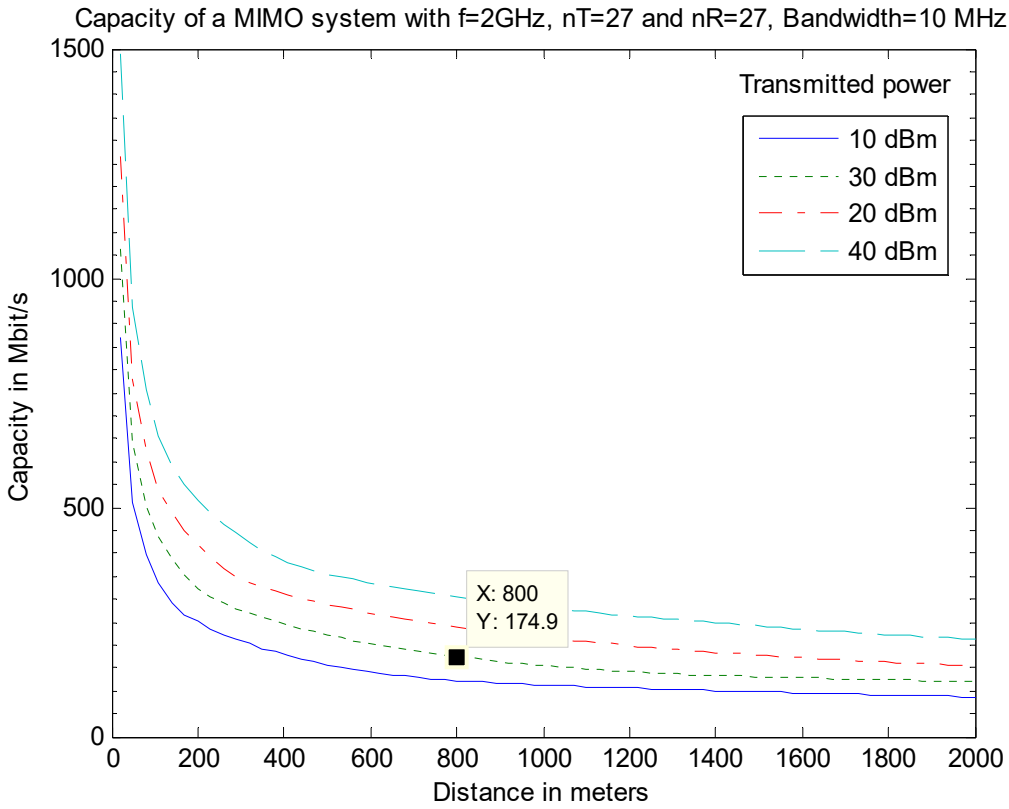

Figure A.64: Capacity of MIMO Linear array N_t=27 and Linear array N_r=27

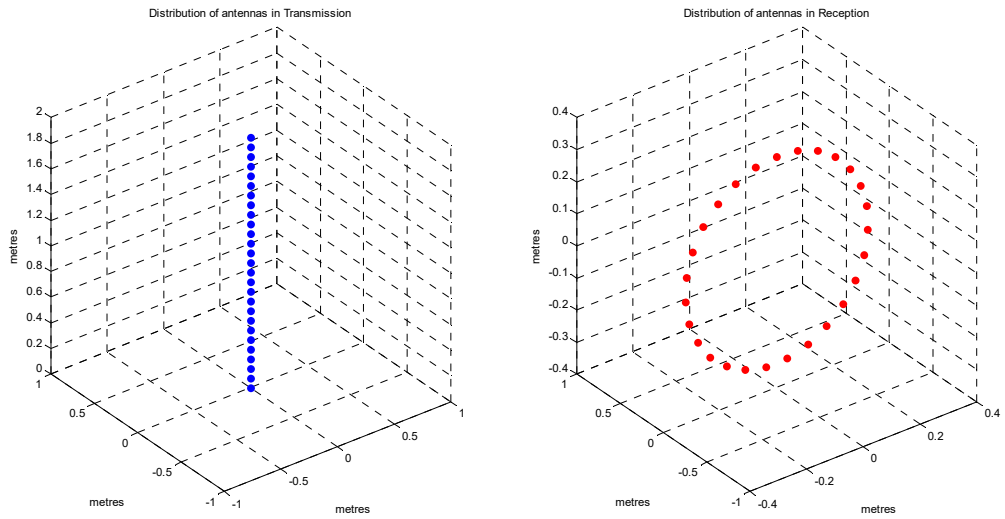

Figure A.65: MIMO Linear array at transmission N_t=27 and Circular array at reception N_r =27

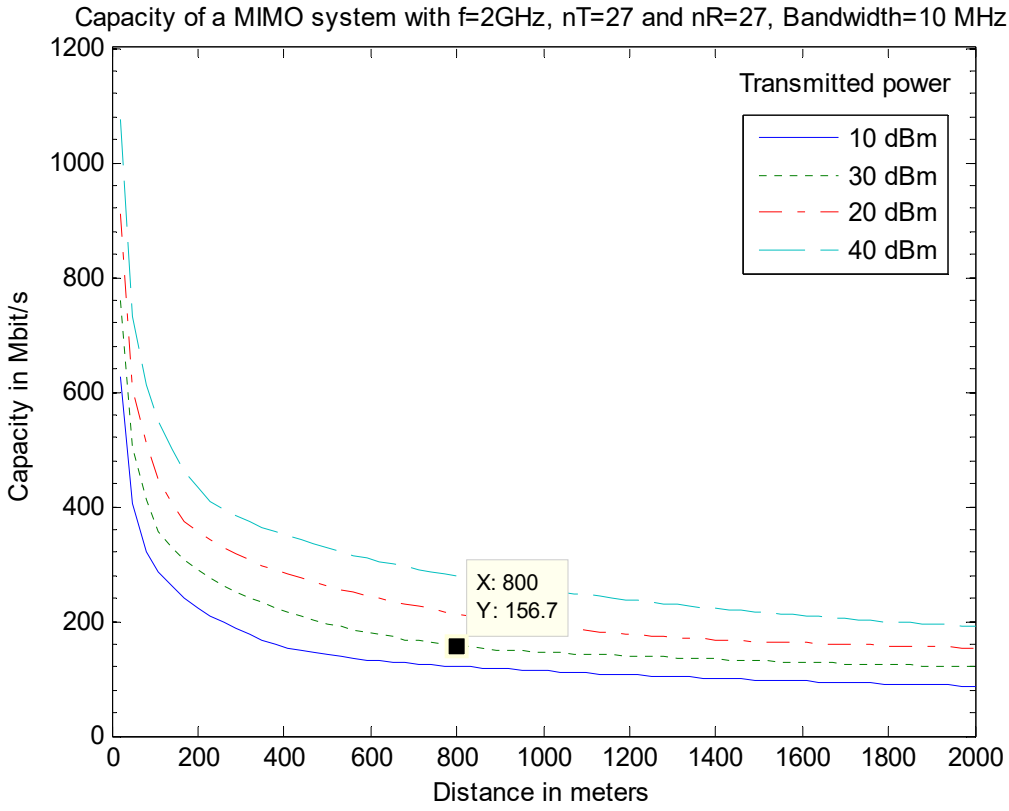

Figure A.66: Capacity of MIMO Linear array N_t=20 and Circular array N_r=20

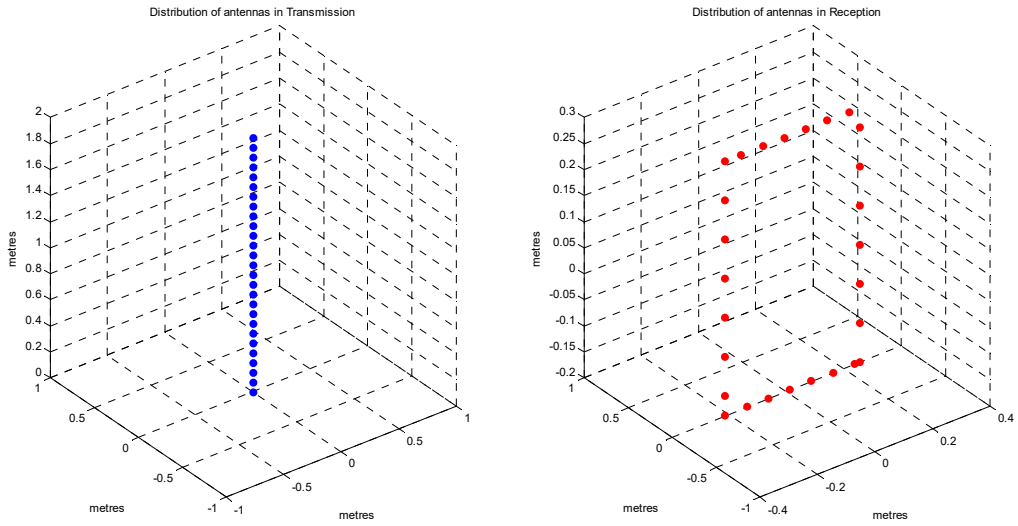

Figure A.67: MIMO Linear array at transmission N_t=27 and Square array at reception N_r =27

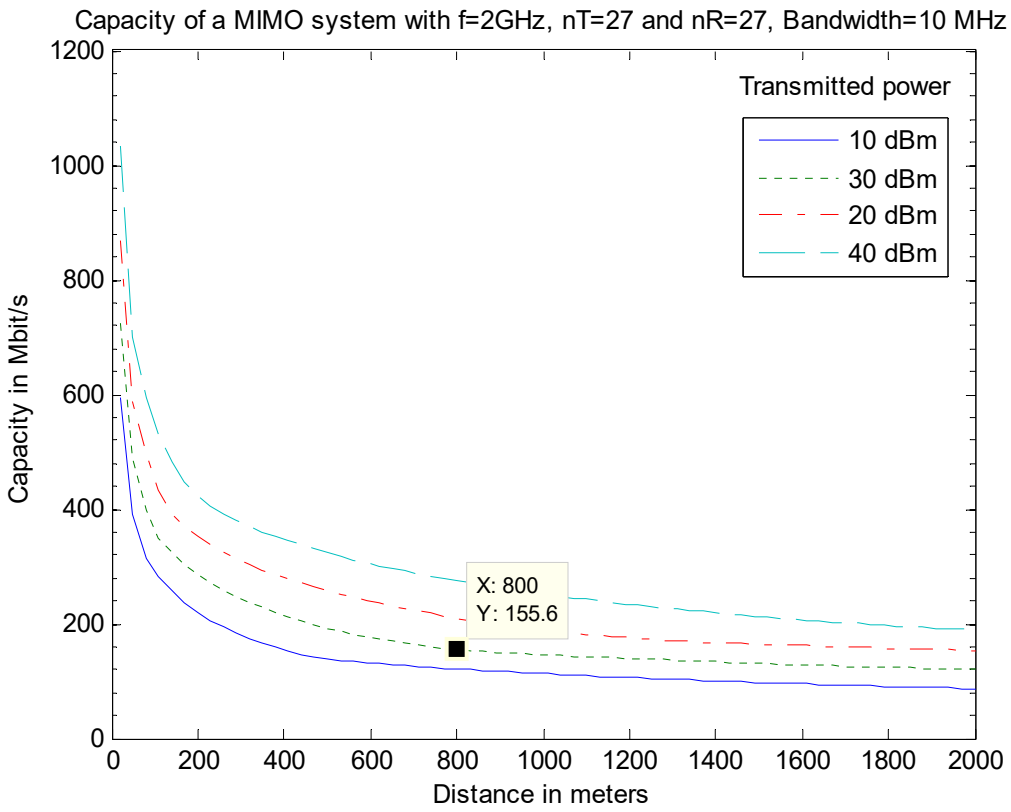

Figure A.68: Capacity of MIMO Linear array N_t=27 and Square array N_r=27

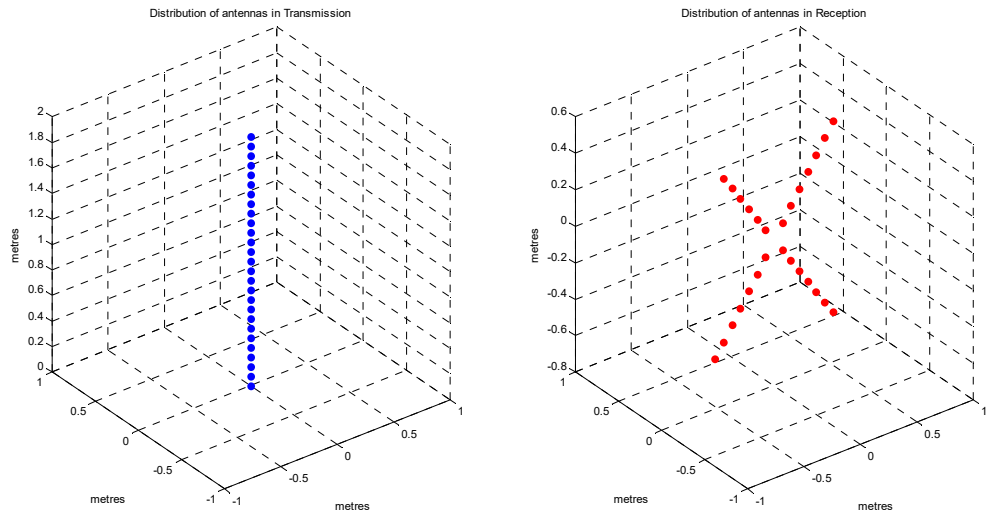

Figure A.69: MIMO Linear array at transmission N_t=27 and C. Squares array at reception N_r =27

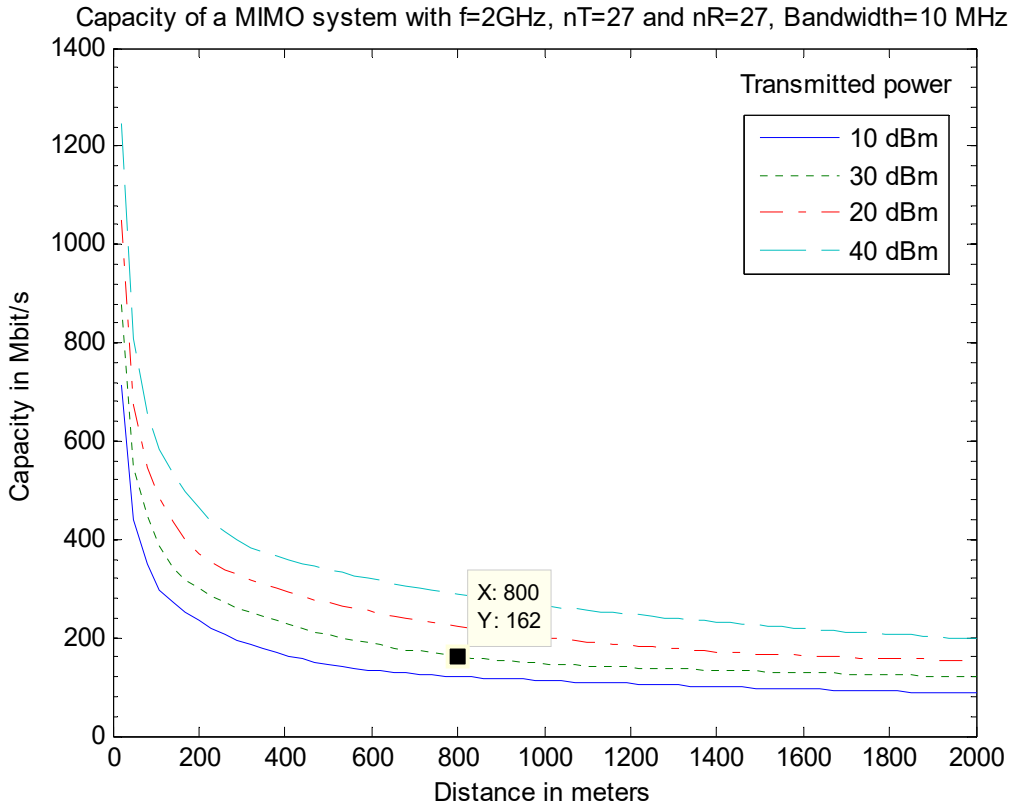

Figure A.70: Capacity of MIMO Linear array N_t=27 and C. Squares array zN_r=27

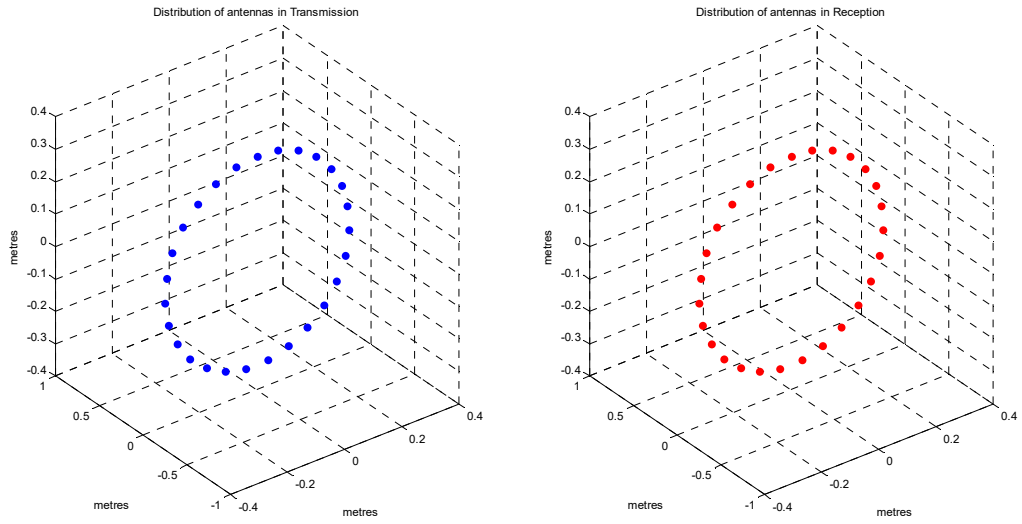

Figure A.71: MIMO Circular array at transmission N_t=27 and Circular array at reception N_r =27

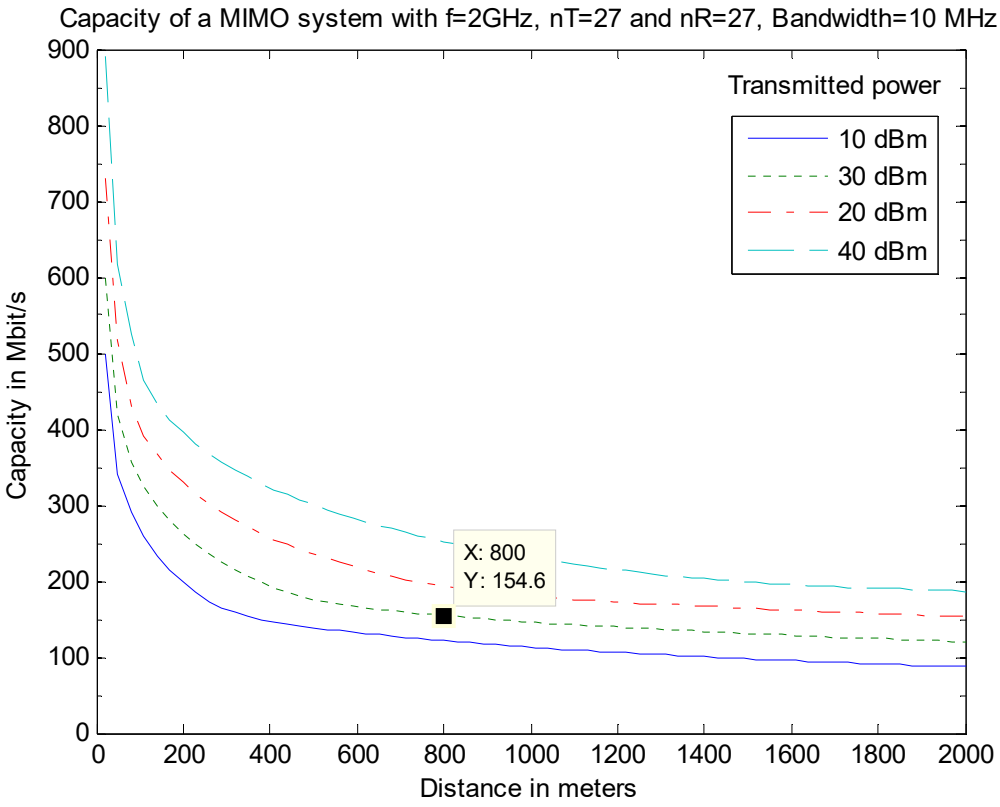

Figure A.72: Capacity of MIMO Circle antenna N_t=27 and Circular array N_r=27

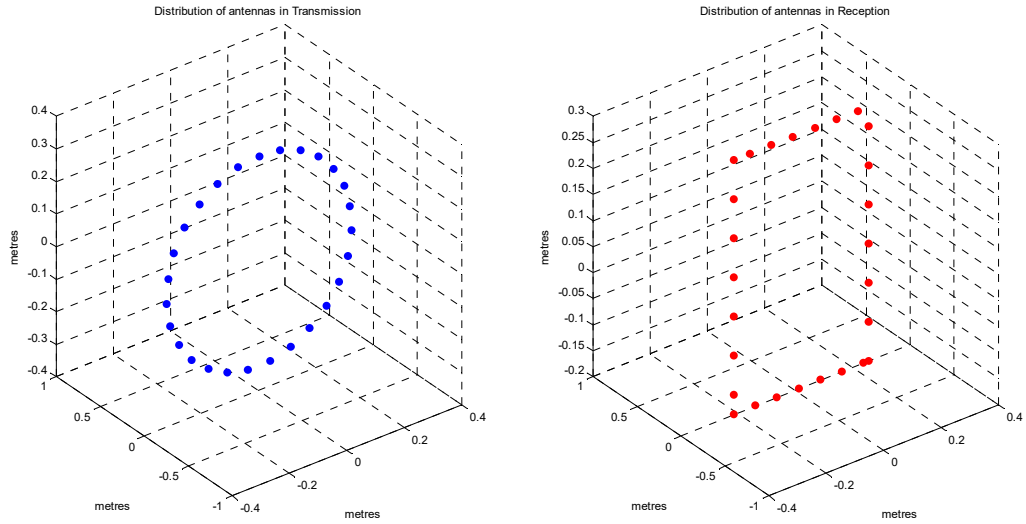

Figure A.73: MIMO Circular array at transmission N_t=27 and Square array at reception N_r =27

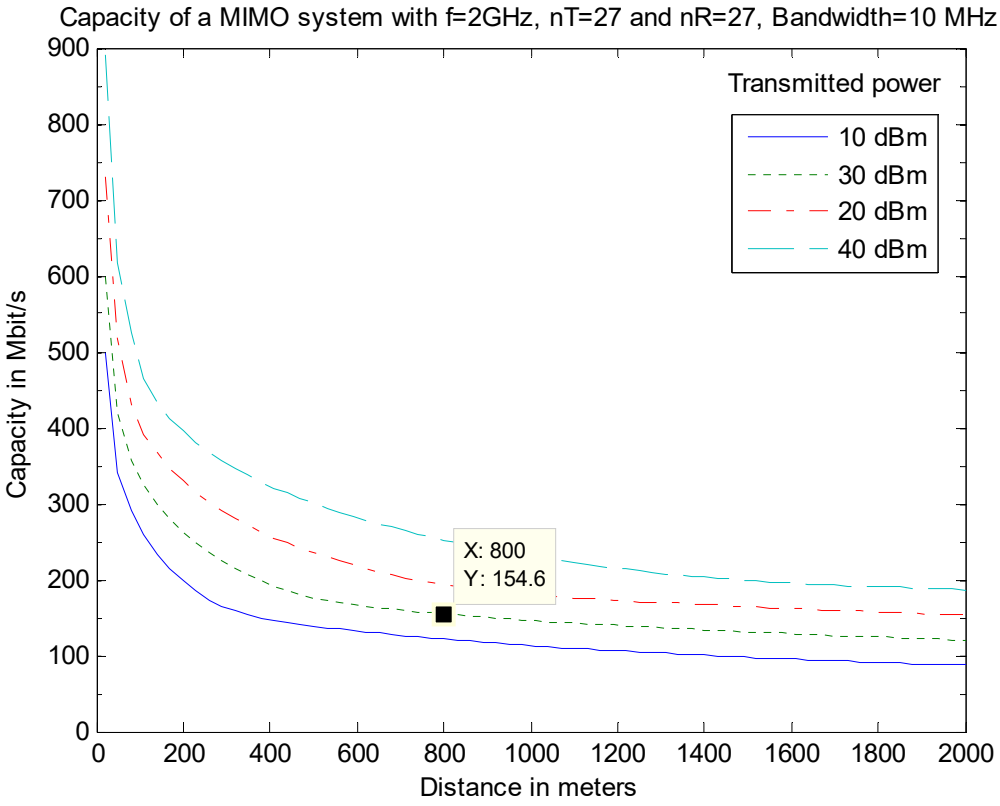

Figure A.74: Capacity of MIMO Circular array N_t=27 and Square array N_r=27

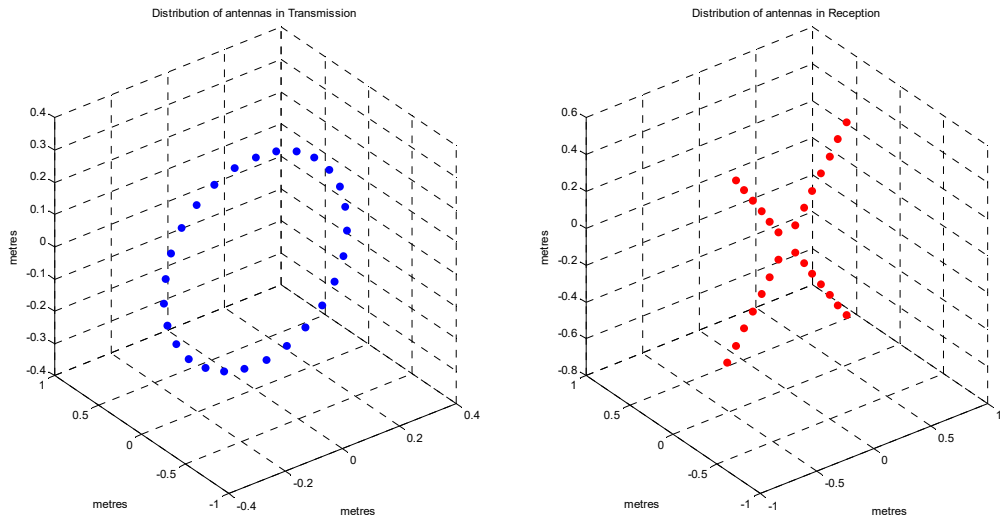

Figure A.75: MIMO Circular array at transmission N_t=27 and C. Squares array at reception N_r =27

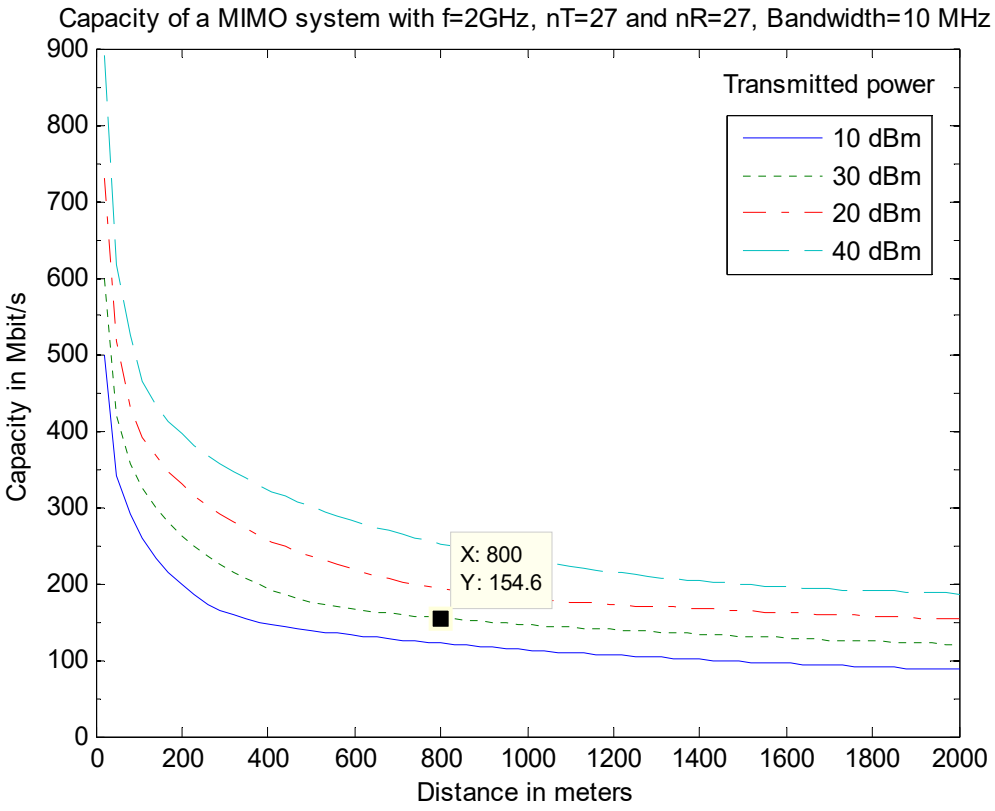

Figure A.76: Capacity of MIMO Circular array N_t=27 and C. Squares array N_r=27

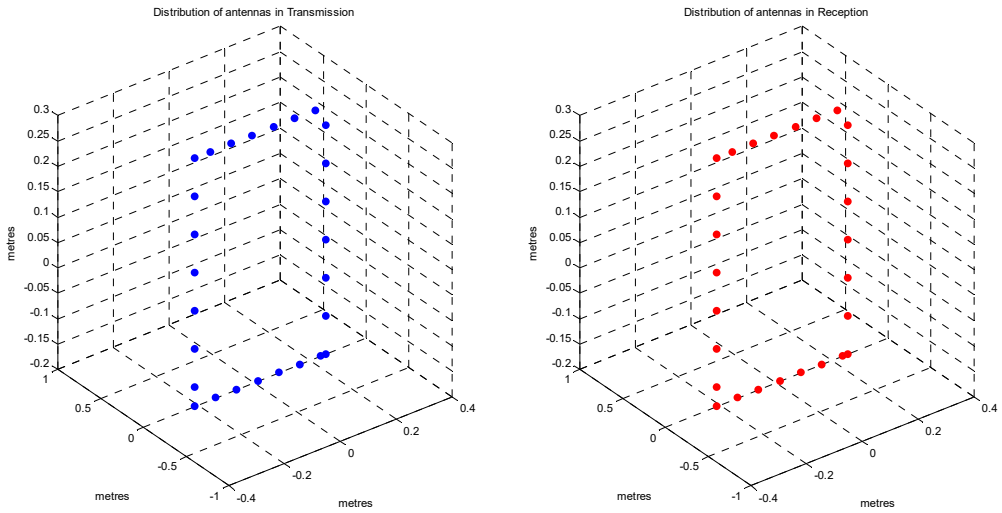

Figure A.77: MIMO Square array at transmission N_t=27 and Square array at reception N_r =27

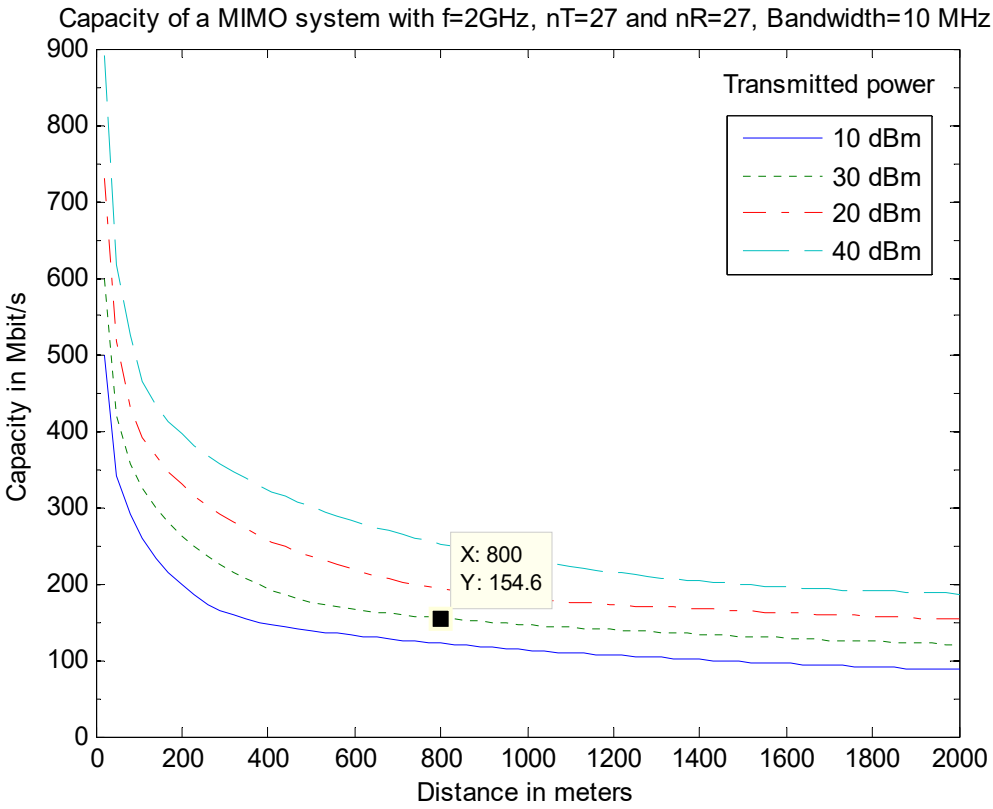

Figure A.78: Capacity of MIMO Square array N_t=27 and Square array N_r=27

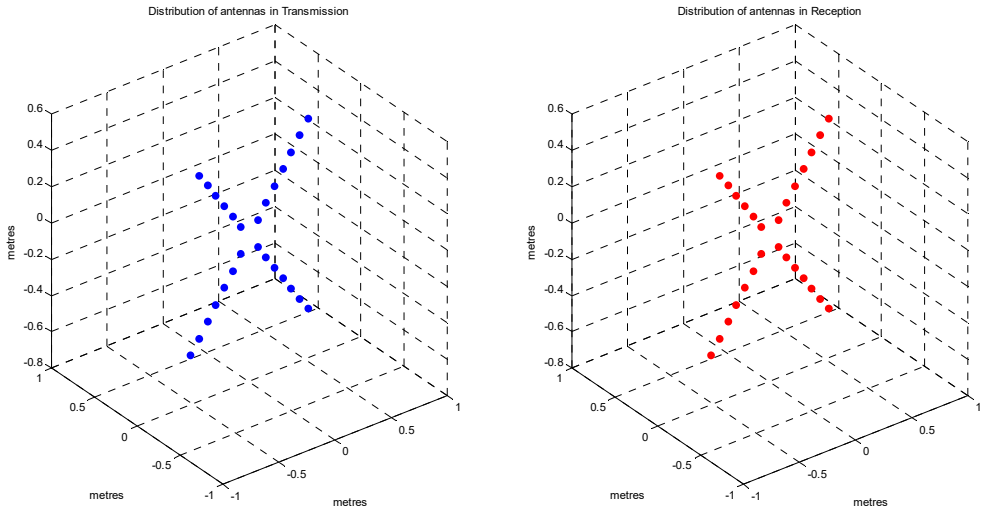

Figure A.79: MIMO C. Squares array at transmission N_t=27 and C. Squares array at reception N_r =27

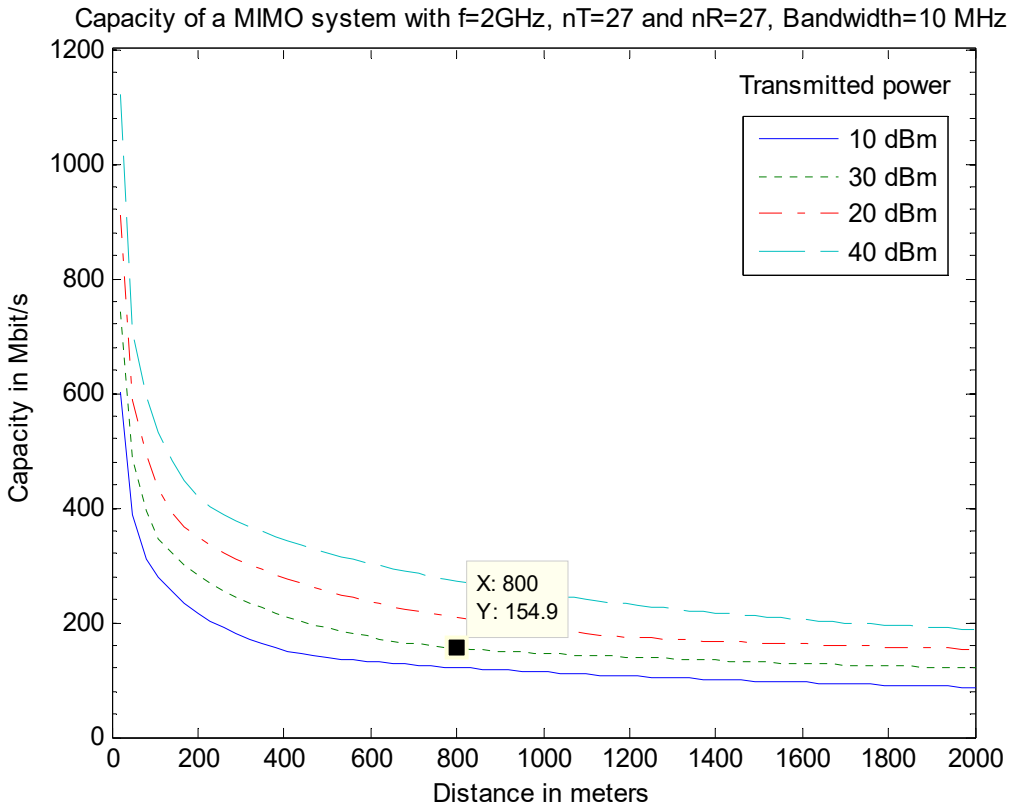

Figure A.80: Capacity of MIMO C. Squares array N_t=27 and C. Squares array N_r=27

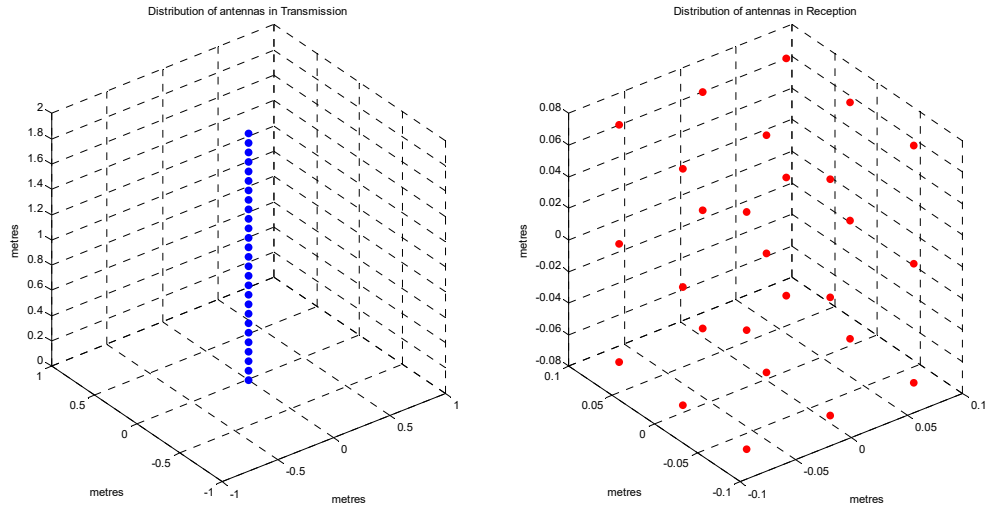

Figure A.81: MIMO Linear array at transmission N_t=27 and Cube array at reception N_r =27

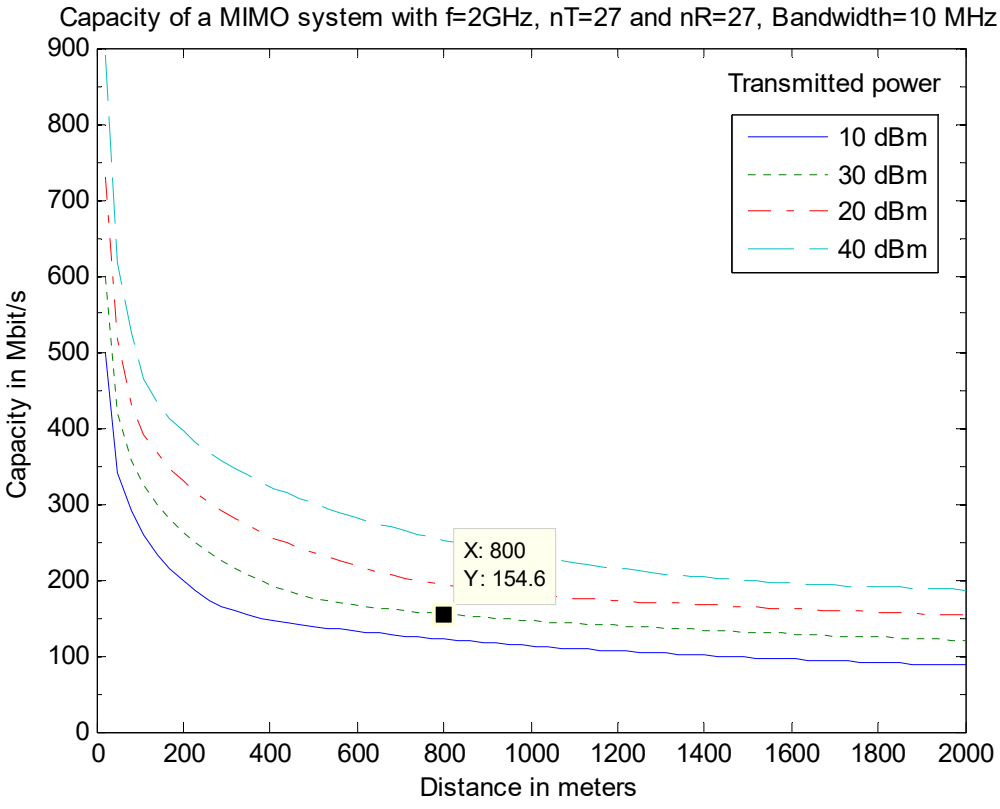

Figure A.82: Capacity of MIMO Linear array N_t=27 and Cube array N_r=27

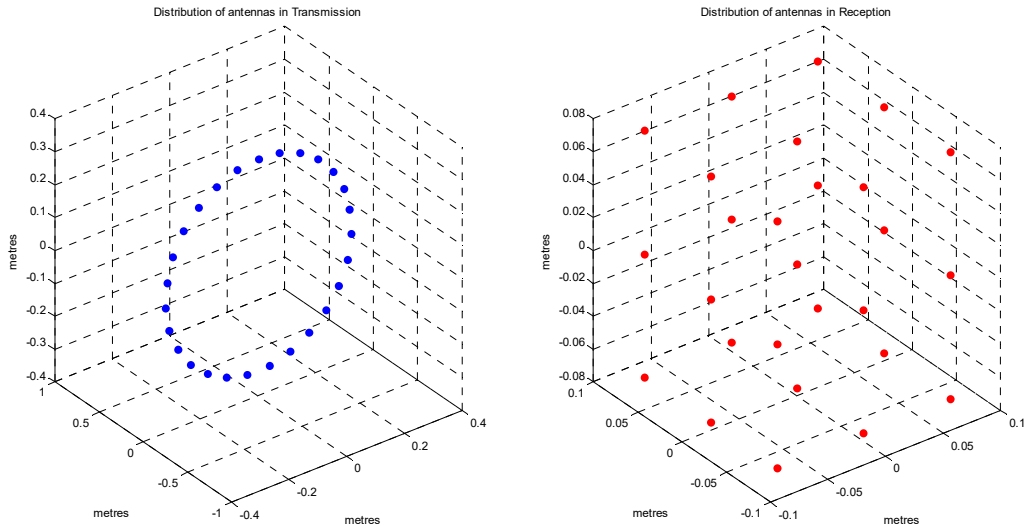

Figure A.83: MIMO Circular array at transmission N_t=27 and Cube array at reception N_r =27

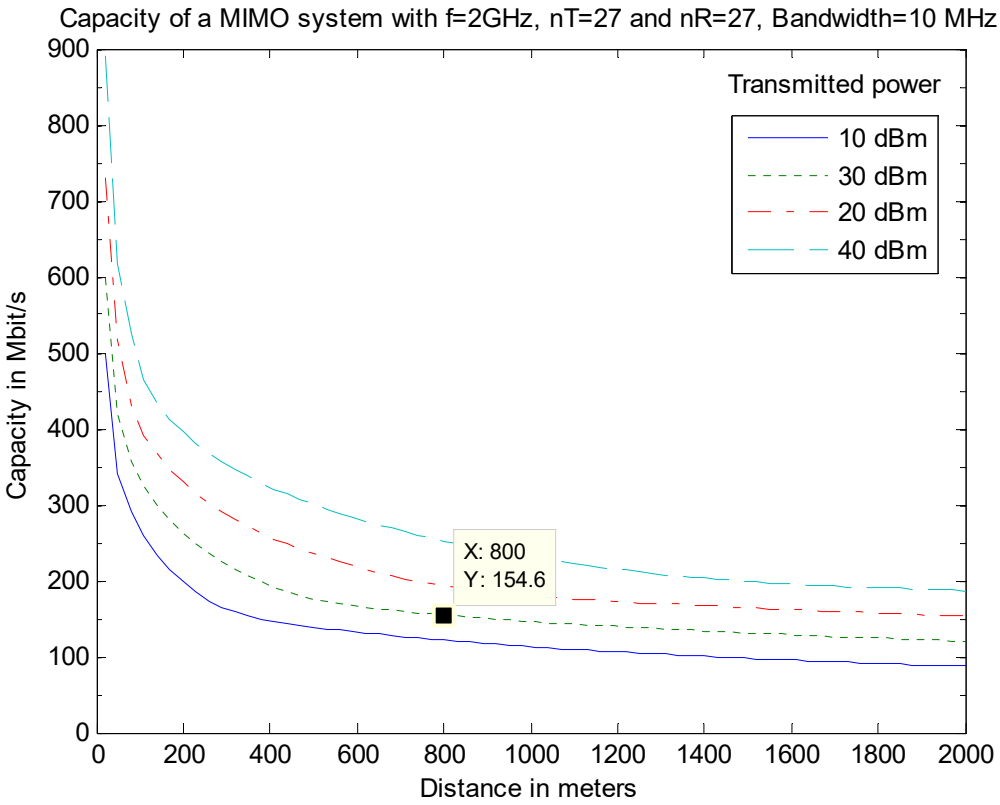

Figure A.84: Capacity of MIMO Circular array N_t=27 and Cube array N_r=27

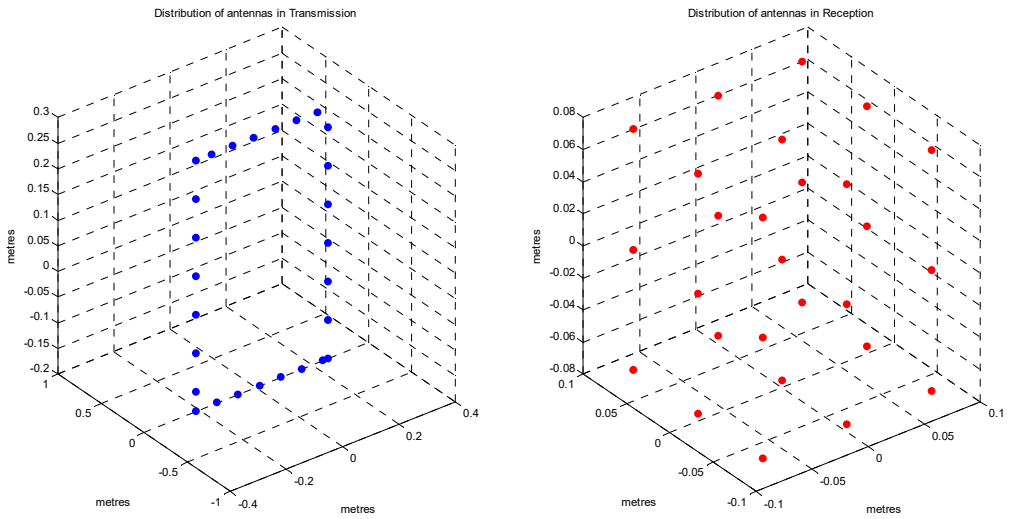

Figure A.85: MIMO Square array at transmission N_t=27 and Cube array at reception N_r =27

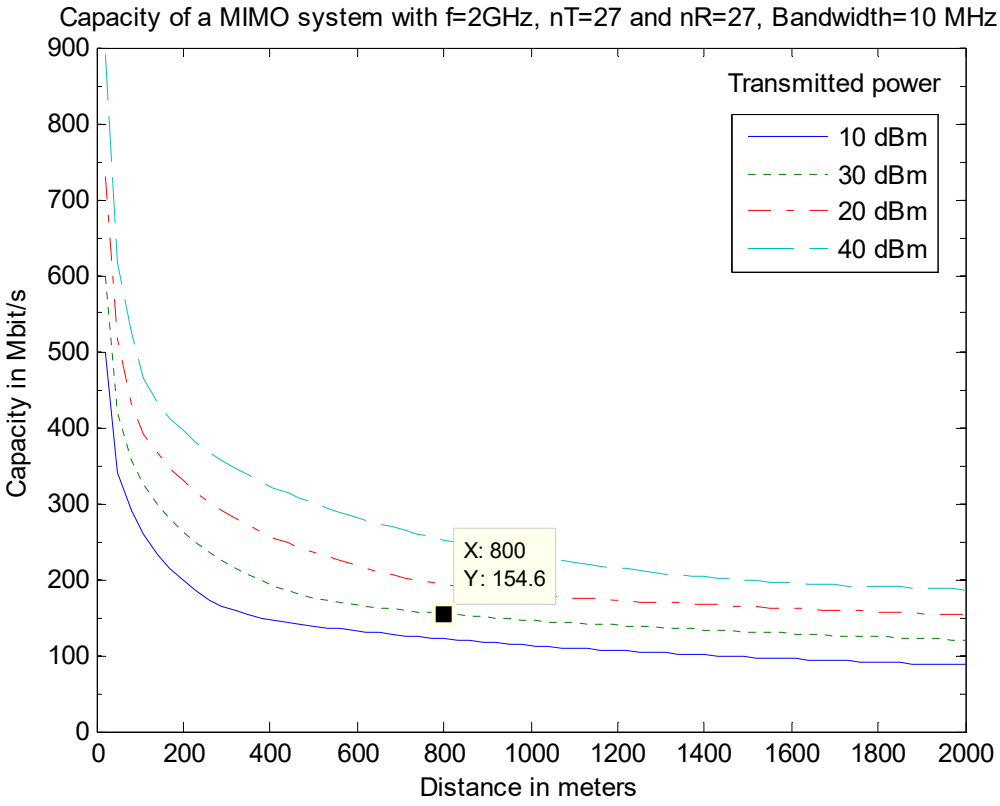

Figure A.86: Capacity of MIMO Square array N_t=27 and Cube array N_r=27

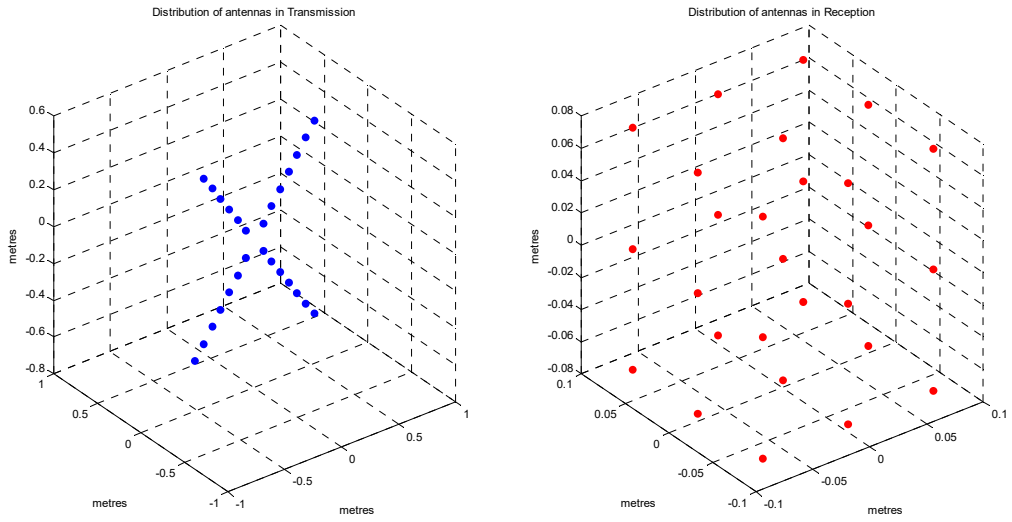

Figure A.87: MIMO C. Squares array at transmission N_t=27 and Cube array at reception N_r =27

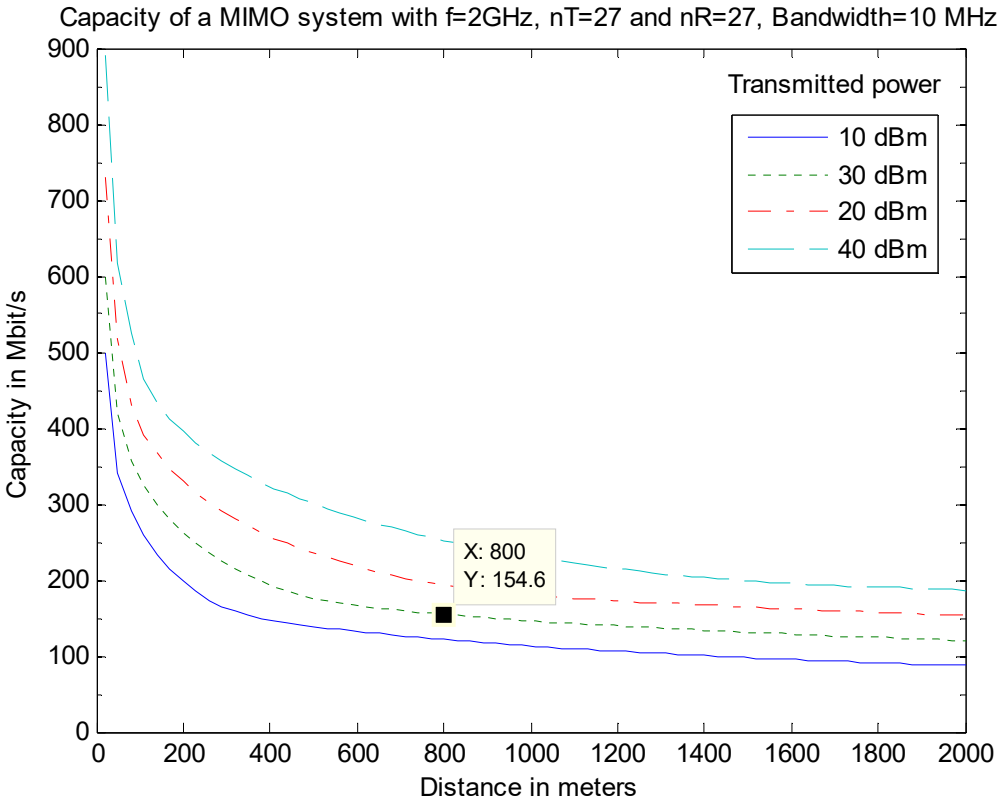

Figure A.88: Capacity of MIMO C. Squares array N_t=20 and Cube array N_r=27

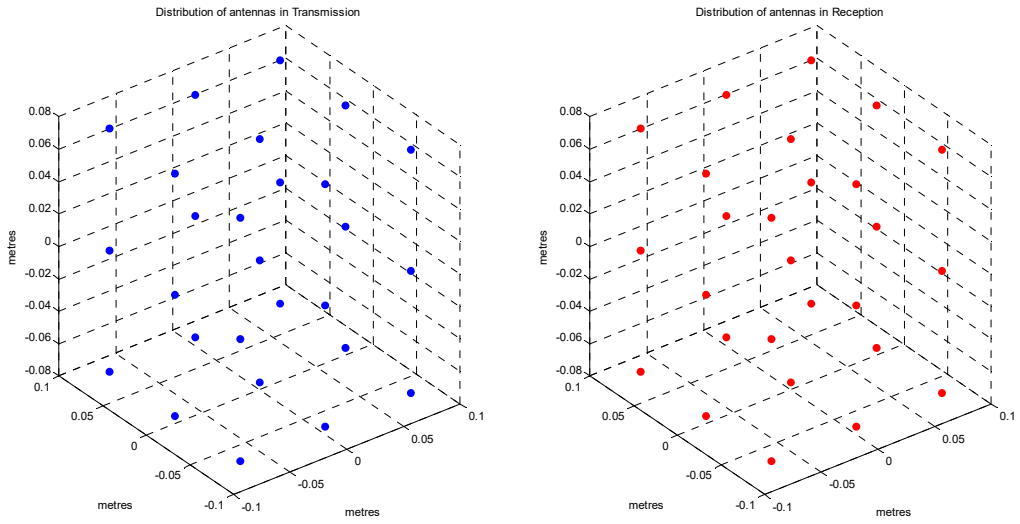

Figure A.89: MIMO Cube array at transmission N_t=27 and Cube array at reception N_r =27

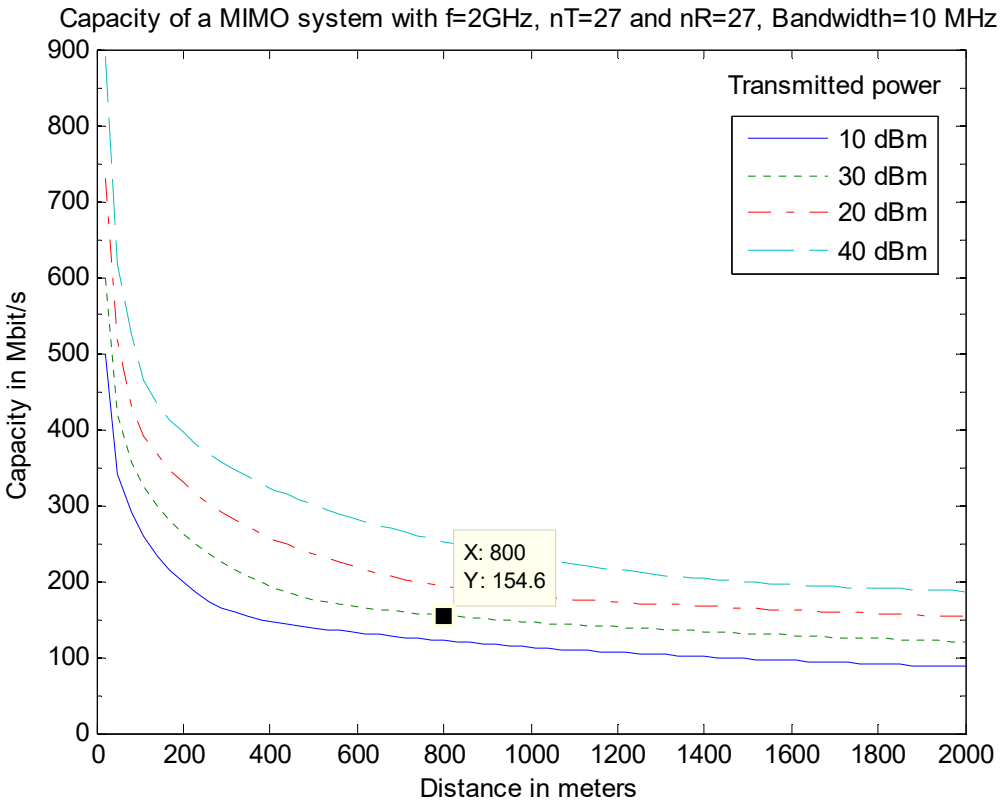

Figure A.90: Capacity of MIMO Cube array N_t=27 and Cube array N_r=27

A.2.4 GSTA

- ***Carrier frequency (f_c):*** 2 GHz
- ***Number of antennas in reception (n_r):*** 20 antennas
- ***Bandwidth (B):*** 10 MHz
- ***Separation between reception antennas ($\Delta_r \lambda_c$):*** 7.5 cm (λ/2)
- ***Angle of incidence1 (∅1):*** $\boldsymbol{\pi/3}$
- ***Angle of incidence2 (∅2):*** **0**
- ***Transmitted power (P):*** 10, 20, 30 and 40 dBm
- ***Noise power (N_0):*** -104 dBm (-174 dBm/Hz)

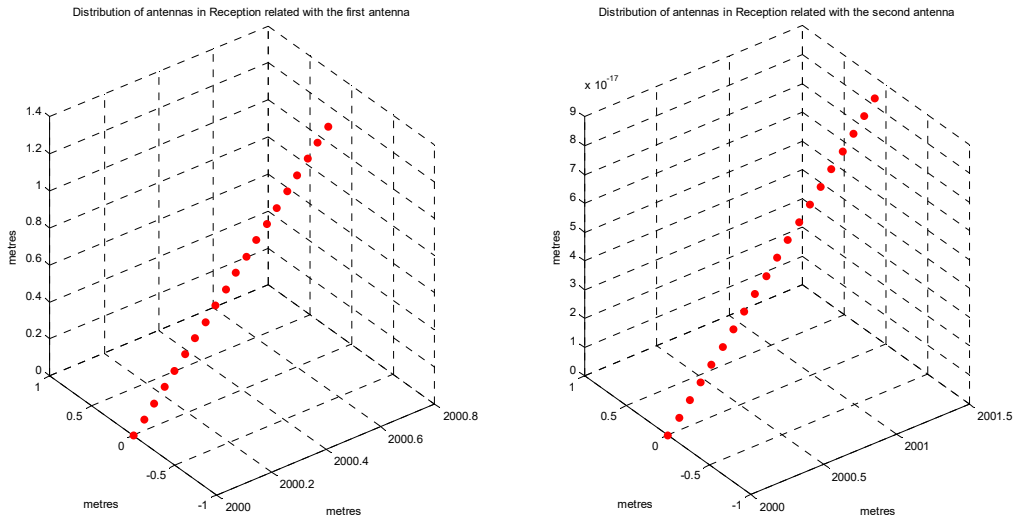

Figure A.91: GSTA Linear array at reception N_r =20 $\emptyset_1 = \frac{\pi}{3}$ $\emptyset_2 = 0$

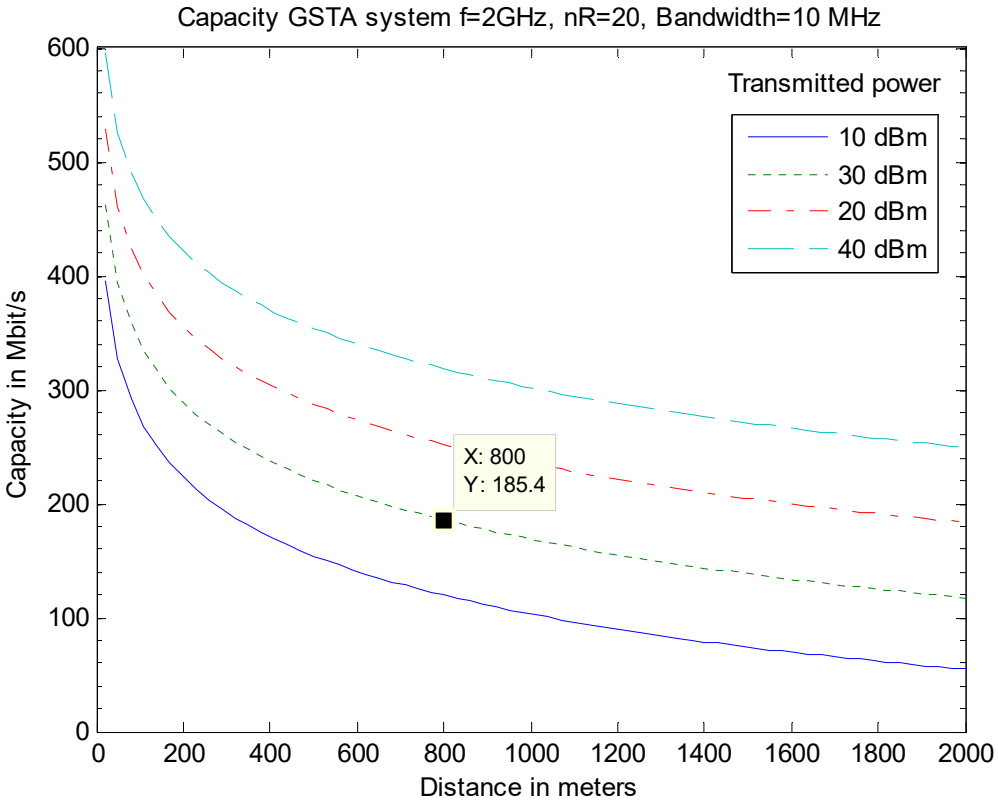

Figure A.92: Capacity of GSTA Linear array N_r=20 $\emptyset_1 = \frac{\pi}{3}$ $\emptyset_2 = 0$

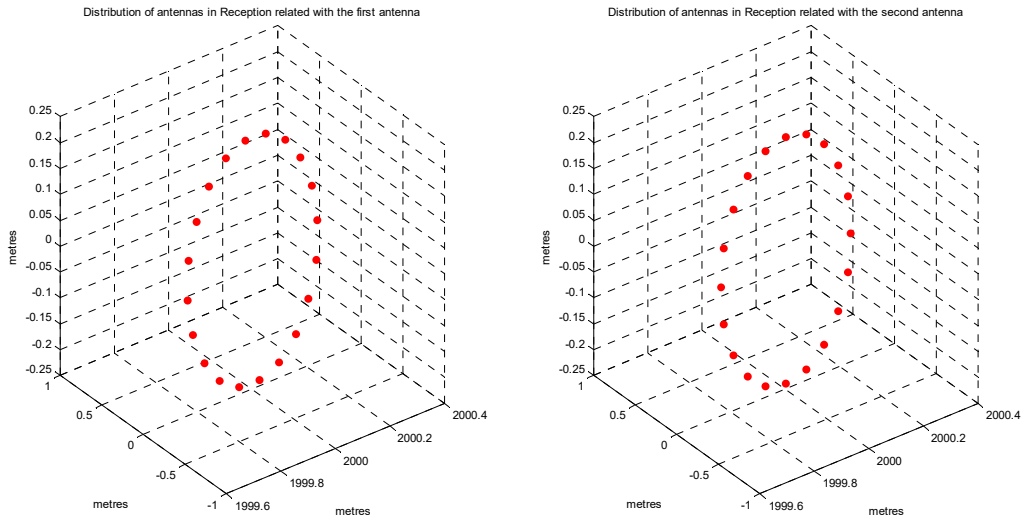

Figure A.93: GSTA Circular array at reception N_r =20 $\emptyset_1 = \frac{\pi}{3}$ $\emptyset_2 = 0$

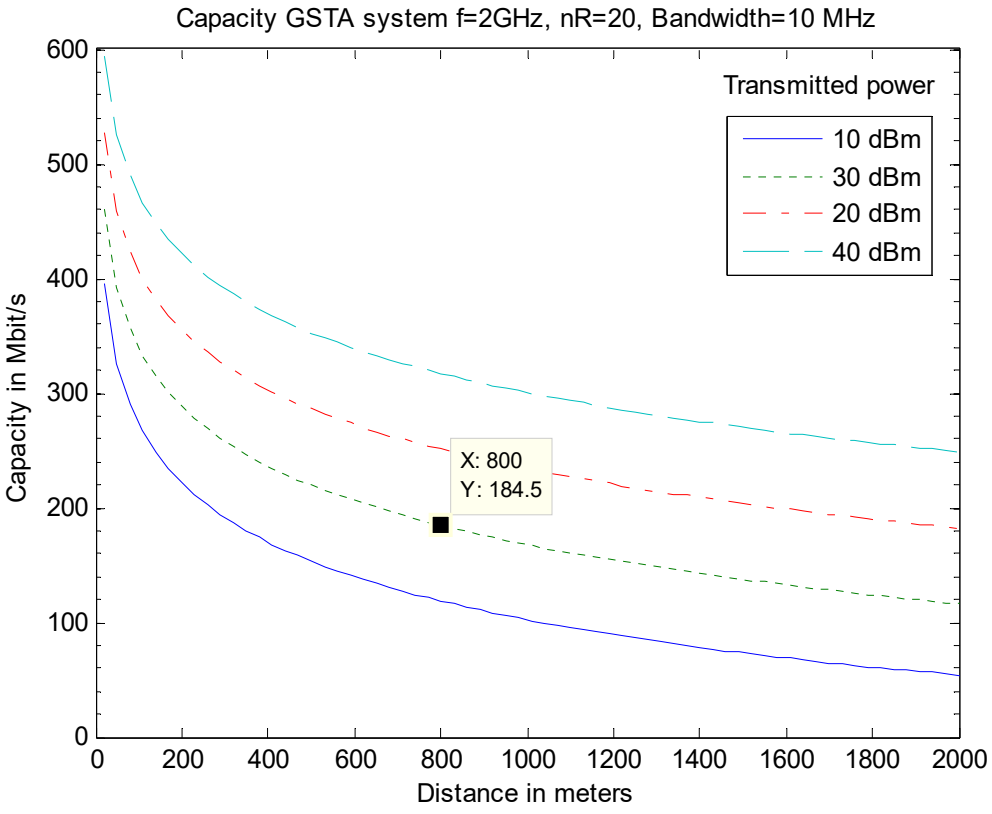

Figure A.94: Capacity of GSTA Circular array N_r=20 $\emptyset_1 = \frac{\pi}{3}$ $\emptyset_2 = 0$

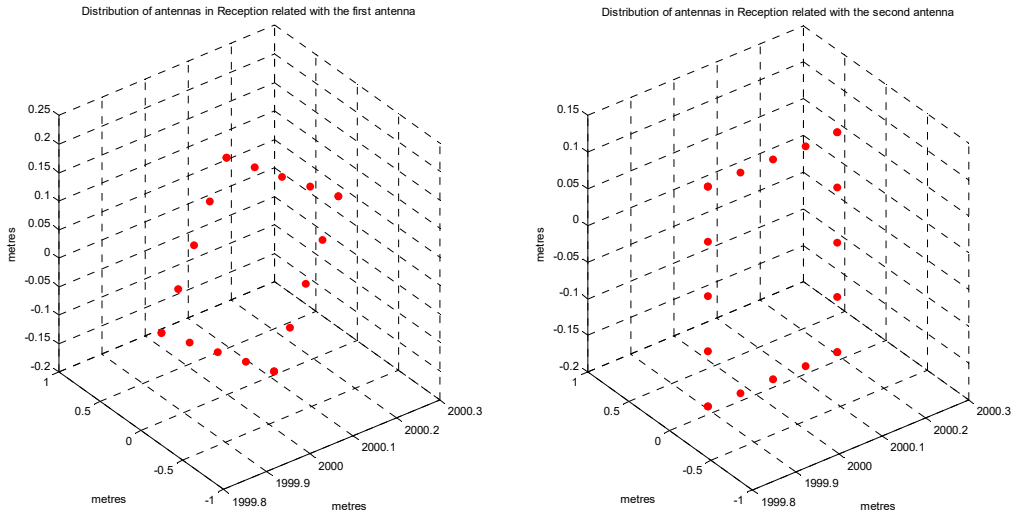

Figure A.95: GSTA Square array at reception N_r =20 $\emptyset_1 = \frac{\pi}{3}$ $\emptyset_2 = 0$

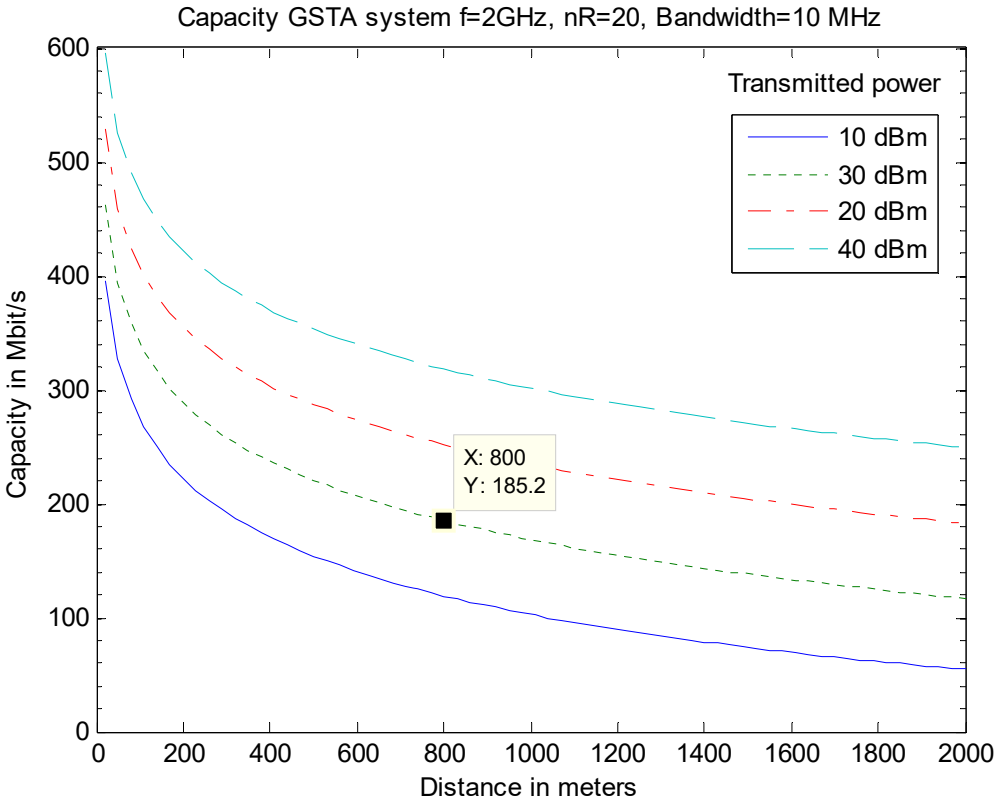

Figure A.96: Capacity of GSTA Square array N_r=20 $\emptyset_1 = \frac{\pi}{3}$ $\emptyset_2 = 0$

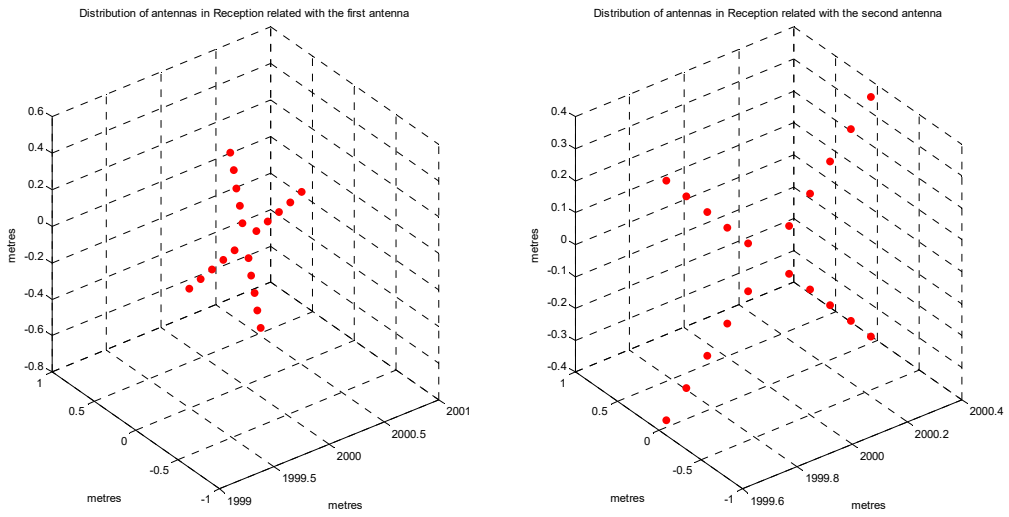

Figure A.97: GSTA C. Squares array at reception N_r =20 $\emptyset_1 = \frac{\pi}{3}$ $\emptyset_2 = 0$

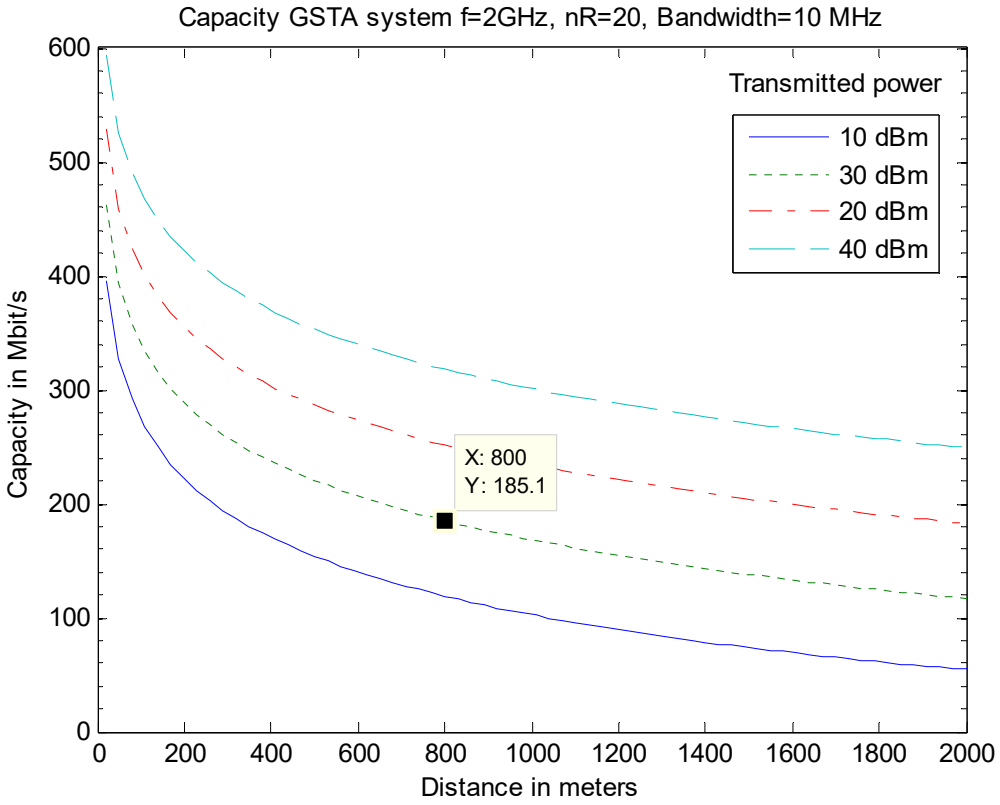

Figure A.98: Capacity of GSTA C. Squares array N_r=20 $\emptyset_1 = \frac{\pi}{3}$ $\emptyset_2 = 0$

- ***Carrier frequency (f_c):*** 2 GHz
- ***Number of antennas in reception (n_r):*** 27 antennas
- ***Bandwidth (B):*** 10 MHz
- ***Separation between reception antennas ($\Delta_r \lambda_c$):*** 7.5 cm (λ/2)
- ***Angle of incidence1 ($\emptyset 1$): $\pi/3$***
- ***Angle of incidence2 ($\emptyset 2$): 0***
- ***Transmitted power (P):*** 10, 20, 30 and 40 dBm
- ***Noise power (N_0):*** -104 dBm (-174 dBm/Hz)

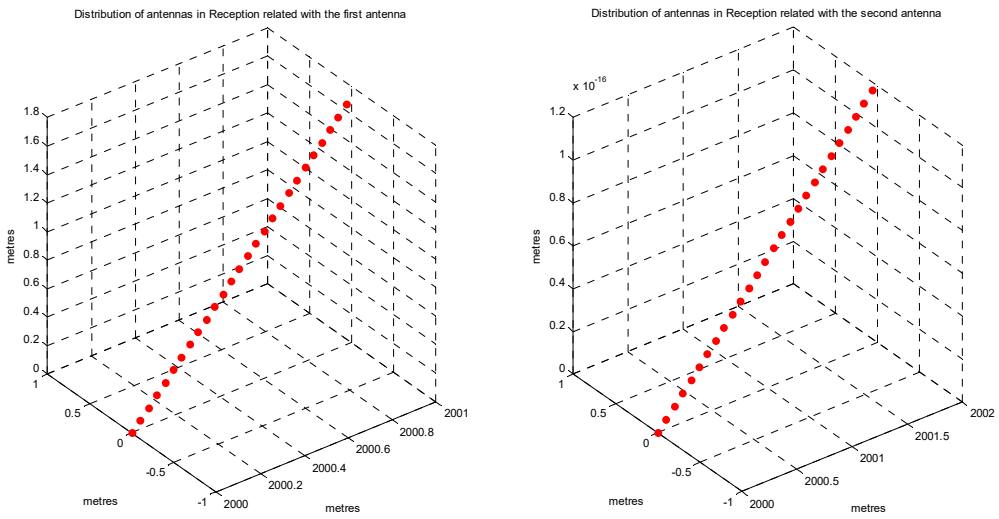

Figure A.99: GSTA Linear array at reception N_r =27 $\emptyset_1 = \frac{\pi}{3}$ $\emptyset_2 = 0$

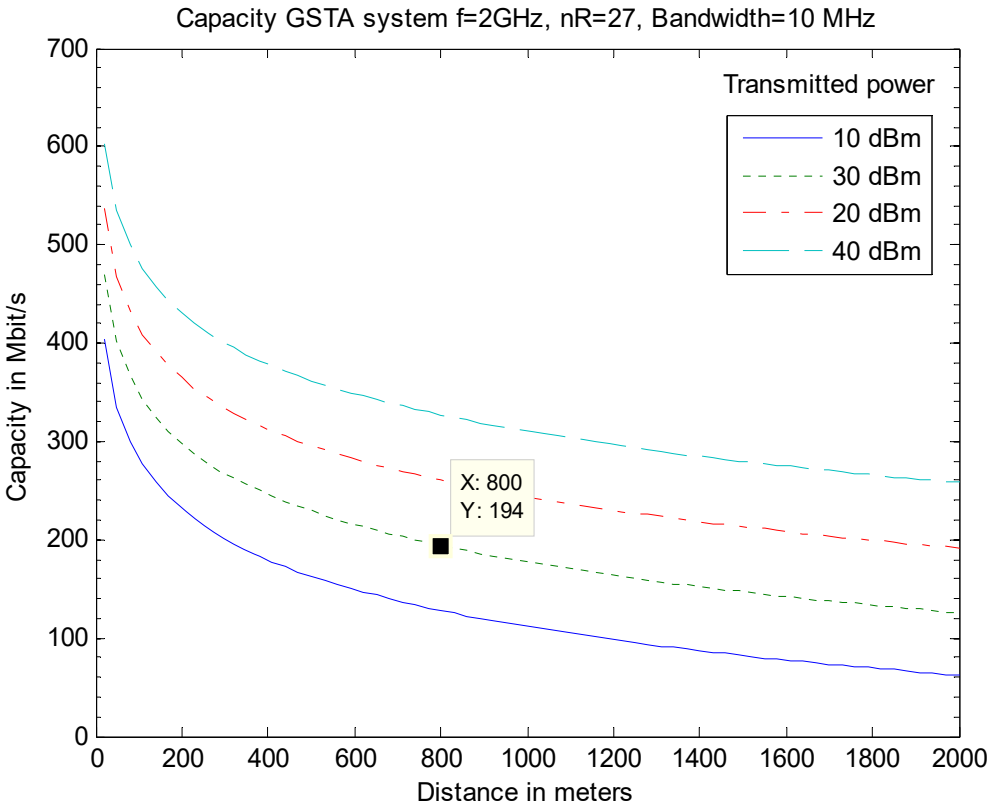

Figure A.100: Capacity of GSTA Linear array N_r=27 $\emptyset_1 = \frac{\pi}{3}$ $\emptyset_2 = 0$

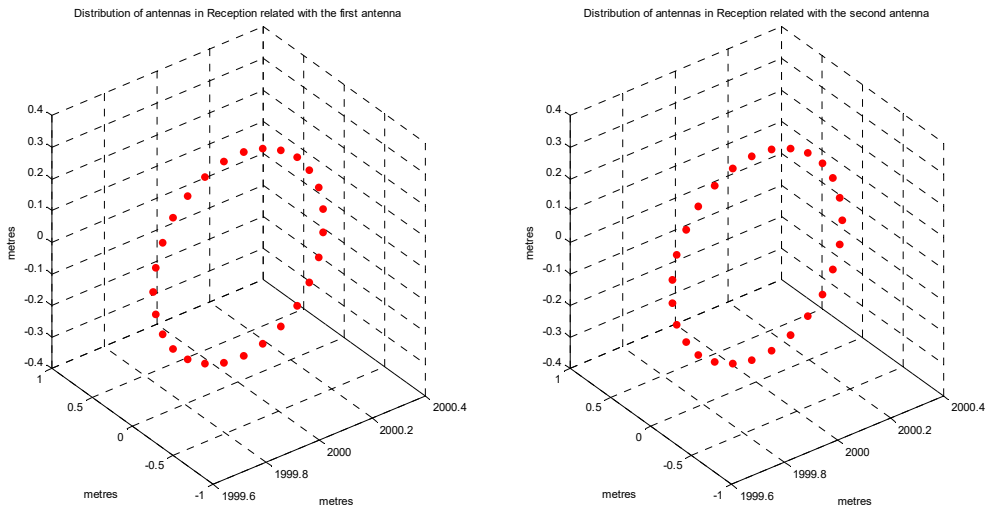

Figure A.101: GSTA Circular array at reception N_r =27 $\emptyset_1 = \frac{\pi}{3}$ $\emptyset_2 = 0$

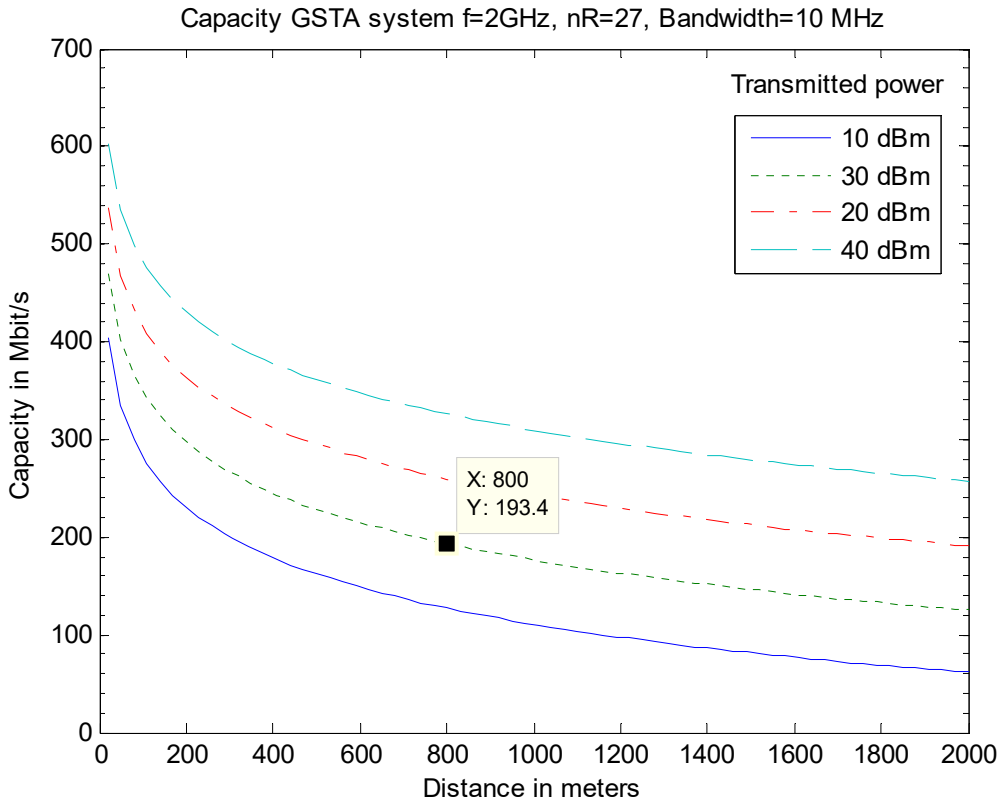

Figure A.102: Capacity of GSTA Circular array N_r=27 $\emptyset_1 = \frac{\pi}{3}$ $\emptyset_2 = 0$

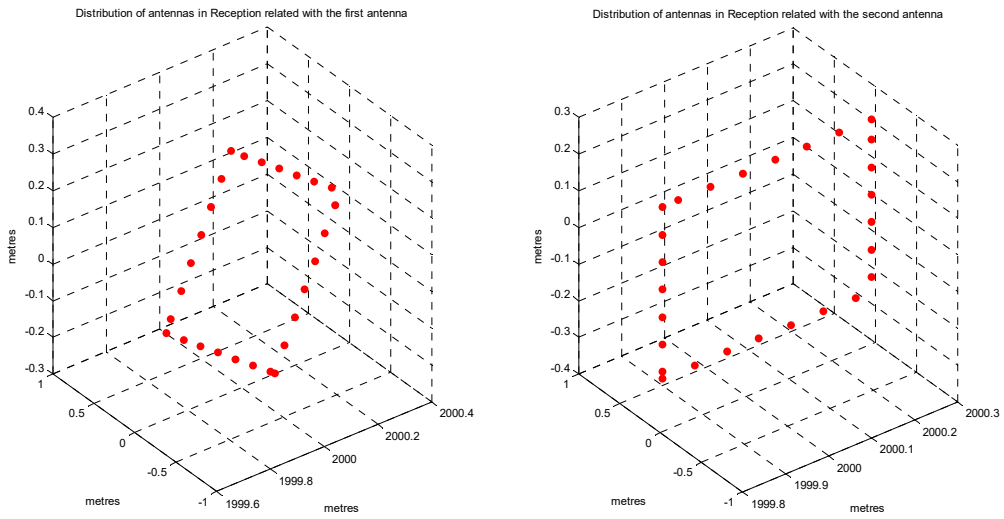

Figure A.103: GSTA Square array at reception $N_r = 27$ $\emptyset_1 = \frac{\pi}{3}$ $\emptyset_2 = 0$

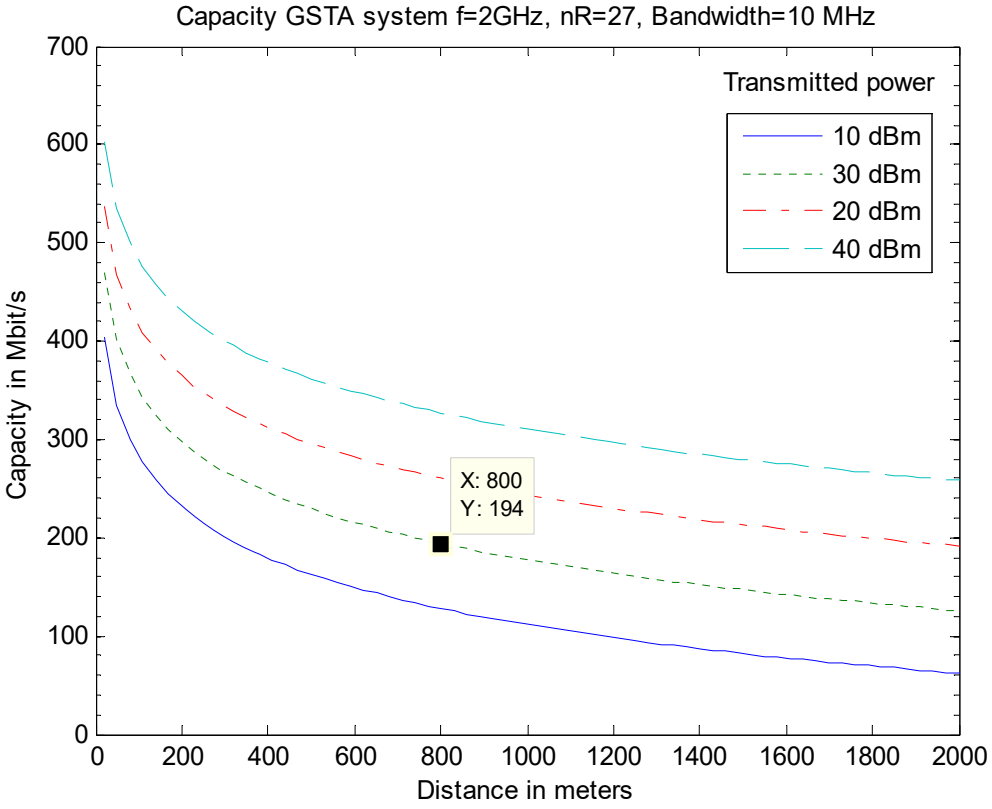

Figure A.104: GSTA Square array at reception $N_r = 27$ $\emptyset_1 = \frac{\pi}{3}$ $\emptyset_2 = 0$

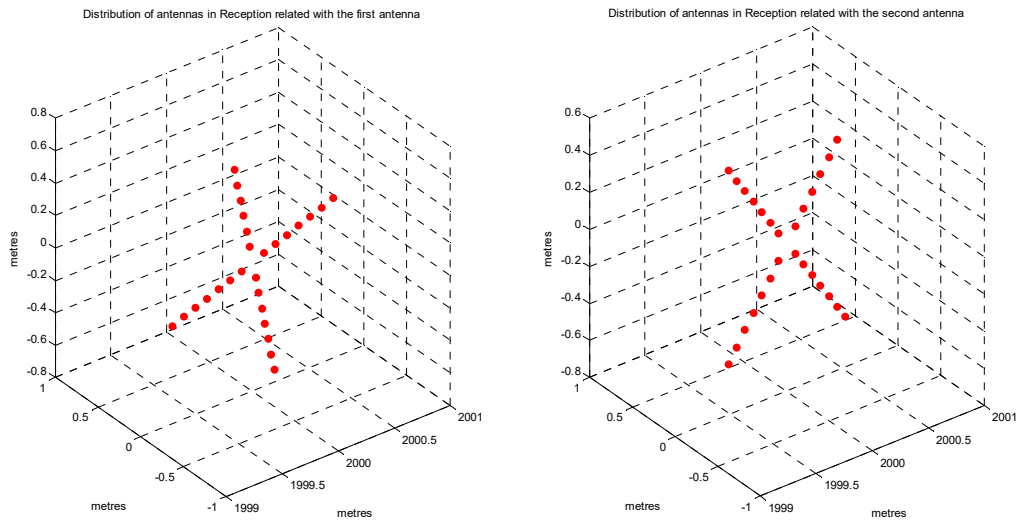

Figure A.105: GSTA C. Squares array at reception N_r =27 $\emptyset_1 = \frac{\pi}{3}$ $\emptyset_2 = 0$

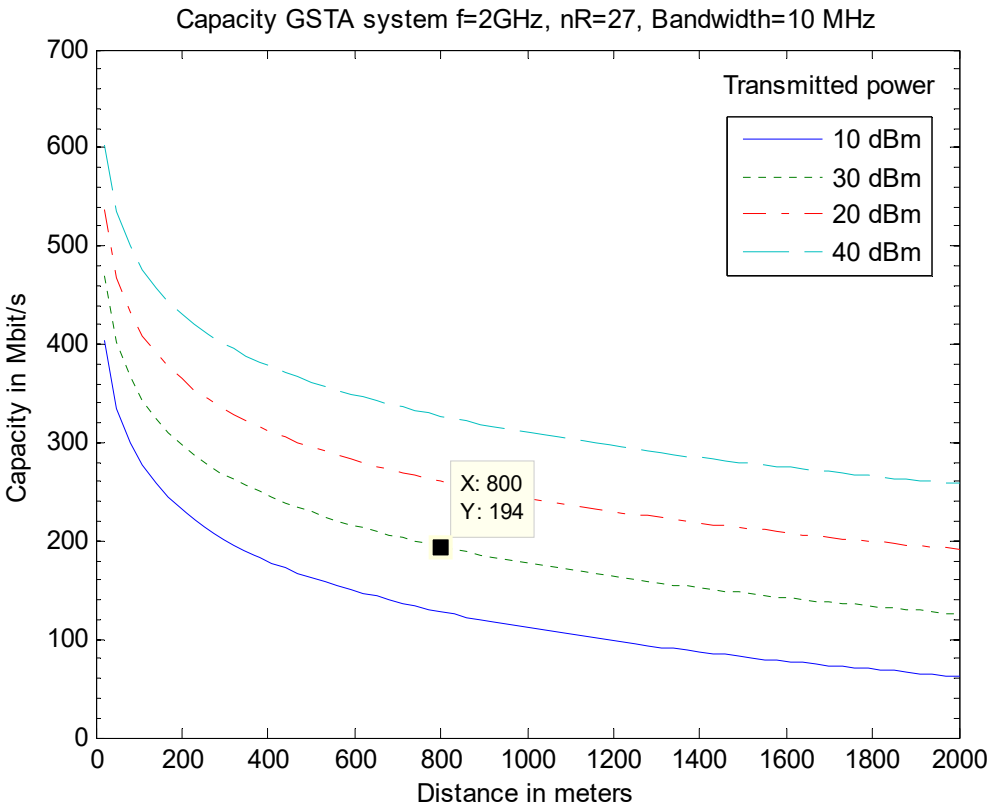

Figure A.106: GSTA C. Squares array at reception N_r =27 $\emptyset_1 = \frac{\pi}{3}$ $\emptyset_2 = 0$

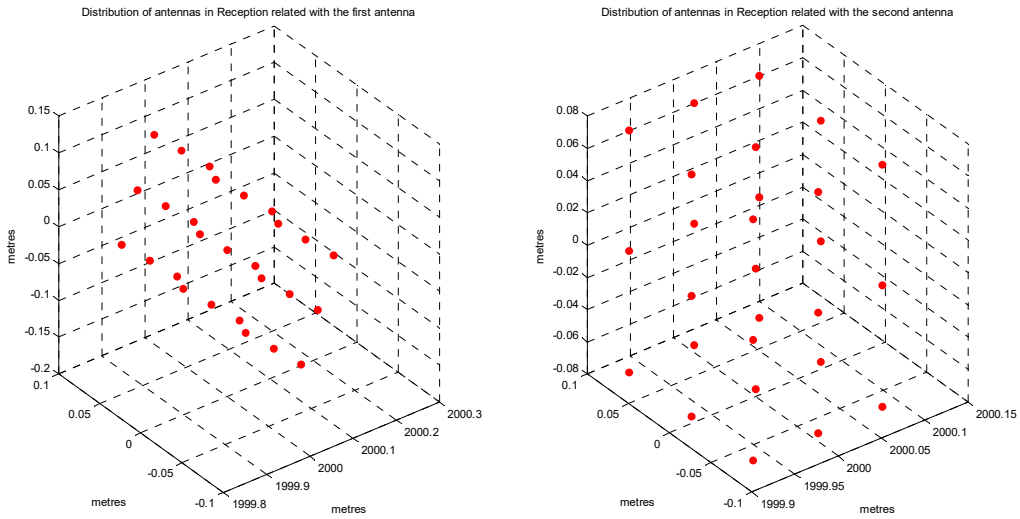

Figure A.107: GSTA Cube array at reception $N_r = 27$ $\emptyset_1 = \frac{\pi}{3}$ $\emptyset_2 = 0$

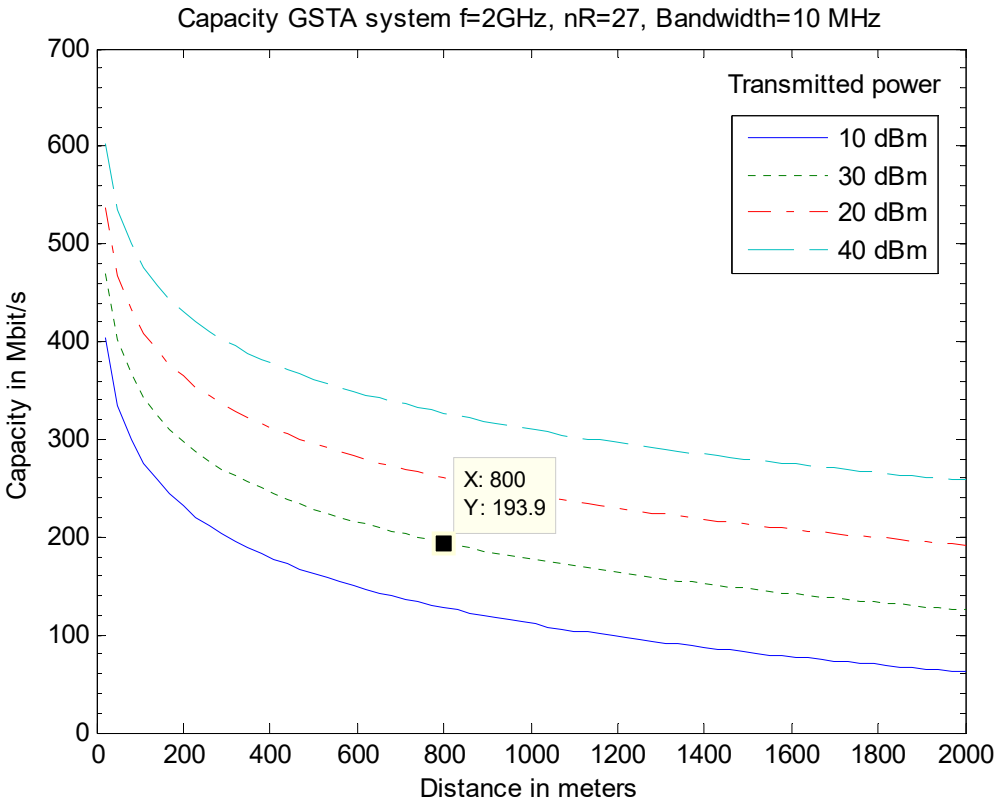

Figure A.108: GSTA Cube array at reception $N_r = 27$ $\emptyset_1 = \frac{\pi}{3}$ $\emptyset_2 = 0$

- ***Carrier frequency (f_c):*** 2 GHz
- ***Number of antennas in reception (n_r):*** 27 antennas
- ***Bandwidth (B):*** 10 MHz
- ***Separation between reception antennas ($\Delta_r \lambda_c$):*** 7.5 cm (λ/2)
- ***Angle of incidence1 ($\emptyset 1$):*** $\mathbf{3\pi/4}$
- ***Angle of incidence2 ($\emptyset 2$):*** $\mathbf{3\pi/4}$
- ***Transmitted power (P):*** 10, 20, 30 and 40 dBm
- ***Noise power (N_0):*** -104 dBm (-174 dBm/Hz)
- ***Angle between spatial signatures $|\cos\theta| = 1$***

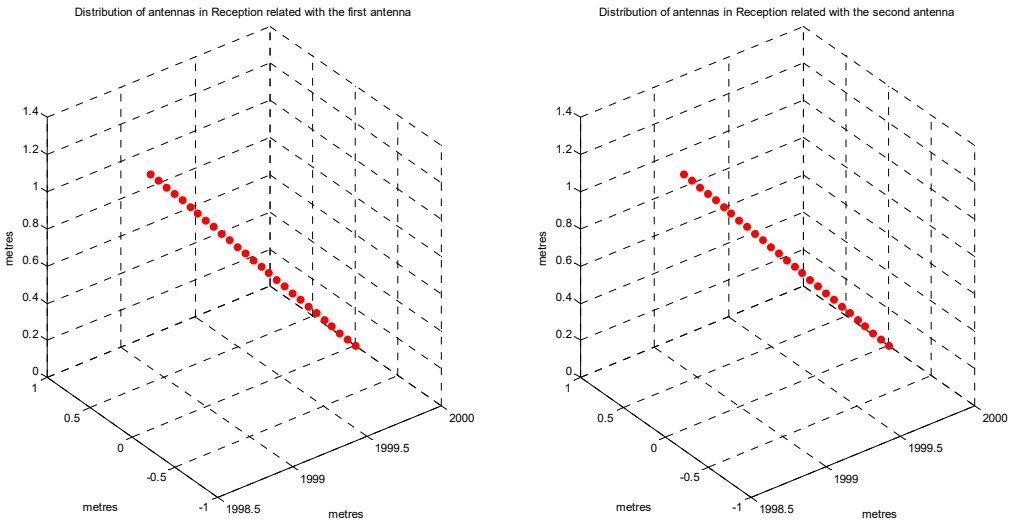

Figure A.109: GSTA Linear array at reception N_r =27 $\emptyset_1 = \frac{3\pi}{4}$ $\emptyset_2 = \frac{3\pi}{4}$

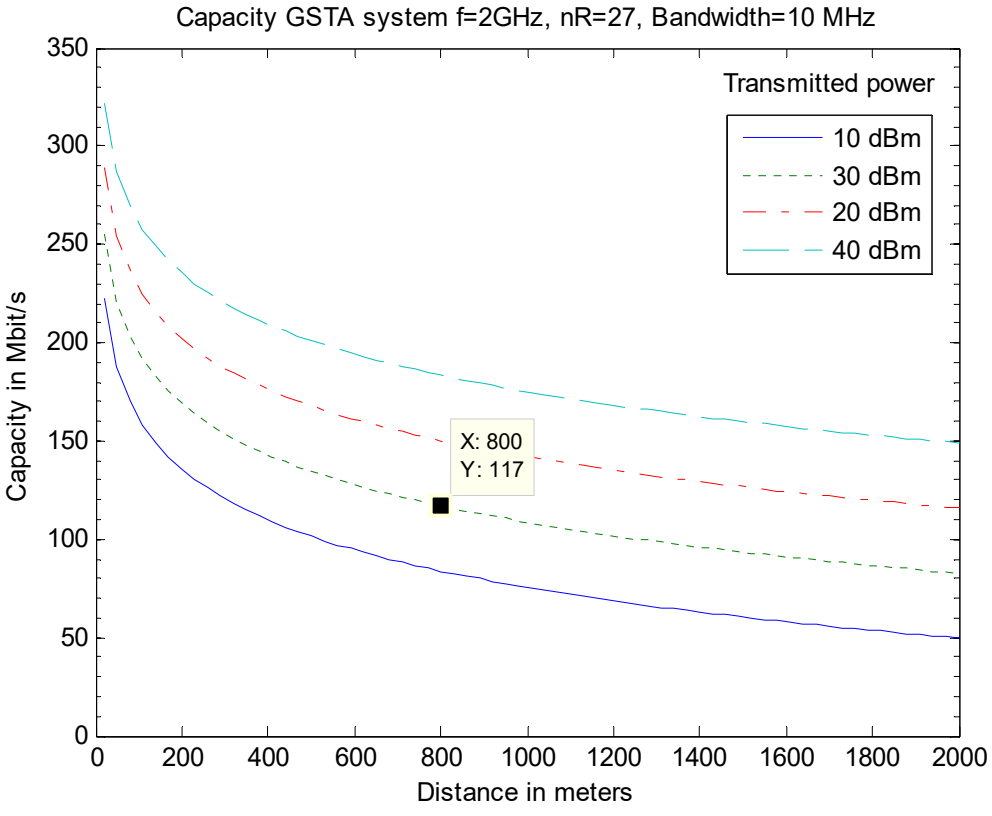

Figure A.110: GSTA Linear array at reception N_r =27 $\emptyset_1 = \frac{3\pi}{4}$ $\emptyset_2 = \frac{3\pi}{4}$

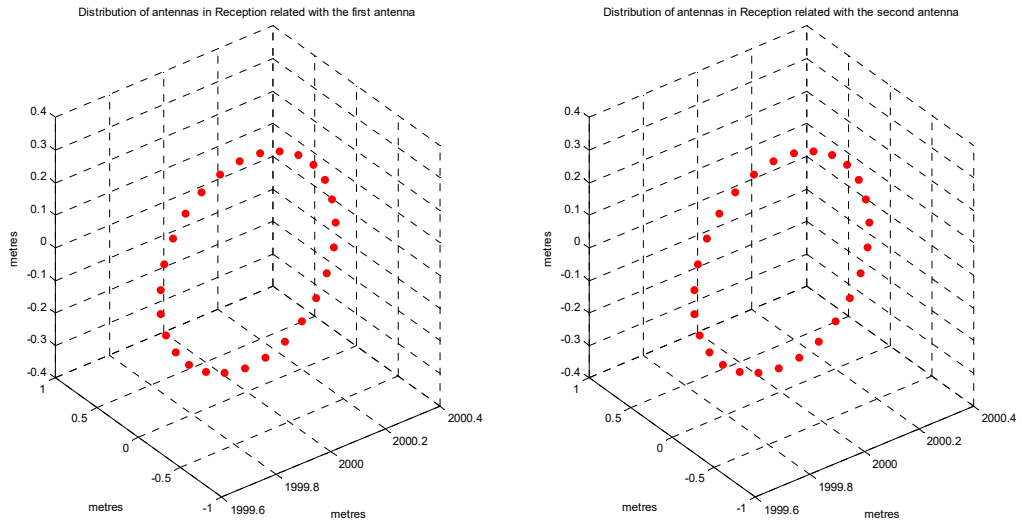

Figure A.111: GSTA Circular array at reception N_r =27 $\emptyset_1 = \frac{3\pi}{4}$ $\emptyset_2 = \frac{3\pi}{4}$

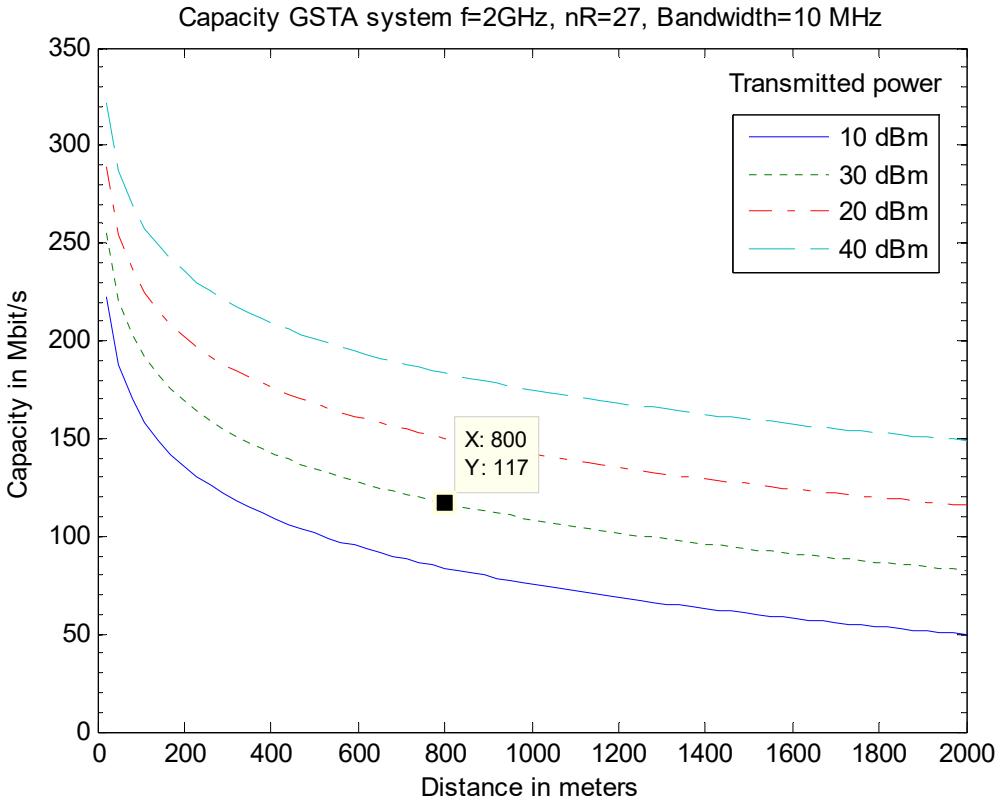

Figure A.112: GSTA Circular array at reception N_r =27 $\emptyset_1 = \frac{3\pi}{4}$ $\emptyset_2 = \frac{3\pi}{4}$

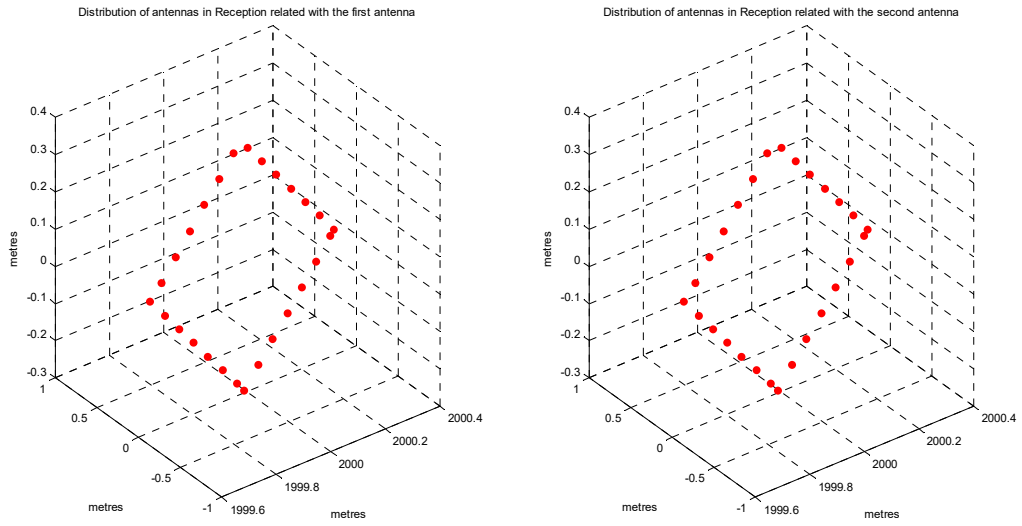

Figure A.113: GSTA Square array at reception N_r =27 $\emptyset_1 = \frac{3\pi}{4}$ $\emptyset_2 = \frac{3\pi}{4}$

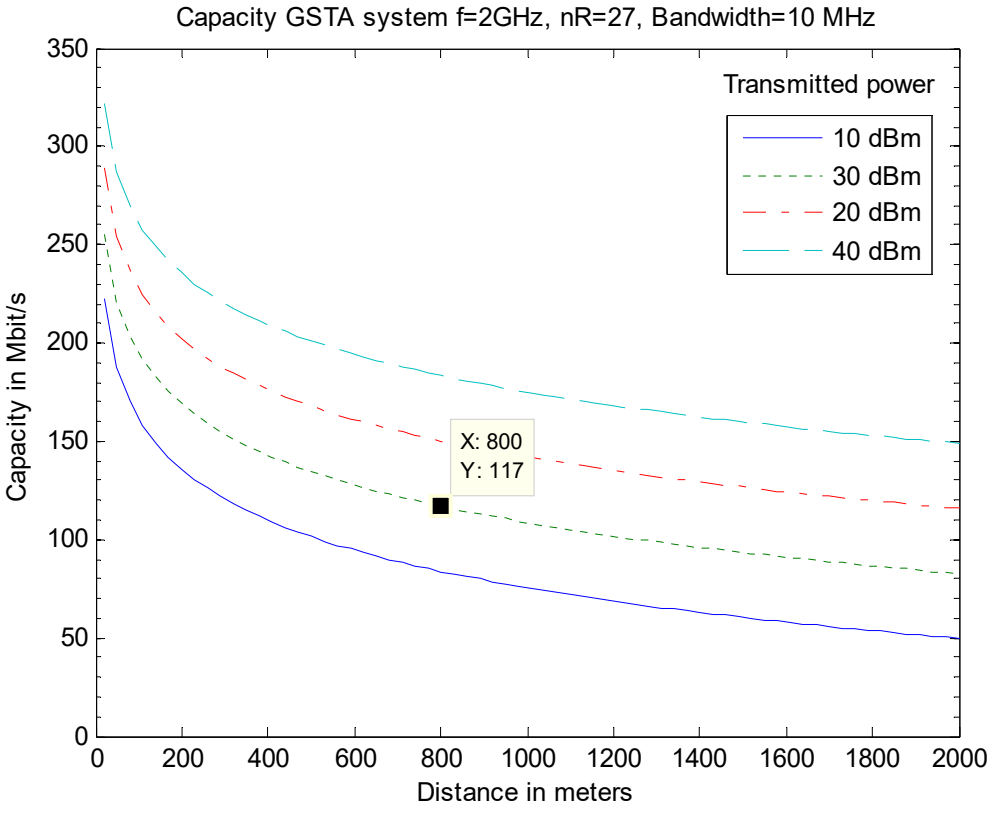

Figure A.114: GSTA Square array at reception N_r =27 $\emptyset_1 = \frac{3\pi}{4}$ $\emptyset_2 = \frac{3\pi}{4}$

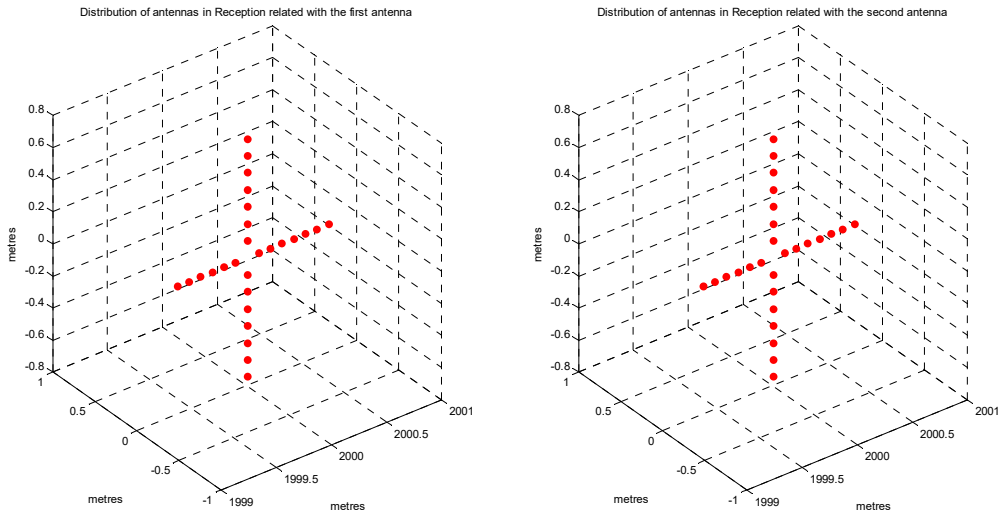

Figure A.115: GSTA C. Squares array at reception N_r =27 $\emptyset_1 = \frac{3\pi}{4}$ $\emptyset_2 = \frac{3\pi}{4}$

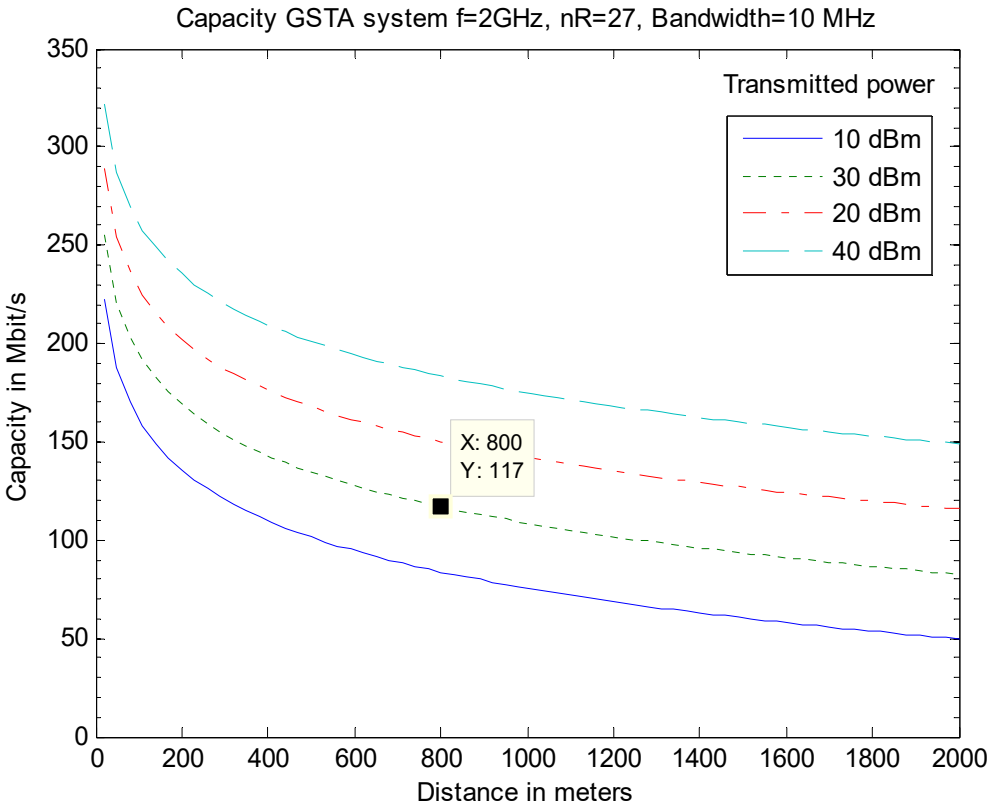

Figure A.116: GSTA C. Squares array at reception N_r =27 $\emptyset_1 = \frac{3\pi}{4}$ $\emptyset_2 = \frac{3\pi}{4}$

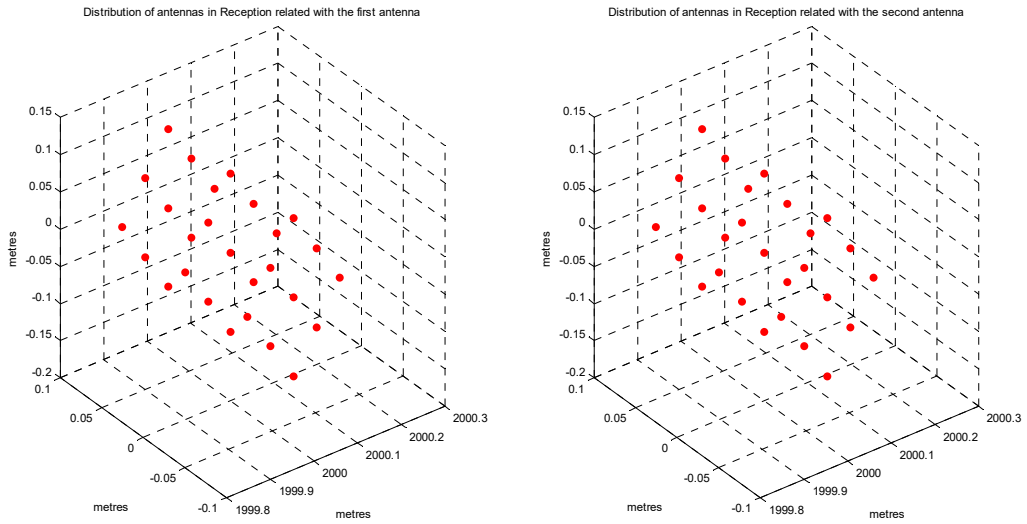

Figure A.117: GSTA Cube array at reception N_r =27 $\emptyset_1 = \frac{3\pi}{4}$ $\emptyset_2 = \frac{3\pi}{4}$

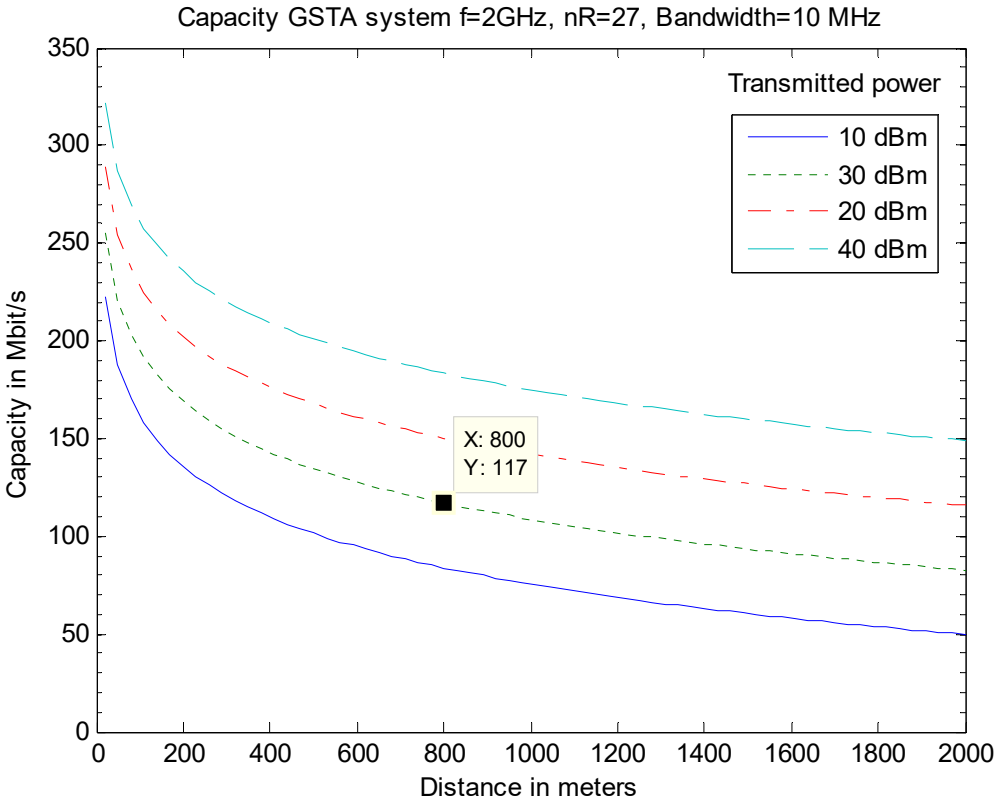

Figure A.118: GSTA Cube array at reception N_r =27 $\emptyset_1 = \frac{3\pi}{4}$ $\emptyset_2 = \frac{3\pi}{4}$

A.2.5 GSRA

- ***Carrier frequency (f_c):*** 2 GHz
- ***Number of antennas in transmission (n_t):*** 20 antennas
- ***Bandwidth (B):*** 10 MHz
- ***Separation between transmission antennas ($\Delta_t \lambda_c$):*** 7.5 cm (λ/2)
- ***Angle of incidence1 ($\emptyset 1$): π***
- ***Angle of incidence2 ($\emptyset 2$): $-\pi/12$***
- ***Transmitted power (P):*** 10, 20, 30 and 40 dBm
- ***Noise power (N_0):*** -104 dBm (-174 dBm/Hz)

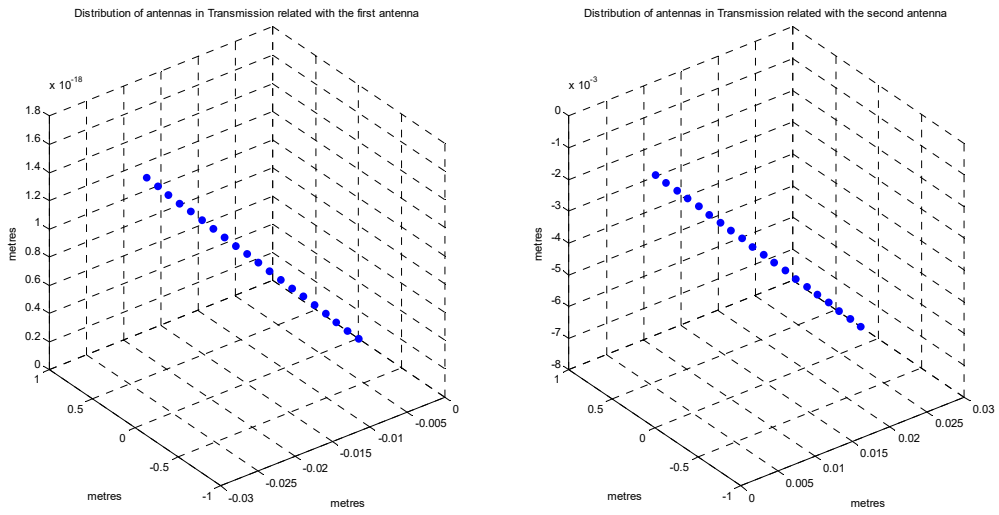

Figure A.119: GSRA Linear array at transmission N_t =20 $\emptyset_1 = \pi$ $\emptyset_2 = -\frac{\pi}{12}$

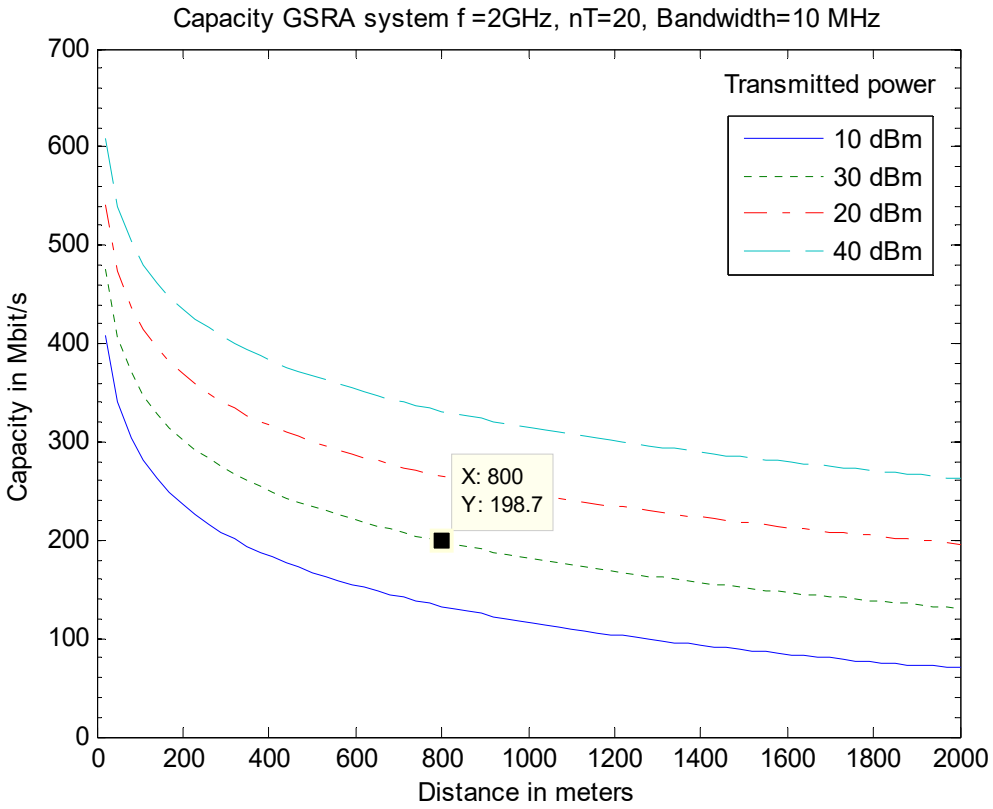

Figure A.120: GSRA Linear array at transmission N_t =20 $\emptyset_1 = \pi$ $\emptyset_2 = -\frac{\pi}{12}$

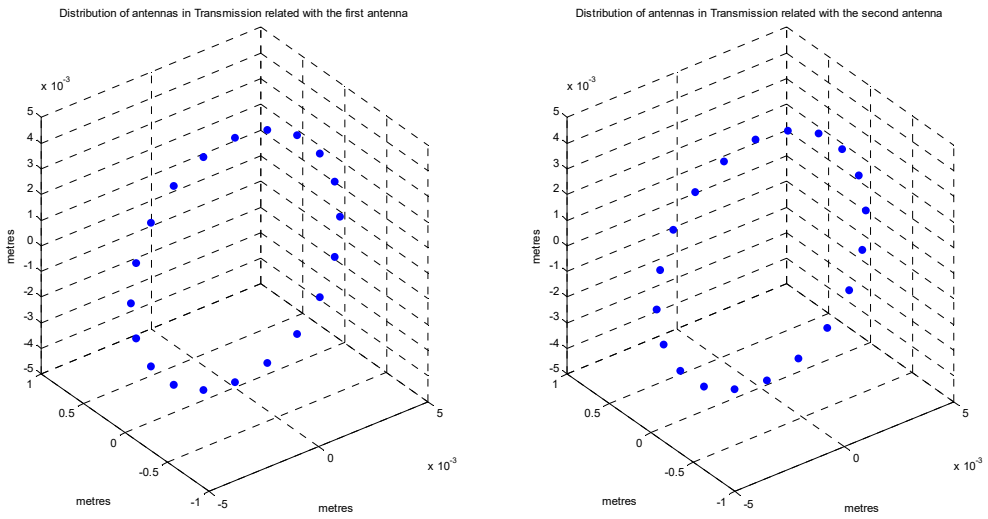

Figure A.121: GSRA Circular array at transmission N_t =20 $\emptyset_1 = \pi$ $\emptyset_2 = -\frac{\pi}{12}$

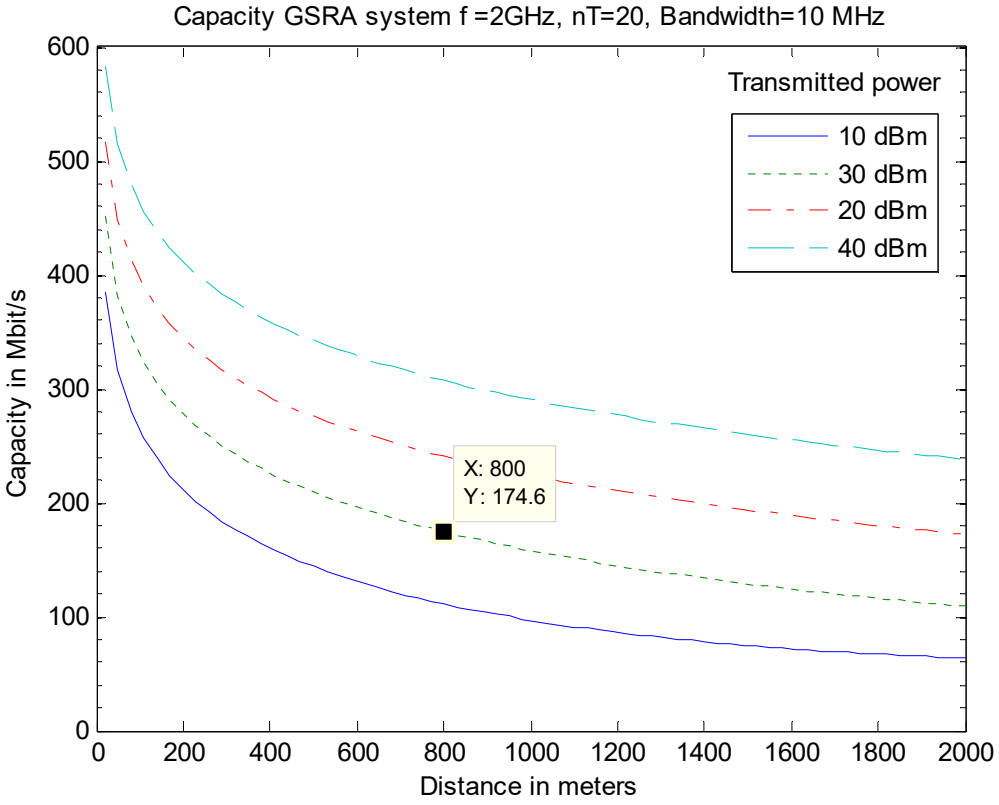

Figure A.122: GSRA Circular array at transmission N_t =20 $\emptyset_1 = \pi$ $\emptyset_2 = -\frac{\pi}{12}$

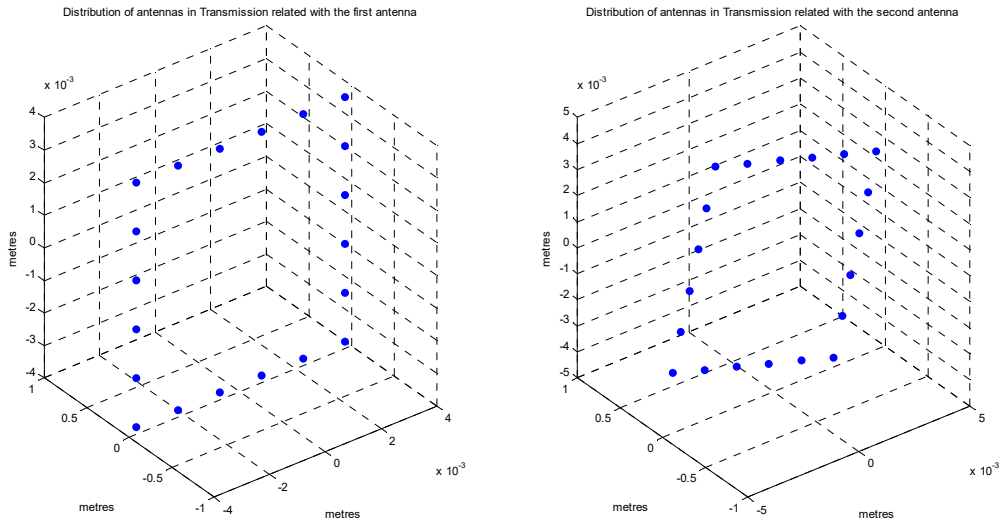

Figure A.123: GSRA Square array at transmission N_t =20 $\emptyset_1 = \pi$ $\emptyset_2 = -\frac{\pi}{12}$

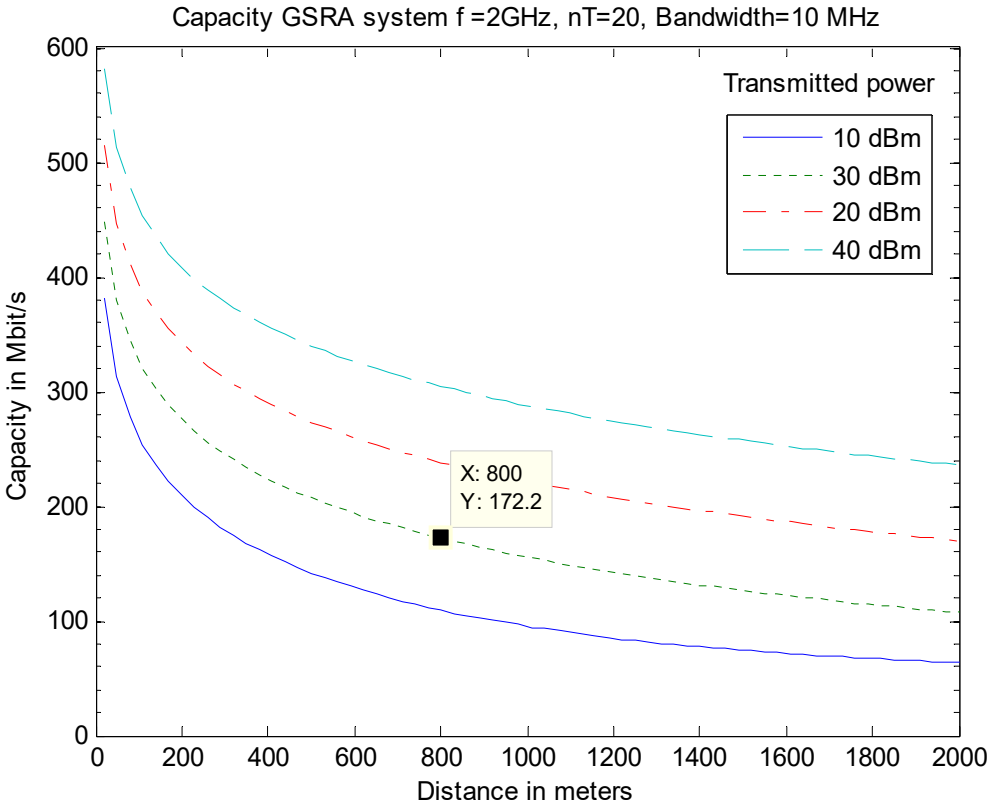

Figure A.124: GSRA Square array at transmission N_t =20 $\emptyset_1 = \pi$ $\emptyset_2 = -\frac{\pi}{12}$

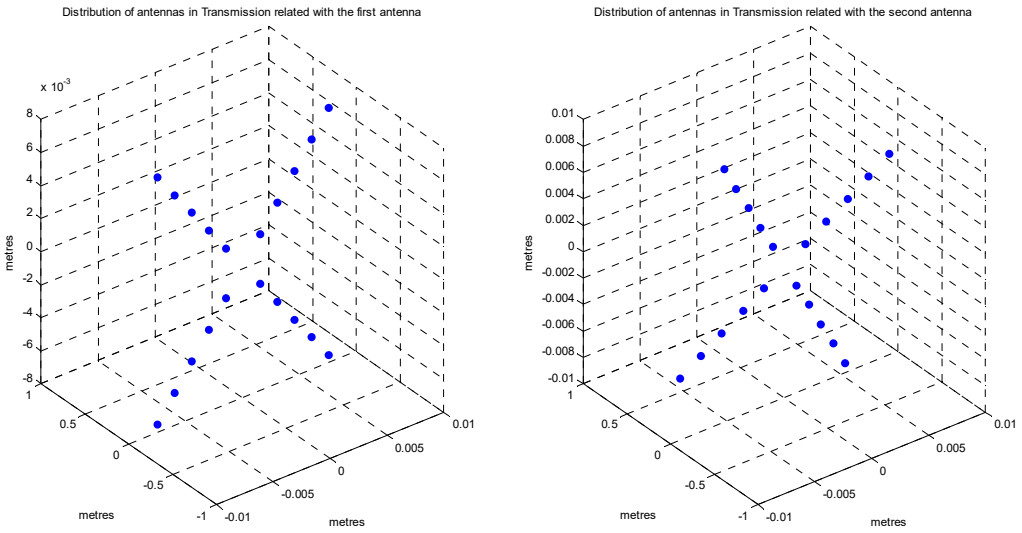

Figure A.125: GSRA C. Squares array at transmission $N_t = 20$ $\emptyset_1 = \pi$ $\emptyset_2 = -\frac{\pi}{12}$

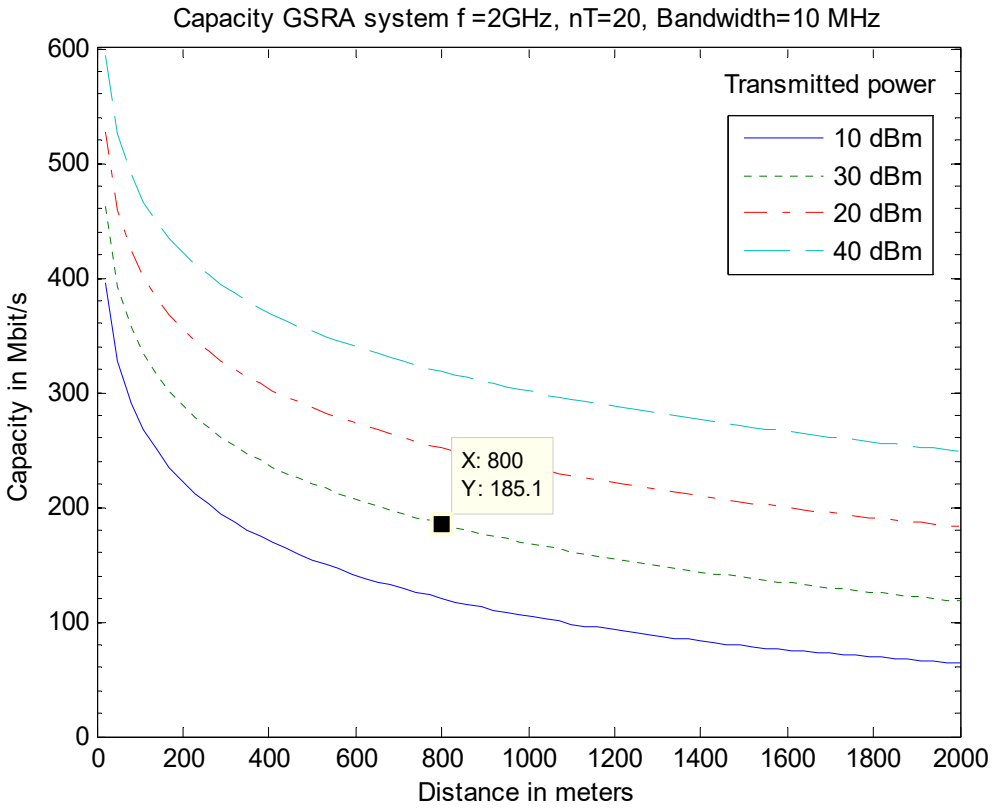

Figure A.126: GSRA C. Squares array at transmission $N_t = 20$ $\emptyset_1 = \pi$ $\emptyset_2 = -\frac{\pi}{12}$

- ***Carrier frequency (f_c):*** 2 GHz
- ***Number of antennas in transmission (n_t):*** 27 antennas
- ***Bandwidth (B):*** 10 MHz
- ***Separation between transmission antennas ($\Delta_t \lambda_c$):*** 7.5 cm (λ/2)
- ***Angle of incidence1 ($\emptyset 1$): π***
- ***Angle of incidence2 ($\emptyset 2$): $-\pi/12$***
- ***Transmitted power (P):*** 10, 20, 30 and 40 dBm
- ***Noise power (N_0):*** -104 dBm (-174 dBm/Hz)

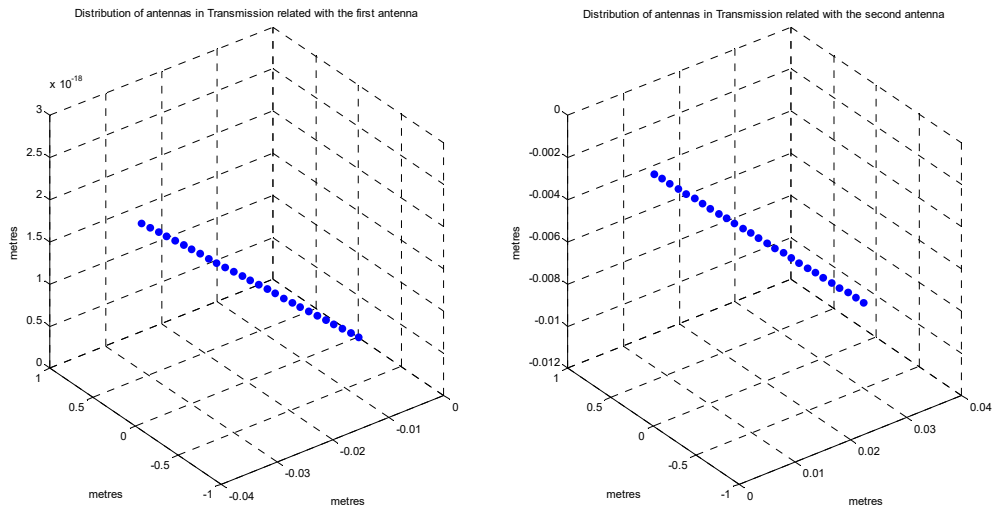

Figure A.127: GSRA Linear array at transmission N_t =27 $\emptyset_1 = \pi$ $\emptyset_2 = -\frac{\pi}{12}$

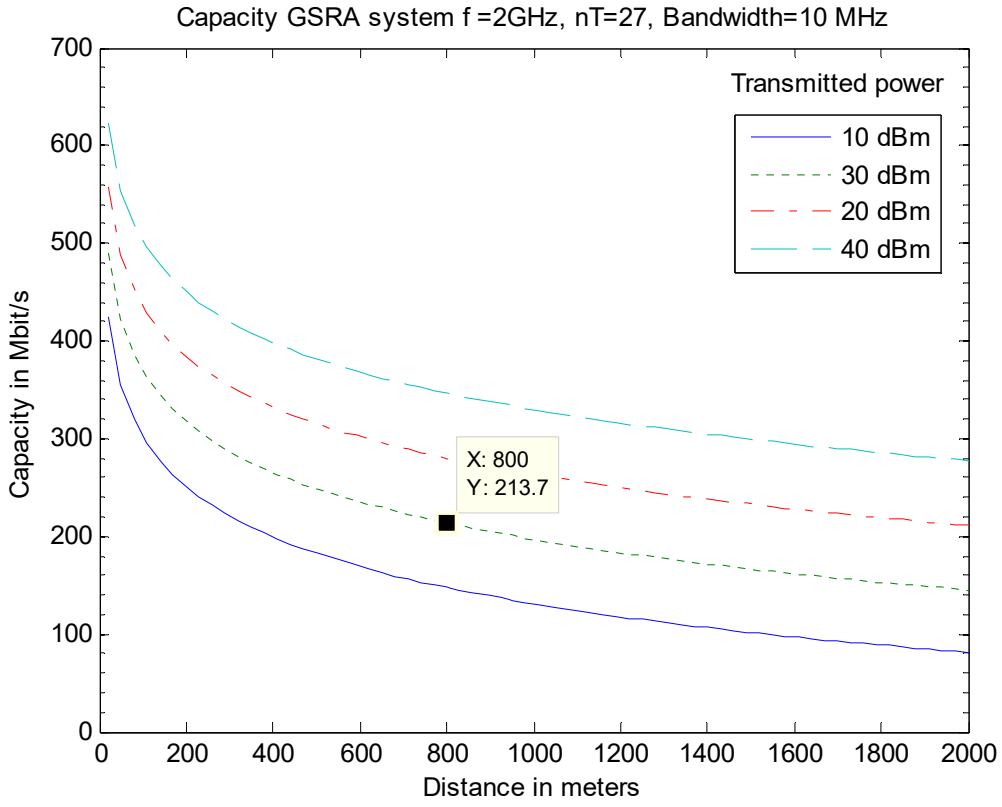

Figure A.128: GSRA Linear array at transmission N_t =27 $\emptyset_1 = \pi$ $\emptyset_2 = -\frac{\pi}{12}$

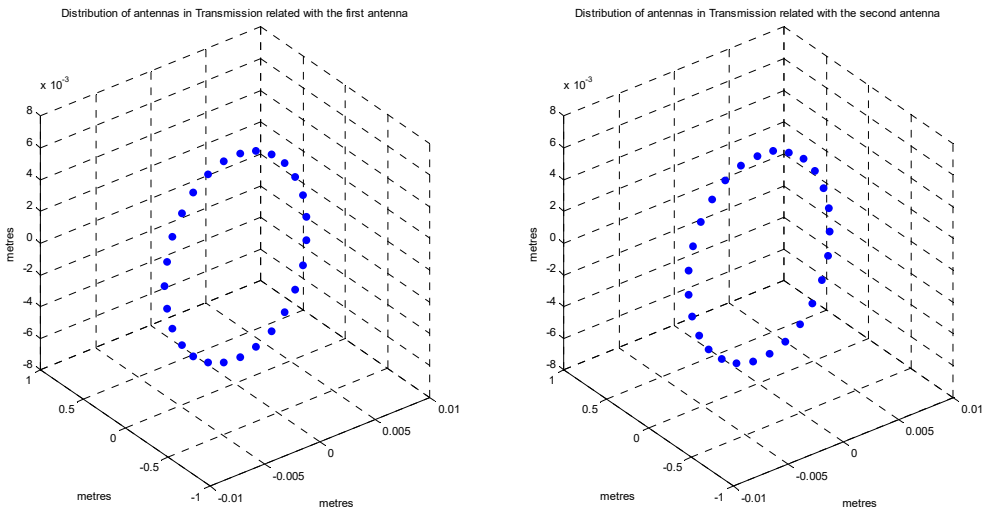

Figure A.129: GSRA Circular array at transmission N_t =27 $\emptyset_1 = \pi$ $\emptyset_2 = -\frac{\pi}{12}$

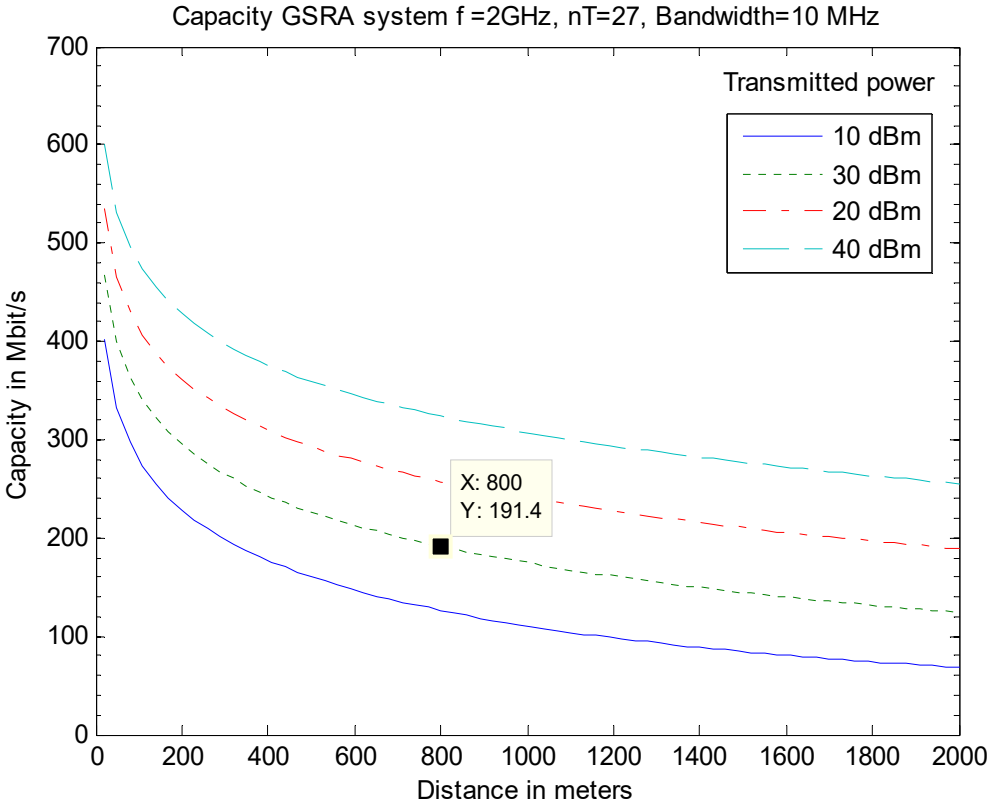

Figure A.130: GSRA Circular array at transmission N_t =27 $\emptyset_1 = \pi$ $\emptyset_2 = -\frac{\pi}{12}$

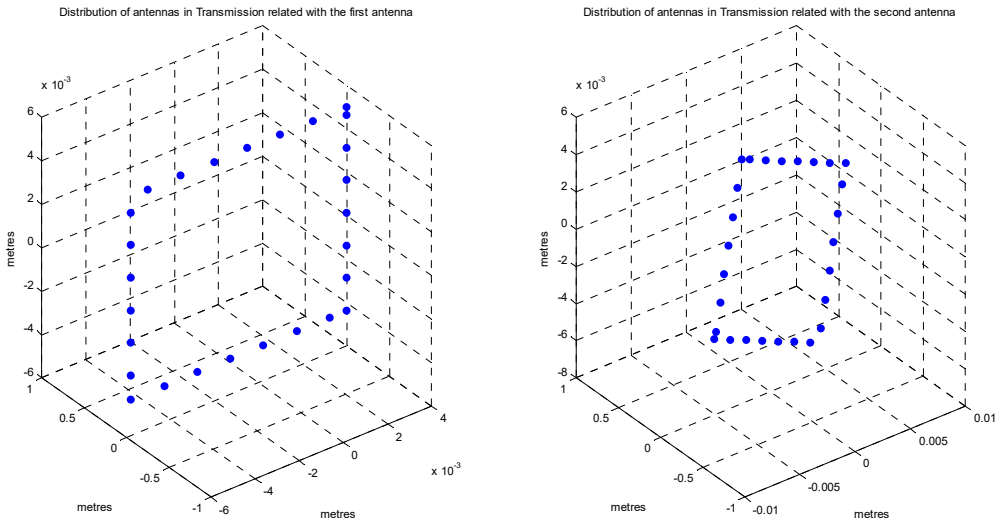

Figure A.131: GSRA Square array at transmission N_t =27 $\emptyset_1 = \pi$ $\emptyset_2 = -\frac{\pi}{12}$

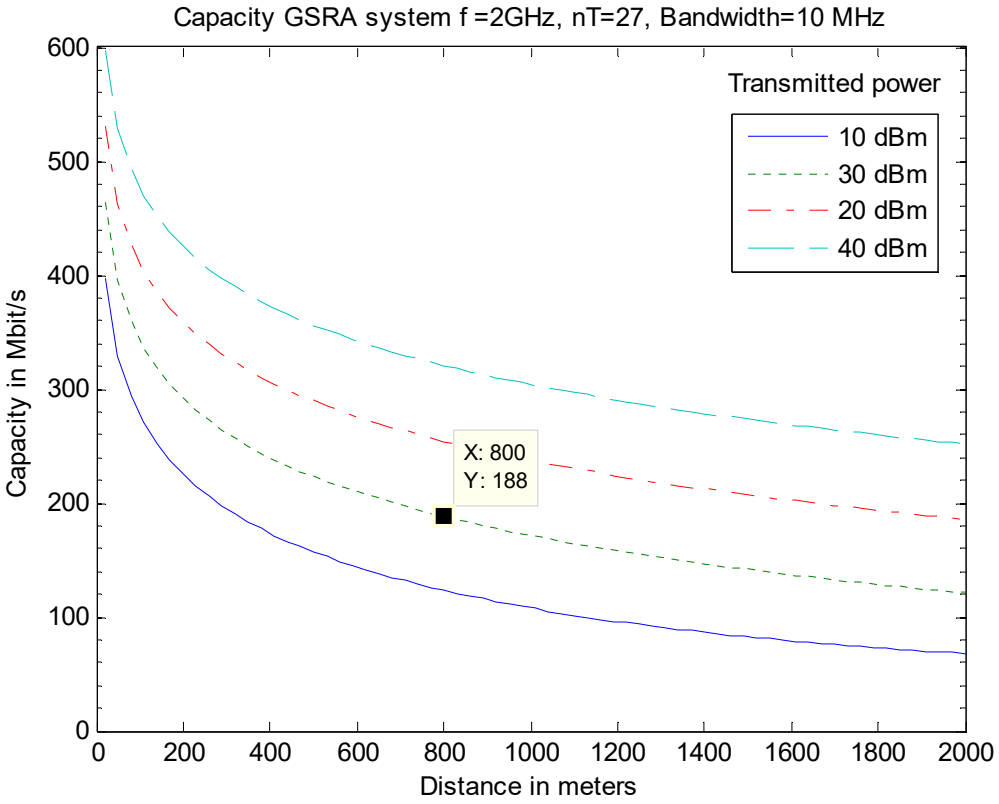

Figure A.132: GSRA Square array at transmission N_t =27 $\emptyset_1 = \pi$ $\emptyset_2 = -\frac{\pi}{12}$

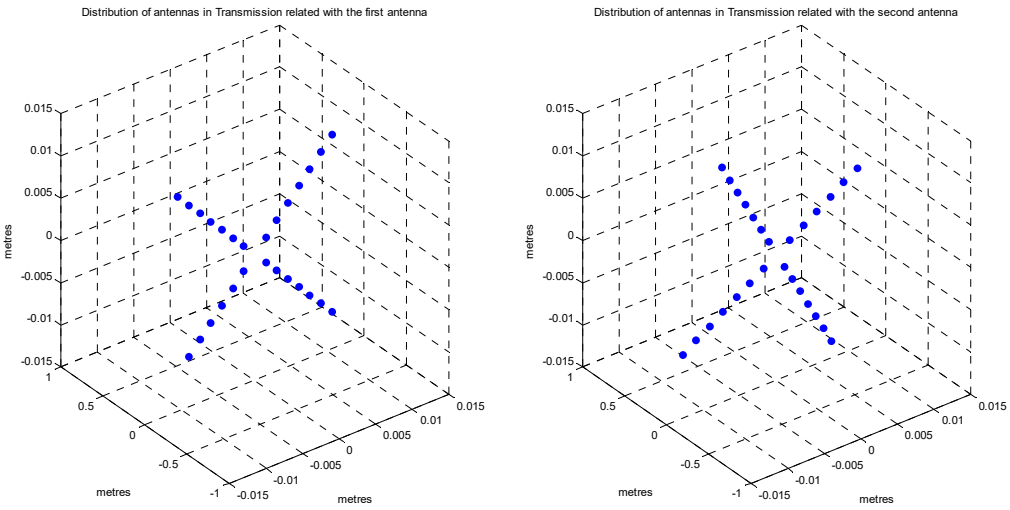

Figure A.133: GSRA C. Squares array at transmission N_t =27 $\emptyset_1 = \pi$ $\emptyset_2 = -\frac{\pi}{12}$

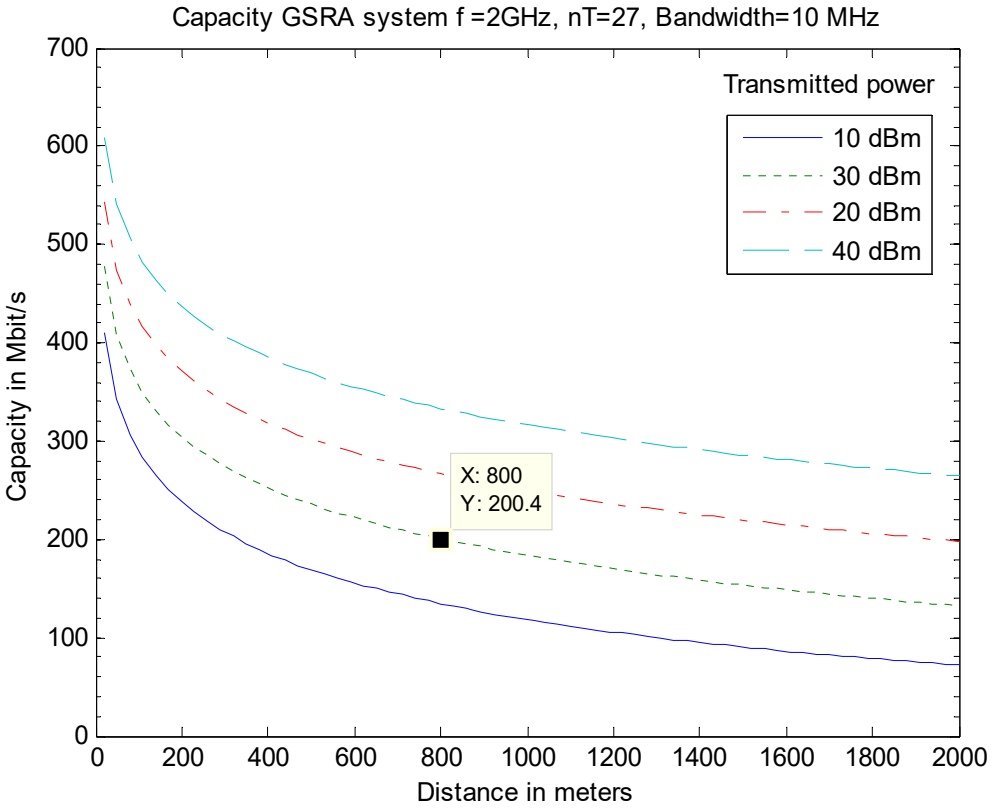

Figure A.134: GSRA C. Squares array at transmission N_t =27 $\emptyset_1 = \pi$ $\emptyset_2 = -\frac{\pi}{12}$

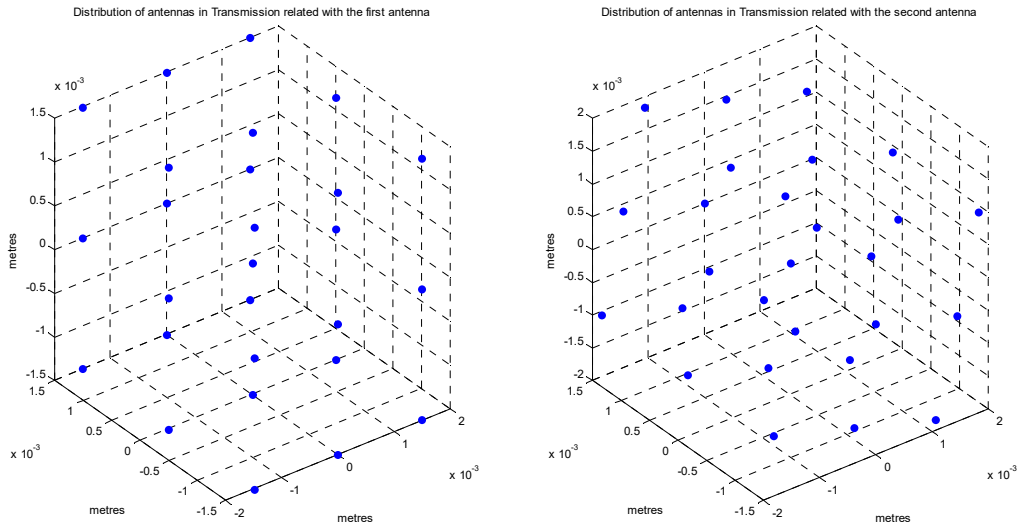

Figure A.135: GSRA Cube array at transmission N_t =27 $\emptyset_1 = \pi$ $\emptyset_2 = -\frac{\pi}{12}$

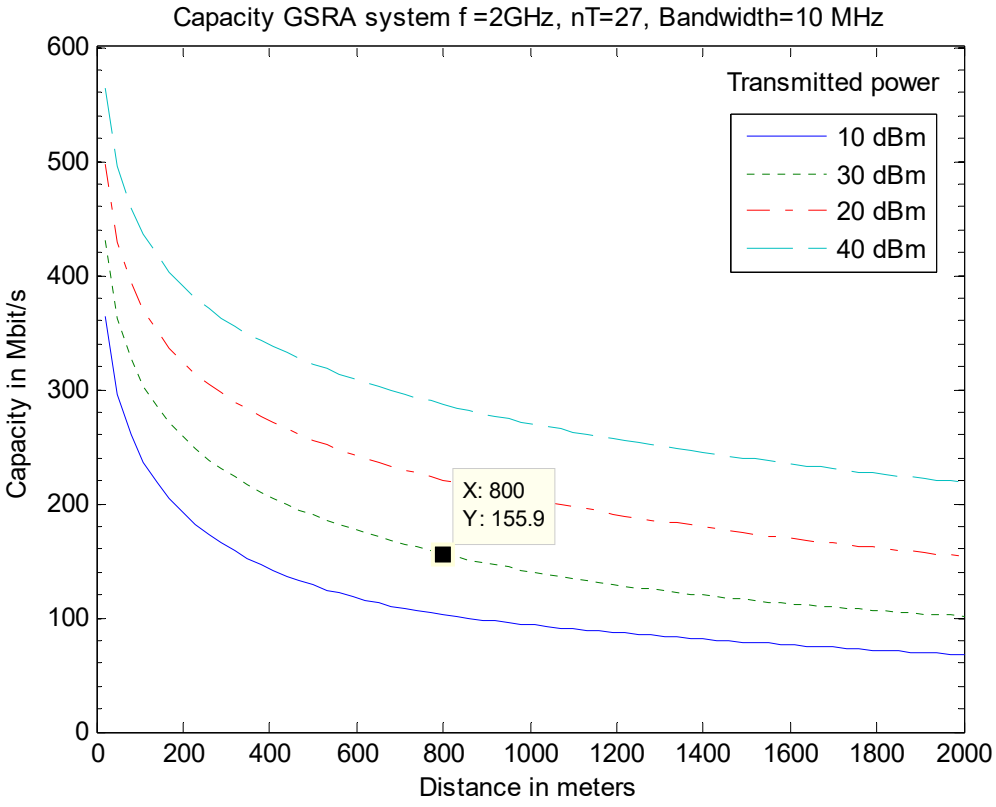

Figure A.136: GSRA Cube array at transmission N_t =27 $\emptyset_1 = \pi$ $\emptyset_2 = -\frac{\pi}{12}$

- ***Carrier frequency (f_c):*** 2 GHz
- ***Number of antennas in transmission (n_t):*** 20 antennas
- ***Bandwidth (B):*** 10 MHz
- ***Separation between transmission antennas ($\Delta_t \lambda_c$):*** 7.5 cm (λ/2)
- ***Angle of incidence1 ($\emptyset 1$): π***
- ***Angle of incidence2 ($\emptyset 2$): $-\pi/5$***
- ***Transmitted power (P):*** 10, 20, 30 and 40 dBm
- ***Noise power (N_0):*** -104 dBm (-174 dBm/Hz)

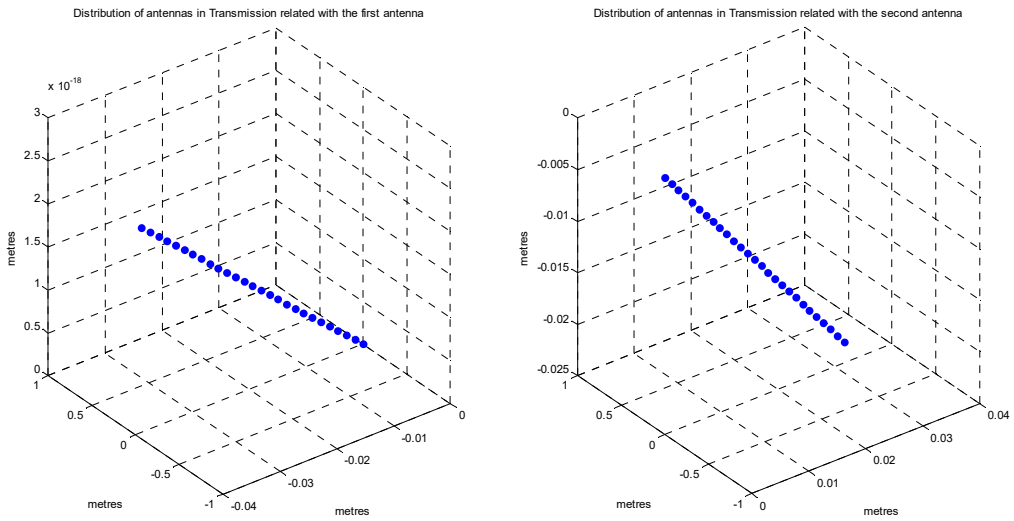

Figure A.137: GSRA Linear array at transmission N_t =27 $\emptyset_1 = \pi$ $\emptyset_2 = -\frac{\pi}{5}$

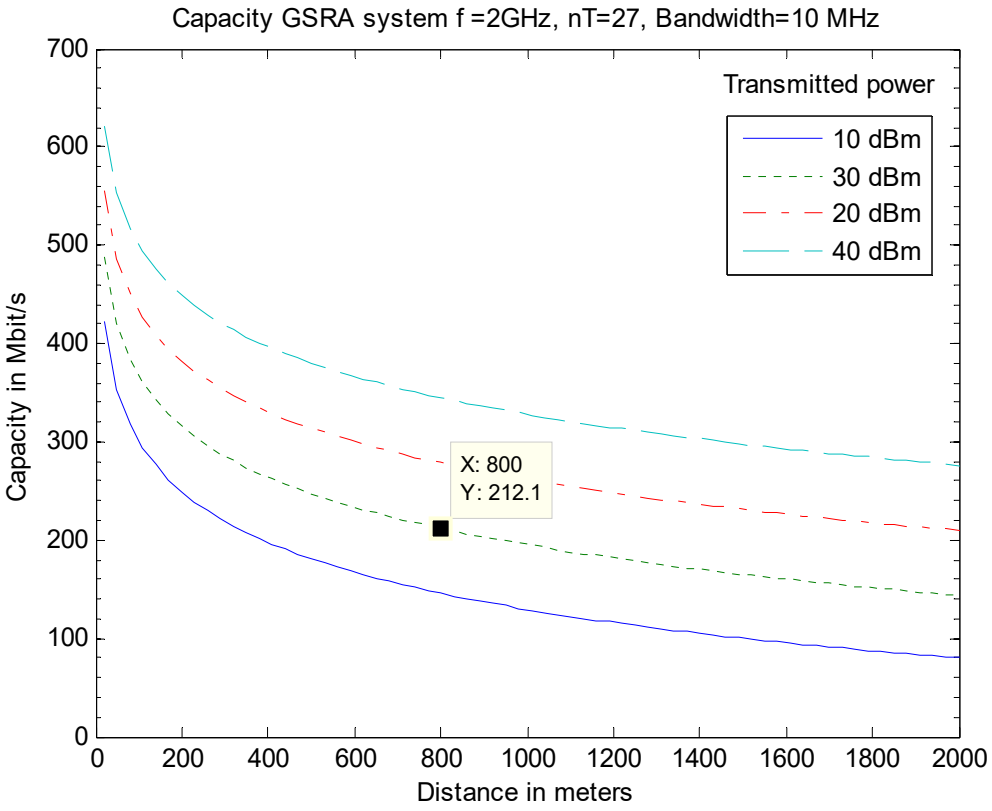

Figure A.138: GSRA Linear array at transmission N_t =27 $\emptyset_1 = \pi$ $\emptyset_2 = -\frac{\pi}{5}$

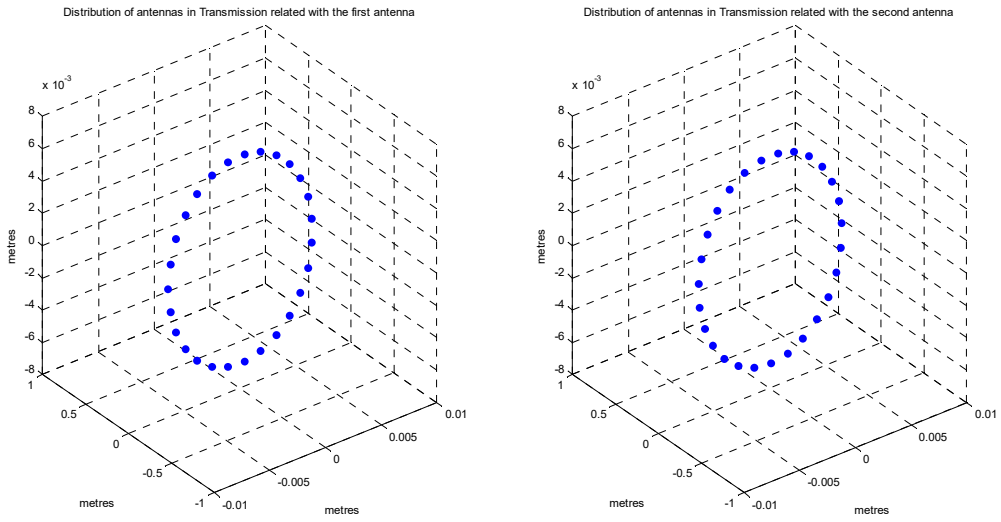

Figure A.139: GSRA Circular array at transmission N_t =27 $\emptyset_1 = \pi$ $\emptyset_2 = -\frac{\pi}{5}$

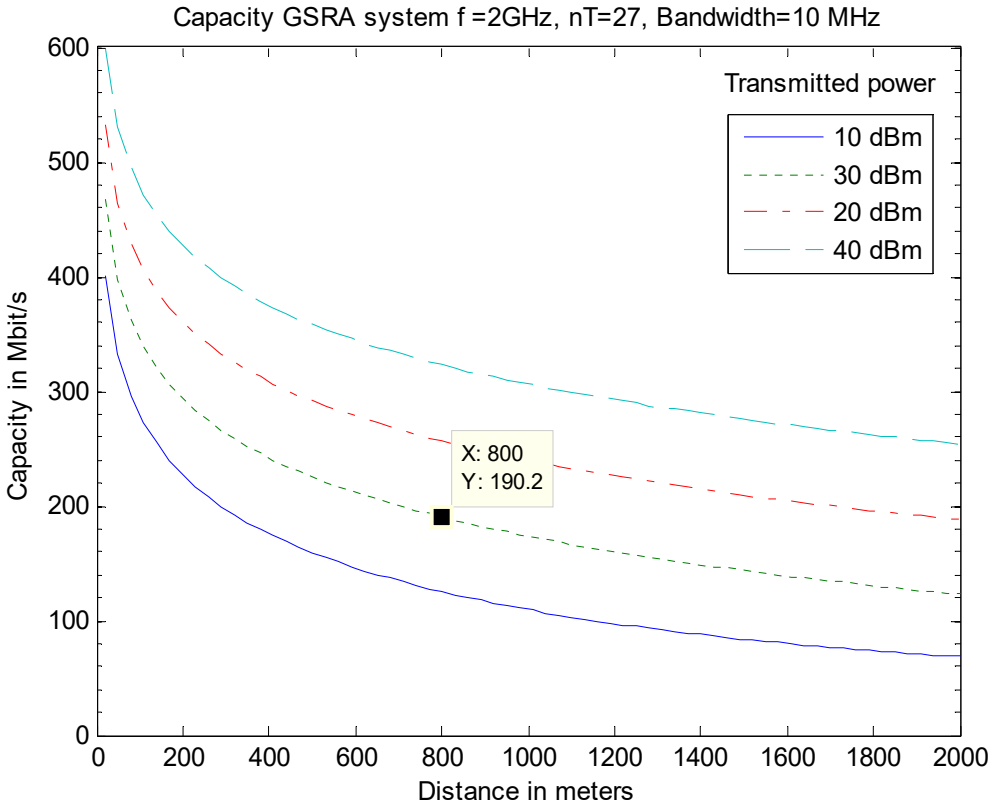

Figure A.140: GSRA Circular array at transmission N_t =27 $\emptyset_1 = \pi$ $\emptyset_2 = -\frac{\pi}{5}$

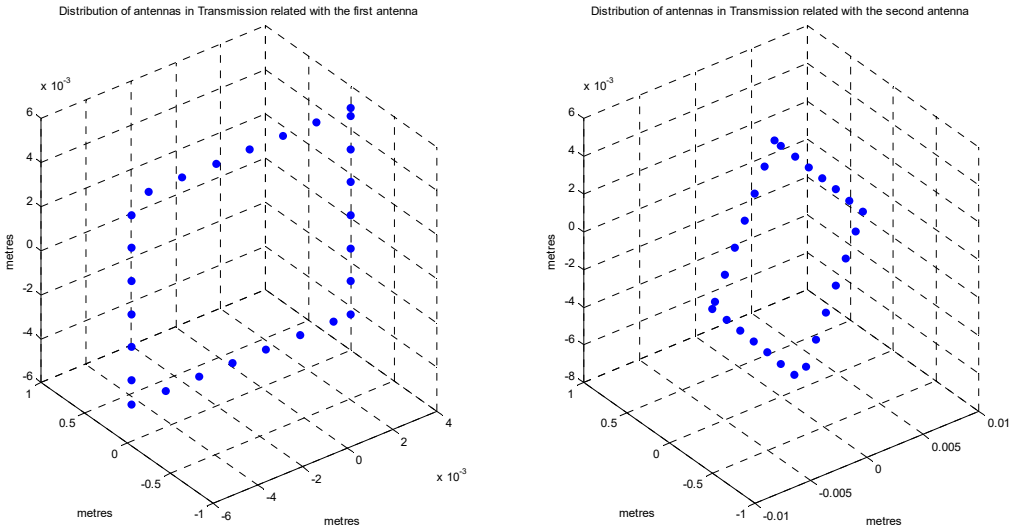

Figure A.141: GSRA Square array at transmission N_t =27 $\emptyset_1 = \pi$ $\emptyset_2 = -\frac{\pi}{5}$

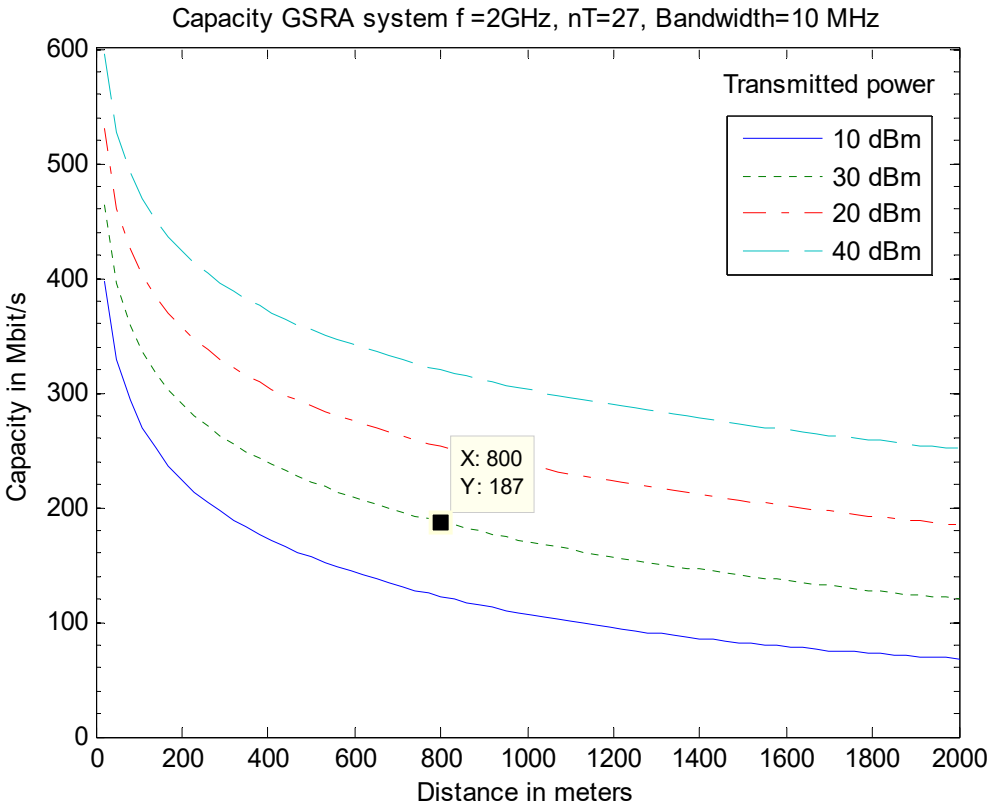

Figure A.142: GSRA Square array at transmission N_t =27 $\emptyset_1 = \pi$ $\emptyset_2 = -\frac{\pi}{5}$

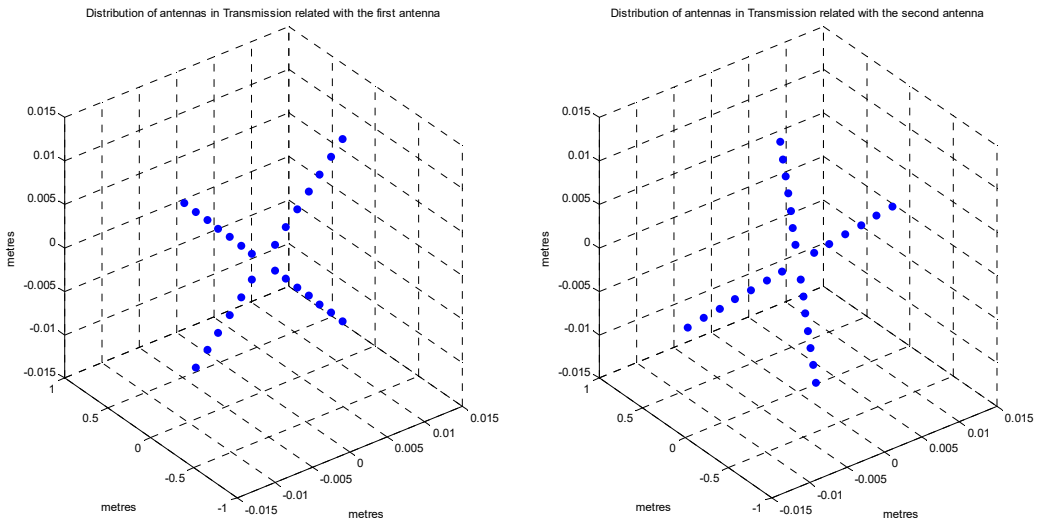

Figure A.143: GSRA C. Squares array at transmission $N_t = 27$ $\emptyset_1 = \pi$ $\emptyset_2 = -\frac{\pi}{5}$

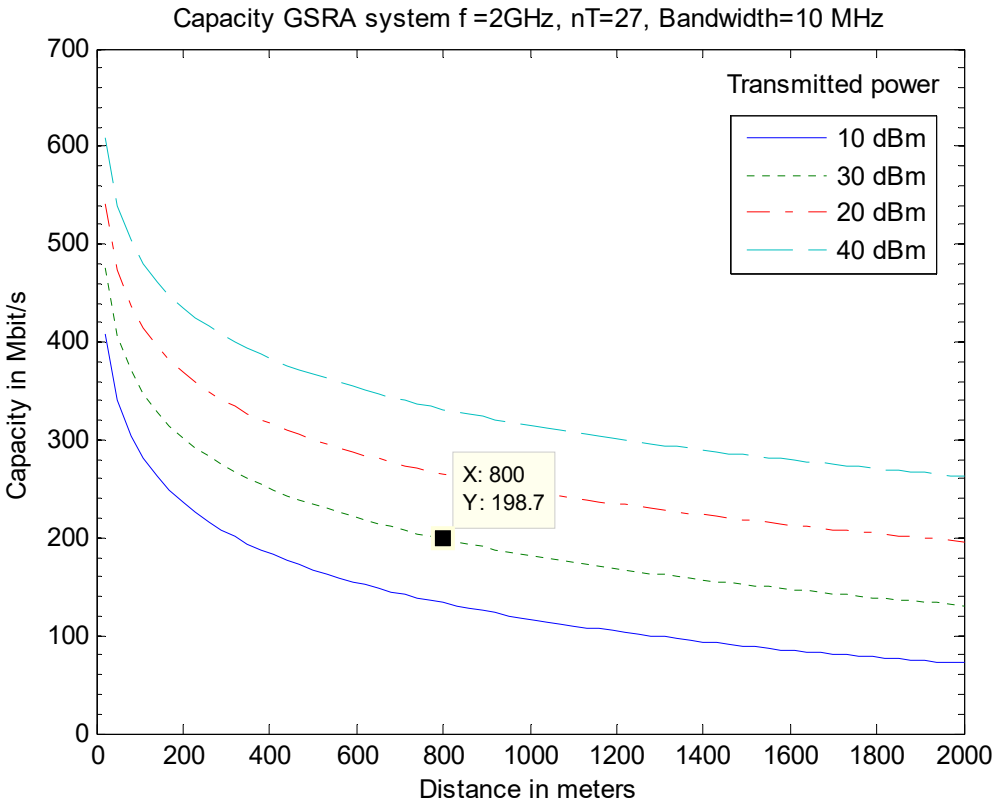

Figure A.144: GSRA C. Squares array at transmission $N_t = 27$ $\emptyset_1 = \pi$ $\emptyset_2 = -\frac{\pi}{5}$

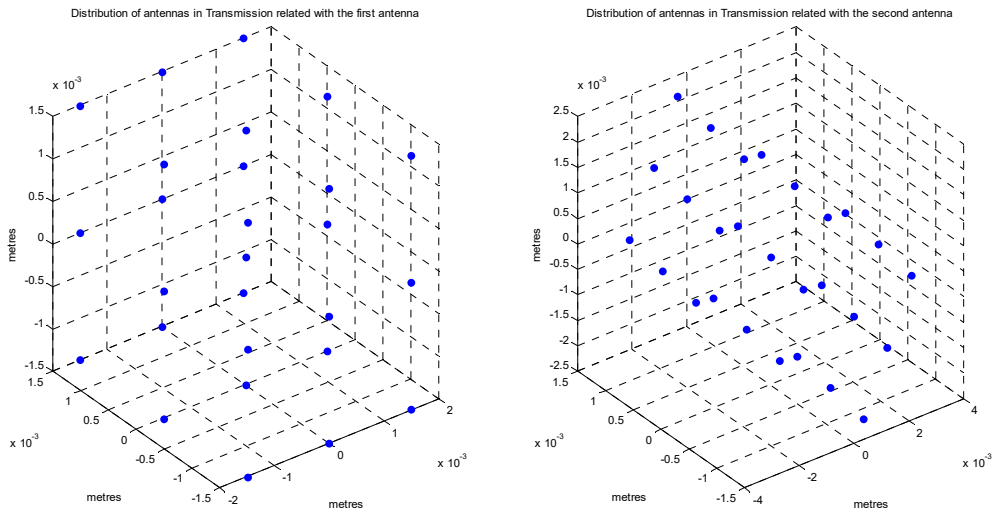

Figure A.145: GSRA Cube array at transmission N_t =27 $\emptyset_1 = \pi$ $\emptyset_2 = -\frac{\pi}{5}$

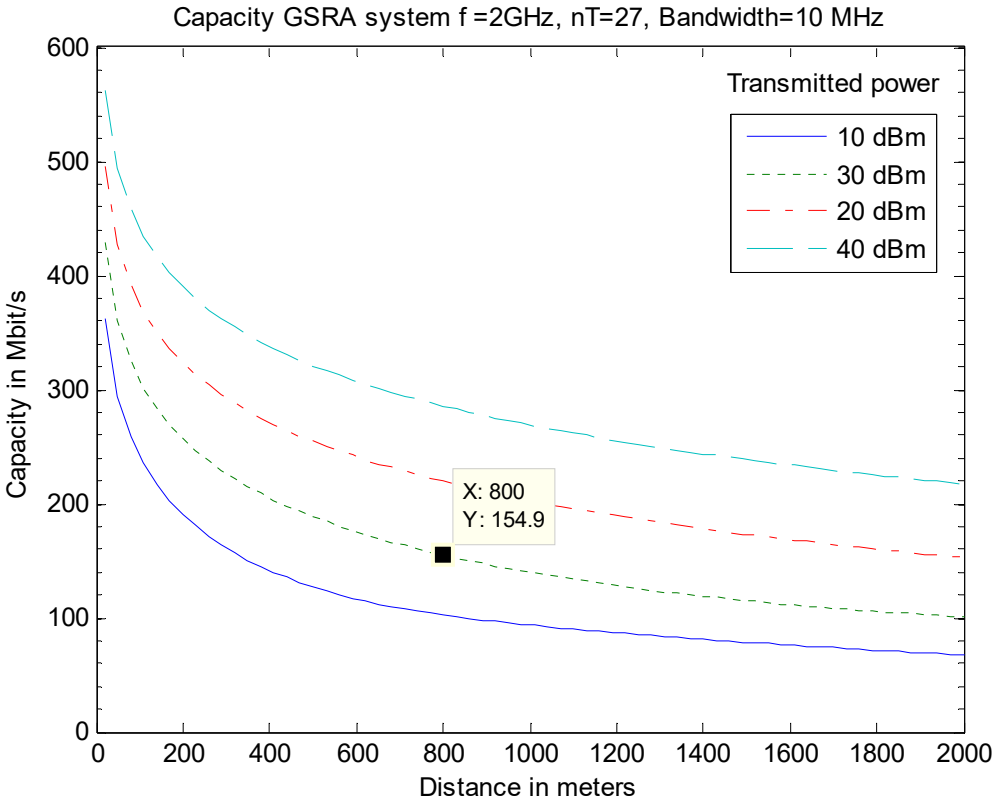

Figure A.146: GSRA Cube array at transmission N_t =27 $\emptyset_1 = \pi$ $\emptyset_2 = -\frac{\pi}{5}$

A.3 Tables

This section contains all the channel matrixes that have been obtained with the models and have been used for the simulations. The matrixes of the MIMO models and simulations are not available because in the simulations we use twenty or more antennas in transmission and the same number of antennas in reception, this creates matrixes of dimension of 20X20, that are too huge to include in the report.

A.3.1 SIMO

Linear Array $N_r = 20$ d = 2km
1.0e-005 *
-0.0753 + 0.1304i
-0.0753 + 0.1304i
-0.0753 + 0.1303i
-0.0753 + 0.1303i
-0.0754 + 0.1303i
-0.0755 + 0.1303i
-0.0755 + 0.1302i
-0.0756 + 0.1301i
-0.0758 + 0.1301i
-0.0759 + 0.1300i
-0.0760 + 0.1299i
-0.0762 + 0.1298i
-0.0764 + 0.1297i
-0.0766 + 0.1296i
-0.0768 + 0.1295i
-0.0770 + 0.1294i
-0.0772 + 0.1292i
-0.0775 + 0.1291i
-0.0777 + 0.1289i
-0.0780 + 0.1287i

Table A.1: Channel matrix SIMO Linear Array N_r=20

Circular Array N_r =20 d = 2km
1.0e-005 *
0.0685 - 0.1340i
-0.0178 + 0.1495i
-0.1091 - 0.1037i
0.0862 - 0.1234i
0.1341 - 0.0684i
0.0862 - 0.1234i
-0.1091 - 0.1037i
-0.0178 + 0.1495i
0.0685 - 0.1340i
-0.0753 + 0.1303i
0.0819 - 0.1263i
-0.1206 + 0.0901i
0.1443 + 0.0427i
0.0638 - 0.1363i
-0.0078 - 0.1503i
0.0638 - 0.1363i
0.1443 + 0.0427i
-0.1206 + 0.0901i
0.0819 - 0.1263i
-0.0753 + 0.1303i

Table A.2: Channel matrix SIMO Circular Array N_r=20

Square Array N_r = 20 d=2km
1.0e-005 *
-0.1303 - 0.0753i
-0.1304 - 0.0753i
-0.1304 - 0.0753i
-0.1304 - 0.0753i
-0.1304 - 0.0753i
-0.1304 - 0.0753i
0.1304 + 0.0753i
-0.1304 - 0.0753i
0.1304 + 0.0753i
-0.1304 - 0.0753i
-0.1304 - 0.0753i
-0.1304 - 0.0753i
-0.1304 - 0.0753i
-0.1304 - 0.0753i
-0.1303 - 0.0753i

-0.1303 - 0.0753i
0.1303 + 0.0753i
-0.1303 - 0.0753i
0.1303 + 0.0753i
-0.1303 - 0.0753i

Table A.3: Channel matrix SIMO Square Array N_r=20

C. Squares Array N_r = 20 d=2km
1.0e-005 *
0.0753 - 0.1304i
0.0753 - 0.1304i
0.0753 - 0.1304i
0.0753 - 0.1304i
-0.0753 + 0.1303i
-0.0753 + 0.1303i
-0.0753 + 0.1303i
-0.0753 + 0.1303i
0.0753 - 0.1303i
0.0753 - 0.1303i
0.0753 - 0.1303i
0.0753 - 0.1303i
-0.0754 + 0.1303i
-0.0754 + 0.1303i
-0.0754 + 0.1303i
-0.0754 + 0.1303i
0.0755 - 0.1303i
0.0755 - 0.1303i
0.0755 - 0.1303i
0.0755 - 0.1303i

Table A.4: Channel matrix SIMO C. Squares Array N_r=20

Linear Array N_r =27 d=2km
1.0e-005 *
-0.0753 + 0.1304i
-0.0753 + 0.1304i
-0.0753 + 0.1303i
-0.0753 + 0.1303i

-0.0754 + 0.1303i
-0.0755 + 0.1303i
-0.0755 + 0.1302i
-0.0756 + 0.1301i
-0.0758 + 0.1301i
-0.0759 + 0.1300i
-0.0760 + 0.1299i
-0.0762 + 0.1298i
-0.0764 + 0.1297i
-0.0766 + 0.1296i
-0.0768 + 0.1295i
-0.0770 + 0.1294i
-0.0772 + 0.1292i
-0.0775 + 0.1291i
-0.0777 + 0.1289i
-0.0780 + 0.1287i
-0.0783 + 0.1286i
-0.0786 + 0.1284i
-0.0790 + 0.1282i
-0.0793 + 0.1280i
-0.0796 + 0.1277i
-0.0800 + 0.1275i
-0.0804 + 0.1273i

Table A.5: Channel matrix SIMO Linear Array N_r=27

Circular Array N_r =27 d=2km
1.0e-005 *
0.0717 - 0.1324i
-0.0445 + 0.1438i
-0.0333 - 0.1468i
0.1410 + 0.0526i
-0.0521 + 0.1412i
-0.1430 + 0.0472i
-0.1491 + 0.0205i
-0.1170 + 0.0947i
0.0518 + 0.1413i
0.1197 - 0.0913i
-0.1499 - 0.0133i
0.1369 + 0.0627i
-0.1306 - 0.0749i
0.1300 + 0.0759i

-0.1225 - 0.0874i
0.0863 + 0.1233i
0.0194 - 0.1493i
-0.1483 + 0.0257i
-0.0236 + 0.1487i
0.0568 + 0.1394i
0.0306 + 0.1474i
-0.0963 + 0.1157i
-0.1160 - 0.0959i
0.1438 - 0.0444i
-0.1025 + 0.1103i
0.0791 - 0.1281i
-0.0754 + 0.1303i

Table A.6: Channel matrix SIMO Circular Array N_r=27

Square Array N_r =27 d=2km
1.0e-005 *
0.1318 - 0.0727i
0.1318 - 0.0727i
0.1318 - 0.0727i
0.1318 - 0.0727i
0.1318 - 0.0727i
0.1318 - 0.0727i
0.1318 - 0.0727i
0.1224 - 0.0877i
0.0692 - 0.1337i
0.0010 - 0.1505i
-0.0675 - 0.1346i
-0.1212 - 0.0893i
-0.1485 - 0.0245i
-0.1435 + 0.0456i
-0.1435 + 0.0456i
-0.1435 + 0.0456i
-0.1435 + 0.0456i
-0.1435 + 0.0456i
-0.1435 + 0.0456i
-0.1435 + 0.0456i
-0.1435 + 0.0456i
-0.1504 - 0.0069i
-0.1308 - 0.0744i
-0.0828 - 0.1257i

-0.0167 - 0.1496i
0.0530 - 0.1409i
0.1112 - 0.1014i

Table A.7: Channel matrix SIMO Square Array N_r=27

C. Squares Array N_r =27 d=2km

1.0e-005
0.0753 - 0.1304i
0.0753 - 0.1304i
0.0753 - 0.1304i
0.0753 - 0.1304i
-0.0753 + 0.1303i
-0.0753 + 0.1303i
-0.0753 + 0.1303i
-0.0753 + 0.1303i
0.0753 - 0.1303i
0.0753 - 0.1303i
0.0753 - 0.1303i
0.0753 - 0.1303i
-0.0754 + 0.1303i
-0.0754 + 0.1303i
-0.0754 + 0.1303i
-0.0754 + 0.1303i
0.0755 - 0.1303i
0.0755 - 0.1303i
0.0755 - 0.1303i
0.0755 - 0.1303i
-0.0755 + 0.1302i
-0.0755 + 0.1302i
-0.0755 + 0.1302i
-0.0755 + 0.1302i
0.0756 - 0.1301i
0.0756 - 0.1301i
0.0756 - 0.1301i

Table A.8: Channel matrix SIMO C. Squares Array N_r=27

Cube Array N_r=27 d=2km
1.0e-005
0.0753 - 0.1304i
0.0753 - 0.1304i
0.0753 - 0.1304i
0.0753 - 0.1304i
0.0753 - 0.1304i
0.0753 - 0.1304i
0.0753 - 0.1304i
0.0753 - 0.1304i
0.0753 - 0.1304i
-0.0753 + 0.1304i
-0.0753 + 0.1304i
-0.0753 + 0.1304i
-0.0753 + 0.1304i
-0.0753 + 0.1304i
-0.0753 + 0.1304i
-0.0753 + 0.1304i
-0.0753 + 0.1304i
-0.0753 + 0.1304i
0.0753 - 0.1304i
0.0753 - 0.1304i
0.0753 - 0.1304i
0.0753 - 0.1304i
0.0753 - 0.1304i
0.0753 - 0.1304i
0.0753 - 0.1304i
0.0753 - 0.1304i
0.0753 - 0.1304i

Table A.9: Channel matrix SIMO Cube Array N_r=27

A.3.2 MISO

Linear Array N_t =20 d=2km
1.0e-005 *
-0.0753 - 0.1304i
-0.0753 - 0.1304i
-0.0753 - 0.1303i
-0.0753 - 0.1303i
-0.0754 - 0.1303i
-0.0755 - 0.1303i

-0.0755 - 0.1302i
-0.0756 - 0.1301i
-0.0758 - 0.1301i
-0.0759 - 0.1300i
-0.0760 - 0.1299i
-0.0762 - 0.1298i
-0.0764 - 0.1297i
-0.0766 - 0.1296i
-0.0768 - 0.1295i
-0.0770 - 0.1294i
-0.0772 - 0.1292i
-0.0775 - 0.1291i
-0.0777 - 0.1289i
-0.0780 - 0.1287i

Table A.10: Channel matrix MISO Linear Array N_t=20

Circular Array N_t=20 d=2km
1.0e-005 *
0.0819 + 0.1263i
-0.1206 - 0.0901i
0.1443 - 0.0427i
0.0638 + 0.1363i
-0.0078 + 0.1503i
0.0638 + 0.1363i
0.1443 - 0.0427i
-0.1206 - 0.0901i
0.0819 + 0.1263i
-0.0753 - 0.1303i
0.0685 + 0.1340i
-0.0178 - 0.1495i
-0.1091 + 0.1037i
0.0862 + 0.1234i
0.1341 + 0.0684i
0.0862 + 0.1234i
-0.1091 + 0.1037i
-0.0178 - 0.1495i
0.0685 + 0.1340i
-0.0753 - 0.1303i

Table A.11: Channel matrix MISO Circular Array N_t=20

Square Array N_t =20 d=2km
1.0e-005 *
0.1303 - 0.0753i
0.1304 - 0.0753i
0.1304 - 0.0753i
0.1304 - 0.0753i
0.1304 - 0.0753i
0.1304 - 0.0753i
-0.1304 + 0.0753i
0.1304 - 0.0753i
-0.1304 + 0.0753i
0.1304 - 0.0753i
0.1304 - 0.0753i
0.1304 - 0.0753i
0.1304 - 0.0753i
0.1304 - 0.0753i
0.1303 - 0.0753i
0.1303 - 0.0753i
-0.1303 + 0.0753i
0.1303 - 0.0753i
-0.1303 + 0.0753i
0.1303 - 0.0753i

Table A.12: Channel matrix MISO Square Array N_t=20

C. Squares Array N_t =20 d=2km
1.0e-005 *
0.0753 + 0.1304i
0.0753 + 0.1304i
0.0753 + 0.1304i
0.0753 + 0.1304i
-0.0753 - 0.1303i
-0.0753 - 0.1303i
-0.0753 - 0.1303i
-0.0753 - 0.1303i
0.0753 + 0.1303i
0.0753 + 0.1303i
0.0753 + 0.1303i
0.0753 + 0.1303i
-0.0754 - 0.1303i

-0.0754 - 0.1303i
-0.0754 - 0.1303i
-0.0754 - 0.1303i
0.0755 + 0.1303i
0.0755 + 0.1303i
0.0755 + 0.1303i
0.0755 + 0.1303i

Table A.13: Channel matrix MISO C. Squares Array N_t=20

Linear Array N_t =27 d=2km
1.0e-005 *
-0.0753 - 0.1304i
-0.0753 - 0.1304i
-0.0753 - 0.1303i
-0.0753 - 0.1303i
-0.0754 - 0.1303i
-0.0755 - 0.1303i
-0.0755 - 0.1302i
-0.0756 - 0.1301i
-0.0758 - 0.1301i
-0.0759 - 0.1300i
-0.0760 - 0.1299i
-0.0762 - 0.1298i
-0.0764 - 0.1297i
-0.0766 - 0.1296i
-0.0768 - 0.1295i
-0.0770 - 0.1294i
-0.0772 - 0.1292i
-0.0775 - 0.1291i
-0.0777 - 0.1289i
-0.0780 - 0.1287i
-0.0783 - 0.1286i
-0.0786 - 0.1284i
-0.0790 - 0.1282i
-0.0793 - 0.1280i
-0.0796 - 0.1277i
-0.0800 - 0.1275i
-0.0804 - 0.1273i

Table A.14: Channel matrix MISO Linear Array N_t=27

Circular Array N_t =27 d=2km
1.0e-005 *
0.0791 + 0.1281i
-0.1025 - 0.1103i
0.1438 + 0.0444i
-0.1160 + 0.0959i
-0.0963 - 0.1157i
0.0306 - 0.1474i
0.0568 - 0.1394i
-0.0236 - 0.1487i
-0.1483 - 0.0257i
0.0194 + 0.1493i
0.0863 - 0.1233i
-0.1225 + 0.0874i
0.1300 - 0.0759i
-0.1306 + 0.0749i
0.1369 - 0.0627i
-0.1499 + 0.0133i
0.1197 + 0.0913i
0.0518 - 0.1413i
-0.1170 - 0.0947i
-0.1491 - 0.0205i
-0.1430 - 0.0472i
-0.0521 - 0.1412i
0.1410 - 0.0526i
-0.0333 + 0.1468i
-0.0445 - 0.1438i
0.0717 + 0.1324i
-0.0754 - 0.1303i

Table A.15: Channel matrix MISO Circular Array N_t=27

Square Array N_t =27 d=2km
1.0e-005 *
-0.0916 + 0.1195i
-0.0916 + 0.1195i
-0.0916 + 0.1194i
-0.0916 + 0.1194i
-0.0916 + 0.1194i
-0.0916 + 0.1194i
-0.0916 + 0.1195i
0.0197 + 0.1492i

-0.0197 - 0.1492i
0.0197 + 0.1492i
-0.0197 - 0.1492i
0.0197 + 0.1492i
-0.0197 - 0.1492i
0.0197 + 0.1492i
0.0197 + 0.1492i
0.0197 + 0.1492i
0.0196 + 0.1492i
0.0197 + 0.1492i
0.0197 + 0.1492i
0.0197 + 0.1492i
0.0198 + 0.1492i
-0.1195 - 0.0915i
0.1195 + 0.0915i
-0.1195 - 0.0915i
0.1195 + 0.0915i
-0.1195 - 0.0915i
0.1195 + 0.0915i

Table A.16: Channel matrix MISO Square Array N_t=27

C. Squares Array N_t =27 d=2km

1.0e-005 *
0.0753 + 0.1304i
0.0753 + 0.1304i
0.0753 + 0.1304i
0.0753 + 0.1304i
-0.0753 - 0.1303i
-0.0753 - 0.1303i
-0.0753 - 0.1303i
-0.0753 - 0.1303i
0.0753 + 0.1303i
0.0753 + 0.1303i
0.0753 + 0.1303i
0.0753 + 0.1303i
-0.0754 - 0.1303i
-0.0754 - 0.1303i
-0.0754 - 0.1303i
-0.0754 - 0.1303i
0.0755 + 0.1303i
0.0755 + 0.1303i

0.0755 + 0.1303i
0.0755 + 0.1303i
-0.0755 - 0.1302i
-0.0755 - 0.1302i
-0.0755 - 0.1302i
-0.0755 - 0.1302i
0.0756 + 0.1301i
0.0756 + 0.1301i
0.0756 + 0.1301i

Table A.17: Channel matrix MISO C. Squares Array N_t=27

Cube Array N_t =27 d=2km
1.0e-005 *
0.0753 + 0.1304i
0.0753 + 0.1304i
0.0753 + 0.1304i
0.0753 + 0.1304i
0.0753 + 0.1304i
0.0753 + 0.1304i
0.0753 + 0.1304i
0.0753 + 0.1304i
0.0753 + 0.1304i
-0.0753 - 0.1304i
-0.0753 - 0.1304i
-0.0753 - 0.1304i
-0.0753 - 0.1304i
-0.0753 - 0.1304i
-0.0753 - 0.1304i
-0.0753 - 0.1304i
-0.0753 - 0.1304i
-0.0753 - 0.1304i
0.0753 + 0.1304i
0.0753 + 0.1304i
0.0753 + 0.1304i
0.0753 + 0.1304i
0.0753 + 0.1304i
0.0753 + 0.1304i
0.0753 + 0.1304i
0.0753 + 0.1304i

Table A.18: Channel matrix MISO Cube Array N_t=27

A.3.3 GSTA

Linear Array N_r =20 SVD_1=0.6734E-5 SVD_2=0.6730E-5 d=2Km	
1.0e-005 *	
-0.0753 + 0.1304i	-0.0753 + 0.1304i
-0.1304 - 0.0753i	0.0753 - 0.1304i
0.0753 - 0.1304i	-0.0753 + 0.1304i
0.1303 + 0.0753i	0.0753 - 0.1304i
-0.0754 + 0.1303i	-0.0753 + 0.1304i
-0.1303 - 0.0754i	0.0753 - 0.1304i
0.0755 - 0.1302i	-0.0753 + 0.1304i
0.1302 + 0.0755i	0.0753 - 0.1304i
-0.0756 + 0.1302i	-0.0753 + 0.1304i
-0.1301 - 0.0757i	0.0753 - 0.1304i
0.0758 - 0.1300i	-0.0753 + 0.1304i
0.1300 + 0.0760i	0.0753 - 0.1304i
-0.0761 + 0.1299i	-0.0753 + 0.1304i
-0.1298 - 0.0762i	0.0753 - 0.1304i
0.0764 - 0.1297i	-0.0753 + 0.1304i
0.1296 + 0.0766i	0.0753 - 0.1304i
-0.0767 + 0.1295i	-0.0753 + 0.1304i
-0.1294 - 0.0769i	0.0753 - 0.1304i
0.0771 - 0.1293i	-0.0753 + 0.1304i
0.1291 + 0.0773i	0.0753 - 0.1304i

Table A.19: Channel matrix GSTA Linear Array N_r=20 $\emptyset_1 = \frac{\pi}{3}$ $\emptyset_2 = 0$

Circular Array N_r=20 SVD_1 =0.6734E-5 SVD_2=0.469E-5 d=2Km	
1.0e-005 *	
-0.1498 - 0.0152i	0.0862 - 0.1234i
0.0350 - 0.1464i	-0.1091 - 0.1037i
0.1301 - 0.0757i	-0.0178 + 0.1495i
0.1161 - 0.0959i	0.0685 - 0.1340i
-0.0359 - 0.1462i	-0.0753 + 0.1303i
-0.1209 + 0.0897i	0.0819 - 0.1263i
0.1494 - 0.0182i	-0.1206 + 0.0901i
-0.1505 + 0.0002i	0.1443 + 0.0427i
0.1505 + 0.0024i	0.0638 - 0.1363i

-0.1463 - 0.0353i	-0.0078 - 0.1503i
0.0880 + 0.1221i	0.0638 - 0.1363i
0.1093 - 0.1035i	0.1443 + 0.0427i
0.0005 - 0.1505i	-0.1206 + 0.0901i
0.0250 - 0.1484i	0.0819 - 0.1263i
0.1446 - 0.0420i	-0.0753 + 0.1303i
-0.0174 + 0.1495i	0.0685 - 0.1340i
-0.0589 - 0.1386i	-0.0178 + 0.1495i
0.0749 + 0.1306i	-0.1091 - 0.1037i
-0.0772 - 0.1292i	0.0862 - 0.1234i
0.1036 + 0.1092i	0.1341 - 0.0684i

Table A.20: Channel matrix GSTA Circular Array N_r=20 $\emptyset_1 = \frac{\pi}{3}$ $\emptyset_2 = 0$

Square Array N_r=20 SVD_1 =0.7116E-5 SVD_2=0.6325E-5 d=2Km

1.0e-005 *	
0.1456 + 0.0382i	-0.1303 - 0.0753i
0.0382 - 0.1456i	0.1303 + 0.0753i
-0.1456 - 0.0382i	-0.1303 - 0.0753i
-0.0383 + 0.1456i	0.1303 + 0.0753i
0.1456 + 0.0383i	-0.1303 - 0.0753i
0.1456 + 0.0383i	-0.1303 - 0.0753i
-0.1172 - 0.0944i	-0.1304 - 0.0753i
0.0685 + 0.1341i	-0.1304 - 0.0753i
-0.0077 - 0.1503i	-0.1304 - 0.0753i
-0.0544 + 0.1404i	-0.1304 - 0.0753i
-0.0544 + 0.1404i	-0.1304 - 0.0753i
-0.1404 - 0.0544i	0.1304 + 0.0753i
0.0544 - 0.1404i	-0.1304 - 0.0753i
0.1404 + 0.0544i	0.1304 + 0.0753i
-0.0544 + 0.1403i	-0.1304 - 0.0753i
-0.0544 + 0.1403i	-0.1304 - 0.0753i
-0.0077 - 0.1503i	-0.1304 - 0.0753i
0.0684 + 0.1341i	-0.1304 - 0.0753i
-0.1173 - 0.0944i	-0.1304 - 0.0753i
0.1456 + 0.0382i	-0.1303 - 0.0753i

Table A.21: Channel matrix GSTA Square Array N_r=20 $\emptyset_1 = \frac{\pi}{3}$ $\emptyset_2 = 0$

C. Squares Array N_r =20 SVD_1 =0.7237E-5 SVD_2=0.6186E-5 d=2Km	
1.0e-005 *	
0.1497 + 0.0154i	0.0753 - 0.1304i
-0.1497 - 0.0154i	0.0753 - 0.1304i
-0.0882 - 0.1220i	0.0753 - 0.1304i
0.0882 + 0.1220i	0.0753 - 0.1304i
-0.0471 - 0.1430i	-0.0753 + 0.1303i
-0.0470 - 0.1430i	-0.0753 + 0.1303i
0.1474 - 0.0307i	-0.0753 + 0.1303i
0.1474 - 0.0306i	-0.0753 + 0.1303i
-0.1113 + 0.1014i	0.0753 - 0.1303i
0.1114 - 0.1013i	0.0753 - 0.1303i
-0.0322 + 0.1470i	0.0753 - 0.1303i
0.0323 - 0.1470i	0.0753 - 0.1303i
0.1380 + 0.0601i	-0.0754 + 0.1303i
0.1379 + 0.0604i	-0.0754 + 0.1303i
-0.1211 - 0.0895i	-0.0754 + 0.1303i
-0.1209 - 0.0897i	-0.0754 + 0.1303i
-0.0015 - 0.1505i	0.0755 - 0.1303i
0.0011 + 0.1505i	0.0755 - 0.1303i
0.1311 - 0.0739i	0.0755 - 0.1303i
-0.1313 + 0.0736i	0.0755 - 0.1303i

Table A.22: Channel matrix GSTA C. Squares Array N_r=20 $\emptyset_1 = \frac{\pi}{3}$ $\emptyset_2 = 0$

Linear Array N_r =27 SVD_1=0.7968E-5 SVD_2=0.7673E-5 d=2Km	
1.0e-005 *	
-0.0753 + 0.1304i	-0.0753 + 0.1304i
-0.1304 - 0.0753i	0.0753 - 0.1304i
0.0753 - 0.1304i	-0.0753 + 0.1304i
0.1303 + 0.0753i	0.0753 - 0.1304i
-0.0754 + 0.1303i	-0.0753 + 0.1304i
-0.1303 - 0.0754i	0.0753 - 0.1304i
0.0755 - 0.1302i	-0.0753 + 0.1304i
0.1302 + 0.0755i	0.0753 - 0.1304i
-0.0756 + 0.1302i	-0.0753 + 0.1304i
-0.1301 - 0.0757i	0.0753 - 0.1304i
0.0758 - 0.1300i	-0.0753 + 0.1304i
0.1300 + 0.0760i	0.0753 - 0.1304i
-0.0761 + 0.1299i	-0.0753 + 0.1304i
-0.1298 - 0.0762i	0.0753 - 0.1304i

0.0764 - 0.1297i	-0.0753 + 0.1304i
0.1296 + 0.0766i	0.0753 - 0.1304i
-0.0767 + 0.1295i	-0.0753 + 0.1304i
-0.1294 - 0.0769i	0.0753 - 0.1304i
0.0771 - 0.1293i	-0.0753 + 0.1304i
0.1291 + 0.0773i	0.0753 - 0.1304i
-0.0776 + 0.1290i	-0.0753 + 0.1304i
-0.1289 - 0.0778i	0.0753 - 0.1304i
0.0780 - 0.1287i	-0.0753 + 0.1304i
0.1286 + 0.0783i	0.0753 - 0.1304i
-0.0786 + 0.1284i	-0.0753 + 0.1304i
-0.1282 - 0.0788i	0.0753 - 0.1304i
0.0791 - 0.1281i	-0.0753 + 0.1304i

Table A.23: Channel matrix GSTA Linear Array N_r=27 $\emptyset_1 = \frac{\pi}{3}$ $\emptyset_2 = 0$

Circular Array N_r=27 SVD_1=0.8622E-5 SVD_2=0.693E-5 d=2Km

1.0e-005 *	
0.0535 - 0.1407i	-0.1337 + 0.0692i
0.1041 + 0.1088i	-0.0032 + 0.1505i
-0.0903 + 0.1205i	0.1493 - 0.0195i
-0.1474 + 0.0306i	-0.1120 - 0.1006i
-0.1474 + 0.0306i	0.0602 + 0.1380i
-0.0903 + 0.1205i	-0.0405 - 0.1450i
0.1041 + 0.1088i	0.0387 + 0.1455i
0.0535 - 0.1407i	-0.0307 - 0.1474i
-0.1260 + 0.0824i	-0.0087 + 0.1503i
0.1431 - 0.0468i	0.0952 - 0.1166i
-0.1454 + 0.0389i	-0.1462 - 0.0358i
0.1459 - 0.0371i	-0.0592 + 0.1384i
-0.1496 + 0.0166i	0.0472 + 0.1430i
0.1430 + 0.0469i	0.0472 + 0.1430i
-0.0576 - 0.1391i	-0.0592 + 0.1384i
-0.1288 + 0.0780i	-0.1462 - 0.0358i
0.0069 + 0.1504i	0.0952 - 0.1166i
0.0600 + 0.1381i	-0.0087 + 0.1503i
0.0069 + 0.1504i	-0.0307 - 0.1474i
-0.1288 + 0.0780i	0.0387 + 0.1455i
-0.0576 - 0.1391i	-0.0405 - 0.1450i
0.1430 + 0.0469i	0.0602 + 0.1380i
-0.1496 + 0.0166i	-0.1120 - 0.1006i

0.1459 - 0.0371i	0.1493 - 0.0195i
-0.1454 + 0.0389i	-0.0032 + 0.1505i
0.1431 - 0.0468i	-0.1337 + 0.0692i
-0.1260 + 0.0824i	-0.1496 + 0.0171i

Table A.24: Channel matrix GSTA Circular Array N_r=27 $\emptyset_1 = \frac{\pi}{3}$ $\emptyset_2 = 0$

Square Array N_r=27 SVD_1=0.8116E-5 SVD_2=0.7516E-5 d=2Km

1.0e-005 *	
-0.0970 - 0.1151i	0.1492 + 0.0197i
-0.1151 + 0.0970i	-0.1492 - 0.0197i
0.0970 + 0.1151i	0.1492 + 0.0197i
0.1151 - 0.0970i	-0.1492 - 0.0197i
-0.0970 - 0.1151i	0.1492 + 0.0197i
-0.1151 + 0.0970i	-0.1492 - 0.0197i
0.0969 + 0.1152i	0.1492 + 0.0197i
0.1478 + 0.0286i	0.1492 + 0.0197i
-0.1232 - 0.0864i	0.1492 + 0.0197i
0.0772 + 0.1292i	0.1492 + 0.0197i
-0.0177 - 0.1495i	0.1492 + 0.0196i
-0.0449 + 0.1437i	0.1492 + 0.0197i
0.0997 - 0.1128i	0.1492 + 0.0197i
-0.1371 + 0.0622i	0.1492 + 0.0197i
-0.1409 - 0.0529i	-0.0197 + 0.1492i
0.0529 - 0.1409i	0.0197 - 0.1492i
0.1409 + 0.0529i	-0.0197 + 0.1492i
-0.0530 + 0.1409i	0.0197 - 0.1492i
-0.1409 - 0.0530i	-0.0197 + 0.1492i
0.0530 - 0.1409i	0.0197 - 0.1492i
0.1409 + 0.0531i	-0.0197 + 0.1492i
-0.1111 + 0.1016i	-0.0197 + 0.1492i
0.0599 - 0.1381i	-0.0197 + 0.1492i
0.0018 + 0.1505i	-0.0196 + 0.1492i
-0.0632 - 0.1366i	-0.0197 + 0.1492i
0.1135 + 0.0989i	-0.0197 + 0.1492i
-0.1440 - 0.0438i	-0.0197 + 0.1492i

Table A.25: Channel matrix GSTA Square Array N_r=27 $\emptyset_1 = \frac{\pi}{3}$ $\emptyset_2 = 0$

C. Squares Array N_r=27 SVD_1=0.7963E-5 SVD_2=0.7678E-5 d=2Km

1.0e-005 *	
0.1497 + 0.0154i	0.0753 - 0.1304i
-0.1497 - 0.0154i	0.0753 - 0.1304i
-0.0882 - 0.1220i	0.0753 - 0.1304i
0.0882 + 0.1220i	0.0753 - 0.1304i
-0.0471 - 0.1430i	-0.0753 + 0.1303i
-0.0470 - 0.1430i	-0.0753 + 0.1303i
0.1474 - 0.0307i	-0.0753 + 0.1303i
0.1474 - 0.0306i	-0.0753 + 0.1303i
-0.1113 + 0.1014i	0.0753 - 0.1303i
0.1114 - 0.1013i	0.0753 - 0.1303i
-0.0322 + 0.1470i	0.0753 - 0.1303i
0.0323 - 0.1470i	0.0753 - 0.1303i
0.1380 + 0.0601i	-0.0754 + 0.1303i
0.1379 + 0.0604i	-0.0754 + 0.1303i
-0.1211 - 0.0895i	-0.0754 + 0.1303i
-0.1209 - 0.0897i	-0.0754 + 0.1303i
-0.0015 - 0.1505i	0.0755 - 0.1303i
0.0011 + 0.1505i	0.0755 - 0.1303i
0.1311 - 0.0739i	0.0755 - 0.1303i
-0.1313 + 0.0736i	0.0755 - 0.1303i
-0.1368 + 0.0628i	-0.0755 + 0.1302i
-0.1370 + 0.0623i	-0.0755 + 0.1302i
0.0139 + 0.1499i	-0.0755 + 0.1302i
0.0133 + 0.1499i	-0.0755 + 0.1302i
0.1132 + 0.0992i	0.0756 - 0.1301i
-0.1127 - 0.0997i	0.0756 - 0.1301i
-0.1425 - 0.0486i	0.0756 - 0.1301i

Table A.26: Channel matrix GSTA C. Squares Array N_r=27 $\emptyset_1 = \frac{\pi}{3}$ $\emptyset_2 = 0$

Cube Array N_r=27 SVD_1=0.8173E-5 SVD_2=0.7455E-5 d=2Km

1.0e-005 *	
-0.0882 - 0.1220i	0.0753 - 0.1304i
-0.0882 - 0.1220i	0.0753 - 0.1304i
-0.0882 - 0.1220i	0.0753 - 0.1304i
0.1220 - 0.0882i	-0.0753 + 0.1304i
0.1220 - 0.0882i	-0.0753 + 0.1304i
0.1220 - 0.0882i	-0.0753 + 0.1304i
0.0882 + 0.1220i	0.0753 - 0.1304i

0.0882 + 0.1220i	0.0753 - 0.1304i
0.0882 + 0.1220i	0.0753 - 0.1304i
0.1304 + 0.0753i	0.0753 - 0.1304i
0.1304 + 0.0753i	0.0753 - 0.1304i
0.1304 + 0.0753i	0.0753 - 0.1304i
-0.0753 + 0.1304i	-0.0753 + 0.1304i
-0.0753 + 0.1304i	-0.0753 + 0.1304i
-0.0753 + 0.1304i	-0.0753 + 0.1304i
-0.1304 - 0.0753i	0.0753 - 0.1304i
-0.1304 - 0.0753i	0.0753 - 0.1304i
-0.1304 - 0.0753i	0.0753 - 0.1304i
-0.1497 - 0.0155i	0.0753 - 0.1304i
-0.1497 - 0.0154i	0.0753 - 0.1304i
-0.1497 - 0.0155i	0.0753 - 0.1304i
0.0154 - 0.1497i	-0.0753 + 0.1304i
0.0154 - 0.1497i	-0.0753 + 0.1304i
0.0154 - 0.1497i	-0.0753 + 0.1304i
0.1497 + 0.0154i	0.0753 - 0.1304i
0.1497 + 0.0154i	0.0753 - 0.1304i
0.1497 + 0.0154i	0.0753 - 0.1304i

Table A.27: Channel matrix GSTA Cube Array N_r=27 $\emptyset_1 = \frac{\pi}{3}$ $\emptyset_2 = 0$

Linear Array N_r=27 SVD_1=0.1106E-4 SVD_2=0 d=2Km

1.0e-005 *	
-0.0753 + 0.1304i	-0.0753 + 0.1304i
0.1493 - 0.0191i	0.1493 - 0.0191i
-0.1056 - 0.1073i	-0.1056 - 0.1073i
-0.0214 + 0.1490i	-0.0214 + 0.1490i
0.1315 - 0.0732i	0.1315 - 0.0732i
-0.1379 - 0.0604i	-0.1379 - 0.0604i
0.0354 + 0.1463i	0.0354 + 0.1463i
0.0950 - 0.1168i	0.0950 - 0.1168i
-0.1505 - 0.0049i	-0.1505 - 0.0049i
0.0871 + 0.1227i	0.0871 + 0.1227i
0.0450 - 0.1437i	0.0450 - 0.1437i
-0.1416 + 0.0512i	-0.1416 + 0.0512i
0.1264 + 0.0817i	0.1264 + 0.0817i
-0.0114 - 0.1501i	-0.0114 - 0.1501i
-0.1126 + 0.0999i	-0.1126 + 0.0999i
0.1477 + 0.0292i	0.1477 + 0.0292i

-0.0661 - 0.1353i	-0.0661 - 0.1353i
-0.0677 + 0.1344i	-0.0677 + 0.1344i
0.1480 - 0.0274i	0.1480 - 0.0274i
-0.1113 - 0.1013i	-0.1113 - 0.1013i
-0.0134 + 0.1499i	-0.0134 + 0.1499i
0.1275 - 0.0800i	0.1275 - 0.0800i
-0.1408 - 0.0531i	-0.1408 - 0.0531i
0.0428 + 0.1443i	0.0428 + 0.1443i
0.0891 - 0.1214i	0.0891 - 0.1214i
-0.1505 + 0.0024i	-0.1505 + 0.0024i
0.0929 + 0.1184i	0.0929 + 0.1184i

Table A.28: Channel matrix GSTA Linear Array N_r=27 $\emptyset_1 = \frac{3\pi}{4}$ $\emptyset_2 = \frac{3\pi}{4}$

Circular Array N_r=27 SVD_1=0.1106E-4 SVD_2=0 d=2Km

1.0e-005 *	
0.0415 + 0.1447i	0.0415 + 0.1447i
-0.0825 - 0.1259i	-0.0825 - 0.1259i
0.0913 + 0.1197i	0.0913 + 0.1197i
-0.0923 - 0.1189i	-0.0923 - 0.1189i
0.1053 + 0.1076i	0.1053 + 0.1076i
-0.1378 - 0.0605i	-0.1378 - 0.0605i
0.1394 - 0.0568i	0.1394 - 0.0568i
0.0240 + 0.1486i	0.0240 + 0.1486i
-0.1264 + 0.0817i	-0.1264 + 0.0817i
-0.1495 + 0.0179i	-0.1495 + 0.0179i
-0.1391 + 0.0576i	-0.1391 + 0.0576i
-0.0288 + 0.1478i	-0.0288 + 0.1478i
0.1495 + 0.0177i	0.1495 + 0.0177i
-0.0758 - 0.1301i	-0.0758 - 0.1301i
0.0080 + 0.1503i	0.0080 + 0.1503i
0.0170 - 0.1496i	0.0170 - 0.1496i
-0.0198 + 0.1492i	-0.0198 + 0.1492i
0.0258 - 0.1483i	0.0258 - 0.1483i
-0.0587 + 0.1386i	-0.0587 + 0.1386i
0.1245 - 0.0846i	0.1245 - 0.0846i
-0.1348 - 0.0670i	-0.1348 - 0.0670i
-0.0779 + 0.1288i	-0.0779 + 0.1288i
0.0398 + 0.1452i	0.0398 + 0.1452i
0.0528 + 0.1410i	0.0528 + 0.1410i
-0.0409 + 0.1449i	-0.0409 + 0.1449i

-0.1505 - 0.0044i	-0.1505 - 0.0044i
0.0590 - 0.1385i	0.0590 - 0.1385i

Table A.29: Channel matrix GSTA Circular Array N_r=27 $\emptyset_1 = \frac{3\pi}{4}$ $\emptyset_2 = \frac{3\pi}{4}$

Square Array N=27 SVD_1=0.1106E-4 SVD_2=0 d=2Km

1.0e-005 *	
-0.0754 + 0.1303i	-0.0754 + 0.1303i
-0.0580 - 0.1389i	-0.0580 - 0.1389i
0.1457 + 0.0379i	0.1457 + 0.0379i
-0.1184 + 0.0930i	-0.1184 + 0.0930i
-0.0023 - 0.1505i	-0.0023 - 0.1505i
0.1212 + 0.0893i	0.1212 + 0.0893i
-0.1445 + 0.0423i	-0.1445 + 0.0423i
-0.1004 + 0.1121i	-0.1004 + 0.1121i
0.1501 + 0.0120i	0.1501 + 0.0120i
-0.0813 - 0.1267i	-0.0813 - 0.1267i
-0.0516 + 0.1414i	-0.0516 + 0.1414i
0.1438 - 0.0446i	0.1438 - 0.0446i
-0.1226 - 0.0874i	-0.1226 - 0.0874i
0.0046 + 0.1505i	0.0046 + 0.1505i
0.1369 + 0.0626i	0.1369 + 0.0626i
-0.0331 - 0.1468i	-0.0331 - 0.1468i
-0.0968 + 0.1153i	-0.0968 + 0.1153i
0.1504 + 0.0071i	0.1504 + 0.0071i
-0.0854 - 0.1239i	-0.0854 - 0.1239i
-0.0469 + 0.1430i	-0.0469 + 0.1430i
0.1422 - 0.0493i	0.1422 - 0.0493i
0.0356 + 0.1463i	0.0356 + 0.1463i
-0.1379 - 0.0603i	-0.1379 - 0.0603i
0.1315 - 0.0732i	0.1315 - 0.0732i
-0.0215 + 0.1490i	-0.0215 + 0.1490i
-0.1055 - 0.1074i	-0.1055 - 0.1074i
0.1493 - 0.0189i	0.1493 - 0.0189i

Table A.30: Channel matrix GSTA Square Array N_r=27 $\emptyset_1 = \frac{3\pi}{4}$ $\emptyset_2 = \frac{3\pi}{4}$

C. Squares Array N_r=27 SVD_1 =0.1106E-4 SVD_2=0 d=2Km	
1.0e-005 *	
-0.0753 + 0.1304i	-0.0753 + 0.1304i
0.1457 + 0.0378i	0.1457 + 0.0378i
-0.0753 + 0.1304i	-0.0753 + 0.1304i
-0.1056 - 0.1073i	-0.1056 - 0.1073i
-0.0753 + 0.1303i	-0.0753 + 0.1303i
-0.0023 - 0.1505i	-0.0023 - 0.1505i
-0.0753 + 0.1303i	-0.0753 + 0.1303i
0.1315 - 0.0732i	0.1315 - 0.0732i
-0.0754 + 0.1303i	-0.0754 + 0.1303i
-0.1445 + 0.0423i	-0.1445 + 0.0423i
-0.0754 + 0.1303i	-0.0754 + 0.1303i
0.0356 + 0.1463i	0.0356 + 0.1463i
-0.0755 + 0.1302i	-0.0755 + 0.1302i
0.0792 + 0.1280i	0.0792 + 0.1280i
-0.0755 + 0.1302i	-0.0755 + 0.1302i
-0.1505 - 0.0046i	-0.1505 - 0.0046i
-0.0757 + 0.1301i	-0.0757 + 0.1301i
0.1023 - 0.1105i	0.1023 - 0.1105i
-0.0757 + 0.1301i	-0.0757 + 0.1301i
0.0445 - 0.1438i	0.0445 - 0.1438i
-0.0758 + 0.1300i	-0.0758 + 0.1300i
-0.1337 - 0.0692i	-0.1337 - 0.0692i
-0.0758 + 0.1300i	-0.0758 + 0.1300i
0.1267 + 0.0812i	0.1267 + 0.0812i
-0.0760 + 0.1299i	-0.0760 + 0.1299i
-0.0311 + 0.1473i	-0.0311 + 0.1473i
-0.0760 + 0.1299i	-0.0760 + 0.1299i

Table A.31: Channel matrix GSTA C. Squares Array N_r=27 $\emptyset_1 = \frac{3\pi}{4}$ $\emptyset_2 = \frac{3\pi}{4}$

Cube Array N_r=27 SVD_1=0.1106E-4 SVD_2=0 d=2Km	
1.0e-005 *	
-0.0753 + 0.1304i	-0.0753 + 0.1304i
-0.0753 + 0.1304i	-0.0753 + 0.1304i
-0.0753 + 0.1304i	-0.0753 + 0.1304i
0.1493 - 0.0191i	0.1493 - 0.0191i
0.1493 - 0.0191i	0.1493 - 0.0191i
0.1493 - 0.0191i	0.1493 - 0.0191i
-0.1056 - 0.1073i	-0.1056 - 0.1073i

-0.1056 - 0.1073i	-0.1056 - 0.1073i
-0.1056 - 0.1073i	-0.1056 - 0.1073i
-0.0581 - 0.1389i	-0.0581 - 0.1389i
-0.0581 - 0.1389i	-0.0581 - 0.1389i
-0.0581 - 0.1389i	-0.0581 - 0.1389i
-0.0753 + 0.1304i	-0.0753 + 0.1304i
-0.0753 + 0.1304i	-0.0753 + 0.1304i
-0.0753 + 0.1304i	-0.0753 + 0.1304i
0.1493 - 0.0191i	0.1493 - 0.0191i
0.1493 - 0.0191i	0.1493 - 0.0191i
0.1493 - 0.0191i	0.1493 - 0.0191i
0.1457 + 0.0378i	0.1457 + 0.0378i
0.1457 + 0.0378i	0.1457 + 0.0378i
0.1457 + 0.0378i	0.1457 + 0.0378i
-0.0581 - 0.1389i	-0.0581 - 0.1389i
-0.0581 - 0.1389i	-0.0581 - 0.1389i
-0.0581 - 0.1389i	-0.0581 - 0.1389i
-0.0753 + 0.1304i	-0.0753 + 0.1304i
-0.0753 + 0.1304i	-0.0753 + 0.1304i
-0.0753 + 0.1304i	-0.0753 + 0.1304i

Table A.32: Channel matrix GSTA Cube Array N_r=27 $\emptyset_1 = \frac{3\pi}{4}$ $\emptyset_2 = \frac{3\pi}{4}$

A.3.4 GSRA

Linear Array N_t=20 SVD_1 =0.1741E-4 SVD_2=0.0413E-5 d=2Km	
1.0e-005 *	
-0.0753 + 0.1304i	-0.1853 - 0.3210i
-0.0669 + 0.1348i	-0.1655 - 0.3316i
-0.0583 + 0.1388i	-0.1451 - 0.3411i
-0.0495 + 0.1422i	-0.1241 - 0.3492i
-0.0405 + 0.1450i	-0.1027 - 0.3561i
-0.0313 + 0.1472i	-0.0809 - 0.3617i
-0.0220 + 0.1489i	-0.0589 - 0.3660i
-0.0126 + 0.1500i	-0.0365 - 0.3688i
-0.0032 + 0.1505i	-0.0141 - 0.3704i
0.0063 + 0.1504i	0.0084 - 0.3706i
0.0157 + 0.1497i	0.0308 - 0.3694i
0.0251 + 0.1484i	0.0532 - 0.3668i
0.0344 + 0.1466i	0.0753 - 0.3629i
0.0435 + 0.1441i	0.0972 - 0.3577i
0.0525 + 0.1411i	0.1187 - 0.3511i
0.0612 + 0.1375i	0.1398 - 0.3433i

0.0697 + 0.1334i	0.1604 - 0.3342i
0.0780 + 0.1288i	0.1803 - 0.3238i
0.0859 + 0.1236i	0.1997 - 0.3123i
0.0935 + 0.1180i	0.2182 - 0.2996i

Table A.33: Channel matrix GSRA Linear Array N_t=20 $\emptyset_1 = \pi$ $\emptyset_2 = -\frac{\pi}{12}$

Circular Array N_t=20 SVD_1=0.1781E-4 SVD_2=0.0173E-5 d=2Km

1.0e-005 *	
-0.0493 + 0.1422i	-0.1291 - 0.3474i
-0.0533 + 0.1408i	-0.1436 - 0.3417i
-0.0595 + 0.1383i	-0.1619 - 0.3334i
-0.0671 + 0.1348i	-0.1820 - 0.3229i
-0.0753 + 0.1304i	-0.2017 - 0.3110i
-0.0832 + 0.1255i	-0.2191 - 0.2989i
-0.0900 + 0.1206i	-0.2328 - 0.2884i
-0.0953 + 0.1165i	-0.2417 - 0.2810i
-0.0986 + 0.1138i	-0.2453 - 0.2778i
-0.0997 + 0.1128i	-0.2435 - 0.2794i
-0.0986 + 0.1138i	-0.2363 - 0.2856i
-0.0953 + 0.1165i	-0.2242 - 0.2952i
-0.0900 + 0.1206i	-0.2078 - 0.3069i
-0.0832 + 0.1255i	-0.1887 - 0.3190i
-0.0753 + 0.1304i	-0.1685 - 0.3302i
-0.0671 + 0.1348i	-0.1493 - 0.3392i
-0.0595 + 0.1383i	-0.1334 - 0.3458i
-0.0533 + 0.1408i	-0.1225 - 0.3498i
-0.0493 + 0.1422i	-0.1180 - 0.3514i
-0.0479 + 0.1427i	-0.1203 - 0.3506i

Table A.34: Channel matrix GSRA Circular Array N_t=20 $\emptyset_1 = \pi$ $\emptyset_2 = -\frac{\pi}{12}$

Square Array N_t=20 SVD_1=0.1782E-4 SVD_2=0.0159E-5 d=2Km

1.0e-005 *	
-0.0539 + 0.1405i	-0.1486 - 0.3396i
-0.0627 + 0.1369i	-0.1689 - 0.3299i
-0.0711 + 0.1327i	-0.1886 - 0.3191i
-0.0793 + 0.1279i	-0.2076 - 0.3070i
-0.0872 + 0.1227i	-0.2259 - 0.2939i

-0.0947 + 0.1170i	-0.2433 - 0.2796i
-0.0947 + 0.1170i	-0.2387 - 0.2836i
-0.0947 + 0.1170i	-0.2341 - 0.2874i
-0.0947 + 0.1170i	-0.2294 - 0.2912i
-0.0947 + 0.1170i	-0.2246 - 0.2949i
-0.0947 + 0.1170i	-0.2198 - 0.2985i
-0.0872 + 0.1227i	-0.2013 - 0.3113i
-0.0793 + 0.1279i	-0.1820 - 0.3229i
-0.0711 + 0.1327i	-0.1621 - 0.3333i
-0.0627 + 0.1369i	-0.1416 - 0.3426i
-0.0539 + 0.1405i	-0.1205 - 0.3505i
-0.0539 + 0.1405i	-0.1262 - 0.3485i
-0.0539 + 0.1405i	-0.1319 - 0.3464i
-0.0539 + 0.1405i	-0.1375 - 0.3442i
-0.0539 + 0.1405i	-0.1431 - 0.3419i

Table A.35: Channel matrix GSRA Square Array N_t=20 $\emptyset_1 = \pi$ $\emptyset_2 = -\frac{\pi}{12}$

C. Squares Array N_t=20 SVD_1=0.1771E-4 SVD_2=0.0252E-5 d=2Km

1.0e-005 *	
-0.0669 + 0.1348i	-0.1709 - 0.3289i
-0.0833 + 0.1254i	-0.2095 - 0.3058i
-0.0833 + 0.1254i	-0.1994 - 0.3124i
-0.0669 + 0.1348i	-0.1601 - 0.3343i
-0.0583 + 0.1388i	-0.1561 - 0.3362i
-0.0910 + 0.1199i	-0.2323 - 0.2888i
-0.0910 + 0.1199i	-0.2131 - 0.3033i
-0.0583 + 0.1388i	-0.1339 - 0.3456i
-0.0495 + 0.1422i	-0.1410 - 0.3428i
-0.0984 + 0.1140i	-0.2539 - 0.2701i
-0.0984 + 0.1140i	-0.2263 - 0.2935i
-0.0495 + 0.1422i	-0.1070 - 0.3549i
-0.0405 + 0.1450i	-0.1257 - 0.3487i
-0.1053 + 0.1076i	-0.2739 - 0.2498i
-0.1053 + 0.1076i	-0.2392 - 0.2832i
-0.0405 + 0.1450i	-0.0794 - 0.3621i
-0.0313 + 0.1472i	-0.1101 - 0.3539i
-0.1119 + 0.1007i	-0.2923 - 0.2280i
-0.1119 + 0.1007i	-0.2515 - 0.2723i
-0.0313 + 0.1472i	-0.0513 - 0.3671i

Table A.36: Channel matrix GSRA C. Squares Array N_t=20 $\emptyset_1 = \pi$ $\emptyset_2 = -\frac{\pi}{12}$

Linear Array N_t=27 SVD_1=0.1988E-4 SVD_2=0.0608E-4 d=2Km

1.0e-005 *	
-0.0753 + 0.1304i	-0.1853 - 0.3210i
-0.0669 + 0.1348i	-0.1655 - 0.3316i
-0.0583 + 0.1388i	-0.1451 - 0.3411i
-0.0495 + 0.1422i	-0.1241 - 0.3492i
-0.0405 + 0.1450i	-0.1027 - 0.3561i
-0.0313 + 0.1472i	-0.0809 - 0.3617i
-0.0220 + 0.1489i	-0.0589 - 0.3660i
-0.0126 + 0.1500i	-0.0365 - 0.3688i
-0.0032 + 0.1505i	-0.0141 - 0.3704i
0.0063 + 0.1504i	0.0084 - 0.3706i
0.0157 + 0.1497i	0.0308 - 0.3694i
0.0251 + 0.1484i	0.0532 - 0.3668i
0.0344 + 0.1466i	0.0753 - 0.3629i
0.0435 + 0.1441i	0.0972 - 0.3577i
0.0525 + 0.1411i	0.1187 - 0.3511i
0.0612 + 0.1375i	0.1398 - 0.3433i
0.0697 + 0.1334i	0.1604 - 0.3342i
0.0780 + 0.1288i	0.1803 - 0.3238i
0.0859 + 0.1236i	0.1997 - 0.3123i
0.0935 + 0.1180i	0.2182 - 0.2996i
0.1007 + 0.1119i	0.2360 - 0.2858i
0.1076 + 0.1053i	0.2529 - 0.2710i
0.1140 + 0.0984i	0.2689 - 0.2551i
0.1199 + 0.0910i	0.2838 - 0.2384i
0.1254 + 0.0833i	0.2978 - 0.2207i
0.1304 + 0.0753i	0.3106 - 0.2022i
0.1348 + 0.0669i	0.3223 - 0.1830i

Table A.37: Channel matrix GSRA Linear Array N_t=27 $\emptyset_1 = \pi$ $\emptyset_2 = -\frac{\pi}{12}$

Circular Array N_t=27 SVD_1=0.2061E-4 SVD_2=0.0269E-4 d=2Km

1.0e-005 *	
-0.0388 + 0.1454i	-0.1045 - 0.3556i
-0.0419 + 0.1446i	-0.1173 - 0.3516i
-0.0469 + 0.1430i	-0.1336 - 0.3457i
-0.0534 + 0.1408i	-0.1525 - 0.3378i
-0.0609 + 0.1377i	-0.1726 - 0.3280i
-0.0691 + 0.1337i	-0.1928 - 0.3165i
-0.0773 + 0.1292i	-0.2119 - 0.3041i
-0.0851 + 0.1242i	-0.2288 - 0.2916i
-0.0921 + 0.1190i	-0.2429 - 0.2800i

-0.0980 + 0.1143i	-0.2536 - 0.2703i
-0.1025 + 0.1102i	-0.2606 - 0.2635i
-0.1056 + 0.1073i	-0.2640 - 0.2602i
-0.1071 + 0.1058i	-0.2635 - 0.2607i
-0.1071 + 0.1058i	-0.2592 - 0.2649i
-0.1056 + 0.1073i	-0.2512 - 0.2725i
-0.1025 + 0.1102i	-0.2397 - 0.2828i
-0.0980 + 0.1143i	-0.2248 - 0.2947i
-0.0921 + 0.1190i	-0.2073 - 0.3073i
-0.0851 + 0.1242i	-0.1878 - 0.3195i
-0.0773 + 0.1292i	-0.1675 - 0.3306i
-0.0691 + 0.1337i	-0.1476 - 0.3400i
-0.0609 + 0.1377i	-0.1292 - 0.3474i
-0.0534 + 0.1408i	-0.1137 - 0.3528i
-0.0469 + 0.1430i	-0.1020 - 0.3563i
-0.0419 + 0.1446i	-0.0950 - 0.3583i
-0.0388 + 0.1454i	-0.0930 - 0.3588i
-0.0378 + 0.1457i	-0.0963 - 0.3579i

Table A.38: Channel matrix GSRA Circular Array N_t=27 $\emptyset_1 = \pi$ $\emptyset_2 = -\frac{\pi}{12}$

Square Array N_t=27 SVD_1=0.2065E-4 SVD_2=0.0239E-4 d=2Km

1.0e-005 *	
-0.0461 + 0.1433i	-0.1353 - 0.3451i
-0.0550 + 0.1401i	-0.1560 - 0.3362i
-0.0637 + 0.1364i	-0.1761 - 0.3262i
-0.0722 + 0.1321i	-0.1955 - 0.3149i
-0.0803 + 0.1273i	-0.2143 - 0.3024i
-0.0882 + 0.1220i	-0.2322 - 0.2889i
-0.0956 + 0.1162i	-0.2493 - 0.2743i
-0.0956 + 0.1162i	-0.2482 - 0.2753i
-0.0956 + 0.1162i	-0.2437 - 0.2793i
-0.0956 + 0.1162i	-0.2391 - 0.2832i
-0.0956 + 0.1162i	-0.2345 - 0.2871i
-0.0956 + 0.1162i	-0.2298 - 0.2908i
-0.0956 + 0.1162i	-0.2250 - 0.2945i
-0.0956 + 0.1162i	-0.2202 - 0.2981i
-0.0920 + 0.1192i	-0.2111 - 0.3047i
-0.0843 + 0.1247i	-0.1922 - 0.3169i
-0.0763 + 0.1298i	-0.1726 - 0.3280i
-0.0680 + 0.1343i	-0.1524 - 0.3379i
-0.0594 + 0.1383i	-0.1316 - 0.3465i

-0.0506 + 0.1418i	-0.1104 - 0.3538i
-0.0416 + 0.1447i	-0.0887 - 0.3599i
-0.0416 + 0.1447i	-0.0931 - 0.3588i
-0.0416 + 0.1447i	-0.0989 - 0.3572i
-0.0416 + 0.1447i	-0.1047 - 0.3556i
-0.0416 + 0.1447i	-0.1105 - 0.3538i
-0.0416 + 0.1447i	-0.1162 - 0.3520i
-0.0416 + 0.1447i	-0.1219 - 0.3500i

Table A.39: Channel matrix GSRA Square Array N_t=27 $\emptyset_1 = \pi\, \emptyset_2 = -\frac{\pi}{12}$

C. Squares Array N_t=27 SVD_1=0.2045E-4 SVD_2=0.0372E-4 d=2Km

1.0e-005 *	
-0.0669 + 0.1348i	-0.1709 - 0.3289i
-0.0833 + 0.1254i	-0.2095 - 0.3058i
-0.0833 + 0.1254i	-0.1994 - 0.3124i
-0.0669 + 0.1348i	-0.1601 - 0.3343i
-0.0583 + 0.1388i	-0.1561 - 0.3362i
-0.0910 + 0.1199i	-0.2323 - 0.2888i
-0.0910 + 0.1199i	-0.2131 - 0.3033i
-0.0583 + 0.1388i	-0.1339 - 0.3456i
-0.0495 + 0.1422i	-0.1410 - 0.3428i
-0.0984 + 0.1140i	-0.2539 - 0.2701i
-0.0984 + 0.1140i	-0.2263 - 0.2935i
-0.0495 + 0.1422i	-0.1070 - 0.3549i
-0.0405 + 0.1450i	-0.1257 - 0.3487i
-0.1053 + 0.1076i	-0.2739 - 0.2498i
-0.1053 + 0.1076i	-0.2392 - 0.2832i
-0.0405 + 0.1450i	-0.0794 - 0.3621i
-0.0313 + 0.1472i	-0.1101 - 0.3539i
-0.1119 + 0.1007i	-0.2923 - 0.2280i
-0.1119 + 0.1007i	-0.2515 - 0.2723i
-0.0313 + 0.1472i	-0.0513 - 0.3671i
-0.0220 + 0.1489i	-0.0942 - 0.3585i
-0.1180 + 0.0935i	-0.3089 - 0.2048i
-0.1180 + 0.0935i	-0.2633 - 0.2608i
-0.0220 + 0.1489i	-0.0229 - 0.3699i
-0.0126 + 0.1500i	-0.0782 - 0.3623i
-0.1236 + 0.0859i	-0.3238 - 0.1805i
-0.1236 + 0.0859i	-0.2747 - 0.2489i

Table A.40: Channel matrix GSRA C. Squares Array N_t=27 $\emptyset_1 = \pi\, \emptyset_2 = -\frac{\pi}{12}$

Cube Array N_t=27 SVD_1=0.2077E-4 SVD_2=0.0074E-4 d=2Km

1.0e-005 *	
-0.0833 + 0.1254i	-0.1994 - 0.3124i
-0.0833 + 0.1254i	-0.1994 - 0.3124i
-0.0833 + 0.1254i	-0.1994 - 0.3124i
-0.0753 + 0.1304i	-0.1801 - 0.3240i
-0.0753 + 0.1304i	-0.1801 - 0.3240i
-0.0753 + 0.1304i	-0.1801 - 0.3240i
-0.0669 + 0.1348i	-0.1601 - 0.3343i
-0.0669 + 0.1348i	-0.1601 - 0.3343i
-0.0669 + 0.1348i	-0.1601 - 0.3343i
-0.0833 + 0.1254i	-0.2045 - 0.3092i
-0.0833 + 0.1254i	-0.2045 - 0.3092i
-0.0833 + 0.1254i	-0.2045 - 0.3092i
-0.0753 + 0.1304i	-0.1853 - 0.3210i
-0.0753 + 0.1304i	-0.1853 - 0.3210i
-0.0753 + 0.1304i	-0.1853 - 0.3210i
-0.0669 + 0.1348i	-0.1655 - 0.3316i
-0.0669 + 0.1348i	-0.1655 - 0.3316i
-0.0669 + 0.1348i	-0.1655 - 0.3316i
-0.0833 + 0.1254i	-0.2095 - 0.3058i
-0.0833 + 0.1254i	-0.2095 - 0.3058i
-0.0833 + 0.1254i	-0.2095 - 0.3058i
-0.0753 + 0.1304i	-0.1905 - 0.3179i
-0.0753 + 0.1304i	-0.1905 - 0.3179i
-0.0753 + 0.1304i	-0.1905 - 0.3179i
-0.0669 + 0.1348i	-0.1709 - 0.3289i
-0.0669 + 0.1348i	-0.1709 - 0.3289i
-0.0669 + 0.1348i	-0.1709 - 0.3289i

Table A.41: Channel matrix GSRA Cube Array N_t=27 $\emptyset_1 = \boldsymbol{\pi}$ $\emptyset_2 = -\frac{\boldsymbol{\pi}}{\mathbf{12}}$

Linear Array N_t=27 SVD_1=0.1999E-4 SVD_2=0.0572E-4 d=2Km

1.0e-005 *	
-0.0753 + 0.1304i	-0.1853 - 0.3210i
-0.0669 + 0.1348i	-0.1688 - 0.3300i
-0.0583 + 0.1388i	-0.1518 - 0.3381i
-0.0495 + 0.1422i	-0.1344 - 0.3454i
-0.0405 + 0.1450i	-0.1167 - 0.3518i
-0.0313 + 0.1472i	-0.0987 - 0.3573i

-0.0220 + 0.1489i	-0.0804 - 0.3618i
-0.0126 + 0.1500i	-0.0619 - 0.3655i
-0.0032 + 0.1505i	-0.0432 - 0.3681i
0.0063 + 0.1504i	-0.0245 - 0.3698i
0.0157 + 0.1497i	-0.0057 - 0.3706i
0.0251 + 0.1484i	0.0132 - 0.3704i
0.0344 + 0.1466i	0.0320 - 0.3693i
0.0435 + 0.1441i	0.0507 - 0.3672i
0.0525 + 0.1411i	0.0693 - 0.3641i
0.0612 + 0.1375i	0.0877 - 0.3601i
0.0697 + 0.1334i	0.1059 - 0.3552i
0.0780 + 0.1288i	0.1238 - 0.3494i
0.0859 + 0.1236i	0.1414 - 0.3426i
0.0935 + 0.1180i	0.1586 - 0.3350i
0.1007 + 0.1119i	0.1754 - 0.3265i
0.1076 + 0.1053i	0.1918 - 0.3172i
0.1140 + 0.0984i	0.2077 - 0.3070i
0.1199 + 0.0910i	0.2230 - 0.2961i
0.1254 + 0.0833i	0.2378 - 0.2844i
0.1304 + 0.0753i	0.2519 - 0.2719i
0.1348 + 0.0669i	0.2654 - 0.2588i

Table A.42: Channel matrix GSRA Linear Array N_t=27 $\emptyset_1 = \pi$ $\emptyset_2 = -\frac{\pi}{5}$

Circular Array N_t=27 SVD_1=0.2063E-4 SVD_2=0.0259E-4 d=2Km

1.0e-005 *	
-0.0388 + 0.1454i	-0.1005 - 0.3568i
-0.0419 + 0.1446i	-0.0943 - 0.3585i
-0.0469 + 0.1430i	-0.0932 - 0.3587i
-0.0534 + 0.1408i	-0.0974 - 0.3576i
-0.0609 + 0.1377i	-0.1065 - 0.3550i
-0.0691 + 0.1337i	-0.1199 - 0.3507i
-0.0773 + 0.1292i	-0.1367 - 0.3445i
-0.0851 + 0.1242i	-0.1559 - 0.3363i
-0.0921 + 0.1190i	-0.1762 - 0.3261i
-0.0980 + 0.1143i	-0.1963 - 0.3144i
-0.1025 + 0.1102i	-0.2150 - 0.3019i
-0.1056 + 0.1073i	-0.2315 - 0.2895i
-0.1071 + 0.1058i	-0.2450 - 0.2781i
-0.1071 + 0.1058i	-0.2551 - 0.2689i
-0.1056 + 0.1073i	-0.2615 - 0.2627i
-0.1025 + 0.1102i	-0.2642 - 0.2600i

-0.0980 + 0.1143i	-0.2630 - 0.2612i
-0.0921 + 0.1190i	-0.2581 - 0.2660i
-0.0851 + 0.1242i	-0.2495 - 0.2741i
-0.0773 + 0.1292i	-0.2373 - 0.2847i
-0.0691 + 0.1337i	-0.2219 - 0.2969i
-0.0609 + 0.1377i	-0.2040 - 0.3095i
-0.0534 + 0.1408i	-0.1843 - 0.3216i
-0.0469 + 0.1430i	-0.1640 - 0.3324i
-0.0419 + 0.1446i	-0.1442 - 0.3415i
-0.0388 + 0.1454i	-0.1263 - 0.3485i
-0.0378 + 0.1457i	-0.1114 - 0.3535i

Table A.43: Channel matrix GSRA Circular Array N_t=27 $\emptyset_1 = \pi$ $\emptyset_2 = -\frac{\pi}{5}$

Square Array N_t=27 SVD_1=0.2066E-4 SVD_2=0.0226E-4 d=2Km

1.0e-005 *	
-0.0461 + 0.1433i	-0.0836 - 0.3611i
-0.0550 + 0.1401i	-0.1018 - 0.3564i
-0.0637 + 0.1364i	-0.1198 - 0.3508i
-0.0722 + 0.1321i	-0.1374 - 0.3442i
-0.0803 + 0.1273i	-0.1548 - 0.3368i
-0.0882 + 0.1220i	-0.1717 - 0.3285i
-0.0956 + 0.1162i	-0.1881 - 0.3194i
-0.0956 + 0.1162i	-0.1911 - 0.3176i
-0.0956 + 0.1162i	-0.2027 - 0.3103i
-0.0956 + 0.1162i	-0.2140 - 0.3026i
-0.0956 + 0.1162i	-0.2250 - 0.2945i
-0.0956 + 0.1162i	-0.2357 - 0.2860i
-0.0956 + 0.1162i	-0.2461 - 0.2771i
-0.0956 + 0.1162i	-0.2562 - 0.2678i
-0.0920 + 0.1192i	-0.2493 - 0.2743i
-0.0843 + 0.1247i	-0.2351 - 0.2866i
-0.0763 + 0.1298i	-0.2202 - 0.2982i
-0.0680 + 0.1343i	-0.2048 - 0.3090i
-0.0594 + 0.1383i	-0.1888 - 0.3190i
-0.0506 + 0.1418i	-0.1724 - 0.3281i
-0.0416 + 0.1447i	-0.1555 - 0.3365i
-0.0416 + 0.1447i	-0.1461 - 0.3407i
-0.0416 + 0.1447i	-0.1334 - 0.3458i
-0.0416 + 0.1447i	-0.1205 - 0.3505i

-0.0416 + 0.1447i	-0.1075 - 0.3547i
-0.0416 + 0.1447i	-0.0943 - 0.3584i
-0.0416 + 0.1447i	-0.0810 - 0.3617i

Table A.44: Channel matrix GSRA Square Array N_t=27 $\emptyset_1 = \pi$ $\emptyset_2 = -\frac{\pi}{5}$

C. Squares Array N_t=27 SVD_1=0.2046E-4 SVD_2=0.037E-4 d=2Km

1.0e-005 *	
-0.0669 + 0.1348i	-0.1565 - 0.3360i
-0.0833 + 0.1254i	-0.1898 - 0.3184i
-0.0833 + 0.1254i	-0.2127 - 0.3035i
-0.0669 + 0.1348i	-0.1808 - 0.3235i
-0.0583 + 0.1388i	-0.1264 - 0.3484i
-0.0910 + 0.1199i	-0.1942 - 0.3157i
-0.0910 + 0.1199i	-0.2385 - 0.2837i
-0.0583 + 0.1388i	-0.1763 - 0.3260i
-0.0495 + 0.1422i	-0.0954 - 0.3582i
-0.0984 + 0.1140i	-0.1985 - 0.3130i
-0.0984 + 0.1140i	-0.2625 - 0.2617i
-0.0495 + 0.1422i	-0.1718 - 0.3284i
-0.0405 + 0.1450i	-0.0636 - 0.3652i
-0.1053 + 0.1076i	-0.2029 - 0.3102i
-0.1053 + 0.1076i	-0.2844 - 0.2377i
-0.0405 + 0.1450i	-0.1672 - 0.3308i
-0.0313 + 0.1472i	-0.0314 - 0.3693i
-0.1119 + 0.1007i	-0.2072 - 0.3074i
-0.1119 + 0.1007i	-0.3042 - 0.2118i
-0.0313 + 0.1472i	-0.1626 - 0.3331i
-0.0220 + 0.1489i	0.0011 - 0.3707i
-0.1180 + 0.0935i	-0.2114 - 0.3044i
-0.1180 + 0.0935i	-0.3215 - 0.1844i
-0.0220 + 0.1489i	-0.1579 - 0.3353i
-0.0126 + 0.1500i	0.0336 - 0.3691i
-0.1236 + 0.0859i	-0.2156 - 0.3015i
-0.1236 + 0.0859i	-0.3365 - 0.1555i

Table A.45: Channel matrix GSRA C. Squares Array N_t=27 $\emptyset_1 = \pi$ $\emptyset_2 = -\frac{\pi}{5}$

Cube Array N_t=27 SVD_1=0.2078E-4 SVD_2=0.071E-4 d=2Km	
1.0e-005 *	
-0.0833 + 0.1254i	-0.2127 - 0.3035i
-0.0833 + 0.1254i	-0.2127 - 0.3035i
-0.0833 + 0.1254i	-0.2127 - 0.3035i
-0.0753 + 0.1304i	-0.1971 - 0.3139i
-0.0753 + 0.1304i	-0.1971 - 0.3139i
-0.0753 + 0.1304i	-0.1971 - 0.3139i
-0.0669 + 0.1348i	-0.1808 - 0.3235i
-0.0669 + 0.1348i	-0.1808 - 0.3235i
-0.0669 + 0.1348i	-0.1808 - 0.3235i
-0.0833 + 0.1254i	-0.2014 - 0.3112i
-0.0833 + 0.1254i	-0.2014 - 0.3112i
-0.0833 + 0.1254i	-0.2014 - 0.3112i
-0.0753 + 0.1304i	-0.1853 - 0.3210i
-0.0753 + 0.1304i	-0.1853 - 0.3210i
-0.0753 + 0.1304i	-0.1853 - 0.3210i
-0.0669 + 0.1348i	-0.1688 - 0.3300i
-0.0669 + 0.1348i	-0.1688 - 0.3300i
-0.0669 + 0.1348i	-0.1688 - 0.3300i
-0.0833 + 0.1254i	-0.1898 - 0.3184i
-0.0833 + 0.1254i	-0.1898 - 0.3184i
-0.0833 + 0.1254i	-0.1898 - 0.3184i
-0.0753 + 0.1304i	-0.1733 - 0.3276i
-0.0753 + 0.1304i	-0.1733 - 0.3276i
-0.0753 + 0.1304i	-0.1733 - 0.3276i
-0.0669 + 0.1348i	-0.1565 - 0.3360i
-0.0669 + 0.1348i	-0.1565 - 0.3360i
-0.0669 + 0.1348i	-0.1565 - 0.3360i

Table A.46: Channel matrix GSRA Cube Array N_t=27 $\emptyset_1 = \pi\, \emptyset_2 = -\frac{\pi}{5}$

Bibliography

[1] Fundamentals of Wireless Communication. https://people.eecs.berkeley.edu/~dtse/Chapters_PDF/Fundamentals_Wireless_Communication_chapter7.pdf

[2] Spatial Channel Model AHG (Combined ad-hoc from 3GPP & 3GPP2)

[3] Wireless Communications, Andrea Goldsmith, Stanford University

[4] Matlab, website http://se.mathworks.com/products/matlab/

[5] Optimal Power Allocation over Parallel Gaussian Broadcast Channels, David N.C. Tse∗ Dept. of Electrical Engineering and Computer Sciences University of California at Berkeley, https://web.stanford.edu/~dntse/papers/broadcast2.pdf

[6] Power Allocation in Wireless Systems Subject to Long-Term and Short-Term Power Constraints, Mostafa Khoshnevisan and J. Nicholas Laneman Department of Electrical Engineering University of Notre Dame, http://www3.nd.edu/~jnl/pubs/icc2011.pdf

[7] Chun-Hung Liu: Lecture Notes, 2014, http://web.it.nctu.edu.tw/~chungliu/courses/WirelessComm/slides/

[8] T. M. Cover and J. A. Thomas, "Elements of Information Theory", John Wiley & Sons, 2003.

[9] Multiple-Input-Multiple-Output (MIMO) Systems, Deke Guo National University of Defense Technology 2012.03, http://www.ntu.edu.sg/home/limo/seminar/MIMO_Deke.pdf

[10] Bigelow, Stephen. Understanding Telephone Electronics. Newnes. p. 16. ISBN 978-0750671750.

[11] Carr, Joseph (2002). RF Components and Circuits. Newnes. pp. 45-46. ISBN 978-0750648448.

[12] Martin Sauter: Communication Systems for the Mobile Information Society, John Wiley, September 2006, ISBN 0-470-02676-6

[13] Singular Value Decomposition Tutorial, Kirk Baker https://www.ling.ohio-state.edu/~kbaker/pubs/Singular_Value_Decomposition_Tutorial.pdf

[14] Arndt, C. (2004), Information Measures: Information and its Description in Science and Engineering, Springer, ISBN 978-3-540-40855-0

[15] Gray, R. M. (2011), Entropy and Information Theory, Springer.